Sources, sinks, and sea lice: determining patch contribution and transient dynamics in marine metapopulations

by

Peter David Harrington

A thesis submitted in partial fulfillment of the requirements for the degree of

Doctor of Philosophy

in

Applied Mathematics

Department of Mathematical and Statistical Sciences
University of Alberta

Abstract

Sea lice are a threat to the health of both wild and farmed salmon and an economic burden for salmon farms. Open-net salmon farms act as reservoirs for sea lice in near coastal areas, which can lead to elevated sea louse levels on wild salmon. With a free living larval stage, sea lice can disperse tens of kilometers in the ocean, both from salmon farms onto wild salmon and between salmon farms. This larval dispersal connects local sea louse populations on salmon farms and thus modelling the collection of salmon farms as a metapopulation can lead to a better understanding of which salmon farms are driving the overall growth of sea lice in a salmon farming region. In this thesis I use metapopulation models to specifically study sea lice on salmon farms in the Broughton Archipelago, BC, and more broadly to better understand the transient and asymptotic dynamics of marine metapopulations.

I begin in Chapter 1 by presenting a brief background on the mathematical concepts used in this thesis and on the biological systems on which it is focused. In Chapter 2 I create a stage-structured metapopulation model for sea lice on salmon farms using age-density equations to capture the complexities of the sea louse life cycle. To identify which salmon farms are acting as sources or sinks of sea lice in a salmon farming region I create a next-generation matrix which distills the essential elements of sea louse dispersal and demography into a single operator. Using the next-generation matrix I investigate the effect of interfarm spacing and environmental variables on the source-sink distribution of salmon farms and show that on the generational scale it is possible for transient dynamics to be different than the long term dynamics of this metapopulation.

In Chapter 3 I further explore the transient dynamics which can occur in general marine and other birth-jump metapopulations. I demonstrate that even in simple linear metapopulation models the transient dynamics can be very different from the asymptotic dynamics of these populations. I show how to connect reactivity and attenuation, measures of the maximum and minimum growth rates that can occur following perturbations, to the source-sink distribution of habitat patches and how reactivity and attenuation can differ from the actual population growth rates when measured in the commonly used ℓ_2 norm. I then demonstrate how to meaningfully measure reactivity in marine metapopulations, where adults typically produce a large number of offspring and thus most would be considered reactive under the classical definition.

In Chapter 4 I use the next-generation matrix developed in Chapter 2 to calculate which salmon farms are acting as the largest source of sea lice in the Broughton Archipelago, BC. The Broughton Archipelago has been ground zero for studying the effects of sea lice on wild salmon and several of the farms are currently being removed in an agreement between the provincial government and local First Nations. I find that several of the farms that are not slated to be removed are acting as the largest sources of sea lice in this region and occur in two distinct clusters. I also find that warming temperatures coupled with high salinities could lead to increased sea louse growth in the Broughton.

In Chapter 5 I calculate the distribution of arrival times for sea lice dispersing between salmon farms in the Broughton Archipelago to disentangle the factors affecting dispersal and cross-infection of sea lice in this region. First, I calculate the arrival time distribution directly using a hydrodynamic model of the Broughton to which I then parameterize a simple advection diffusion model of the arrival time distribution. I use the simple model to show that there an intermediate distance between farms can maximize cross infection, and the specific distance which maximizes cross infection depends on the magnitude of the current and temperature of the ocean. I conclude

the thesis in Chapter 6 by contextualizaing the results within the broader literature and discussing limitations, potential for future work, and management implications of sea lice on salmon farms.

Preface

This thesis has been structured as paper based where Chapters 2,3,4, and 5 are the four main components of original work. Mark A. Lewis was a supervisory author on all chapters and contributed to the ideas of each chapter and gave feedback on the writing of the thesis. Other contributions are noted below.

Chapter 2 has been published as: Peter D. Harrington and Mark A. Lewis, (2020) "A next-generation approach to calculate source–sink dynamics in marine metapopulations", *Bulletin of Mathematical Biology*, 82, pp. 1–44, doi:10.1007/s11538-019-00674-1. I was responsible for model development, analysis, and manuscript composition. Mark A. Lewis was a supervisory author and contributed to the ideas of the manuscript as well as manuscript edits.

Chapter 3 has been accepted for publication in *SIAM Journal on Applied Dynamical Systems* as : Peter D. Harrington, Mark A. Lewis and Pauline van den Driessche, "Reactivity, Attenuation, and Transients in Metapopulations". I was responsible for model development, analysis, and manuscript composition. Pauline van den Driessche and Mark A. Lewis were supervisory authors on this chapter and contributed to the ideas of this manuscript and gave feedback on the writing.

Chapter 4 will soon be submitted for publication as: Peter D. Harrington, Danielle L. Cantrell, Michael G. G. Foreman, Ming Guo, and Mark A. Lewis, "Calculating the timing and probability of arrival for sea lice dispersing between salmon farms". I was responsible for model development, analysis, and manuscript composition. Danielle L. Cantrell provided code that was used to generate the Kernel Density Estimations for this chapter, and gave feedback on the writing. Michael G.G. Foreman and Ming

Guo were involved in the original development of the Broughton FVCOM and particle tracking models, and gave feedback on the writing. Mark A. Lewis was a supervisory author and contributed to the ideas of the manuscript as well as manuscript edits.

Chapter 5 will soon be submitted for publication as: Peter D. Harrington, Danielle L. Cantrell, and Mark A. Lewis, "Calculating patch contribution and persistence in marine metapopulations with next-generation matrices: the case of sea lice on salmon farms". I was responsible for model development, analysis, and manuscript composition and Mark A. Lewis was a supervisory author and contributed to the ideas of the manuscript as well as manuscript edits.

Acknowledgements

There are so many people that have supported me over the length of this PhD and have helped me grow to become a better scientist and a better person. If you do not see your name here, know that it is only because I have run out of room. First and foremost, I would like to thank my supervisor, Mark Lewis, for his help with just about everything. Mark, you are incredibly kind and patient, and have shown me the importance of both being a good scientist and doing good science. Throughout my PhD I have often felt hopeless, but whenever we meet your energy, passion, and support brings me new energy and excitement for the work I'm doing. You sent me out to Salmon Coast Field Station as soon as I started my PhD and allowed me to keep returning after I fell in love with the community, the place, and the fieldwork. Because of you I'm probably one of the only math graduate students that got to spend their summers on a boat catching salmon.

I want to thank Junling Ma and Pauline van den Driessche for welcoming me at UVic and showing me just how fast a paper can come together when everyone is extremely focused. Pauline, I also want to thank you for your support on the third chapter of this thesis, you are one of the most friendly, passionate, and endlessly energetic scientists I know and it has been a pleasure working with you. Thank you Danielle Cantrell for your work on the fourth and fifth chapters of this thesis, they would have been much more difficult without your help. Thanks also to the members of my committee, Subhash Lele and Thomas Hillen for your guidance, especially around how much work is too much work to try and complete in a PhD.

Thank you to the Lewis lab for your advice, support and friendship throughout the years, especially to Dean, Jody, Nathan, Sam and Melodie for showing me how to finish a PhD. Thank you Kim Wilke-Budinski, for helping make the logistical aspects of this PhD more fun and for taking care of everyone in the lab over the years. Special thanks also to Chris Heggerud, you helped me get through classes, figure out research, and took me skiing. This PhD would not nearly have been as enjoyable if you weren't going through one at the same time, and congratulations on beating me to the finish line.

Thank you to everyone at Salmon Coast Field Station, you taught me so much and created such a welcoming environment for a rogue mathematician. I would try and name all of you, but then invariably I would leave someone out. Special thanks to Lauren and Steph for teaching me how to spot sea lice, and Andrew and Chris for teaching me how to drive a boat, it must have taken a lot of patience.

I want to thank my teaching mentors, Dinuka Gunaratne, John Nychka, and Shawn Desaulniers. You have all helped me realize how passionate I was about teaching and have helped guide me onwards to a teaching career.

I also want to acknowledge the financial support that I have received from an NSERC Canadian Graduate Master's Scholarship, an Alberta Graduate Excellence Scholarship, a Queen Elizabeth II Scholarship, and other smaller scholarships that I have received from the University of Alberta Math Department over the years.

Lastly I want to thank my friends and family for your endless support and for making this PhD a (mostly) fun time. Thank you to my (somewhat now dispersed) Vancouver crew: Chris, Jo, Rosy, Chloe, Jer, Warren, Laura, Kai, Jon, Lauren, Lolo, Jayne, and Vincent - your support, joy, and laughter meant more than you know and you always made me feel like I had a home to come back to. Thank you to Hannah and Griffin for supporting me through so much of this journey even if not till then end. Thank you Simon, for putting up with me for so long, for showing me how to fall in love with winter and Edmonton, for being my squash buddy, and for moving with me more times than anyone should have to. Thank you Emma, for your tremendous support especially at the end of this PhD, and for always being a willing adventure buddy despite your many injuries, your unbridled enthusiasm for all things is infectious. Thank you Mom, Dad, and Ben, for your unconditional support through this PhD and for always believing in me, even when I didn't believe in myself. Finally, thank you Alex and Whites. Whites, for always being there for me in a way that only a cat can, and Alex, thank you for always taking care of me, especially when I was most stressed, I truly don't know if I could have finished this thesis without your love and support.

Table of Contents

List of Tables

List of Figures

Chapter 1

Introduction

Sea lice (*Lepeophtheirus salmonis*) are a marine ectoparasite that can feed on the epidermal tissues, blood and muscles of salmon (Costello, 2006). They occur naturally in low densities on wild salmon, but salmon farms in near coastal ecosystems provide a stationary host for sea lice on which they can survive year round and the density of salmon in the farms can lead to large sea louse outbreaks (Bateman et al., 2016; Costello, 2009a; Frazer et al., 2012; Krkošek et al., 2011b; Rogers et al., 2013). With a free living larval stage, sea lice can disperse tens of kilometers in the ocean between different salmon farms and from salmon farms onto wild salmon. When salmon farms are located along the migration routes of wild salmon, dispersal of sea lice away from farms leads to elevated levels of sea lice on wild salmon, which can cause additional mortality and morbidity (Brauner et al., 2012; Godwin et al., 2015; Godwin et al., 2017; Krkošek et al., 2011a; Krkošek et al., 2006a; Krkošek et al., 2005; Peacock et al., 2020). For pink salmon, high sea lice numbers on nearby salmon farms have been correlated with population level declines (Krkošek et al., 2011b; Krkošek et al., 2007).

The Broughton Archipelago is a group of islands on the west coast of Canada that has been at the center of the debate of the effect of sea lice from salmon farms on wild salmon (Brooks, 2005; Brooks and Stucchi, 2006; Krkošek et al., 2011b; Krkošek et al., 2008; Krkošek et al., 2007; Krkošek et al., 2006a; Krkošek et al., 2005; Krkošek et al., 2006b; Marty et al., 2010; Riddell et al., 2008). The area has historically had several active salmon farms located along the migratory routes of wild pink and chum salmon and much of the early debate was surrounding the ability of simple advection diffusion equations to accurately capture the complex current patterns that govern dispersal of sea lice in this region. Due to the concern around the threat that sea lice from salmon farms pose to wild salmon, several farms are now being removed in an agreement between governments of British Columbia and the Kwikwasut'inuxw

Haxwa'mis, 'Namgis, and Mamalilikulla First Nations (Brownsey and Chamberlain, 2018) and after 2023 the remaining salmon farms must be approved by both the local First Nations and the provincial government in order to continue to operate.

In the context of salmon farms and the threat of sea lice to wild salmon in the Broughton Archipelago, the motivating idea behind this thesis is to model sea louse populations as a connected metapopulation, in order to identify which salmon farms were having the largest effect on the growth of sea lice in this region. Some of the focus is on short timescales, so that the farms which are having the largest initial effect on sea louse population growth can be identified and treated early. However, many other species have juvenile stages which disperse between habitat patches and adult stages which remain on a patch, sometimes referred to as birth-jump populations, which can be modelled as a metapopulation. For marine species which are declining, the metapopulation framework can be used to identify which habitat patches to protect in order to maintain persistence of the metapopulation, and has been used to design Marine Protected Areas and marine reserves (Bode et al., 2006; Botsford et al., 2009; Burgess et al., 2014; Costello et al., 2010; Crowder et al., 2000; Figueira, 2009; Fox et al., 2016; Kritzer and Sale, 2006; Watson et al., 2011).

Therefore there are two main threads in this thesis: using mathematics to understand sea louse transmission between salmon farms in the Broughton Archipelago, and contributing more broadly to the understanding of transient and asymptotic dynamics of birth-jump metapopulations. The structure of this thesis is as follows. First, in the remainder of Chapter 1 I provide a more extensive background on metapopulation models and sea lice on salmon farms, including examples of marine and birth-jump metapopulations, as well as an overview of the relevant mathematical concepts used in this thesis. In Chapter 2 I construct a model for sea lice on salmon farms where maturation and survival are age dependent and answer the following questions: How do we classify habitat patches as sources or sinks in a continuous time, continuous age metapopulation; and how does this relate to the contribution of sea lice populations on individual salmon farms located in a channel? In Chapter 3 I investigate the transient dynamics that can occur in birth-jump metapopulations and answer the questions: how are the transient dynamics different from the long-term dynamics of birth jump metapopulations; and how can we connect the transient dynamics to the source-sink classification of habitat patches? In Chapter 4 I apply the source-sink classification developed in Chapter 2 to connectivity and demography data from the Broughton Archipelago and answer the questions: Which farms are acting as the largest sources of sea lice in this system; and what is the effect of farm removal the sea louse metapopulation? In Chapter 5 I investigate the timing of arrival for sea lice

dispersing between two salmon farms and answer the questions: can simple advection-diffusion equations adequately describe the arrival of sea lice dispersing between two farms; and how does the interaction between farm spacing and sea louse maturation affect the level of cross-infection between farms. Lastly I conclude in Chapter 6 with a discussion of the significance of the results of the thesis and their applications to sea lice on salmon farms and other marine and birth-jump metapopulations.

1.1 Metapopulations

A metapopulation is a collection of subpopulations located on discrete habitat patches, where the subpopulations are connected via dispersal (Hanski, 1998). The interpatch dispersal is not so low that the population dynamics of an individual patch can be adequately captured in isolation of other patches or so high that the dynamics of the entire metapopulation can be described without consideration of local subpopulations. The metapopulation concept was originally formulated by Levins (1969) where the fraction of occupied habitat patches was modelled in a metapopulation where subpopulations on local habitat patches go extinct and are recolonized through dispersal from other subpopulations. Since this original formulation metapopulation models have grown to include spatially explicit patch occupancy models as well as models where the population density on each patch is modelled explicitly (Amarasekare and Nisbet, 2001; Bani et al., 2019; Botsford et al., 1994; Gyllenberg and Hanski, 1997; Hanski and Thomas, 1994; Kritzer and Sale, 2004; Marculis and Hastings, 2021). Modelling connected subpopulations under the metapopulation framework has been successful in capturing the dynamics that occur in both terrestrial and marine systems (Hanski, 1999; Kritzer and Sale, 2006; Ovaskainen and Saastamoinen, 2018; Watson et al., 2012).

In most marine metapopulations, the dispersal between habitat patches occurs in a pelagic larval stage and the remaining life stages are confined to the habitat patch on which the larvae settle (Cowen and Sponaugle, 2009; White et al., 2019). Once thought to be open subpopulations with continuous exchanges of larvae, it is now recognized that most adult subpopulations depend directly on the degree of larval exchange between habitat patches (Cowen et al., 2000; Cowen and Sponaugle, 2009; White et al., 2019). Research into larval dispersal in marine metapopulations has led to a greater understanding of the population dynamics of many marine species including Dungeness crab, sea urchins, barnacles, corals and coral reef fish, sea turtles, mussels and many benthic marine species (Botsford et al., 1994; Carson et al., 2011; Cowen and Sponaugle, 2009; Jones et al., 2009; Mayorga-Adame et al., 2017; Robson

et al., 2017; Roughgarden et al., 1988; White et al., 2019). In marine systems the metapopulation concept has also been used in the planning of Marine Protected Areas and the citing of marine reserves (Bode et al., 2006; Botsford et al., 2009; Burgess et al., 2014; Costello et al., 2010; Crowder et al., 2000; Figueira, 2009; Fox et al., 2016; Kritzer and Sale, 2006; Watson et al., 2011).

While most of this thesis is primarily focused on marine metapopulations, many of the analyses apply more broadly to a class of biological metapopulation models where dispersal occurs in the first life stage. These are a subset of birth-jump processes (Hillen et al., 2015) and include all of the marine populations listed above, but also include many plant species where seeds are carried between suitable habitat patches (Husband and Barrett, 1996) and insect species where there is a large dispersal event, such as the spruce budworm (Williams and Liebhold, 2000) and mountain pine beetle (Safranyik and Carroll, 2007).

1.1.1 Sea lice on salmon farms

As mentioned at the start of the introduction, a specific birth-jump metapopulation on which much of this thesis is focused is sea louse populations on salmon farms. In high densities sea lice can lead to additional morbidity and mortality of adult salmon (Pike and Wadsworth, 1999), and lesions and stress from sea louse infestation make adult salmon susceptible to secondary infections, all of which have led to large economic consequences for salmon farms (Costello, 2009b). At one point sea lice have been estimated to cost the global aquaculture industry 6% of its product value a year (Costello, 2009a), and cost the Norwegian salmon farming industry $436 million USD a year (Abolofia et al., 2017). For wild juvenile salmon infestation with sea lice can lead to physiological and behavioural effects (Brauner et al., 2012; Godwin et al., 2015; Godwin et al., 2017; Krkošek et al., 2011a) and high infestation can result in mortality (Krkošek et al., 2007).

Due to the economic and environmental consequences of sea lice on salmon farms, sea lice are a well studied species. Since the 1990s there has been a growing body of literature on the effect of temperature and salinity on the development time and survival of sea lice through their life stages (Aldrin et al., 2017; Connors et al., 2008; Groner et al., 2014; Johnson and Albright, 1991; Samsing et al., 2016; Skern-Mauritzen et al., 2020; Stien et al., 2005; Stige et al., 2021). Higher temperatures lead to faster development and higher salinities lead to increased survival, though the estimates of development time and survival vary between studies. In the last decade there has also been a growing body of literature quantifying the dispersal

of sea lice away from salmon farms. Some of the work is statistical, relying on sea lice population counts on salmon farms to infer seaway distance dispersal kernels (Aldrin et al., 2017; Aldrin et al., 2013; Kristoffersen et al., 2013) but much of the work on dispersal comes from coupling large scale computational ocean circulation models to particle tracking simulations in order to estimate the trajectories of sea lice larvae subject to realistic ocean currents (Adams et al., 2012; Adams et al., 2015; Cantrell et al., 2021; Cantrell et al., 2018; Kragesteen et al., 2018; Samsing et al., 2017; Samsing et al., 2019; Sandvik et al., 2021; Sandvik et al., 2020; Stucchi et al., 2011). The development of realistic larval dispersal models, coupled with well studied maturation and survival functions, make sea lice on salmon farms an ideal system to study in the metapopulation framework.

1.2 Key concepts and mathematical frameworks

There are several key concepts and mathematical frameworks which I use in this thesis to answer the questions posed at the start of the introduction.

1.2.1 Next-generation matrices

One of the primary mathematical frameworks that I use throughout this thesis is the next-generation matrix. Next-generation matrices were originally popularized in epidemiology as a simple method to calculate the basic reproduction number, R_0, in compartmental disease models (Diekmann et al., 1990; Diekmann et al., 2010; van den Driessche and Watmough, 2002) to determine whether an epidemic will occur in a susceptible population. In epidemiological models, the entries of the next-generation matrix give the number of new infections produced in compartment i from an initial infection in compartment j over one generation, and thus the next-generation matrix maps the current infections in each stage to the new number of infections produced after one generation. In ecological models, the next-generation matrix can be used to track the number of new individuals produced in a compartment, rather than the number of new infections. This is especially useful in metapopulation models to track the number of new individuals produced on each habitat patch from an initial individual on a specific habitat patch. As I show in Chapter 2 and Chapter 4, the next-generation matrix can be calculated for metapopulation models formulated in discrete time, continuous time, and continuous time and continuous age, in each case distilling the processes of maturation, survival, and dispersal between patches into a single matrix. In heterogeneous aquatic populations, next-operators have been

used to calculate both the source-sink distribution and persistence of the population (Huang et al., 2016; Huang and Lewis, 2015; Krkošek and Lewis, 2010; Mckenzie et al., 2012a).

1.2.2 Sources and sinks

In the metapopulation framework habitat patches are often classified into sources or sinks based on how the subpopulations on local habitat patches are estimated to contribute to the metapopulation (Bode et al., 2006; Crowder et al., 2000; Figueira, 2009; Figueira and Crowder, 2006; Pulliam, 1988; Runge et al., 2006; Theuerkauf et al., 2021). This was first formalized in work by Pulliam (1988) who defined source patches as habitat patches on which the local population has a positive growth rate at low densities in the absence of dispersal, and sink patches as habitat patches on which the local population has a negative growth rate. However, in marine metapopulations dispersal can play a large role in the effect of a specific habitat patch on the metapopulation due to the large scale over which larvae can disperse. Recognizing the limitations of the definition of source and sink patches in the absence of dispersal, both Runge et al. (2006) and Figueira and Crowder (2006) created new classifications of source and sink patches which include both the productivity of the local population on a habitat patch (growth rate) and dispersal away from the habitat patch. Under these new classifications a habitat patch will be a source if an adult can produce more than one new adult over the entire metapopulation, and patch will be a sink if an adult cannot self-replace over the entire metapopulation. For a source patch, the adult does not need to produce more than one adult on that same habitat patch, but rather on all habitat patches together, and so patches can be defined as sources under this updated classification even if they were classified as sinks according to Pulliam (1988).

Habitat patches can also be classified into sources and sinks by measuring the contribution of an individual on one habitat patch to the entire metapopulation with the next-generation matrix. The entries of the next-generation for metapopulation models are the number of new individuals produced in patch i from an initial individual on patch j over a generation. Therefore the column sums give the total number of new individuals produced in the metapopulation from an initial individual on a given patch. If one individual on a patch produces more than one individual over the entire metapopulation, then the habitat patch can be classified as a source, otherwise habitat patch can be classified as a sink.

1.2.3 Metapopulation persistence

In marine metapopulations the scale of larval dispersal away from a local habitat often means that habitat patches that are defined as sources, due to their positive contribution over the entire metapopulation, cannot persist in isolation due to insufficient larval retention around any specific patch (White et al., 2019). Therefore preserving a persistent marine metapopulation and the establishment of successful marine protected areas or marine reserves may require more than preserving the source patches in a metapopulation. For a marine metapopulation to persist if no single patch can persist in isolation there must be sufficient larval exchange between closed loops of habitat patches such that an individual can produce more than one new individuals over all patches in the loop over several generations (Burgess et al., 2014; Hastings and Botsford, 2006). Sink patches may be part of this closed loop if they exchange sufficient larvae back to the source patches so on average over several generations an individual can self-replace over the loop. Determining if a metapopulation can persist can be difficult as it therefore requires estimating local demographic rates on habitat patches as well as quantifying the level of dispersal between habitat patches, but is necessary in designing Marine Protected Areas in which the protected habitat patches can persist even if the unprotected patches are exploited (Burgess et al., 2014; Carson et al., 2011; Dedrick et al., 2021; Garavelli et al., 2018; Puckett and Eggleston, 2016; Theuerkauf et al., 2021; White et al., 2010). In terms of the next-generation matrix for metapopulation models, persistence can be evaluated using the basic reproduction number, R_0, calculated as the spectral radius of the next-generation matrix. The basic reproduction number, R_0, can be interpreted as the number of new individuals produced by one average individual, and thus if $R_0 > 1$, the metapopulation will persist.

1.2.4 Transient dynamics

Transient dynamics can often be very different than the long term dynamics of ecological systems (Caswell and Neubert, 2005; Hastings, 2001; Hastings, 2004; Hastings et al., 2018; Hastings et al., 2021; Hastings and Higgins, 1994; Lloyd and May, 1996; Lutscher and Wang, 2020; Mari et al., 2019; Mari et al., 2017; Morozov et al., 2020; Neubert et al., 2002; Neubert et al., 2004; Wang et al., 2019). These transient dynamics can sometimes be long-lived and difficult to differentiate from the asymptotic dynamics over intervals in which they are measured in ecological systems, or they can be relatively short-lived. In patch occupancy metapopulation models, the length of transients has been shown to be determined by both local population dynamics and

connectivity of the landscape (Ovaskainen and Hanski, 2002). In marine metapopulations where dispersal is asymmetrical, a small amount of stochasticity can even lead to continued transient growth, so that the metapopulation can persist with stochastic perturbations even if it would go extinct without them (Aiken and Navarrete, 2011).

To investigate the transient dynamics that can occur in birth-jump metapopulations we use three metrics which quantify the degree of transient growth or decay that can occur following the perturbation of an equilibrium. Reactivity, initially introduced by Neubert and Caswell (1997), is the maximum possible growth rate of a system over all possible perturbations to an equilibrium. If the maximum growth rate is positive, then equilibrium is said to be reactive and there is a solution that will initially grow even if it eventually decays. Along with reactivity Neubert and Caswell (1997) also defined the amplification envelope, which measures the how large solutions can grow over time following initial perturbations. In contrast, attenuation, defined by Townley and Hodgson (2008), is the minimum initial growth rate of a system over all possible perturbations to an equilibrium. If the minimum growth rate is negative then the equilibrium attenuates, and thus there is a solution which initially decays even if it eventually grows. Reactivity and attenuation are most interesting when they are different from the long-term stability of a system: when an equilibrium is reactive but stable so that certain solutions initially grow but eventually decay, or when an equilibrium attenuates but is unstable so that certain solutions initially decay but eventually grow. It is in these situations which reactivity and attenuation have been extensively studied (Caswell and Neubert, 2005; Lutscher and Wang, 2020; Mari et al., 2017; Neubert and Caswell, 1997; Stott et al., 2011; Townley and Hodgson, 2008; Verdy and Caswell, 2008) and on which we focus in birth-jump metapopulations in Chapter 3 of this thesis. In the context of sea lice of salmon farms, we demonstrate that if salmon farm populations are located along the side of a channel, then the system can be reactive and the introduction of small amount of sea lice on the first farm can lead to large transient growth and cause outbreaks on downstream farms.

1.2.5 First passage time

For sea lice to successfully disperse between salmon farms they must both arrive in the vicinity of the second farm and be infectious at the time of arrival. If salmon farms are too close together they could be swept by before they become infectious and if they are too far away then sea lice may not survive to arrive in the vicinity of the second farm. The cross-infection between farms thus relies heavily on the time is takes for sea lice to disperse between farms, and to investigate this process we use

theory from first passage time.

The first passage time of an individual or a particle is defined as the time at which they first pass by or arrive at given location (Berg, 1983; Redner, 2001). First passage time models are common in physics but were first introduced in an ecological context by Berg (1983). Since their introduction they have been used to understand the effect of the landscape on animal movement and the time required for animals to locate prey (Kurella et al., 2015; McKenzie et al., 2009; Mckenzie et al., 2012b). Empirically calculated first passage times have been used to measure the habitat use of an animal by measuring the time that it takes for the animal to leave a circle of a given radius (Fauchald and Tveraa, 2003; Le Corre et al., 2014; Webber et al., 2020). When modeling the first passage time of a group of individuals or particles, different individuals may first arrive at the point of interest at different times, and so to model the first passage time of any random individual it is useful to calculate a distribution of first passage times. From this distribution, the mean first passage time of a random individual can be calculated, as well as the variance of first passage times among individuals and the overall probability that the individual arrives at any point in time. Sea lice dispersing between and successfully arriving onto salmon farms can be modelled as a first-passage time process, and in Chapter 5 of this thesis I build on first passage time methods to calculate the arrival time distribution of sea lice arriving on one salmon farm after leaving another farm.

1.3 Thesis overview

Each chapter of this thesis is generally focused on marine metapopulations, and some are specifically focused on sea lice populations on salmon farms in the Broughton Archipelago, as detailed at the start of the introduction. Chapters 2 through 5 are meant to be understood independently of each other, as they have either been published, are accepted for publication, or soon to be submitted for publication. As detailed in the preface, Chapter 2 has been published in the *Bulletin of Mathematical Biology*, Chapter 3 has been accepted in the *SIAM Journal on Applied Dynamical Systems*, and Chapters 4 and 5 are soon to be submitted to journals for publication. Below I detail the contents of each chapter, including how I will answer the questions posed at the start of the introduction.

In Chapter 2 I construct a next-generation matrix for a marine metapopulation model using age dependent maturation and survival functions and demonstrate how it can be used to calculate source and sink habitat patches, as well as metapopulation persistence. I investigate the effect of environmental variables on the contribution of

habitat patches in a simplified system of sea lice on salmon farms in a channel and show how the next-generation matrix can provide useful biological insight into the transient and asymptotic dynamics of the metapopulation.

In Chapter 3 I analyse the transient dynamics that can arise in marine and other birth-jump metapopulations. I provide simple examples of metapopulations where the transient dynamics are very different than the asymptotic dynamics and show how the choice of norm affects the calculations of reactivity and attenuation in metapopulations. I then connect reactivity and attenuation to the source-sink classification of habitat patches and demonstrate how to meaningfully measure reactivity when metapopulations are stage-structured, with a focus on marine metapopulations.

In Chapter 4 I demonstrate how to use the next-generation matrix to calculate the contribution of local habitat patches to marine metapopulations and evaluate metapopulation persistence under a variety of modeling frameworks. I calculate a specific next-generation matrix for sea lice populations on salmon farms in the Broughton Archipelago to identify which salmon farms are the largest sources of sea lice in this region, evaluate the effect of the current farm removals, and investigate the effect of environmental variables on metapopulation growth.

In Chapter 5 I develop a simple, mechanistic, advection-diffusion model for the arrival time distribution of sea lice dispersing between two different salmon farms, building on the theory of first passage times. I use the arrival time distribution to calculate the level of cross-infection between salmon farms, given by the probability that a sea louse leaving one farm eventually arrives onto the other farm. I then calculate the arrival time directly for two farms in the Broughton Archipelago using numerical flows from a hydrodynamic model, coupled with a particle tracking model, to fit the simple mechanistic model and find realistic parameter estimates. I then use the parameterized mechanistic model to investigate the effect of environmental variables and farm placement on the cross infection between farms.

In Chapter 6 I discuss the significance of the results of this thesis, their limitations, their implications for management, the potential for future work, and situate the thesis within the broader literature of sea lice on salmon farms and marine metapopulations.

Chapter 2

A next-generation approach to calculate source-sink dynamics in marine metapopulations

2.1 Introduction

Source-sink theory was developed to better understand population dynamics in connected populations. Originating from work by Levins (1969) using metapopulation models, source-sink theory attempts to explain how certain population patches in poor environments can be sustained by population patches in more favourable environments. Population patches in poor environments are labelled 'sinks', because these populations could not be sustained in the absence of dispersal. 'Sources' are then population patches that can sustain themselves in the absence of dispersal. Levins used metapopulation models to study source-sink dynamics, with patch occupancy as the state variable. These models as well as other types of related models have greatly contributed to the rich body of work on source-sink theory (Amarasekare and Nisbet, 2001; Figueira and Crowder, 2006; Hanski, 1998; Pulliam, 1988).

Critical to the theory of source-sink dynamics is the concept of dispersal. Dispersal is the mechanism by which source populations can rescue sink populations from extinction. Some theoretical models have modelled dispersal implicitly, and have investigated how dispersal rates can change the source-sink dynamics of a population (Gyllenberg and Hanski, 1997). Others have modelled dispersal explicitly (Hastings, 1982), which is important when the rates or mechanisms of dispersal are understood. The rates and mechanisms of dispersal also differ largely between terrestrial and marine systems. In terrestrial systems, it is often adults that are capable of dispersing between population patches. In many marine systems, adults are confined to habitat patches, and dispersal occurs through the release of pelagic larvae, which spread

through the ocean to other patches (Cowen and Sponaugle, 2009).

For marine species, modelling dispersal explicitly has led to advancements in understanding the degree of connectivity between different marine subpopulations (Figueira and Crowder, 2006). While there is evidence that some larval populations are well mixed in an ocean environment (Cowen et al., 2000), both theoretical advection-diffusion models for larval movement between patches (Alexander and Roughgarden, 1996; Botsford et al., 1994) and computational hydrodynamic models (Cowen and Sponaugle, 2009; Watson et al., 2012), have been successful at reproducing patterns of connectivity observed in marine systems. While hydrodynamic models are very useful in understanding connectivity in the specific systems for which they are parameterized, advection-diffusion models can be applied more generally to give insights into the connectivity of subpopulations. In either framework, modelling dispersal explicitly can illuminate the level of connectivity between marine subpopulations of several species.

Corals and coral reef fish (Cowen et al., 2006; Jones et al., 2009), barnacles (Roughgarden et al., 1988), Dungeness crabs (Botsford et al., 1994), sea urchins (Botsford et al., 1994), and many benthic marine species (Cowen and Sponaugle, 2009) have relatively sedentary adult stages that are confined to habitat patches, with larvae that disperse between patches. In fact, it is estimated that up to 70% of benthic invertebrates have a pelagic larval phase, capable of dispersal (Mileikovsky, 1971). Adult subpopulations for these meroplanktonic species, species with a planktonic larval stage, then act as connected metapopulations which are connected through larval dispersal (Botsford et al., 1994). For these marine metapopulations, local environmental conditions determine survival and productivity of adult population patches, and regional environmental conditions determine the degree of pelagic larval dispersal, as environmental conditions between patches affect the growth and survival of larvae. Both local and regional environmental conditions will then affect the source-sink distribution of the different marine habitat patches. Accurately modelling the source-sink distribution of marine metapopulations is especially important when this information is used to design conservation management actions, such as marine protected areas. When creating marine protected areas, determining the level of dispersal between population patches, as well as the productivity of local patches is critical. Protecting productive source patches which are capable of dispersing to sink patches may be essential in sustaining the connected metapopulations (Planes et al., 2009).

However, for certain parasitic or invasive marine species, we may be interested in controlling the spread of the species, rather than conserving the existing population. One such species of importance on which we focus specifically in our application

section is *Lepeoptheirus salmonis*, also known as sea lice. Sea lice are a marine ectoparasite that feed on the epidermal tissues of salmon (Costello, 2006). When sea lice are present in high densities their salmonid hosts can experience additional morbidity and mortality (Costello, 2006; Krkošek et al., 2011b), as well reduced foraging ability (Godwin et al., 2017). Salmon farms in coastal ecosystems present stationary hosts for sea lice, on which sea lice can survive year round (Rogers et al., 2013). Sea lice are a large economic issue facing salmon farms worldwide, and have previously cost the global aquaculture industry 6% of its product value a year (Costello, 2009b). These farms act as population patches on which sea lice can grow until maturity. Adult females exude egg strings and release larvae which can spread between salmon farms via coastal currents and ocean mixing. This larval dispersal between farms can connect sea lice populations on different farms within a specific region (Aldrin et al., 2017). The larval dispersal also transmits sea lice between farmed salmon and wild salmon migrating past farms (Krkošek et al., 2006a), and has been shown to lead to population declines in Pacific pink salmon populations (Krkošek et al., 2007). To protect both farmed and wild salmon populations from the effects of sea lice, salmon farms now use a variety of treatment measures to reduce sea lice levels when populations outbreak (Aaen et al., 2015). However, in many regions sea lice have developed resistance to some of the most effective chemical treatments (Aaen et al., 2015), and even in regions without resistance sea lice continue to pose a threat to wild salmon (Bateman et al., 2016). Due to the economic and ecological importance of controlling sea lice on salmon farms, we use salmon farms as an example to study the source-sink distribution of habitat patches under different environmental conditions, as well as the effect of treatment.

To study source-sink distributions in sea lice and other meroplanktonic marine populations on habitat patches we use a next generation approach. Next generation operators have a rich history in epidemiology (Diekmann et al., 1990; Diekmann et al., 2010; van den Driessche and Watmough, 2002), and are often used to determine whether an infectious epidemic will occur in a population, by calculating the basic reproduction number, R_0. Recently, next generation operators have been used to analyse heterogeneous aquatic populations (Huang et al., 2016; Huang and Lewis, 2015; Krkošek and Lewis, 2010; Mckenzie et al., 2012a). The next-generation operator can be used to map the current number of individuals at each life stage in a heterogeneous environment to the new number of individuals at each life stage after one generation. If populations exist in discrete patches, then this next generation operator can be formulated as a next generation matrix. The next generation approach distills the complex process of dispersal between patches and stage-structured

survival and growth on a patch into a single operator. In ecological systems, the next generation operator has been used to determine population persistence, but has also been used to determine the source-sink distribution of a population (Huang et al., 2016; Krkošek and Lewis, 2010; Mckenzie et al., 2012a).

Specifically, new measures of persistence, $R_\delta(x)$, $R_{\text{loc}}(x)$, R_u and R_l have been defined using next generation operators. $R_{\text{loc}}(x)$ is the number of new individuals produced at location x in the absence of dispersal, and thus can be used to measure the fundamental niche of a population (Huang et al., 2016). $R_\delta(x)$ is the number of new individuals produced over the entire population from one individual starting at spatial position x (Huang et al., 2016). It takes into account both growth and survival at location x, and dispersal from location x. If one individual at x produces less than one individual over the entire landscape, then $R_\delta(x) < 1$, and the location x is defined as a sink. If $R_\delta(x) > 1$, then x is defined as a source. Pulliam (1988) originally defined a source habitat as a habitat that can sustain itself in isolation, and a sink habitat as one that cannot sustain itself in isolation, assuming low poulation density. However, this definition can give rise to connected patches of sink habitats that persist (Armsworth, 2002). A benefit of the $R_\delta(x)$ measure, is that it does not allow for connected patches of sinks to persist. Lastly, R_u and R_l are then defined as the maximum and minimum R_δ taken over all possible locations, respectively, and are shown to be the intergenerational growth rate under the best and worst possible initial conditions (Huang and Lewis, 2015). They can therefore be useful in determining bounds for intergenerational growth, as well as R_0.

Another method of measuring the contribution that each patch provides to the total population is to look at the contribution of each patch to R_0 (Hurford et al., 2010). This approach uses the left and right eigenvectors associated with R_0 to determine the contribution of each patch if the population were distributed according the right eigenvector. In the application section we build on and apply all of these persistence measures and next generation theory to determine the source-sink distribution on the discrete population patches in our system under different environmental conditions.

The final concept in this chapter borrowed from epidemiology is the type reproduction number (Heesterbeek and Roberts, 2007; Lewis et al., 2019; Roberts and Heesterbeek, 2003). The type reproduction number is a measure of the control effort needed when control is targeted at a certain type of individual in a heterogeneous population. For patch models, this is often the control effort required on a certain patch so that the total population cannot grow. Type reproduction numbers need not only be used to determine control, they can also determine the amount of enhancement effort required on a patch so that the entire population will grow. We

use the concept of type reproduction number in the application section to determine the treatment level required for sea lice on a salmon farm so that the entire sea lice population is controlled.

In this chapter we use a next generation approach to quantify the source-sink distribution of marine meroplanktonic populations where subpopulations are confined to local habitat patches and are connected via larval dispersal. First we present a stage-structured model for a general marine population, composed of several sessile stages which survive and reproduce on a population patch. The final adult sessile stage gives birth to planktonic larvae, which disperse between patches. The dispersal of larvae is modelled explicitly by approximating hydrodynamic ocean movement using the Fokker-Plank equation. Next, we construct a next generation matrix for this model, and prove that the spectral radius of the next generation matrix determines whether or not the species can persist. Lastly we apply different persistence measures to sea lice populations on salmon farms, to answer several key questions around the source-sink dynamics of sea lice on salmon farms:

1. What is the source-sink distribution of salmon farms in a channel?
2. How does the source-sink distribution change with respect to environmental variables?
3. Are there certain parameter regions in which local outbreaks can occur, but not global outbreaks?
4. What is the effect of treating a single salmon farm for sea lice control on the transient and asymptotic dynamics?
5. What is the effect of an environmental gradient on patch contributions to R_0 and the source-sink distribution?

2.2 The stage-structured patch model

To study the source-sink distribution of a marine metapopulation we consider a marine species with m life stages that is spreading between n spatial patches. We are interested in identifying which habitat patches are acting as sources and which are acting as sinks. Our focus is populations at low densities, typically near the extinction equilibrium. Determining the source-sink distribution can also uncover transient dynamics that may be substantially different than the long term asymptotic dynamics of the population. To investigate the source-sink distribution, we construct a next

generation matrix for our model, and we show in a later section on applications (section 3.5) how to use the column sums of the next generation matrix to determine the source-sink distribution.

We are interested in modelling a marine meroplanktonic species where the larval (first) stage is the only stage capable of dispersing between population patches. The remaining juvenile and adult stages are confined to a single population patch. We call these stages confined to a patch sessile stages, though in reality they could be motile but restricted to the habitat patch; such is the case for sea lice or reef fish. We assume that the last adult stage is the only stage capable of reproduction. This is the case for sea lice, on which we focus specifically in the applications section, but is also the case for other marine species mentioned in the introduction, depending on how stages are grouped. During the larval stage, we assume there is a latent period during which the newly released larva cannot attach to a new patch. Here we define larvae not capable of attaching to a new patch as latent, and larvae capable of attaching to a new patch as active. Larvae are therefore first released from a patch as latent larvae, and then mature into active larvae, at which time they are capable of attaching to a new patch. Some marine species have larval stages that are active directly after release (Mileikovsky, 1971), and so for these species we can ignore the latent larval stage.

In both larval and sessile stages an individual will either die or mature to the next stage, with the exception of the last sessile stage where individuals give birth instead of maturing. We choose to model the number of individuals in each stage using density equations, so that we are tracking the density of individuals in a given stage that have spent a time units in the stage at time t. Modelling the population using density equations allows for the probability of survival in a stage, as well as the probability of maturing to the next stage, to depend on a, the amount of time already spent in the stage. When modelling populations using ordinary differential equations (ODEs), it is assumed that stage durations are always exponentially distributed (Feng et al., 2007). However, this assumption is oversimplistic for many marine populations including sea lice.

While modelling using density equations allows for more generality in the survival and maturation of an individual, it is more difficult to include density dependence in this framework. However, source and sink populations are typically categorized in the context of low population densities, especially when calculated through a next generation operator (Krkošek and Lewis, 2010), and thus we do not expect density dependence to play a crucial role in the context of source-sink dynamics for the problems considered. Our metapopulation model will therefore ignore the density

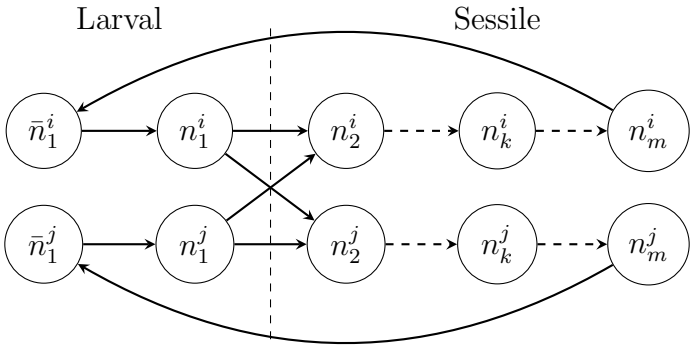

Figure 2.1: The structure of the life cycle graph for a marine species with m stages on two patches. The top row shows the stages associated with patch i and the bottom row shows the stages associated with patch j. The larval stages on the left have just left their respective patches, and the recruitment onto a patch occurs as the larval stage n_1 arrives on a patch as a sessile individual in stage n_2.

dependent effects that could influence survival and maturation at both high and low densities. This model is then most useful for investigating the impact of connectivity among habitat patches at low population densities, in populations where habitat patches are not resource limited, or where populations are artificially managed to remain at low densities. It is in this context of negligible density dependence that we ask the five questions given at the end of the introduction.

2.2.1 Derivation of the stage-structured patch population model

In this section we derive a system of density equations that model the change in population density on each habitat patch in our connected metapopulation. The general structure of the model, consisting of sessile stages confined to a habitat patch connected by larval dispersal can be seen from the life cycle graph for two subpopulations (Figure 5.1). To mathematically describe our model, we first give the general structure for the density of sessile individuals in stage k on patch i.

Let $n_k^i(t,a)$ be the density of individuals with stage-age a at time t, in stage k on patch i. Then

$$n_k^i(t,a) = \begin{cases} B_k^i(t-a)S_k^i(a)M_k^i(a) & t > a \\ n_{k,0}^i(a-t)\frac{S_k^i(a)M_k^i(a)}{S_k^i(a-t)M_k^i(a-t)} & 0 < t < a \\ n_{k,0}^i(a) & t = 0 \end{cases} \tag{2.1}$$

for $k = 2, \ldots, m-1$. Here $B_k^i(t)$ is the rate at which individuals are entering stage k on patch i at time t, $S_k^i(a)$ is the probability that an individual survives longer than a

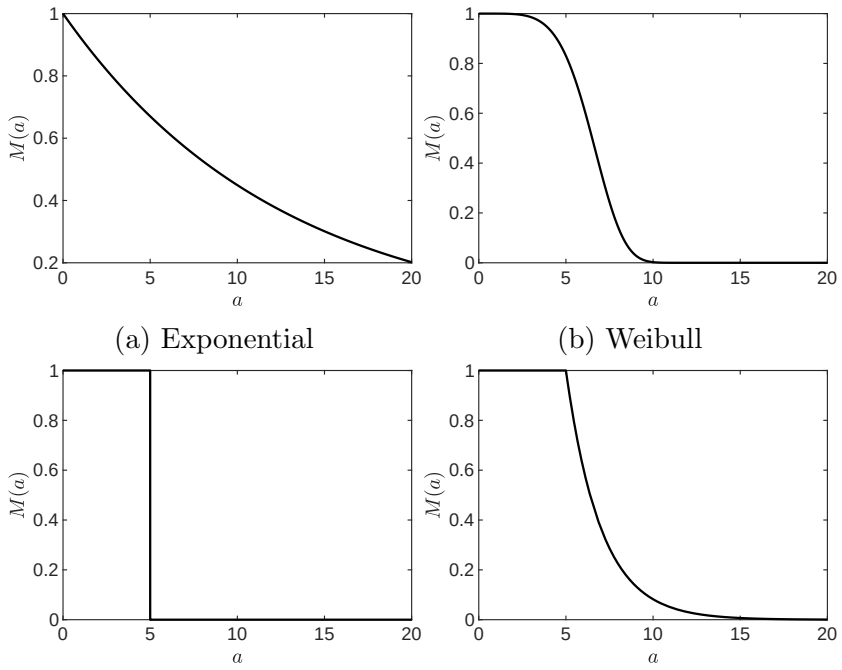

(a) Exponential

(b) Weibull

(c) Step function

(d) Step function and exponential

Figure 2.2: A selection of $M_k^i(a)$ functions that have been used in sea lice population models. When a constant maturation rate is assumed, as in Krkošek et al. (2012a), $M_k^i(a)$ is represented as an exponential function, shown in a). b) The Weibull survival function was used by Aldrin et al. (2017) to avoid strict minimum development times, and constant maturation rates. c) The step function was used by Revie et al. (2005), where it is assumed that all sea lice in a stage mature at the same time. d) A combination of a step function and exponential function was used by Stien et al. (2005), where the step function is used to enforce a minimum development time, after which the exponential is used to capture a constant maturation rate.

time units in a stage, given that they have not yet matured, $M_k^i(a)$ is the probability that an individual takes longer than a time units to mature to the next stage, given that they have survived, and $n_{k,0}^i(a)$ is the initial density of individuals with age a. We assume that both $S_k^i(a)$ and $M_k^i(a)$ are non-negative and non-increasing functions, with $S_k^i(0) = M_k^i(0) = 1$, and that $S_k^i(a)$ and $M_k^i(a)$ are L^1 functions, so $\int_0^\infty S_k^i(a)da < \infty$ and $\int_0^\infty M_k^i(a)da < \infty$. We also assume that survival and maturation in a given stage are independent. A selection of $M_k^i(a)$ functions that have been used for sea lice models are shown in Figure 2.2.

Individuals with stage age $a > t$ must have entered the stage at time $t - a$, with rate $B_k^i(t - a)$, and then survived until stage age a with probability $S_k^i(a)M_k^i(a)$; the density of these individuals is given by the first line of Equation 4.5. If individuals have stage age $a < t$, then they were already in the stage at $t = 0$, with density

$n^i_{k,0}(a-t)$, and the probability that they survive to stage age a, given that they were present at stage age $a-t$, is $S^i_k(a)M^i_k(a)/S^i_k(a-t)M^i_k(a-t)$; the density of these individuals is given by the second line of Equation 4.5. This formula for $n^i_k(t,a)$ is also the solution to the McKendrick-von Foerster partial differential equation (Keyfitz and Keyfitz, 1997; McKendrick, 1925):

$$\begin{aligned}\frac{\partial n^i_k(t,a)}{\partial t}+\frac{\partial n^i_k(t,a)}{\partial a} &= -\mu^i_k(a)n^i_k(t,a)\\ n^i_k(t,0) &= B^i_k(t)\\ n^i_k(0,a) &= n^i_{k,0}(a)\\ \mu^i_k(a) &= -\frac{(M^i_k(a)S^i_k(a))'}{M^i_k(a)S^i_k(a)},\end{aligned}$$

which can be found by integrating along the characteristic curves, as shown in Appendix 2.6.1.

The larval (first) stage, which is capable of spreading between patches, includes both a latent and active stage. During the latent larval stage, individuals spread away from a patch, but are not capable of attaching to another patch. They then enter the active stage, where they are capable of attaching to another patch. To distinguish between the two stages, let $\bar{n}^i_1(t,a)$ be the density of latent larvae released from patch i with stage age a, and $n^i_1(t,a)$ be the density of active larvae. Let $\bar{S}^i_1(a)$ be the survival function for the latent stage, and let $M^i_1(a)$ the maturation function for the larval stage, so that $M^i_1(a)$ is the probability that a latent larva has not yet matured into an active larva, given it has survived.

During the active stage, instead of maturing, active larvae will be removed from this stage when they arrive on another patch. Let $f^{ij}(a)$ be the arrival time density function for an active larva spreading from patch j to patch i, where $\int_{a_1}^{a_2} f^{ij}(a)da$ is the probability that the active larva arrives on patch i between stage age a_1 and a_2. Let $F^{ij}(a)=\int_0^a f^{ij}(\tau)d\tau$, then $1-F^{ij}(a)$ is the probability that the larva has not yet arrived on a patch i by stage age a, given that it has not died. The physical process underlying the arrival time density function is shown in detail in Section 2.2.4, and a typical $f^{ij}(a)$ is shown in Figure 2.3. In Section 2.2.4, we also show that if we define $f^j(a)$ as the arrival time density for an active larvae leaving patch j to arrive on any patch, then $f^j(a)=\sum_{i=1}^n f^{ij}(a)$, and $F^j(a)=\sum_{i=1}^n F^{ij}(a)$.

Let $S^i_1(a)$ be the survival function for the active larvae leaving patch i. The density

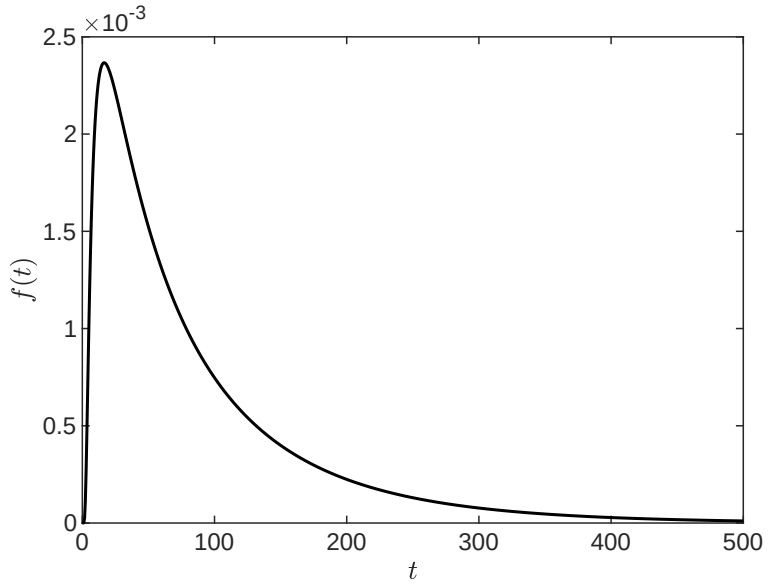

Figure 2.3: The arrival time density, $f^{ij}(t)$, as a function of time, t, for larvae leaving patch j and arriving on patch i. Movement from patch j to patch i is described in section 2.2.4. Here patch j was located at $x = 0$, patch i at $x = 15$, with additional parameters $v = 1$, $D = 5$, $\alpha = 0.1$, $\Delta = 0.8$. A 1 dimensional domain was used, with no other patches present.

of latent larvae in stage $k = 1$ leaving patch i is:

$$\bar{n}_1^i(t,a) = \begin{cases} \bar{B}_1^i(t-a)\bar{S}_1^i(a)M_1^i(a) & t > a \\ \bar{n}_{1,0}^i(a-t)\frac{\bar{S}_1^i(a)M_1^i(a)}{\bar{S}_1^i(a-t)M_1^i(a-t)} & 0 < t < a \\ \bar{n}_{1,0}^i(a) & t = 0 \end{cases},$$

and the density of active larvae is:

$$n_1^i(t,a) = \begin{cases} B_1^i(t-a)S_1^i(a)(1-F^i(a)) & t > a \\ n_{1,0}^i(a-t)\frac{S_1^i(a)(1-F^i(a))}{S_1^i(a-t)(1-F^i(a-t))} & 0 < t < a \\ n_{1,0}^i(a) & t = 0 \end{cases}.$$

The last sessile adult stage also requires a different density equation from rest of the sessile stages, for during this stage individuals cannot mature any longer, they can only survive. For $k = m$ the density of individuals on a patch i is:

$$n_m^i(t,a) = \begin{cases} B_m^i(t-a)S_m^i(a) & t > a \\ n_{m,0}^i(a-t)\frac{S_m^i(a)}{S_m^j(a-t)} & 0 < t < a \\ n_{m,0}^i(a) & t = 0 \end{cases}.$$

To complete our model we need to define $B_k^i(t)$, which is the rate that individuals enter each stage. For stages $3, \ldots, m$, $B_k^i(t)$ will be the rate at which individuals from stage $i-1$ are maturing to stage i:

$$B_k^i(t) = \int_0^\infty n_{k-1}^i(t,a) m_{k-1}^i(a) da,$$

where $m_k^i(a) = -M_k^{i\prime}(a)/M_k^i(a)$ is the instantaneous maturation rate for individuals in stage k with stage age a. Multiplying the current density by $m_k^i(a)$ and integrating across all stage ages gives the total density of individuals maturing at time t.

Individuals in the last stage give birth to latent larvae in the first stage. Let $b^i(a)$ be the stage age dependent birth rate in patch i, then $\bar{B}_1^i(t)$ is given by:

$$\bar{B}_1^i(t) = \int_0^\infty n_m^i(t,a) b^i(a) da.$$

The latent larvae then mature into active larvae in the first stage with rate:

$$B_1^i(t) = \int_0^\infty \bar{n}_1^i(t,a) m_1^i(a) da.$$

Individuals enter the second stage on patch i by arriving as active larvae, which are spreading from all patches. The instantaneous rate that an active larva, travelling from patch j to patch i, arrives on patch i as a larva in the second stage, is $f^{ij}(a)/(1-F^j(a))$. Therefore we have

$$B_2^i(t) = \sum_{j=1}^n \int_0^\infty n_1^{ij}(t,a) f^{ij}(a)/(1-F^j(a)) da.$$

Combining all of these equations, the age density of individuals is

$$\bar{n}_1^i(t,a) = \begin{cases} \underbrace{\bar{B}_1^i(t-a)\bar{S}_1^i(a)M_1^i(a)}_{\text{entered at } t-a\text{, survived to } a} & t > a \\ \underbrace{\bar{n}_{1,0}^i(a-t)\dfrac{\bar{S}_1^i(a)M_1^i(a)}{\bar{S}_1^i(a-t)M_1^i(a-t)}}_{\text{present at a-t, survived to a}} & 0 < t < a \\ \underbrace{\bar{n}_{1,0}^i(a)}_{\text{initial density}} & t = 0 \end{cases} \qquad k = 1, \quad (2.2)$$

$$n_1^i(t,a) = \begin{cases} B_1^i(t-a)S_1^i(a)(1-F^i(a)) & t > a \\ n_{1,0}^i(a-t)\frac{S_1^{ij}(a)(1-F^i(a))}{\bar{S}_1^i(a-t)(1-F^i(a-t))} & 0 < t < a \\ n_{1,0}^i(a) & t = 0 \end{cases} \qquad k = 1,$$

$$n_k^i(t,a) = \begin{cases} B_k^i(t-a)S_k^i(a)M_k^i(a) & t > a \\ n_{k,0}^i(a-t)\frac{S_k^i(a)M_k^i(a)}{S_k^i(a-t)M_k^i(a-t)} & 0 < t < a \\ n_{k,0}^i(a) & t = 0 \end{cases} \qquad k = 2, \ldots, m-1,$$

$$n_m^i(t,a) = \begin{cases} B_m^i(t-a)S_m^i(a) & t > a \\ n_{m,0}^i(a-t)\frac{S_m^i(a)}{S_m^i(a-t)} & 0 < t < a \\ n_{m,0}^i(a) & t = 0 \end{cases} \qquad k = m,$$

$$\bar{B}_1^i(t) = \int_0^\infty n_m^i(t,a)b^i(a)da,$$

$$B_1^i(t) = \int_0^\infty \bar{n}_1^i(t,a)m_1^i(a)da,$$

$$B_2^i(t) = \sum_{j=1}^n \int_0^\infty n_1^j(t,a)f^{ij}(a)/(1-F^j(a))da,$$

$$B_k^i(t) = \textstyle\int_0^\infty n_{k-1}^i(t,a)m_{k-1}^i(a)da \qquad k = 3, \ldots, m,$$

These equations can also be expressed in an integral form, by substituting the equations for $n_k^i(t,a)$ into $B_k^i(t)$, and tracking the total number of parasites in each patch at each stage, $N_k^i(t) = \int_0^\infty n_k^i(t,a)da$. System 4.16 then becomes:

$$
\begin{aligned}
\bar{N}_1^i(t) &= \underbrace{\int_0^t \bar{B}_1^i(t-a)\bar{S}_1^i(a)M_1^i(a)da}_{\text{entered at } t-a\text{, survived to } a} + \underbrace{\int_t^\infty \bar{n}_{1,0}^i(a-t)\frac{\bar{S}_1^i(a)M_1^i(a)}{\bar{S}_1^i(a-t)M_1^i(a-t)}da}_{\text{present at a-t, survived to a}} \\
N_1^i(t) &= \int_0^t B_1^i(t-a)S_1^i(a)(1-F^i(a))da \\
&\quad + \int_t^\infty n_{1,0}^i(a-t)\frac{S_1^i(a)(1-F^i(a))}{S_1^i(a-t)(1-F^i(a-t))}da \\
N_k^i(t) &= \int_0^\infty B_k^i(t-a)S_k^i(a)M_k^i(a)da \\
&\quad + \int_t^\infty n_{k,0}^i(a-t)\frac{S_k^i(a)M_k^i(a)}{S_k^i(a-t)M_k^i(a-t)}da, \quad k=2,\ldots,m-1 \\
N_m^i(t) &= \int_0^t B_m^i(t-a)S_m^i(a)da + \int_t^\infty n_{m,0}^i(a-t)\frac{S_m^i(a)}{S_m^i(a-t)}da \\
\bar{B}_1^i(t) &= \int_0^t B_m^i(t-a)S_m^i(a)b^i(a)da + \int_t^\infty n_{m,0}^i(a-t)\frac{S_m^i(a)b^i(a)}{S_m^i(a-t)}da \qquad (2.3) \\
B_1^i(t) &= \int_0^t \bar{B}_1^i(t-a)\bar{S}_1^i M_1^i(a)m_1^i(a)da \\
&\quad + \int_t^\infty \bar{n}_{1,0}^i(a-t)\frac{\bar{S}_1^i(a)M_1^i(a)m_1^i(a)}{\bar{S}_1^i(a-t)M_1^i(a-t)}da \\
B_2^i(t) &= \sum_{j=1}^n \int_0^t B_1^j(t-a)S_1^j f^{ij}(a)da \\
&\quad + \sum_{j=1}^n \int_t^\infty n_{1,0}^{ij}(a-t)\frac{S_1^j(a)f^{ij}(a)}{S_1^j(a-t)(1-F^j(a-t))}da \\
B_k^i(t) &= \int_0^t B_{k-1}^i(t-a)S_{k-1}^i(a)M_{k-1}^i(a)m_{k-1}^i(a)da \\
&\quad + \int_t^\infty n_{k-1,0}^i(a-t)\frac{S_{k-1}^i(a)M_{k-1}^i(a)m_{k-1}^i(a)}{S_{k-1}^i(a-t)M_{k-1}^i(a-t)}da, \quad k=3,\ldots,m
\end{aligned}
$$

Here we have constructed an stage-structured model for a marine population with several sessile stages on local habitat patches connected by larval dispersal. We have formulated our model as both a system of age density equations (system 4.16), which we find most intuitive, as well as a system of integral equations (system 2.3).

2.2.2 Reduction to a system of ODEs

It is also possible to reduce Equation 4.16 to a system of ODEs under some strong assumptions. We do not believe that these assumptions are sufficiently realistic for benthic marine species with dispersing larvae. However, we include this reduction here

as an illustrative example of how Equation 4.16 can be connected to the more familiar ODE model structure. We start by assuming that time till maturation and time to death are both exponential waiting times. We also need to make this assumption for the arrival time. This arrival time distribution is no longer be directly solved through the more realistic advection diffusion equation (2.7), given in section 2.2.4 and shown in Figure 2.3. However, the new exponential rate could be an approximation by using the average arrival time generated by the advection diffusion equation.

Here we will use the lower case letter as the exponential rate associated with the survival or maturation function. For example, $M_k^i(a) = e^{-m_k^i a}$, and $S_k^i(a) = e^{-s_k^i a}$. For the arrival time, we now assume that there is a constant rate of arrival of larvae, f^{ij}, from a source patch j to a receiving patch i. We can then formulate $f^j(a)$, the distribution of arrival times for a larva leaving patch j to arrive on any other patch, as the exponential function $f^j(a) = \sum_{i=1}^n f^{ij} e^{-\sum_{i=1}^n f^{ij} a}$. By formulating the arrival times using constant rates, we lose the spatial structure of the system, so that patches are now only distinguished by their arrival time rates, f^{ij}.

To reduce the system of density equations to a system of ODEs, it is easiest to use the McKendrick-von Foerster formulation of the model (Appendix 2.6.1). We simply integrate the different versions of Equation 2.14 of equations over all ages, so $N_k^i(t) = \int_0^\infty n_k^i(t,a)da$. The resulting model is as follows:

$$
\begin{aligned}
\frac{d}{dt}\bar{N}_1^i(t) &= b^i N_m^i(t) - (\bar{s}_1^j + m_1^j)\bar{N}_1^j(t) && k = 1 \\
\frac{d}{dt}N_1^j(t) &= m_1^j \bar{N}_1^j - (s_1^j + \sum_{i=1}^n f^{ij})N_1^j(t) && k = 1 \\
\frac{d}{dt}N_2^i(t) &= \sum_{j=1}^n f^{ij} N_1^j(t) - (s_2^i + m_2^i)N_2^i(t) && k = 2 \\
\frac{d}{dt}N_k^i(t) &= m_{k-1}^i N_{k-1}^i(t) - (s_k^i + m_k^i)N_k^i(t) && k = 3, \ldots, m-1 \\
\frac{d}{dt}N_m^i(t) &= m_{m-1}^i N_{m-1}^i(t) - s_m^i N_m^i(t) && k = m
\end{aligned}
\tag{2.4}
$$

Here we have also assumed the birth rate of latent larvae on each patch is constant. The reduction of our full system of equations (4.16) to a system of ODEs results in the loss of the age structure present in our original model as well as stronger model assumptions. However, formulating the model as a system of ODEs allows for a more familiar comparison between our model and other population models.

2.2.3 The next generation matrix for the patch model

In this section we define the next generation matrix for our model. In the application section we show how this next generation matrix can be used to identify source and sink habitat patches, using the column sums of this matrix. We also show how the source-sink distribution can be used to determine transient dynamics in our model. Next generation matrices are often used to describe new infections in compartmental disease models (Diekmann et al., 1990; Diekmann et al., 2010; van den Driessche and Watmough, 2002), though here we use the next generation matrix to describe the growth and spread of marine organisms between patches. In the classic formulation of a next generation matrix, the (i, j) entry describes the number of new infections in the ith compartment produced by one new infection in the jth compartment. In our model, since we are tracking individuals and not infections, we need to define "new" individuals. We choose to define "new" individuals as those first entering a patch at stage $k = 2$. We choose $k = 2$ as the first stage because this is the first sessile stage where individuals arrive on a patch and can be counted.

In our model we have n patches and m stages so in total we have $n \times m$ compartments. However, the only new individuals are produced in stage $k = 2$. We could create a next generation matrix of size $nm \times nm$, but it would only have n non-zero rows, as there is only one stage on every patch where new individuals are produced. This next generation matrix is referred to the next generation matrix with large domain, K_L, by Diekmann et al. (2010). Instead we can group all stages together for a single patch, so that the (i, j) entries of our next generation matrix are the number of new individuals (stage $k = 2$) produced on patch i, from one new individual on patch j. This is referred to as the next generation matrix K by Diekmann et al. (2010), as we have removed all compartments which cannot have "new" individuals, and are only tracking the production of "new" individuals in compartments that start with "new" individuals. We will elaborate on the details of this process in section 2.3.1.

For our system (4.16), the (i, j) entry of the next generation matrix, K is

$$K(i,j) = \prod_{k=2}^{m-1} \left(\int_0^\infty S_2^j(t) M_2^j(t) m_2^j(t) dt \right) \left(\int_0^\infty S_m^j(t) b^j(t) dt \right) \left(\int_0^\infty \bar{S}_1^j(t) M_1^j(t) m_1^j(t) dt \right) \left(\int_0^\infty S_1^j(t) f^{ij}(t) dt \right). \quad (2.5)$$

In order to understand which patches may be acting as sources or sinks, we can look at the column sums of the different spatial patches. The sum of column j is the total number of new individuals (stage $k = 2$) produced on all patches from one new individual on patch j. If the sum of column j is larger than one, then each

new individual on patch j is producing more than one new individual on all patches. Therefore patch j is a source. Similarly if the sum of column j is less than one then patch j is a sink. We will expand on and formalize this quantification of source-sink dynamics in section 3.5.

The general structure of our model and next generation matrix allows it to be readily applied to a number of systems. However, in order to examine the effect of changing biological environments on the next generation matrix, it is useful to look at specific survival and maturation functions, $S_k^j(t)$ and $M_k^j(t)$, for each stage k, and on each patch j. Suppose we let $S_k^j(t)$ be the survival function associated with the exponential distribution: $S_k^j(t) = e^{-\mu_k^j t}$. This means that in each stage and on each patch the instantaneous death rate, μ_k^j is constant, and does not depend on the time spent in the stage. This is a common biological assumption, as mortality is often governed primarily the external environment and is often independent of age. For sea lice, this is assumed for most population models (Adams et al., 2015; Aldrin et al., 2017; Krkošek et al., 2006a; Revie et al., 2005).

Next, we consider a simplifying case where the maturation probability density function (p.d.f.), $-M_k^j(t)'$, is the gamma distribution. There are several reasons for this choice. First, the gamma distribution can be unimodal, and therefore biologically represents a situation in which the highest probability of maturing to the next stage is at some intermediate age. This is the case for sea lice, which have a minimum required development time before they can mature through a stage (Johnson and Albright, 1991). Second, the gamma distribution can reduce to the exponential distribution, and, in a limiting case, to the delta distribution. Exponential and delta maturation p.d.f.s have both been used to model sea lice (Krkošek et al., 2012a; Revie et al., 2005), and their maturation functions $M_k^j(t)$ are shown in Figure 2.2. When the gamma distribution is reduced to an exponential distribution, our system of density equations (4.16) can be reduced to an ODE system (section 2.2.2). When the gamma distribution is reduced to a Dirac delta distribution, our system could be formulated as a system of discrete delay differential equations. The gamma distribution is also similar to the Weibull distribution, which has been used to model sea lice (Aldrin et al., 2017), as both distributions are continuous, unimodal, and can be reduced to exponential distributions. Lastly, the integration of the gamma distribution multiplied by the exponential distribution is simple to evaluate analytically, and thus our expression for the next generation matrix does not become overly complicated. If we use β_k^j as the rate parameter and a_k^j as the shape parameter then the maturation

function becomes

$$-\frac{d}{dt}M_k^j(t) = M_k^j(t)m_k^j(t) = \frac{{\beta_k^j}^{a_k^j} x^{a_k^j-1} e^{-\beta_k^j x}}{\Gamma(a_k^j)}.$$

The last function to define explicitly is the age dependant birth rate, $b(t)$. Here we assume that the birth rate is constant, $b(t) = b$, so larvae are produced at a constant rate as soon as an individual enters their final stage of maturation. This is a biologically reasonable assumption, and again simplifies our calculations analytically. Our arrival time function, $f^{ij}(t)$ is derived in section 2.2.4, and thus cannot be assumed to have any particular form.

Under all the stated assumptions, the next generation matrix simplifies to:

$$K(i,j) = \prod_{k=2}^{m-1} \left(\frac{{\beta_k^j}^{a_k^j}}{(\beta_k^j + \mu_k^j)^{a_k^j}} \right) \left(\frac{b}{\mu_m^j} \right) \left(\frac{{\beta_1^j}^{a_1^j}}{(\beta_1^j + \bar{\mu}_1^j)^{a_1^j}} \right) \left(\int_0^\infty e^{-\mu_1^j t} f^{ij}(t) dt \right). \quad (2.6)$$

Here we have shown that the next generation matrix distills the essential quantities of larval dispersal between population patches as well as growth and survival on local patches into a single operator. From the next generation matrix we can calculate the source-sink distribution of our connected metapopulation. By approximating the maturation functions as gamma distributions and survival functions as exponential functions the form of the matrix can be simplified, while maintaining sufficient generality to approximate several realistic biological systems.

2.2.4 The arrival time of larvae moving between patches

In this section we formally define and demonstrate the calculation of the arrival time density, $f^{ij}(t)$. In previous sections we have focused on stages that grow on distinct patches and now we turn our attention to the first, or larval stage, which is spreading between patches. We allow the larval stage to have a latent period, where the larvae cannot arrive at the second patch even if it passes by. The larvae then mature into an active larvae, and during the active phase may arrive on a new patch. We include this latent period to allow our model to be applicable to various marine organisms where the first larval stage is not capable of attaching to a habitat patch, though the latency period can also easily be removed.

To formally define the arrival time distribution, let T be a random variable which describes the time from maturation that an active larva arrives on any patch, after it is released as a latent larva from patch j. If the larva does not arrive on a patch

then we say T is infinite. Then $\int_{t_1}^{t_2} f^j(t)dt = \Pr(t_1 < T < t_2)$, so that $f^j(t)$ is the distribution of arrival times for larvae leaving patch j. We will also show that $f^j(t) = \sum_{i=1}^{n} f^{ij}(t)$, where f^{ij} is the distribution of arrival times for an active larvae from patch j arriving on patch i. In order to determine $f^j(t)$ and $f^{ij}(t)$, we will first solve an equation governing the movement of the larvae between patches, for both the latent and active larval stages.

We are interested in approximating the movement of larvae between habitat patches in a marine environment, so we approximate movement using the Fokker-Plank equation, or advection diffusion equation in the case of constant diffusion. This equation has previously been used to model the dispersal of sea lice larvae away from salmon farms (Krkošek et al., 2006a), as well as barnacle and crab larvae along the California coast (Alexander and Roughgarden, 1996; Botsford et al., 1994). The diffusion term represents the effect of tides and ocean mixing, and the advection term represents any flow due to constant currents, potentially generated by river outflow, or other sources.

To allow for local hydrodynamic movement in a protected patch, we divide the total larvae produced at a patch into a fraction r that remain locally around the patch, and the remaining fraction q that enter the larger ocean environment and are then influenced by advection and diffusion. The fraction q that enter the channel are still able to rearrive on their natal patch.

To determine movement between patches and subsequently arrival on habitat patches in our model, we use the Fokker-Plank equation in a one dimensional domain. We use a one dimensional domain because coastlines can typically be approximated by a one-dimensional domain, and in the application section we apply our model to salmon farms located in a channel. However, the advection diffusion equation could easily be structured in its two dimensional form, if the model was to be used to analyse marine species where patches did not simply lie in a channel or along a coastline.

Let $\bar{p}^j(x,t)$ be the probability density function for the location of the latent larvae leaving patch j into the channel environment as a function of time. The larvae are released from patch j and then we assume the movement of the larvae between patches is governed by the Fokker-Plank equation:

$$\begin{aligned} \frac{\partial}{\partial t}\bar{p}^j(x,t) &= -\frac{\partial}{\partial x}\left(v(x)\bar{p}^j(x,t)\right) + \frac{\partial^2}{\partial x^2}\left(D(x)\bar{p}^j(x,t)\right) \\ \bar{p}^j(x,0) &= qh(x-x_j)/\Delta, \end{aligned} \tag{2.7}$$

where Δ is the size of the patch, and $h(x) = 1$ when $x \in [-\Delta/2, \Delta/2]$ and $h(x) = 0$ otherwise. $D(x)$ is the diffusion coefficient and $v(x)$ is the advection coefficient of the

environment.

Latent larvae then mature into active larvae. In section 2.2 we defined $M_1^j(a)$ as the probability that a latent larvae released from patch j has not yet matured into an active larva, and $m_1^j(a)$ as the instantaneous rate of maturation. Using these two previously defined functions, $M_1^j(a)m_1^j(a)$ is therefore the probability density function associated with maturation. If $\bar{T}$ is the time it takes for the latent larva to mature into an active larva after it is released, then $\int_{t_1}^{t_2} M_1^j(t)m_1^j(t)dt = \Pr(t_1 < \bar{T} < t_2)$. Once larvae mature into active larvae they continue to move according to the Fokker-Plank equation, but now they arrive on patch i with rate α_i as they pass by. Let $p^j(x,t)$ be the probability density function of the active larvae travelling from patch j, then $p^j(x,t)$ is given by:

$$\begin{aligned} \frac{\partial}{\partial t}p^j(x,t) = &-\frac{\partial}{\partial x}\left(v(x)p^j(x,t)\right) + \frac{\partial^2}{\partial x^2}\left(D(x)p^j(x,t)\right) \\ &- \sum_{i=1}^{n} \alpha_i h(x-x_i)p^j(x,t) \\ p^j(x,0) = &\int_0^\infty M_1^j(\tau)m_1^j(\tau)\bar{p}^j(x,t)d\tau. \end{aligned} \tag{2.8}$$

Local larvae that remain at a patch also mature according to the same maturation function. As they do not spread between patches, the density of active larvae that are in local water column around patch j, P^j, can be described by the ordinary differential equation:

$$\begin{aligned} \frac{d}{dt}P^j(t) &= -\alpha_j^r P^j(t) \\ P(0) &= r\int_0^\infty M_1^j(\tau)m_1^j(\tau)d\tau, \end{aligned} \tag{2.9}$$

where α_j^r, is the rate of arrival of the local larvae. We allow α_j^r to differ from α_j, the rate of arrival of larvae moving between patches.

We now consider the arrival time of an active larva. Let T be the time of arrival of the active larva on any patch, starting from the time it became active. Let the probability that the larva has not yet arrived on a patch at time t, $\Pr(T > t)$ be given by $A(t)$. Equation 2.8 also describes the density of parasites that have not yet arrived on any patch, and so $A(t) = \int_{-\infty}^{\infty} p^j(x,t)dx + P^j(t)$. To determine the relationship between $f^j(t)$ and $A(t)$, we can see that $\int_0^t f^j(\tau)d\tau = \Pr(T < t)$, and $A(t) = \Pr(T > t)$, thus $\int_0^t f^j(\tau)d\tau = 1 - A(t)$, or alternatively $f^j(t) = -dA(t)/dt$.

Integrating equation 2.8 over all space, adding equation 2.9, and substituting $f^j(t) = -dA/dt$ we find

$$f^j(t) = \sum_{i=1}^{n} \alpha_i \int_{x_i-\Delta/2}^{x_i+\Delta/2} p^j(x,t)dx + \alpha_j^r P^j(t),$$

as we require $\lim_{x\to\infty} p^j(x,t) = 0$ and $\lim_{x\to\infty} \frac{\partial}{\partial x} p^j(x,t) = 0$ for Equation 2.8 to be unique and well defined. We can then split the distribution for arrival time onto any patch, $f^j(t)$, into a sum of the arrival time distributions for each patch i. Let

$$f^{ij}(t) = \alpha_i \int_{x_i-\Delta/2}^{x_i+\Delta/2} p^j(x,t)dx$$

be the distribution of arrival time for an active larvae produced from patch j arriving on patch i, for $i \neq j$. For $i = j$,

$$f^{jj}(t) = \alpha_j \int_{x_j-\Delta/2}^{x_j+\Delta/2} p^j(x,t)dx + \alpha_r^j P^j(t).$$

Then we can rewrite $f^j(t)$ as

$$f^j(t) = \sum_{i=1}^{n} f^{ij}(t).$$

Therefore, if we can solve for $p^j(x,t)$, we can solve for $f^j(t)$ and $f^{ij}(t)$. In the application section we solve for the arrival time numerically. The approximate analytical solution of $f^{ij}(t)$ is the focus of Chapter 5.

Calculating the arrival time density function for larvae leaving one patch and arriving on another allows us to characterize the larval movement between a transmitting and receiving patch using a single function. This arrival time density function is incorporated into our full model to characterize larval dispersal between patches. In this section we have presented the derivation for our full model (system 4.16) and demonstrated how larval dispersal between patches and growth and survival on patches determine metapopulation dynamics. We have also constructed a next generation matrix for our model, which distils the essential information required to determine the source-sink distribution of our system.

2.3 Mathematical analysis of the model and next generation matrix

In this section we present the details of the construction of the next generation matrix, as well as proofs detailing the relationship between the stability of our model and the spectral radius of the next generation matrix.

2.3.1 Constructing the next generation matrix

The next generation matrix extracts the essential information of our model into a single operator. The elements of the matrix quantify the effect of an individual

from one patch on other patches, and the column sums identify source and sink patches. Here we present the details of the construction of the next generation matrix, beginning with one patch and then abstracting to multiple patches.

The next general matrix for a one patch system

To construct the next generation matrix for a single patch we need to calculate the number of new individuals produced on patch i from one initial individual on patch i in each stage. To calculate the number of new (stage $k = 2$) individuals produced on patch i by an initial individual at $t = 0$ starting on that same patch, we calculate the rate of production of new individuals at time t. We call this rate $\gamma(t)$. We then integrate $\gamma(t)$ over all t to calculate the total number of individuals produced.

For one initial individual in stage $k = 2$ to be producing new offspring, it must survive and mature through each stage and produce larvae which spread back to the patch. Let r_k be the time that the individual spends in stage k. For stages $k = 2, \ldots, m-1$ the probability that the individual survives to r_k in stage k is $S_k^i(r_k)M_k^i(r_k)$ and the rate at which they mature to the next stage is $m_k^i(r_k)$. For stage $k = m$ the probability that they survive to r_m is $S_m^i(r_m)$ and the rate at which they are producing larvae is $b^i(r_m)$. The probability that latent larvae survive to $\bar{r}_1$ is $\bar{S}_1^i(\bar{r}_1)M_1^i(\bar{r}_1)$ and the rate at which they mature into active larvae is $m_1^i(\bar{r}_1)$. The probability that active larvae ($k = 1$) survive to r_1 is $S_1^i(r_1)(1 - F^i(r_1))$ and the rate at which they attach as $k = 2$ individuals is $f^{ii}(r_1)/(1 - F^i(r_1))$.

To calculate the rate of production at time t, $\gamma(t)$, we multiply the survival probabilities and maturation rates in each of the stages and integrate over all possible r_k. At time t, we must have $0 \leq \bar{r}_1 + \sum_1^m r_k \leq t$, so we can rewrite $r_m = t - \sum_1^{m-1} r_k - \bar{r}_1$ before integrating over all other possible r_k. We calculate

$$\gamma(t) = \int_0^t \int_0^{t-r_{m-1}} \int_0^{t-r_{m-1}-r_{m-2}} \cdots \int_0^{t-\sum_2^{m-1} r_k} S_2^i(r_2)M_2^i(r_2)m_2^i(r_2)\ldots$$
$$S_{m-1}^i(r_{m-1})M_{m-1}^i(r_{m-1})m_{m-1}^i(r_{m-1})S_m^i(t - \sum_1^{m-1} r_k - \bar{r}_1)b^i(t - \sum_1^{m-1} r_k - \bar{r}_1)\times$$
$$\bar{S}_1^i(\bar{r}_1)M_1^i(\bar{r}_1)m_1^i(\bar{r}_1)S_1^i(r_1)f^{ii}(r_1)d\bar{r}_1 dr_1 \ldots dr_{m-1}.$$

Then, integrating $\gamma(t)$ over all t and using the convolution theorem,

$$\int_0^\infty f(t) * g(t)dt = \int_0^\infty f(t)dt \int_0^\infty g(t)dt$$

we calculate the number of new individuals on patch i produced from an initial individual in stage $k = 2$ on patch i to be:

$$\left(\prod_{k=2}^{m-1}\int_0^\infty S_k^i(t)M_k^i(t)m_k^i(t)\right)\left(\int_0^\infty S_m^i(t)b^i(t)dt\right)$$
$$\left(\int_0^\infty \bar{S}_1^i(t)M_1^i(t)m_1^i(t)\right)\left(\int_0^\infty S_1^i(t)f^{ii}(t)dt\right).$$

To calculate the next generation matrix with large domain, K_L, (Diekmann et al., 2010), we can also calculate the number of new individuals ($k = 2$) produced on patch i, from initial individuals in the other stages. Repeating the process described above, we find that the number of new individuals produced on patch i from an initial individual in stage $k = l$, for $2 \leq l \leq m$, is

$$\left(\prod_{k=l}^{m-1}\int_0^\infty S_k^i(t)M_k^i(t)m_k^i(t)\right)\left(\int_0^\infty S_m^i(t)b^i(t)dt\right)$$
$$\left(\int_0^\infty \bar{S}_1^i(t)M_1^i(t)m_1^i(t)\right)\left(\int_0^\infty S_1^i(t)f^{ii}(t)dt\right).$$

We can repeat the same process for $k = 1$ (where now we group the latent and active larval stages for simplicity). The (i, j) entries of the next generation matrix with large domain, K_L, are the number of new (stage $k = 2$) individuals in stage i produced from an initial individual in stage j. Therefore

$$\begin{aligned}
K_L(2,l) &= \left(\prod_{k=l}^{m-1}\int_0^\infty S_k^i(t)M_k^i(t)m_k^i(t)\right)\left(\int_0^\infty S_m^i(t)b^i(t)dt\right)\\
&\quad\left(\int_0^\infty \bar{S}_1^i(t)M_1^i(t)m_1^i(t)\right)\left(\int_0^\infty S_1^i(t)f^{ii}(t)dt\right) \quad 2 \leq l \leq m-1,\\
K_L(2,m) &= \left(\int_0^\infty S_m^i(t)b^i(t)dt\right)\left(\int_0^\infty \bar{S}_1^i(t)M_1^i(t)m_1^i(t)\right)\\
&\qquad\left(\int_0^\infty S_1^i(t)f^{ii}(t)dt\right),\\
K_L(2,1) &= \left(\int_0^\infty \bar{S}_1^i(t)M_1^i(t)m_1^i(t)\right)\left(\int_0^\infty S_1^i(t)f^{ii}(t)dt\right),\\
K_L(i,j) &= 0 \quad i \neq 2.
\end{aligned}$$

The next generation matrix with large domain, K_L, can then be reduced to the next generation matrix, K, through the process described by Diekmann et al. (2010). Essentially we multiply K_L from the left and right by matrices which isolate the relevant entries where new individuals are produced from other new individuals. In

this case, let E be an $n \times 1$ matrix with a 1 in row 2, and zeros elsewhere. Then $K = E^T K_L E$. The entries of the next generation matrix are the number of new individuals ($k = 2$) in stage i produced by an individual in stage j, though here we only include stages where new individuals can be produced. In our one patch example, because new individuals can only be produced in stage $k = 2$, our next generation matrix, K, for one patch is simply the scalar:

$$K = \left(\prod_{k=2}^{m-1} \int_0^\infty S_k^i(t) M_k^i(t) m_k^i(t) \right) \left(\int_0^\infty S_m^i(t) b^i(t) dt \right) \left(\int_0^\infty \bar{S}_1^i(t) M_1^i(t) m_1^i(t) \right) \left(\int_0^\infty S_1^i(t) f^{ii}(t) dt \right).$$

While the next generation matrix, K, and next generation matrix with large domain, K_L, have different sizes and different entries, their spectral radii are equal (Diekmann et al., 2010).

The next generation matrix for the multiple patch system

Calculating the remaining entries of the next generation matrix, K, for the multiple patch model, using the same process as in the previous subsection, is relatively straightforward. In this case we restrict ourselves to calculating K, and no longer K_L, though K_L can also easily be calculated in the same way as in the previous section. We want to calculate the number of new individuals produced on patch i from an initial individual on patch j. In order for an individual to produce new individuals on patch i, it must first survive and mature on patch j, and then produce larvae that successfully travel to patch i. The majority of $K(i, j)$ will be the same as $K(j, j)$, as the individual must mature on patch j before producing larvae. Only now, instead of the larvae travelling back to j, they must successfully spread to i. Therefore the last multiplication factor which will now be $\int_0^\infty S_1^j(t) f^{ij}(t) dt$, instead of $\int_0^\infty S_1^j(t) f^{jj}(t) dt$. With this replacement we can see that we have the same formula for $K(i, j)$ as given by (2.5). In the following sections we will also make the assumption that K is irreducible. Physically, this means that larvae have a positive probability of arriving on any patch when leaving from a given patch. Recall that $f^{ij}(t) = \alpha_i \int_{-\infty}^{\infty} p^j(x, t) dx$, where $p^j(x, t)$ is the solution to the advection diffusion equation from section 2.2.4. The solution to the advection diffusion equation is positive everywhere, so $p(x, t) > 0$, and thus $f^{ij}(t) > 0$ for all (i, j).

Here we have presented the construction of the next generation matrix for our stage-structured model on one patch as well as on multiple patches. We have explicitly

shown how to reduce the next generation matrix with large domain to the next generation matrix on one patch, and we have demonstrated the process for multiple patches.

2.3.2 Model stability analysis

In this section we will demonstrate that $R_0 = \rho(K)$ determines the stability of the zero equilibrium for the system (4.16).

Calculating the model equilibrium

First, we show that the zero equilibrium is the only equilibrium in our system. It should be noted here that system (4.16) is the solution to a linear system of age structured PDEs, and so we expect the zero equilibrium to be the only equilibrium. However, we include the details for completeness. Assume the system is at equilibrium, so that $n_k^i(t,a) = n_k^i(a)^*$, and $B_k^i(t) = B_k^{i\,*}$. Now we solve for $B_1^{i\,*}$ using system (4.5):

$$
\begin{aligned}
B_1^{i\,*} &= \int_0^\infty \bar{n}_1(a)^* m_1^i(a) da \\
&= \int_0^\infty \bar{B}_1^{i\,*} \bar{S}_1^i(a) M_1^i(a) m_1^i(a) da \\
&= \int_0^\infty n_m^i(a)^* b^i(a) da \int_0^\infty \bar{S}_1^i(a) M_1^i(a) m_1^i(a) da \\
&= \int_0^\infty B_m^{i\,*} S_m^i(a) b^i(a) da \int_0^\infty \bar{S}_1^i(a) M_1^i(a) m_1^i(a) da \\
&= \int_0^\infty n_{m-1}^i(a)^* m_{m-1}^i(a) da \int_0^\infty S_m^i(a) b^i(a) da \int_0^\infty \bar{S}_1^i(a) M_1^i(a) m_1^i(a) da \\
&= \int_0^\infty B_{m-1}^{i\,*} S_{m-1}^i(a) M_{m-1}^i(a) m_{m-1}^i(a) da \int_0^\infty S_m^i(a) b^i(a) da \\
&\qquad \int_0^\infty \bar{S}_1^i(a) M_1^i(a) m_1^i(a) da \\
&= B_2^{i\,*} \left(\prod_{k=2}^{m-1} \int_0^\infty S_k^i(a) M_k^i(a) m_k^i(a) da \right) \left(\int_0^\infty S_m^i(a) b^i(a) da \right) \\
&\qquad \left(\int_0^\infty \bar{S}_1^i(a) M_1^i(a) m_1^i(a) da \right) \\
&= \sum_{j=1}^n \int_0^\infty n_1^j(a)^* f^{ij}(a) / (1 - F^j(a)) da \left(\prod_{k=2}^{m-1} \int_0^\infty S_k^i(a) M_k^i(a) m_k^i(a) da \right) \\
&\qquad \left(\int_0^\infty S_m^i(a) b^i(a) da \right) \left(\int_0^\infty \bar{S}_1^i(a) M_1^i(a) m_1^i(a) da \right) \\
&= \sum_{j=1}^n B_1^{j\,*} \left(\int_0^\infty S_1^j(a) f^{ij}(a) da \right) \left(\prod_{k=2}^{m-1} \int_0^\infty S_k^i(a) M_k^i(a) m_k^i(a) da \right) \\
&\qquad \left(\int_0^\infty S_m^i(a) b^i(a) da \right) \left(\int_0^\infty \bar{S}_1^i(a) M_1^i(a) m_1^i(a) da \right).
\end{aligned}
$$

Let us define a matrix $\mathbf{S}$ entry-wise such that

$$
\begin{aligned}
S(i,j) = \left(\int_0^\infty S_1^j(a) f^{ij}(a) da \right) &\left(\prod_{k=2}^{m-1} \int_0^\infty S_k^i(a) M_k^i(a) m_k^i(a) da \right) \\
&\left(\int_0^\infty S_m^i(a) b^i(a) da \right) \left(\int_0^\infty \bar{S}_1^i(a) M_1^i(a) m_1^i(a) da \right).
\end{aligned}
$$

Then we can write the equations for $B_1^{i\,*}$ for each farm i in matrix notation as

$$
B_1{}^* = \mathbf{S} B_1{}^*.
$$

This equation can only have a solution if $\det(\mathbf{S} - \mathbf{I}) = 0$. However, as we have general functions $f^{ij}(a)$, $S_k^i(a)$, and $M_k^i(a)$, we therefore require $B_1^* = 0$, from which we can

recursively deduce that $B_k^* = 0$ for all k. Therefore the zero equilibrium is the only equilibrium for this system.

Determining the stability of the equilibrium using R_0

Next we prove that the spectral radius of the next generation operator, $R_0 = \rho(K)$, determines the stability of the zero equilibrium of the full system (4.16). Again the result would be generally expected, based on the theory in Diekmann et al. (2010), but we include the details here for completeness.

Theorem 2.1. *Assume the next generation matrix, K, is irreducible. Then*

1. *if $R_0 < 1$ then the zero equilibrium of system 4.16 is globally stable.*
2. *if $R_0 > 1$ then the zero equilibrium of system 4.16 is unstable.*

Proof. To analyse the stability of the zero equilibrium we consider small perturbations to the equilibrium and examine their growth or decay. At the equilibrium we have $B_k^i(t) = 0$ for all k, i. Consider a small perturbation of the form $B_k^i(t) = \bar{B_k^i} e^{\lambda t}$ to each of the $B_k^i(t)$. Similar to the calculation of the equilibrium, we will construct a recursive equation for $\bar{B}_1^i$ and then reformulate as a matrix equation for all patches. Using the equation for $B_k^i(t)$ in system (4.16) we find

$$
\begin{aligned}
\bar{B}_1^i &= e^{-\lambda t} B_1^i(t) \\
&= e^{-\lambda t} \int_0^\infty \bar{n}_1^i(t,a) m_1^i(a) da \\
&= e^{-\lambda t} \int_0^\infty \bar{B}_1^i(t-a) \bar{S}_1^i(a) M_1^i(a) m_1^i(a) da \\
&= e^{-\lambda t} \int_0^\infty \bar{\bar{B}}_1^i e^{\lambda(t-a)} \bar{S}_1^i(a) M_1^i(a) m_1^i(a) da \\
&= \bar{\bar{B}}_1^i \int_0^\infty e^{-\lambda a} \bar{S}_1^i(a) M_1^i(a) m_1^i(a) da \\
&= e^{-\lambda t} \bar{B}_1^i(t) \int_0^\infty e^{-\lambda a} \bar{S}_1^i(a) M_1^i(a) m_1^i(a) da \\
&= e^{-\lambda t} \int_0^\infty n_m^i(t,a) b^i(a) da \int_0^\infty e^{-\lambda a} \bar{S}_1^i(a) M_1^i(a) m_1^i(a) da \\
&= e^{-\lambda t} \int_0^\infty B_m^i(t-a) S_m^i(a) b^i(a) da \int_0^\infty e^{-\lambda a} \bar{S}_1^i(a) M_1^i(a) m_1^i(a) da \\
&= e^{-\lambda t} \int_0^\infty \bar{B}_m^i e^{\lambda(t-a)} S_m^i(a) b^i(a) da \int_0^\infty e^{-\lambda a} \bar{S}_1^i(a) M_1^i(a) m_1^i(a) da \\
&= \bar{B}_m^i \int_0^\infty e^{-\lambda a} S_m^i(a) b^i(a) da \int_0^\infty e^{-\lambda a} \bar{S}_1^i(a) M_1^i(a) m_1^i(a) da \\
&= \bar{B}_2^i \left(\prod_{k=2}^{m-1} \int_0^\infty e^{-\lambda a} S_k^i(a) M_k^i(a) m_k^i(a) da \right) \\
&\quad \left(\int_0^\infty e^{-\lambda a} S_m^i(a) b^i(a) da \right) \left(\int_0^\infty e^{-\lambda a} \bar{S}_1^i(a) M_1^i(a) m_1^i(a) da \right) \\
&= \sum_{j=1}^n \bar{B}_1^j \left(\int_0^\infty e^{-\lambda a} S_1^j(a) f^{ij}(a) da \right) \left(\prod_{k=2}^{m-1} \int_0^\infty e^{-\lambda a} S_k^i(a) M_k^i(a) m_k^i(a) da \right) \\
&\left(\int_0^\infty e^{-\lambda a} S_m^i(a) b^i(a) da \right) \left(\int_0^\infty e^{-\lambda a} \bar{S}_1^i(a) M_1^i(a) m_1^i(a) da \right).
\end{aligned}
$$

Define

$$
\mathbf{L}(\lambda) = \begin{bmatrix}
L_1^{11}(\lambda) \bar{L}_1^1(\lambda) \prod_{k=2}^m L_k^1(\lambda) & \dots & L_1^{1n}(\lambda) \bar{L}_1^1(\lambda) \prod_{k=2}^m L_k^1(\lambda) \\
\vdots & \ddots & \vdots \\
L_1^{n1}(\lambda) \bar{L}_1^n(\lambda) \prod_{k=2}^m L_k^n(\lambda) & \dots & L_1^{nn}(\lambda) \bar{L}_1^n(\lambda) \prod_{k=2}^m L_k^n(\lambda)
\end{bmatrix}
$$

with

$$L_k^i(\lambda) = \begin{cases} \int_0^\infty e^{-\lambda a} S_k^i(a) M_k^i(a) m_k^i(a) da & k = 2, \ldots, m-1 \\ \int_0^\infty e^{-\lambda a} S_m^i(a) b^i(a) da & k = m \end{cases}$$
$$\bar{L}_1^i(\lambda) = \int_0^\infty e^{-\lambda a} \bar{S}_1^i(a) M_1^i(a) m_1^i(a) da$$
$$L_1^{ij}(\lambda) = \int_0^\infty e^{-\lambda a} S_1^{ij}(a) f^{ij}(a) da.$$

Then again we can write the equations for each $\bar{B}_1^i$ for each patch i in matrix notation as

$$(\mathbf{L}(\lambda) - \mathbf{I})\bar{B}_1 = 0.$$

We are looking for non-trivial solutions where $\bar{B}_1 \neq 0$, and therefore require

$$\det(\mathbf{L}(\lambda) - \mathbf{I}) = 0. \tag{2.10}$$

This is the characteristic equation for our system. If the root λ satisfies $\Re(\lambda) < 0$ then the zero equilibrium is stable, and if $\Re(\lambda) > 0$ then the zero equilibrium is unstable. Furthermore, as our system 4.16 is linear, if the equilibrium is locally stable it will be globally stable.

We know that because λ is a root of (2.10) then $1 \in \sigma(\mathbf{L}(\lambda))$, where $\sigma(\mathbf{L}(\lambda))$ is the spectrum of $\mathbf{L}(\lambda)$. We also know from the definition of system 4.16 that $\bar{B}_1$ must be non-negative, and from (2.10) that $\bar{B}_1$ is the eigenvector associated with an eigenvalue of 1. $\mathbf{L}(\lambda)$ is irreducible, because K is irreducible, and the eigenvalue associated with a non-negative eigenvector of an irreducible matrix is the spectral radius of the matrix (Theorem 2.1, Li and Schneider (2002)). Thus $\rho(\mathbf{L}(\lambda)) = 1$.

1) If $R_0 < 1$, then $\rho(\mathbf{L}(0)) = \rho(K) = R_0 < 1$. If $\Re(\lambda) > 0$ then $\mathbf{L}(0) \geq \mathbf{L}(\lambda)$ entry wise, and so $\rho(\mathbf{L}(\lambda)) \leq \rho(\mathbf{L}(0)) < 1$ (Corollary 8.1.19, Horn and Johnson (2012)). Therefore in order for $\rho(\mathbf{L}(\lambda)) = 1$ we require $\Re(\lambda) < 0$.

2) If $R_0 > 1$, then $\rho(\mathbf{L}(0)) > 1$. If $\Re(\lambda) < 0$ then $\mathbf{L}(0) \leq \mathbf{L}(\lambda)$ entry wise and so $\rho(\mathbf{L}(\lambda)) \geq \rho(\mathbf{L}(0)) > 1$. Therefore in order for $\rho(\mathbf{L}(\lambda)) = 1$ we require $\Re(\lambda) > 0$. □

Corollary 2.2. *If the number of new individuals produced on a given patch k, from an initial individual starting on patch k, is greater than one, so $K(k,k) > 1$, then $R_0 > 1$.*

Proof. If $K(k,k) > 1$, then we can decompose $K = A + B$, where

$$B(i,j) = \begin{cases} 1 & i = j = k \\ 0 & \text{otherwise,} \end{cases}$$

and A is still non-negative. Because A is non-negative, we can see that $K > B$, and so by Corollary 8.1.19 Horn and Johnson (2012), $\rho(K) > \rho(B) = 1$. □

Here we have demonstrated that $R_0 = \rho(K)$ determines the stability of the zero equilibrium for system 4.16. Earlier in this section we presented the details of the construction of the next generation matrix, K, for the stage-structured population on both one and multiple habitat patches.

2.4 Applications

In this section we discuss applications of the next generation matrix and the effect of different environmental variables on the next generation matrix. The next generation matrix is a useful tool to quantify the effect of individuals from one patch on other patches. Here we will show how to use the column sums in the matrix to determine the source-sink dynamics of the network, and how this relates to R_0. We will also show how the column sums can be used to investigate the transient dynamics of the system, and how these may differ from the asymptotic dynamics. We then investigate how the left and right eigenvectors can provide insight into the contributions of each patch to R_0. Using salmon farms as a motivating example we structure the application section to answer the key questions posed at the end of the introduction.

2.4.1 Salmon farms distributed in a channel

Here we present an example of patches in a linear array and in the following sections will demonstrate how both the source-sink distribution and persistence measures change as a function of the distance between patches. This example is motivated by sea lice spreading between salmon farms in a channel. Salmon farms act as habitat patches for sea lice, as the non-larval sea lice stages require a salmonid host on which to feed, and the salmon are themselves confined to the net pens in the farms. The larval sea lice stages are released into the water column and are capable of spreading between salmon farms in a given region. In both Norway and Canada, many salmon farms are located in sheltered coastal channels or fjords (Aldrin et al., 2017; Krkošek et al., 2006a). We therefore use a one dimensional domain to calculate the arrival time of sea lice spreading between farms.

In the following examples we consider 5 patches or farms of width Δ, each separated by some distance x_0 (Figure 2.4). We consider systems where there is no maturation delay from the latent to active larval stage, and where all larvae enter the channel, so that none remain locally. The absorption rate for larvae when they pass by a patch

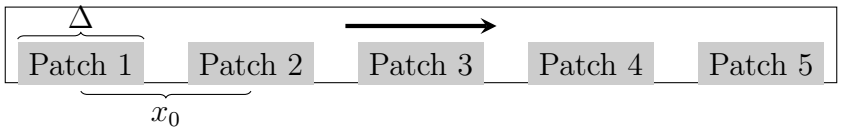

Figure 2.4: Patches, or salmon farms arranged in a channel. The width of each patch is Δ and the distance between the center of each patch is x_0. The arrow above the patches indicates the direction of advection.

is small, and in most examples diffusion is larger than advection. This represents a coastal channel environment in which ocean mixing is more prevalent than any constant currents generated by river outflow. It is in this environment that we answer the five questions posed above.

2.4.2 What is the source-sink distribution of salmon farms in a channel?

First, we show how to use the next generation matrix to determine the source-sink distribution of farms. Recent work has used R_0 theory to define two measures of persistence of a species on a continuous landscape, $R_{\text{loc}}(x)$ and $R_\delta(x)$, using the next generation operator (Huang et al., 2016; Krkošek and Lewis, 2010; Mckenzie et al., 2012a). $R_{\text{loc}}(x)$ is the number of new individuals produced at location x in the absence of dispersal, and can be used as a measure of the fundamental niche in certain scenarios. In our model, dispersal is a key environmental feature for the larval stage of the marine organism, and while we allow some percentage of larvae to remain at a patch, it is not realistic that any large percentage would remain and avoid dispersal. Therefore $R_{\text{loc}}(x)$ is not relevant for our model.

The second persistence measure, $R_\delta(x)$, is the number of new individuals produced over the entire network from one individual at location x. It takes into account both growth and survival at location x, and dispersal from location x. If one individual at x produces less than one individual over the entire landscape, then $R_\delta(x) < 1$, and the location x is defined as a sink. If $R_\delta(x) > 1$, then x is defined as a source. The spectral radius of the next generation operator, R_0, determines species persistence over the entire landscape. When using this measure it is not possible for connected patches of sinks to persist. In this section we build on and apply this theory to determine the source-sink distribution on the discrete population patches in our system using the next generation matrix.

In our system of n patches, let $R_\delta(j)$ be the number of new individuals on all patches produced from one individual on patch j. In terms of our next generation

matrix K (Equation 2.5),

$$R_\delta(j) = \sum_{i=1}^{n} K(i,j).$$

If for patch j, $R_\delta(j) > 1$, then j is a source, and if $R_\delta(j) < 1$, then j is a sink. $R_0 = \rho(K)$ is still needed to determine if the populations on the connected patches will persist or perish, however there are some nice persistence results that follow directly from $R_\delta(j)$.

First, a connected network consisting only of sinks cannot persist. Using this new measure, for a connected network of sinks, we have $R_\delta(j) < 1$ for all j. There is a nice result concerning R_0 for non-negative irreducible matrices (Horn and Johnson, 2012) which states that

$$\min_{1\le j\le n} \sum_{i=1}^{n} K(i,j) \le \rho(K) \le \max_{1\le j\le n} \sum_{i=1}^{n} K(i,j).$$

Substituting the definition of R_δ and R_0 this can be restated as

$$\min_{1\le j\le n} R_\delta(j) \le R_0 \le \max_{1\le j\le n} R_\delta(j). \tag{2.11}$$

Therefore if $R_\delta(j) < 1$ for all j, then $R_0 < 1$ as well. Secondly, a connected network consisting only of sources cannot perish. Here, $R_\delta(j) > 1$ for all j, and so $R_0 > 1$ as well. Similarly, if any diagonal entry of the next generation matrix is greater than one, $K(j,j) > 1$, then $R_0 > 1$. This can be seen from Corollary 2.2. Biologically, this result means a population on a network will persist if the network contains at least one patch which is self sustaining in the absence of dispersal from other patches. However, there are also other situations in which the network can persist. In summary, $R_\delta(j)$, the jth column sum of the next generation matrix, is necessary to determine if a patch j is a source or a sink, and R_0, the spectral radius of the next generation matrix, is necessary to determine the persistence of the total population.

2.4.3 How does the source-sink distribution change with respect to environmental variables?

In this section we examine the effect of advection and diffusion on R_0 and R_δ, using the example of 5 patches in a channel, shown in Figure 2.4. First we study the effect of varying diffusion on R_0 across different interfarm separation distances, x_0. In Figure 2.5 the diffusion coefficient, D, is decreased from 5 to 1 and the change in R_0 is shown as a function of x_0. For small values of x_0, R_0 is larger when there is less diffusion. When there is less diffusion, each patch has a greater probability of

self infecting, because there is less immediate dispersal away from the patch. When the patches are overlapping, they act as one patch, which is why R_0 is larger at small x_0 when there is less diffusion. This is also why the horizontal asymptote for R_0 is larger for smaller diffusion. For intermediate values of x_0 an interesting phenomenon occurs. As the separation distance, x_0 increases, R_0 for low diffusion drops below R_0 for high diffusion. When diffusion is low, it is more difficult for individuals to disperse against the direction of advection, and so as x_0 increases, individuals from Patch 5 begin to only contribute to other individuals on Patch 5. As will be shown when examining the effect of advection, Patch 5 becomes a sink for small values of x_0, and so the other patches are contributing individuals to Patch 5, which cannot sustain them.

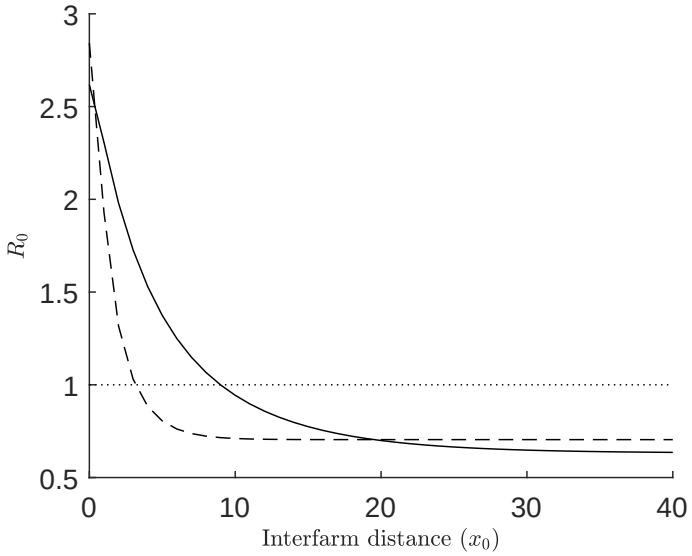

Figure 2.5: R_0 as a function of x_0, for $D = 5$, $v = 1$, solid line; $D = 1$, $v = 1$, dashed line. The remaining parameter values are $\alpha = 0.1$, $g^{ij}(t) = 0$, $\Delta = 0.8$, $S^{ij}(t) = e^{-0.05t}$. The survival, maturation, and birth functions for the sessile stages were combined so that $\prod_{k=2}^{m-1} \left(\int_0^\infty S_2^j(t) M_2^j(t) m_2^j(t) dt\right) \left(\int_0^\infty S_m^j(t) b^j(t) dt\right) = 10$.

Next, we study the effect that advection has on R_0 and R_δ across different interfarm distances, x_0. For different values of advection, both R_0 and R_δ, as functions of x_0, have the same shape as R_0 shown in Figure 2.5. Therefore we find it most illuminating to examine the effect of advection on the ratio of R_δ/R_0. Biologically, R_0 is the number of new individuals produced in the population, from one typical individual, and $R_\delta(j)$ is the number of new individuals produced in the population, from one individual starting on patch j. Therefore the ratio $R_\delta(j)/R_0$ can be seen as the relative multiplication factor of the number of new individuals in the population produced by one individual starting on patch j, compared to one typical individual.

If $R_\delta(j)/R_0 > 1$ then an individual on patch j is contributing more than the typical individual, and if $R_\delta(j)/R_0 < 1$, then it is contributing less. Of course, it is also important to also track if each R_δ and R_0 are greater or less than one, so that it is known which patches are sources, which are sinks, and whether or not the total population is growing.

In Figure 2.6, R_δ/R_0 is plotted as a function of the interfarm separation distance, x_0 for different values of v. The switch in each curve from black to grey marks where $R_\delta \leq 1$. Using the R_δ measure, we can see that for low x_0 all patches are sources. As x_0 increases, Patch 5 becomes a sink, with $R_0 > 1$, and then as x_0 continues to increase, R_0 falls below 1. Therefore in this linear array, there is some critical separation distance, beyond which the population patches are not sufficiently connected for the total population to persist. Even after this critical distance, some patches are still sources with $R_\delta > 1$, and it takes a larger separation distance x_0 for all patches to become sinks.

Both R_0 and R_δ change when v increases from 0.1 to 1. As v increases, it takes a much smaller separation distance, x_0, for R_0 to fall below 1. Increasing v not only reduces retention of individuals on each patch, but also inhibits individuals from better dispersing against the direction of advection. Therefore when v is lowered, there is greater dispersal among neighbouring patches, but less long distance dispersal in the direction of advection, from Patch 1 to Patch 5. There are two other interesting behaviours that should also be highlighted. First, is that $\max_{1\leq i\leq n} R_\delta(i)$ is achieved at Patch 3 when advection is low, compared to Patch 1 when advection is high. We can see the transition as Patch 1 becomes a larger source as v increases. Second, the critical separation distances, for which each R_δ falls below one and becomes a sink, come closer together, as the decrease in advection makes the behaviour on all patches more similar.

In both examples where diffusion and advection were changed, for large separation distances, $R_0 < 1$. However, this is due to the parameters controlling the birth, survival, and maturation functions for these examples. For other parameter values, certain values of v and D could result in $R_0 > 1$ for large x_0 and some could result in $R_0 < 1$. Here we have shown how R_0 and the source-sink distribution, quantified by R_δ, change as a function of the diffusion and advection in the system, as well as the interfarm seperation distance, x_0.

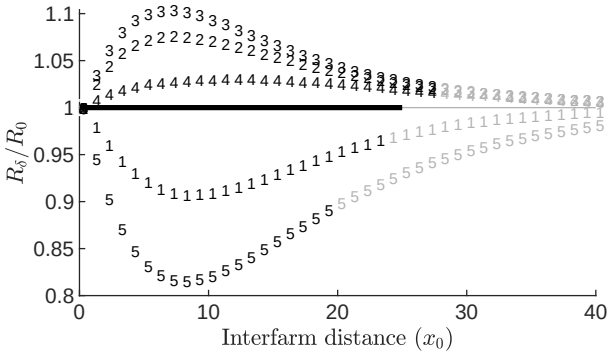

(a) Low advection ($v = 0.1$)

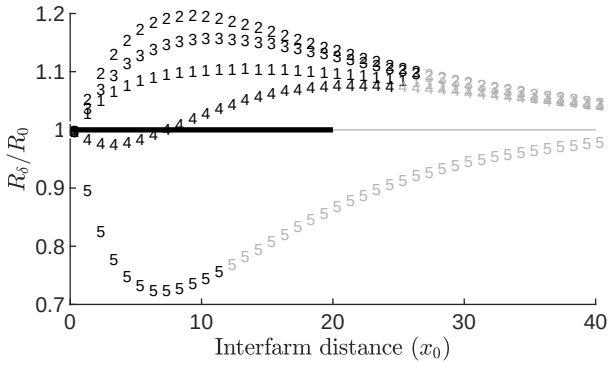

(b) Medium advection ($v = 0.4$)

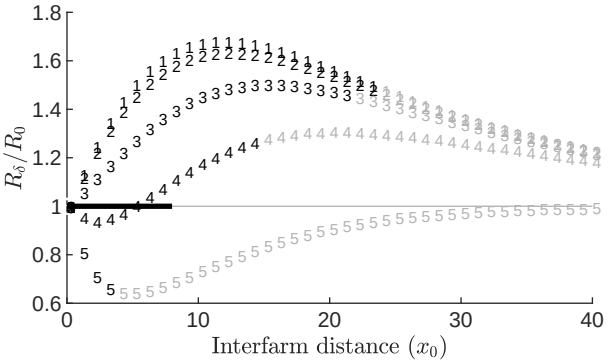

(c) High advection ($v = 1$)

Figure 2.6: R_δ/R_0 for each patch when $D = 5$. When each curve is black $R_\delta > 1$, and when the curve is grey $R_\delta \leq 1$. The switch from black to grey on the solid line indicates when $R_0 = 1$. The remaining parameters are the same as in Figure 2.5.

2.4.4 Are there certain parameter regions in which local outbreaks can occur, but not global outbreaks?

Interesting transient dynamics can occur if we consider networks of patches with $R_0 < 1$, but where some patches are sources, and networks with $R_0 > 1$, but where some patches are sinks. In these network arrangements, the value of R_0 still determines the global persistence of the total population, but the initial conditions determine whether the population will begin by increasing or decreasing. To consider these dynamics we let $N(g)$ be the vector of sea lice populations on each patch, in generation g. Then, in terms of generational time, the population will update according to

$$N(g+1) = KN(g),$$

with the initial condition N_0, which is a vector of the initial sea lice populations on each patch. For example, consider the next generation matrix K with parameter values that are the same as for Figure 2.6c. At $x_0 = 8$, $R_0 > 1$, but $R_\delta(5) < 1$. Therefore the total population ($\sum_i N_i(g)$) will increase eventually, but will start by decreasing if our initial population is all in Patch 5 ($N_0 = [0\ 0\ 0\ 0\ 1]^T$). In fact, for $x_0 = 8$, if we begin with 1 individual in Patch 5, it takes 23 generations before the total population increases above 1, as shown in Figure 2.7. Similarly, for $x_0 = 10$, $R_0 < 1$ but $R_\delta(1) > 1$. In this case the population will eventually decrease, but will begin by increasing if the initial population is in Patch 1 ($N_0 = [1\ 0\ 0\ 0\ 0]^T$). If we start with 1 individual in Patch 1, it takes 41 generations before the total population falls below 1. In this configuration, this means that there would be a local outbreak, but not a global sea lice outbreak.

To attempt to quantify the effect of the source and sink patches on transient dynamics more formally, we use notation from Huang and Lewis (2015). They define

$$R_l = \min_{1\le j\le n} \sum_{i=1}^{n} K(i,j) = \min_{1\le j\le n} R_\delta(j),$$

which is shown to be the intergenerational growth rate under the worst possible initial conditions, and

$$R_u = \max_{1\le j\le n} \sum_{i=1}^{n} K(i,j) = \max_{1\le j\le n} R_\delta(j),$$

which is shown to be the intergenerational growth rate under the best possible initial conditions (Huang and Lewis, 2015). Equation 2.11 can then be restated using R_l and R_u as

$$R_l \le R_0 \le R_u.$$

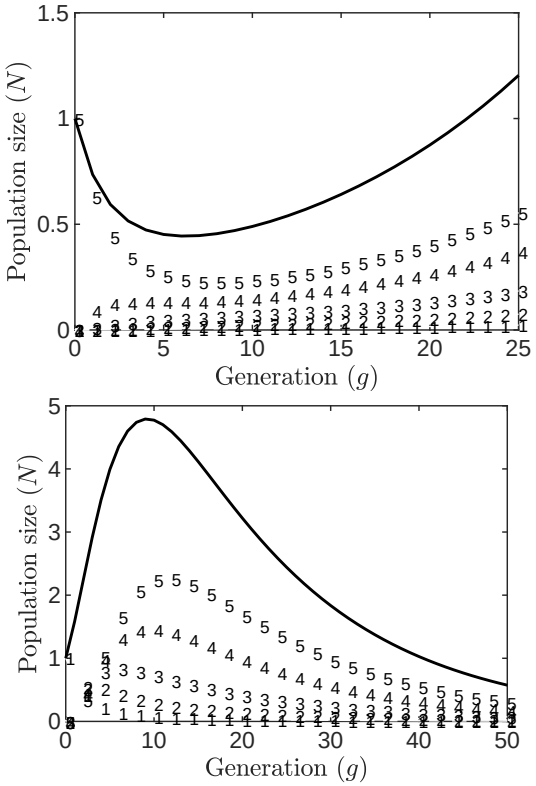

Figure 2.7: The population of sea lice ($N_i(g)$) on each patch i in each generation (g) after one initial individual is released on a patch. Let $N(g)$ be a vector of patch populations, then in generational time the population updates according to $N(g+1) = KN(g)$, with the initial condition N_0, which is a vector of the initial sea lice populations on each patch. The black line shows the total population size ($\sum_i N_i(g)$). Parameter values are the same as Figure 2.6. In a), we fix $x_0 = 8$, so that $R_0 > 1$, and release the initial individual on patch 5 ($N_0 = [0\ 0\ 0\ 0\ 1]^T$). In b) we fix $x_0 = 10$, so that $R_0 < 1$, and release the initial individual on patch 1 ($N_0 = [1\ 0\ 0\ 0\ 0]^T$).

In essence, R_l is the growth rate in the first generation if our population is initially at the worst sink patch, and R_u is the growth rate if we are at the best source patch. Therefore R_l and R_u are useful measures to quantify potential transient dynamics, and also retain key information about the source-sink distribution. If $R_l < 1$ then there is at least one patch acting as a sink, and if $R_u > 1$ then there is at least one patch acting as a source. In the following section, we examine how R_l, R_u, and R_0 change with different variables, instead of considering R_δ for every patch.

2.4.5 What is the effect of treating a single farm on the transient and asymptotic dynamics?

In this section we examine the effect that treating specific farms have on R_l, R_u, and R_0. We define treatment as reduced survival and maturation on a patch or farm, affecting stages k through m, but not affecting the larval stage. On salmon farms, treatment is used to reduce sea lice levels and is typically administered orally to farmed salmon (Rogers et al., 2013). Reduced survival and maturation could also be the result of poor environmental conditions at a patch, such as low salinity and temperature in the case of sea lice. We also view treatment through the lens of type reproduction numbers, and the effort required for control on a patch to reduce $R_0 = 1$.

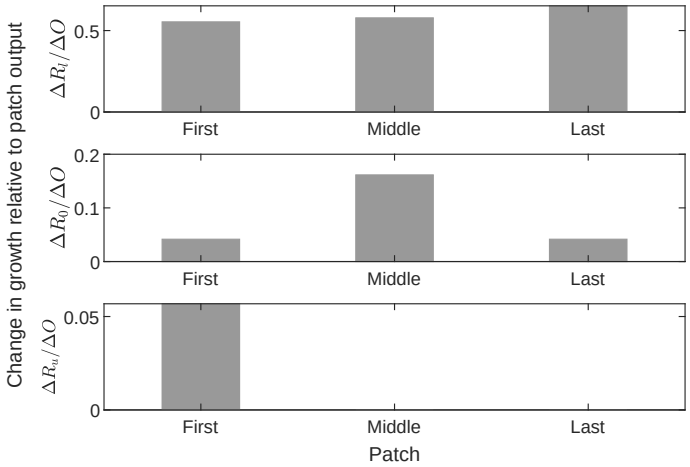

Figure 2.8: The change in R_l, R_0, and R_u when the output from the First patch (Patch 1), Middle Patch (Patch 3) or Last Patch (Patch 5) is reduced from 10 to 1. Parameter values for this figure are $\alpha = 0.1$, $D = 5$, $v = 1$, $g^{ij}(t) = 0$, $\Delta = 0.8$, $S^{ij}(t) = e^{-0.05t}$, $x_0 = 8.4$. The survival, maturation, and birth functions for the sessile stages were combined so that $O = \prod_{k=2}^{m-1} \left(\int_0^\infty S_2^j(t) M_2^j(t) m_2^j(t) dt\right) \left(\int_0^\infty S_m^j(t) b^j(t) dt\right) = 10$, and for the reduced patch $O = \prod_{k=2}^{m-1} \left(\int_0^\infty S_2^j(t) M_2^j(t) m_2^j(t) dt\right) \left(\int_0^\infty S_m^j(t) b^j(t) dt\right) = 1$

To first examine the effect of treatment on the transient and asymptotic dynamics, we treat Patch 1, Patch 3, and Patch 5 separately. In the direction of advection these

patches are the first, middle, and last patches respectively (Figure 2.4). Figure 2.8 shows the change in R_l, R_u, and R_0 for the system when either the first, middle, or last patch has a reduced output (ΔO), from treatment. Perhaps the most interesting result is that if either the first or last patch has reduced output, the change in the R_0 value remains the same. The first patch is the patch that produces the most individuals on other patches, and the last patch is the patch that receives the most individuals from other patches. If we consider the reduced output as treatment, then if we treat either the patch that produces the most individuals, or the patch that receives the most individuals, the effect on R_0 will be the same. However, if we treat the middle patch, we have a larger change in R_0. Therefore treating the middle patch is more effective if we want to reduce long term population growth.

If treating the first or last patch has the same effect on R_0, then how might it change the transient dynamics of the system? We can see that if we treat the first patch, then the change in R_u is larger than if we treat either the middle or last patch, where there is no change. Therefore if we treat the first patch, the maximum possible growth rate is reduced, and thus we can reduce the severity of a local outbreak. However, if we treat the first patch the change in R_l is less than if we treat either the middle or last patch. Therefore treating the first patch results in a larger minimum possible growth rate.

We can also examine the effect of treatment using the type reproduction number (Heesterbeek and Roberts, 2007; Lewis et al., 2019; Roberts and Heesterbeek, 2003). The type reproduction number measures the control effort required to control a certain patch to reduce $R_0 = 1$. The type reproduction number can also been generalized to the target reproduction number, if control is not applied to an entire patch, to specific inter patch infections. To define the type reproduction number we divide the next generation matrix $K = [k_{ij}]$ into two matrices, $K = B + C$, where C is the target matrix associated with control, and B is the residual matrix. If we are interested in controlling patch i, then $C_i = [c_{ij}]$, with $c_{ij} = k_{ij}$ for $1 \leq i \leq n$ and $j = i$, and $c_{ij} = 0$ otherwise. Then $B = K - C$. To control patch i such that we can reduce $R_0 = 1$, we require $\rho(B) < 1$. The type reproduction number T_{C_i} is then defined by $\rho(C_i(I - B)^{-1})$, and $1 - 1/T_{C_i}$ is the fraction that output from patch i must be reduced in order for $R_0 = 1$. The controlled next generation matrix would then be $\frac{1}{T_{C_i}}C_i + (K - C_i)$, and would have $\rho(K) = 1$.

Consider the patch arrangement and parameter values as shown in Figure 2.8. In this case $R_0 > 1$, but when we are considering control of either the first, middle, or last patch, and creating target matrices C, we still have $\rho(B) < 1$. To create the target matrix C_1 associated with control on the first patch, we take the first column of K as

the first column of C_1, and put zeros in all other entries. Likewise to treat the middle patch we take the 3rd column of K as the third column of C_3, with zeros elsewhere, and to treat the last patch we take the last column of K as the last column of C_5 with zeros elsewhere. Using the formula for the type reproduction number given above, we calculate $T_{C_1} = T_{C_5} = 3.6$, and $T_{C_3} = 1.2$. This demonstrates that it requires a greater control effort to treat the first or last patch, to reduce $R_0 = 1$, than is required if treating the middle patch.

Here we have shown that either using the type reproduction number or directly examining the effect of treatment, that more treatment is required to control the first or last patch than the middle patch. Moreover, treating the first patch produces the largest change in R_u, the largest intergeneration growth rate, and treating the last patch produces the largest change in R_l, the minimum intergenerational growth rate.

2.4.6 What is the effect of an environmental gradient on patch contributions to R_0 and the source-sink distribution?

A different approach to measuring the contribution of each patch to the metapopulation is to use the right and left eigenvectors associated with R_0 (Hurford et al., 2010). This approach measures the contributions that each patch has on R_0 if the population is proportioned relative to the right eigenvector of the next generation matrix.

First, from the Perron-Frobenius Theorem, we know that the eigenvalue for which the spectral radius of K is achieved is real. Then, we can write this eigenvalue, R_0, using the left eigenvector, w, and the right eigenvector, v, as

$$R_0 = \frac{w^T K v}{w^T u}.$$

If we rescale w and v so that $w^T v = 1$, then we can rewrite R_0 as

$$R_0 = v_1 \sum_{i=1}^{n} K(i,1) w_i + v_2 \sum_{i=1}^{n} K(i,2) w_i + \cdots + v_n \sum_{i=1}^{n} K(i,n) w_i. \tag{2.12}$$

Equation 2.12 can then be interpreted as the sum of the contributions of each patch to R_0, when the population is proportioned relative to the right eigenvector (Hurford et al., 2010). If we look at the first term in this sum, which is the contribution of patch 1, v_1 is the relative proportion of the population that is in patch 1. This proportion, v_1, is then multiplied by $\sum_{i=1}^{n} K(i,1) w_i$, where each $K(i,1)$ is the number of new individuals produced on patch i from one individual on patch 1, and w_i is the

reproductive value of patch i. Therefore the first term in Equation 2.12 measures the proportion of the population that is in patch 1 multiplied by the effect that individuals from patch 1 will have on future growth after they give birth to larvae which disperse to other patches. For ease of future reference, we define

$$R_c(j) = v_j \sum_{i=1}^{n} K(i,j) w_i$$

as the contribution of patch j to R_0. We can therefore rewrite equation 2.12 as

$$R_0 = \sum_{j=1}^{n} R_c(j) \tag{2.13}$$

Interestingly, the relative source-sink measure of a patch, $R_\delta(j)$, can be very different from the relative contribution measure, $R_c(j)$. In certain instances, for a given patch j, we can have $R_\delta(j) = \min_{1 \le i \le n} R_\delta(i) < 1$, so that patch j is the largest sink in the population. However, that same patch j, may have $R_c(j) = \max_{1 \le i \le n} R_c(i)$, with $R_0 > 1$, so that if the population is distributed according to v, patch j has the largest contribution to R_0. R_0 is greater than 1, so the population is growing. This means that in one generation, one individual from patch j is contributing the least to the total population, but over several generations, patch j is having the largest contribution to the total growth of the population.

As an example, we examine how the intergenerational growth measures change if we put the patches in an environmental gradient. Salmon farms are often located along ocean channels, where rivers feed into the source of these channels. This creates a salinity gradient along the channel, where farms located closest to the river have the lowest salinity and farms furthest from the river have the highest salinity. Lower salinity results in a reduction in sea lice survival at each stage (Johnson and Albright, 1991). Often the river output at the source of the channel is also the source of advection in the channel, though there may be systems in which the average advection is in the opposite direction due to strong ocean currents. First we consider the less likely case, where the first patch (or farm) has the largest output, and the last patch has the least. In this case output decreases in the direction of advection. Next we will consider the more realistic case where output increases in the direction of advection. This would be the common case for salmon farms in a channel where the first farm is located closest to the river output, which is where salinity is lowest and so the patch output is also the lowest, and the river is the source of advection in the system. For reference, the average output from all patches is the same as the output for a single patch when there is no gradient.

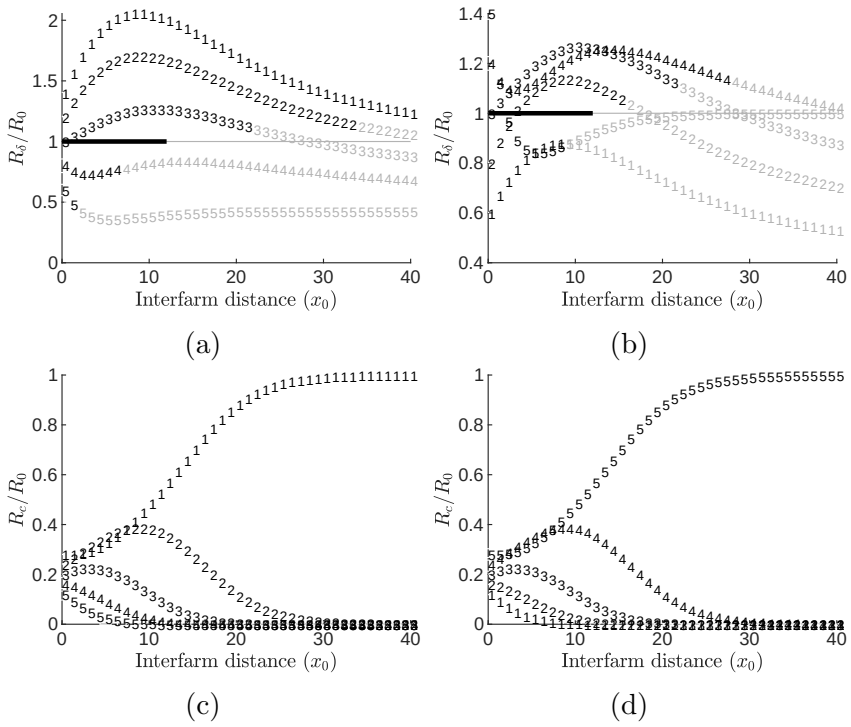

Figure 2.9: R_δ/R_0 and R_c/R_0 are shown as a function of x_0. Subfigures 2.9a and 2.9c are when the output decreases in the direction of advection, and 2.9b and 2.9d are when output increases. For subfigures 2.9a and 2.9b, when each curve is black $R_\delta > 1$, and when the curve is grey $R_\delta \leq 1$. The switch from black to grey on the solid line indicates when $R_0 = 1$. Parameter values for this figure are $\alpha = 0.1$, $D = 5$, $v = 1$, $g^{ij}(t) = 0$, $\Delta = 0.8$, $S^{ij}(t) = e^{-0.05t}$. The survival, maturation, and birth functions for the sessile stages were combined so that in the case of constant patch output, the output is $O = \prod_{k=2}^{m-1} \left(\int_0^\infty S_2^j(t) M_2^j(t) m_2^j(t) dt\right) \left(\int_0^\infty S_m^j(t) b^j(t) dt\right) = 10$. To construct the environmental gradient, the largest output was $1.4 \times O$, then $1.2 \times O$, then O, then $0.8 \times O$, then $0.6 \times O$.

We use R_δ/R_0 and R_c/R_0 as the intergenerational growth measures, for which we examine the effect of an environmental gradient. While R_δ/R_0 can be thought of as the relative multiplication factor of the number of new individuals in the population produced by one individual on patch j, compared to a typical individual, R_c/R_0 is simply the relative contribution of the patch to R_0, within the framework of left and right eigenvectors. In Figure 2.9, both R_δ/R_0 and R_c/R_0 are plotted as a function of x_0, for an environmental gradient in the direction of advection and for a gradient in the opposite direction.

First, what cannot be seen easily from Figure 2.9, is that R_0 is the same when patch output increases or decreases in the direction of advection. Interestingly, both of these R_0 values are larger than for patches without any gradient. When comparing R_δ/R_0 values, the relative spread of R_δ/R_0 is larger when patch output decreases in the direction of advection. Here, Patch 1 has the largest R_δ/R_0 value. Interestingly, when we look at R_c/R_0, the relative contribution to R_0, we can see that there is an intermediate distance x_0 where if the population is distributed relative to the right eigenvector, Patch 2 would be contributing more to R_0 than Patch 1, even though Patch 1 is the larger source.

We observe even more interesting behaviour when we look at R_δ/R_0 and R_c/R_0 when patch output increases in the direction of advection. Here, the relative ordering of $R_\delta(j)/R_0$ values change for different values of x_0. Patch 3 and 4 are the largest sources for most x_0, until they become sinks (when numbers switch from black to grey). Patch 5 starts as the largest source when $x_0 = 0$, but is the first to become a sink (along with Patch 1), around $x_0 = 9$. However, if we look at the plot of R_c, then for some x_0, Patch 5 is the largest contributor to R_0. In fact, at $x_0 = 9$, Patch 5 is a sink with the smallest R_δ, $R_\delta(5) = \min_{1\leq i\leq 5} R_\delta(i) < 1$. Therefore in the absence of dispersal from other patches, the population on Patch 5 would perish. However, for $x_0 = 9$, $R_0 > 1$ and $R_c(5) = \max_{1\leq i\leq 5} R_c(i)$. Therefore the population is growing, and moreover Patch 5 would be the largest contributor to growth if the population was distributed according the right eigenvector.

What we can also see from Figures 2.9a and 2.9b is that when the patch output decreases in the direction of advection, the relative ordering of the R_δ/R_0 values of the patches are the same as when there is no gradient (Figure 2.6c). However, when patch output increases in the direction of advection, the relative ordering of R_δ depends on the interfarm separation distance x_0. In this case the farm with the largest output is not the largest source, nor is the farm with the lowest output the largest sink. Here, knowing the local environmental conditions that determine sessile output does not directly inform the source-sink distribution of the patch network.

In this application section we have demonstrated how the next generation matrix can be used to determine the source-sink distribution of a metapopulation, as well as other persistence measures, each of which quantifies some useful information about our population. We applied these different persistence measures to examine populations of sea lice on salmon farms, and to answer the five questions posed at the end of the introduction.

2.5 Discussion

In this chapter we constructed a model for a meroplanktonic marine species, in which the larval stage is capable of dispersing between habitat patches, and the later sessile stages remain confined to a single habitat patch. This type of model is applicable to corals and coral reef fish (Cowen et al., 2006; Jones et al., 2009), barnacles (Roughgarden et al., 1988), Dungeness crabs (Botsford et al., 1994), sea urchins (Botsford et al., 1994), and many benthic marine species (Cowen and Sponaugle, 2009). We modelled the growth and survival of sessile stages on a habitat patch using arbitrary survival and maturation functions so that our model is applicable to a breadth of different systems. To model the dispersal between patches in the larval stage, we approximated hydrodynamic movement, so that rates of larval movement between patches have an underlying mechanistic model. We then constructed the next generation matrix, K, for this model. The next generation matrix distils the key elements of the model into a matrix from which we can determine the source-sink distribution among patches using the column sums. We denote the jth column sum by $R_\delta(j)$ and showed that if $R_\delta(j) < 1$ then patch j is a sink and if $R_\delta(j) > 1$ then patch j is a source. We also proved that the basic reproduction number $R_0 = \rho(K)$ determines the stability of the zero equilibrium of our model, so that if $R_0 > 1$ then the population grows, and if $R_0 < 1$ then the population goes extinct.

Using salmon farms as an example, we investigated how the source-sink distribution can change as a function of patch separation distance, and how often there is a critical separation distance for each patch, at which point a patch changes from a source to a sink. We demonstrated that increasing the ratio of advection to diffusion between patches increases the difference in critical separation distance between patches. We also demonstrate how $R_\delta(j)$ can be used to determine the transient dynamics of the salmon farm system, and how these transient dynamics can persist over several generations, and differ from the asymptotic dynamics determined by R_0 (Section 2.4.4, Figure 2.7). We investigated the effect of treatment of a single patch on the patch dynamics using the concept of type reproduction numbers and found that treating the

middle patch in a channel results in the greatest reduction in R_0, but that treating the first patch results in the greatest reduction in the maximum R_δ. Lastly, we looked at differing local productivity on patch dynamics, determined the contribution that each patch has to R_0, and demonstrated how this can also differ from $R_\delta(j)$.

Next generation matrices have a long history in epidemiology, where they have been used to calculate the number of new infections produced in one compartment when a newly infectious individual is introduced in another compartment (Diekmann et al., 1990; Diekmann et al., 2010; van den Driessche and Watmough, 2002). Our approach in constructing a next generation matrix for a stage-structured model with arbitrary stage durations and larval flow between patches extends recent use of next generation operators in ecology (Huang et al., 2016; Huang and Lewis, 2015; Krkošek and Lewis, 2010; Mckenzie et al., 2012a). Much of the previous work has used continuous space next generation operators to determine the source-sink distribution of populations in streams or lakes. There, the movement of individuals through the water is also described by partial differential equations, though individuals can be produced at any point in space. In our work, we describe the movement of larvae between patches using advection diffusion equations, though, as larvae can only be produced on certain population patches, our linear operator can be formulated as a matrix. Our work also extends work of Huang and Lewis (2015), where the next generation matrix was used to determine the transient dynamics in a system and how they differ from the asymptotic dynamics determined by R_0 in a model of salmonids. The minimum R_δ was shown to determine whether it is possible for the population to initially decline, even if it eventually grows, and the maxiumum R_δ was shown to determine whether it is possible for the population to initially grow, even if it declines. We re-emphasize the finding that while R_0 determines the long term dynamics of a system, it cannot also characterize the transient dynamics. We also advocate for further use of the next generation approach in ecology, as the next generation operators are often able to distil relevant ecological information into a simple operator.

Our model formulation as a set of age density equations, rather than a set of distributed delay equations, or partial differential equations, follows the work of Feng and Thieme (2000). There, arbitrary survival and maturation functions were used to model the progression of an infection with a finite number of infections stages, all of which have general length distributions. The generality of the survival and maturation functions used in our model allow us to calculate the next generation matrix for a wide breadth of model formulations. For example, in models of sea lice populations on salmon, studies have used a variety of different maturation functions. When discrete differential equations are used (Adams et al., 2015; Revie et al., 2005),

all lice of a given stage mature at the same age. The maturation function, $M_k^i(a)$, can then be formulated using step functions, as $M_k^i(a) = 1 - H(a - \tau)$. Here $H(a)$ is the Heaviside function and τ is the development time. When linear delay differential equations are used to model sea lice development (Stien et al., 2005), there is some minimum development time, after which sea lice mature at a constant rate. The maturation function for our model could then be written as $M_k^i(a) = 1 - H(a - \tau)(1-e^{-m(a-\tau)})$, where τ is now the minimum development time, and m is the constant rate of maturation. Weibull functions have the nice property that the probability of maturing is largest at some intermediate age, and have thus also been used to describe maturation functions, without requiring a fixed minimum development time or fixed maturation time (Aldrin et al., 2017). Here the maturation function can be written as $M_k^i(a) = e^{(-\lambda a)^p}$, where λ is the scale parameter, and p is the shape parameter for the Weibull distribution. Even though all of these models are formulated using different equations, by identifying the maturation and survival functions used, we can reformulate these models as age density equations, given by system 4.16, and therefore calculate the next generation matrix for all these different types of models using equation 2.5. However, our model explicitly calculates rates of larval movement using the Fokker-Plank equation, and therefore the arrival time component of our model and next generation matrix will remain different from the above mentioned models.

While the general structure of our model allows us to calculate the next generation matrix for a variety of survival and maturation functions, one of the limitations of our model is that we do not include density dependence. To include density dependence in our model, the partial differential equation formulation of the model would no longer be set a of McKendrick-von Foerster equations (Keyfitz and Keyfitz, 1997; McKendrick, 1925), as shown in Appendix 2.6.1. They could, however, be reformulated as a series of Gurtin McCamy equations (Gurtin and MacCamy, 1974), where now $\mu_k^i(a) = \mu_k^i(a, N_1^i, \ldots, N_m^i)$, and $B_k^i(t) = B_k^i(t, N_1^i, \ldots, N_m^i)$ where $N_k^i = \int_0^\infty n_k^i(t, a)da$. Most of the sea lice population models previously mentioned (Adams et al., 2015; Aldrin et al., 2017; Revie et al., 2005; Stien et al., 2005) do not include density dependence in their model formulations, as the assumption is that sea lice are regulated before they reach high enough densities to exhibit negative density dependence, and that there is no Allee affect at low densities. However, using Anderson-May host parasite equations, Krkošek et al. (2012b), demonstrated evidence of an Allee effect of sea lice on wild salmon, so that at low densities there is mate limitation, and thus a reduced birth rate. Modifying the birth rate of larvae to include mate limitation at low densities would be interesting future work. In mod-

elling the populations of other marine species on habitat patches, it has been shown that if external recruitment to populations is much larger than self-recruitment, then it is not necessary to include negative density dependence at high population densities to control for unbounded growth (Armsworth, 2002). However the inclusion of negative density dependence is necessary to prevent unbounded growth of populations when self recruitment to a population is large. The addition of density dependence to our model would therefore allow it to be applicable to a broader set of species at equilibrium densities.

With respect to sea lice on salmon farms, we use the advection diffusion equation to approximate hydrodynamic ocean flow between farms due to the success of modelling the transmission of nauplii onto wild salmon with the same advection diffusion equation. In the Broughton Archipelago, a region at the center of the debate of the effect of salmon farms on wild salmon, advection diffusion equations were used to model nauplii and copepodid movement, where nauplii were released as point sources from salmon farms (Krkošek et al., 2006a). Copepodids could then attach to wild salmon migrating past these salmon farms, and Krkošek et al. (2006a) were able to correlate the spatial distribution of sea lice on wild salmon with the spatial position of salmon farms. The accuracy of the approximation of ocean current using an advection diffusion equation in the Broughton Archipelago has been debated (Brooks, 2005), as well as the use of a constant maturation rate from nauplii to copepodids. We believe that the advection diffusion equation is a useful approximation to ocean circulation in channels, especially when hydrodynamic models are not available, though we include a general maturation delay in our model, so that the maturation of larvae can parameterized accurately to different species.

In the context of sea lice on salmon farms, we also estimated the effect of sea lice treatment on a salmon farm network using measures of both transient and asymptotic dynamics. In the next generation framework, we defined treatment as a reduction in the survival and/or maturation in the sessile stages on a farm. Salmon farms typically apply a parasiticide, emamectin benzoate, into the salmon feed to treat sea lice infestations (Rogers et al., 2013). We assumed that treating a salmon farm is therefore equivalent to reducing the survival through the different sessile stages on farm. We investigated the effect of treating the first, middle, and last farm in a channel. We found that treating the middle farm resulted in the greatest reduction in R_0, and that if either the first or last farm where treated, then the reduction in R_0 was the same. However, treating the first farm resulted in the greatest reduction in R_u, the maximum intergenerational growth rate, and treating the last farm resulted in the greatest reduction in R_l, the minimum intergenerational growth rate.

If we are interested in preventing long term outbreaks, reducing R_0 is important. However, in the case of the salmon aquaculture industry, frequent sea lice treatments prevent long term growth of sea lice. In this case it may be more important to prevent local outbreaks, as even local outbreaks of sea lice on salmon farms can have negative effects on migrating wild salmon (Bateman et al., 2016). Treating the first farm would thus most reduce the magnitude of a local outbreak. This result contradicts simulation studies of salmon farm dynamics in Scotland (Adams et al., 2015). This study found the farm influx (number of lice coming into a farm), was a better predictor of management impact than farm outflux (number of lice coming from a farm), even though when unmanaged lice density was accounted for, influx and management impact were only weakly correlated. In our work, relative influx can be calculated using the difference in row sums, and relative outflux could be calculated using relative column sums. In our model the first farm has the highest outflux, and the last farm in the channel has the highest influx. Perhaps this difference is due to the fact that the farm with the highest influx is most likely to outbreak, and thus treating that farm will be the most effective at reducing the total sea lice population. Whereas, if the farm with the highest outflux is treated, then the worst possible initial outbreak decreases, even if this initial outbreak is less likely to happen. The difference between the results found in this chapter and from Adams et al. (2015) highlight the complexity of designing effective management actions to control sea lice.

The largest limitation of our model, if applied to specific biological systems, is the use of the advection diffusion equation to approximate ocean movement, rather than a hydrodynamic model. While the advection diffusion equation may be a good approximation in a channel environment (Krkošek et al., 2006a), the use of a hydrodynamic model to approximate larval movement between patches rather than an advection diffusion equation would greatly improve the accuracy and relevance of the model to a specific region. Recently, there have been several studies which have used hydrodynamic models to accurately model the transmission of sea lice between salmon farms (Adams et al., 2015; Cantrell et al., 2018; Foreman et al., 2009), as well as the transmission of other marine larvae between population patches. These studies often quantify the amount of larval connectivity between patches by pairing particle tracking models with ocean circulation models, such as FVCOM (Chen et al., 2006). Connectivity matrices can then be constructed by tracking the number of particles released from one patch that pass by another patches. Most recently, Cantrell et al. (2018) used kernel density estimation on the output of the particle tracking model to quantify infection pressure of sea lice from a particular salmon farm. Depending on the method that these models use to estimate larval connectivity between patches, the

arrival time that we calculate in this chapter from the advection diffusion equation, could easily be calculated from these detailed hydrodynamic models. The connectivity matrices often calculated in these papers could then be reformulated as next generation matrices using survival and maturation functions specific to the species studied, so that the source-sink distribution of populations can be directly calculated, and so that the entries have a more relevant biological meaning. We believe that the combination of connectivity matrices from hydrodynamic models with next generation matrices is an exciting area of future work to understand the population dynamics of specific systems, and is our focus in Chapter 4 of this thesis.

2.6 Appendix for Chapter 2

2.6.1 Derivation from McKendrick-von Foerster PDE

Here we derive equation 4.5 by solving the McKendrick von-Foerster PDE:

$$\begin{aligned} \frac{\partial n_k^i(t,a)}{\partial t} + \frac{\partial n_k^i(t,a)}{\partial a} &= -\mu_k^i(a) n_k^i(t,a) \\ n_k^i(t,0) &= B_k^i(t) \\ n_k^i(0,a) &= \tilde{n}_k^i(a) \\ \mu_k^i(a) &= -\frac{\left(M_k^i(a) S_k^i(a)\right)'}{M_k^i(a) S_k^i(a)} \end{aligned} \tag{2.14}$$

First, for simplicity we drop the indexes k and i so that $n_k^i(t,a) = n(t,a)$. Then, we solve this linear partial differential equation using the method of characteristics. The goal is to reduce the partial differential equation into an ordinary differential equation of one variable along certain characteristic curves in a and t. To do this we parameterize $a = a(s)$ and $t = t(s)$, so that $n(t(s), a(s))$ is now a function of the single variable s. Differentiating $n(t(s), a(s))$ with respect to s:

$$\frac{dn}{ds} = \frac{\partial n}{\partial t}\frac{dt}{ds} + \frac{\partial n}{\partial a}\frac{da}{ds} \tag{2.15}$$

Now we choose the characteristic curves $a(s)$ and $t(s)$ such that

$$\frac{da}{ds} = 1 \quad \text{and} \quad \frac{dt}{ds} = 1.$$

Then substituting equation 2.14 into equation 2.15 we arrive at the ordinary differential equation:

$$\frac{d}{ds} n(t(s), a(s)) = -\mu(a(s)) n(t(s), a(s)) \tag{2.16}$$

Solving for the characteristic curves, $t(s)$ and $a(s)$, we find

$$t(s) = s + t_0 \quad \text{and} \quad a(s) = s + a_0.$$

Then, solving for $n(t(s), a(s))$ in equation 2.16 we find:

$$\begin{aligned} n(t(s), a(s)) &= n(t(0), a(0)) e^{-\int_0^s \mu(x+a_0)dx} \\ &= n(t(0), a(0)) e^{-\int_{a_0}^{a_0+s} \mu(y)dy} \\ &= n(t(0), a(0)) e^{\int_{a_0}^{a_0+s} \frac{(M(y)S(y))'}{M(y)S(y)}dy} \\ &= n(t(0), a(0)) e^{\int_{a_0}^{a_0+s} \frac{d}{dy}\log(M(y)S(y))dy} \\ &= n(t(0), a(0)) \frac{M(a_0+s)S(a_0+s)}{M(a_0)S(a_0)} \end{aligned} \tag{2.17}$$

Now we have two boundary conditions to impose, one at $t = 0$ and one at $a = 0$. Together, the two boundaries intersect all characteristic curves, and so equation 2.17 is the unique solution to equation 2.14 for all $a \geq$, $t \geq 0$. From the form of our characteristic equations for $a(s)$ and $t(s)$, it is clear that all characteristics are lines $t = a + b$ in the a-t plane. The line $t = a$ divides the a-t plane into two regions: $t \leq a$ and $t > a$. Characteristic curves for which $t \leq a$ intersect the boundary $t = 0$ at some point $(t, a) = (0, a_0)$. Substituting $t = s$ and $a = s + a_0$ into equation 2.17 we find

$$\begin{aligned} n(t, a) &= n(0, a - t)\frac{M(a)S(a)}{M(a-t)S(a-t)} \\ &= n_0(a - t)\frac{M(a)S(a)}{M(a-t)S(a-t)}. \end{aligned}$$

Similarly, characteristic curves for which $t > a$ intersect the $a = 0$ boundary at some point $(t, a) = (t_0, 0)$. Substituting $t = s + t_0$ and $a = s$ into equation 2.17, we find

$$\begin{aligned} n(t, a) &= n(t - a, 0)M(a)S(a) \\ &= B(t - a)M(a)S(a). \end{aligned}$$

Therefore together we have

$$n(t, a) = \begin{cases} B(t-a)M(a)S(a) & t > a \\ n_0(a-t)\frac{M(a)S(a)}{M(a-t)S(a-t)} & 0 < t < a \\ n_0(a) & t = 0 \end{cases}$$

Chapter 3

Reactivity, Attenuation, and Transients in Metapopulations

3.1 Introduction

Transient dynamics, those that occur over short timescales, can often be vastly different from the asymptotic or long term dynamics of ecological systems. However, throughout the history of mathematical biology much of the work has focused on determining the asymptotic dynamics of biological systems. While the study of long-term dynamics has given ecologists many tools to analyze the behaviour of populations, these tools are often not the same as those required to understand transient dynamics. Recently Hastings et al. (2018) have shown that transient dynamics are much more ubiquitous than previously assumed and long transients occur in many different ecological systems, from plankton and coral to voles and grouse. Studying the transient dynamics of an ecological system can give useful insight into the different processes that may occur after a disturbance, change in environmental conditions, or change in human intervention to a system. In some marine systems that are driven by environmental fluctuations, such as the Dungeness crab, transient dynamics may in fact be key to understanding how these systems behave (Higgins et al., 1997).

There has also been a recent push to characterize the different types of systems that display long transient dynamics that differ significantly from their asymptotic dynamics (Hastings, 2001; Hastings, 2004; Hastings et al., 2018; Morozov et al., 2020). Hastings et al. (2018) have loosely categorized four different drivers of long transient dynamics in ecological systems: ghost attractors and crawl-bys, slow-fast dynamics, high dimensionality, and stochastic noise. These categories are not always distinct and certain systems may indeed fall into multiple categories. For example, a predator prey system may have a crawl-by past a saddle that drives the transient

dynamics in this system, but this could also be thought of as a difference in timescales of the predator decline due to lack of prey. For metapopulations the main driver of transient dynamics is often the high dimensionality arising due to spatial structure, though these transient dynamics may be exacerbated by the other drivers as well.

Some of the earliest studies of systems that could generate long transients were systems with spatial structure (Hastings and Higgins, 1994; Lloyd and May, 1996). It seems intuitive that spatial structure or spatial heterogeneity can drive some sort of transient dynamics in a system. If individuals start in one location in a habitat, especially a poor habitat, then it will take time before they can spread over the entire habitat and the long-term population dynamics begin to emerge. What is surprising is that spatial structure can also give rise to so called long-lived transients, where the transient dynamics are extensive enough that they continue on timescales past which we typically measure biological populations (Hastings and Higgins, 1994).

One method of adding spatial structure to a population is to formulate it as a metapopulation, where distinct populations live on habitat patches that are connected via dispersal or migration. Metapopulation models were originally proposed by Levins (1969) to model patch occupancy in habitats consisting of isolated habitat patches, but these early models used space implicitly rather than explicitly. Later metapopulation models have included space explicitly by allowing for differing habitat quality on patches or differing dispersal between patches (Gyllenberg et al., 1997; Hanski and Thomas, 1994), though often these models are focused on the proportion of occupied patches rather than the population size on each patch. However, many marine metapopulation models as well as epidemiological metapopulation models explicitly track the number of individuals on each patch as well as movement or dispersal between patches (Arino and van den Driessche, 2003; Armsworth, 2002; Figueira and Crowder, 2006; Lloyd and May, 1996). In this chapter we model the metapopulation structure following this spatially explicit framework where individuals are tracked rather than the proportion of occupied patches.

Another benefit of the metapopulation framework is that habitat patches can be classified into source patches and sink patches. This classification can occur in many different ways (Figueira and Crowder, 2006; Krkošek and Lewis, 2010; Pulliam, 1988), but commonly a source is a productive habitat patch and a sink is a poor habitat patch. Early measures of sources and sinks were mainly focused on connectivity between patches, however more recently it has been understood that it is the interplay between patch connectivity and local patch productivity that characterizes patches as sources or sinks, especially in marine metapopulations. One of the new and easily tractable metrics that embodies this relationship comes from the theory of

next-generation matrices and the basic reproduction number, R_0. This framework, originally developed in epidemiology, has been used to characterize sources and sinks in populations of mussels, salmon, and sea lice on salmon farms (Harrington and Lewis, 2020; Huang and Lewis, 2015; Krkošek and Lewis, 2010).

While metapopulation theory has previously been used to classify patches as sources and sinks, other metrics have been used to characterize the transient dynamics of systems. Reactivity was initially introduced by Neubert and Caswell (1997) to measure the maximum initial growth rate of a system over all possible perturbations from an equilibrium. If the maximum initial growth rate is positive, then the system is reactive. Complementing reactivity is the amplification envelope, which is a measure of how large solutions can grow over time after initial perturbations. Later, Townley and Hodgson (2008) introduced attenuation as the opposite metric to measure initial decline of populations; a system attenuates if the minimum possible growth rate declines following a perturbation. Reactivity and attenuation are then most interesting when they are different from the stability of the equilibrium of a system — when a system attenuates but is unstable, or is reactive but stable — and it is on these situations that we focus this chapter. Biologically these are populations that begin by declining but eventually increase, or begin by increasing but eventually decline.

It should be noted that reactivity, attenuation and the amplification envelope are all defined from the linearization of a non-linear system about an equilibrium. These measures are therefore most useful around hyperbolic equilibria, where the dynamics of the non-linear system can be well approximated by the dynamics of the linear system. If an equilibrium is not hyperbolic, then the trajectories in the non-linear system may no longer be similar to the linearization by which reactivity, attenuation, and the amplification envelope are defined. Even around a hyperbolic equilibrium the trajectories of the non-linear and linearized systems may diverge as they move away from the equilibrium. Here we use the technique of linearization to determine reactivity and attenuation as others have before us, but want to emphasize these caveats as they are often brushed over in the transient literature.

In this chapter we apply these transient measures of growth to a class of biological metapopulation models where there is no migration between population patches, only birth on new patches. These are a subset of birth-jump processes (Hillen et al., 2015) and include models for marine meroplanktonic species, where larvae can travel through the ocean between population patches but adults remain confined to a habitat patch. Specific species that exhibit this structure include sea lice (Adams et al., 2015), corals and coral reef fish (Cowen et al., 2006; Jones et al., 2009), barnacles (Roughgarden et al., 1988), Dungeness crabs (Botsford et al., 1994), sea urchins

(Botsford et al., 1994), and many other benthic marine species (Cowen and Sponaugle, 2009). This type of system also encompasses many plant species where seeds are carried between suitable habitat patches (Husband and Barrett, 1996), and depending on the census timing could also include insect species where there is one large dispersal event between habitat patches, such as the spruce budworm (Ludwig et al., 1978; Morris, 1963; Williams and Liebhold, 2000) and mountain pine beetle (Safranyik and Carroll, 2007). Lastly this class of models also includes multi-patch or multi-city epidemiological metapopulation models where infections can spread between patches, for example infected residents of a city may travel and infect residents of other cities before returning home (Arino and van den Driessche, 2003). We focus on the transient dynamics that can occur around the extinction state of these systems.

The aims of this chapter are threefold. The first is of a technical nature: if we want to study reactivity and attenuation, what norm should we use and how do we calculate these quantities from the dynamical system? In section 3.2 we demonstrate how to calculate reactivity and attenuation using the biologically intuitive ℓ_1 norm in birth-jump metapopulations, and in section 3.6 we show how to add a weighting to this norm to calculate reactivity and attenuation if the metapopulation is stage-structured. The second aim of this chapter is pedagogical, to provide simple examples of metapopulations that exhibit interesting transient behaviour that is different from their asymptotic behaviour as well as transient behaviour that is different depending on the norm. In section 3.2 we provide examples that illuminate the difference between reactivity and attenuation in the ℓ_1 and ℓ_2 norms, in section 3.3 we provide examples that illustrate the potential difference between the transient and asymptotic dynamics of metapopulations, and in section 3.4 we provide an example of how increasing the number of habitat patches can accentuate this difference. The last aim of this chapter, and the focus of section 3.5, is to connect reactivity and attenuation to the source-sink classification of habitat patches, of which there exists a large body of literature in marine metapopulations, thus relating these instantaneous and generational transient measures of growth and decay.

Chronologically the chapter is structured as follows. In section 3.2 we use the ℓ_1 norm as a biologically intuitive measure of reactivity and attenuation in birth-jump metapopulations and provide examples to demonstrate how measurement in this norm differs from the commonly used ℓ_2 norm. In section 3.3 we use simple two-patch metapopulation examples to demonstrate that the transient dynamics of these systems can be vastly different from their asymptotic dynamics, and in section 3.4 we provide an example of how increasing the number of habitat patches in a metapopulation can enhance this difference. In section 3.5 we show how to connect

the reactivity and attenuation of a metapopulation to the source-sink classification of habitat patches, and in section 3.6 we show how to appropriately measure the reactivity and attenuation of a metapopulation when the population is stage structured using a weighted ℓ_1 norm.

3.2 Extending the general theory of transients to metapopulations

In this section we apply the metrics of reactivity (Neubert and Caswell, 1997) and attenuation (Townley and Hodgson, 2008) to the zero equilibrium of general systems of single-species metapopulations and thus focus on the transient dynamics that can occur around the extinction state of these systems. In order to present our work in a general form, we model the dynamics of a metapopulation of a single species on n patches around the zero equilibrium with the system:

$$x'(t) = Ax(t) \qquad x(0) = x_0, \tag{3.1}$$

where $A = [a_{ij}]$ is a real irreducible Metzler matrix ($a_{ij} \geq 0$ for all $i \neq j$) of order n, $x(t)$ is a population vector containing the population of the species on each patch, and the initial condition x_0 is a small perturbation of the zero equilibrium. This most often represents the linearization of a non-linear system, which more completely captures the dynamics of the population, but could also represent the full dynamics of a linear system if density dependence was not important to the population dynamics.

For the analyses in this chapter we focus on biologically realistic single-species metapopulations where the entries of $x(t)$ are non-negative when beginning with a non-negative initial perturbation, x_0. This condition is equivalent to requiring that A be an essentially non-negative (Metzler) matrix, such that all the off-diagonal entries of A are non-negative (Thm 2.4, Thieme (2009)). Biologically this means that the presence of individuals on one patch cannot contribute to the decline of a population on another patch and that the population on each patch will not become negative.

3.2.1 Reactivity and attenuation using the ℓ_1 norm

To analyze the transient dynamics of this metapopulation we begin by introducing some definitions from Neubert and Caswell (1997). An equilibrium is *reactive* if there is an initial perturbation x_0 such that the initial growth rate of the total population is positive. The mathematical definition of reactivity from Neubert and Caswell (1997),

using notation from Lutscher and Wang (2020), is:

$$\bar{\sigma}_\omega = \max_{||x_0||_\omega \neq 0} \left[\frac{1}{||x(t)||_\omega} \frac{d||x(t)||_\omega}{dt} \bigg|_{t=0} \right], \tag{3.2}$$

where $x(t)$ is a solution to eq. (3.1) and ω specifies the norm to be used to calculate reactivity, if the ℓ_1 norm is used then $\omega = 1$ and if the ℓ_2 norm is used then $\omega = 2$. If $\bar{\sigma}_\omega > 0$ then the equilibrium is reactive, and if $\bar{\sigma}_\omega \leq 0$ then the equilibrium is not reactive. Neubert and Caswell (1997) use the ℓ_2 norm to measure the population size and show that $\bar{\sigma}_2$ is the maximum eigenvalue of $(A + A^T)/2$. However, the ℓ_2 norm lacks a reasonable biological interpretation, and so others have instead used the ℓ_1 norm to define reactivity (Huang and Lewis, 2015; Stott et al., 2011; Townley et al., 2007). Biologically, the ℓ_1 norm,

$$||x||_1 = \sum_{i=1}^{n} |x_i|, \tag{3.3}$$

can be interpreted as the total population on all patches of a metapopulation whereas the ℓ_2 norm,

$$||x||_2 = \sqrt{\sum_{i=1}^{n} x_i^2}, \tag{3.4}$$

is the Euclidean distance of the total population away from the origin. We show in this work that the ℓ_1 norm is convenient to determine reactivity from the population matrix A in single species metapopulations.

In contrast, an equilibrium *attenuates* if there is an initial perturbation x_0 for which the initial growth rate of the total population declines (Townley and Hodgson, 2008). This is formally defined as

$$\underline{\sigma}_\omega = \min_{||x_0||_\omega \neq 0} \left[\frac{1}{||x(t)||_\omega} \frac{d||x(t)||_\omega}{dt} \bigg|_{t=0} \right]. \tag{3.5}$$

If $\underline{\sigma}_\omega < 0$ then the equilibrium attenuates, and if $\underline{\sigma}_\omega \geq 0$ then the equilibrium does not attenuate.

Comparing the definitions of attenuation and reactivity we can see that it is possible for an equilibrium to be both reactive and to attenuate, if there are certain initial perturbations for which $\bar{\sigma}_\omega > 0$ is achieved and others such that $\underline{\sigma}_\omega < 0$. In relation to the stability of an equilibrium, all stable equilibria attenuate and all unstable equilibria are reactive (Theorem 3.3). Reactivity and attenuation are then most interesting when they are different from the stability of the equilibrium: when an equilibrium is reactive but stable, so that the total population initially grows but

eventually declines, or when an equilibrium attenuates but is unstable, so that the total population declines but eventually grows. It should also be noted that the only systems that are not reactive and do not attenuate are those in which the total population size remains constant for all time. In this chapter we sometimes refer to the reactivity and attenuation of a system, rather than an equilibrium, and in this case we are referring to the reactivity and attenuation of the zero equilibrium, around which we have linearized a system.

The last measures that we define here to use in some later sections are the *amplification envelope* and the *maximum amplification*. The amplification envelope is the maximum possible deviation of a solution away from the steady state at time t after any initial perturbation x_0, which Neubert and Caswell (1997) define mathematically as:

$$\rho(t) = \max_{||x_0|| \neq 0} \frac{||x(t)||}{||x_0||}. \tag{3.6}$$

The maximum amplification is simply the maximum of the amplification envelope over all time:

$$\rho_{\max} = \max_{t \geq 0} \rho(t) = \max_{\substack{t \geq 0 \\ ||x_0|| \neq 0}} \frac{||x(t)||}{||x_0||}. \tag{3.7}$$

We do not use ω to differentiate between norms here as we only use the amplification envelope and maximum amplification with the ℓ_1 norm in sections 3.3.1 and 3.4. The amplification envelope need not be achieved by a single perturbation that produces a maximal solution for all time, rather different perturbations may produce the maximal deviation for different times. While reactivity and attenuation quantify the short time response to a perturbation, the amplification envelope and maximum amplification quantify how large a perturbation can become and how long growth can last. It is for these purposes that we use the amplification envelope and maximum amplification in sections 3.3.1 and 3.4.

Now before quantifying the reactivity and attenuation of the entire metapopulation, let us first determine the initial growth rate of the population if we begin with one individual on patch j. We call this initial growth rate λ_j, and mathematically we define

$$\lambda_j = \sum_{i=1}^{n} x_i'(0),$$

with $x_0 = e_j$, where e_j is the vector of length n with 1 in the jth entry and 0s elsewhere. In terms of system 3.1 this simplifies to the jth column sum of A,

$$\lambda_j = \sum_{i=1}^{n} a_{ij}.$$

The initial growth rate for a given patch j, λ_j, can also be calculated from the lifecycle digraph as the sum of all the outgoing birth rates from a patch minus the death rate on that patch, where any paths describing movement of individuals between patches are ignored. See figs. 3.3, 3.5, 3.7 and 3.8 for examples of lifecycle graphs and Caswell (2000) for further reference. We can then connect this patch specific initial growth rate with the total growth rate, or reactivity, using the following lemma.

Lemma 3.1. *Reactivity under the ℓ_1 norm in eq.* (3.2) *is equal to the maximum column sum of A in system (3.1),*

$$\bar{\sigma}_1 = \max_{1\le j\le n} \lambda_j = \max_{1\le j\le n} \sum_i a_{ij}.$$

Proof. Since $x_j \ge 0$ for all j, the absolute value signs in eq. (3.2) can be dropped and so

$$\begin{aligned}\bar{\sigma}_1 &= \max_{||x_0||_1=1} \left[\frac{d||x||_1}{dt}\bigg|_{t=0}\right] = \max_{||x_0||_1=1} \left[\frac{d}{dt}\sum_{i=1}^{n} x_i\bigg|_{t=0}\right] \\ &= \max_{||x_0||_1=1} \left[\sum_{i=1}^{n} \frac{d}{dt}x_i\bigg|_{t=0}\right] = \max_{||x_0||_1=1} \left[1^T x'\bigg|_{t=0}\right]\end{aligned}$$

where 1^T is a row vector where every entry is equal to 1. Substituting $x' = Ax$ from (3.1) gives

$$\bar{\sigma}_1 = \max_{||x_0||_1=1} \left[1^T A x_0\right] = \max_{||x_0||_1=1} \left[\sum_{j=1}^{n} \left(\sum_{i=1}^{n} a_{ij}\right) x_{0j}\right].$$

Now let k be such that $\sum_{i=1}^{n} a_{ik} = \max_{1\le j\le n} \sum_{i=1}^{n} a_{ij}$. Then, with $||x_0||_1 = 1$,

$$\sum_{j=1}^{n} \left(\sum_{i=1}^{n} a_{ij}\right) x_{0j} \le \left(\sum_{i=1}^{n} a_{ik}\right) \sum_{j=1}^{n} x_{0j} = \left(\sum_{i=1}^{n} a_{ik}\right),$$

with equality when $x_{0j} = \begin{cases} 1 & j = k \\ 0 & j \ne k \end{cases}$. Therefore

$$\bar{\sigma}_1 = \max_{1\le j\le n} \left(\sum_{i=1}^{n} a_{ij}\right) = \max_{1\le j\le n} \lambda_j.$$

□

With a similar proof we can connect the patch specific initial growth rate to attenuation via the following lemma:

Lemma 3.2. *Attenuation under the ℓ_1 norm in eq.* (3.5) *is equal to the minimum column sum of A in system (3.1),*

$$\underline{\sigma}_1 = \min_{1\leq j\leq n} \lambda_j = \min_{1\leq j\leq n} \sum_i a_{ij}.$$

It should be noted, as can be seen in the proof of Lemma 3.1, that the maximum possible growth rate occurs if the initial population is all on the patch with the maximum λ_j, and the minimum possible growth rate occurs if the initial population is all on the patch with the minimum λ_j.

3.2.2 Comparing reactivity in the ℓ_1 and ℓ_2 norms

Here we present some examples of systems that are reactive in ℓ_1 but not in ℓ_2 and vice versa to illuminate the difference between measuring reactivity in the two norms. It has previously been noted that reactivity depends on the norm and scaling (Lutscher and Wang, 2020; Neubert and Caswell, 1997) and the following examples help clarify the underlying biological and mathematical meaning of the two norms.

Example 1

First, we present an example that is reactive in ℓ_2 but not in ℓ_1. Reactivity in ℓ_2, $\bar{\sigma}_2$, can be calculated as the maximum eigenvalue of $(A + A^T)/2$ (Neubert and Caswell, 1997). Take system (3.1) with

$$A = \begin{bmatrix} -1 & 0 \\ 1 & 0 \end{bmatrix}.$$

This system simply redistributes individuals from patch 1 to patch 2, and the phase plane is shown in fig. 3.1. It is not reactive in the ℓ_1 norm ($\bar{\sigma}_1 \leq 0$) because the total population size is not increasing, but it is reactive in ℓ_2 ($\bar{\sigma}_2 > 0$). This highlights how measuring reactivity in the ℓ_2 norm can at times defy our biological expectation of what reactivity should mean — the growth of a population — and reinforces our rationale for using the ℓ_1 norm to measure reactivity in metapopulations. While the matrix A is reducible and this system is only semi-stable, and thus may be considered a borderline example, if a_{22} is replaced by a small negative number, $-\epsilon$, and a_{12} is replaced by a small positive number, $\epsilon/2$, then for sufficiently small ϵ, A will be irreducible and the system will now be stable, but will still be reactive in ℓ_2 and not in ℓ_1.

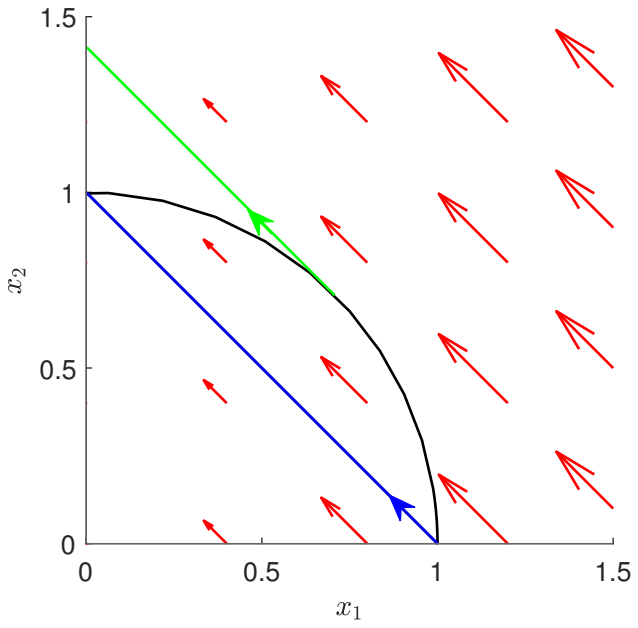

Figure 3.1: The phase plane for system (3.1) with $A = \begin{bmatrix} -1 & 0 \\ 1 & 0 \end{bmatrix}$, which is reactive in ℓ_2 but not in ℓ_1. The line $x_1 + x_2 = 1$ and the circle $x_1^2 + x_2^2 = 1$ geometrically depict $||x|| = 1$ in the ℓ_1 and ℓ_2 norms respectively. The derivative vectors for the phase plane are shown in red and two different initial trajectories are shown in green and blue. The green trajectory is an example that is reactive in ℓ_2, but not in ℓ_1, and the blue trajectory is another example that is not reactive in ℓ_1.

Example 2

The second example, which is reactive in ℓ_1 but not in ℓ_2 is system (3.1) with

$$A = \begin{bmatrix} -1 & 3/2 \\ 1/3 & -1 \end{bmatrix},$$

where the phase plane is shown in fig. 3.2. Now the system is reactive in ℓ_1 ($\bar{\sigma}_1 > 0$) because if we start with one individual on the second patch (the dynamics governed by the second row of A) the total population grows, but in such a way that it will not be reactive in ℓ_2 ($\bar{\sigma}_2 \leq 0$). This example demonstrates that again reactivity in ℓ_2 can defy our biological expectation of reactivity, but now in the opposite way. Here the total population grows, yet the system is not reactive in ℓ_2. Note that this system is equivalent to system (3.9) with $\epsilon = 3$.

Together, the two examples highlight the differences that can occur when measuring reactivity in different norms and the caution that should be taken when interpreting

reactivity in the ℓ_2 norm biologically. Here we only present examples that are reactive in ℓ_2 but not in ℓ_1 and vice versa but it is also possible to find examples of systems that attenuate in ℓ_2 but not in ℓ_1.

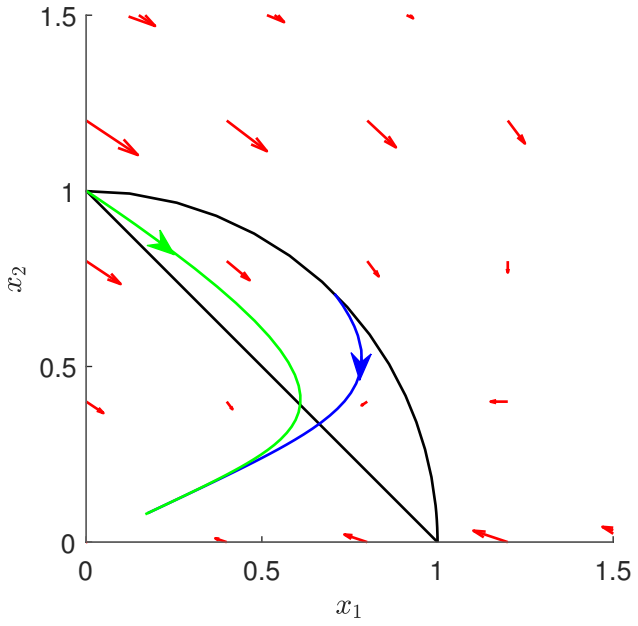

Figure 3.2: The phase plane for system (3.1) with $A = \begin{bmatrix} -1 & 3/2 \\ 1/3 & -1 \end{bmatrix}$, which is reactive in ℓ_1 but not in ℓ_2. The line $x_1 + x_2 = 1$ and the circle $x_1^2 + x_2^2 = 1$ geometrically depict $||x|| = 1$ in the ℓ_1 and ℓ_2 norms respectively. The derivative vectors for the phase plane are shown in red and two different initial trajectories are shown in green and blue. The green trajectory is an example that is reactive in ℓ_1, but not in ℓ_2, and the blue trajectory is another example that is not reactive in ℓ_2.

3.2.3 The relationship between stability and reactivity/attenuation

Now that we have presented two examples that demonstrate the difference between reactivity in the ℓ_1 and ℓ_2 norms, we show that in any norm if an equilibrium is asymptotically stable it attenuates, and if an equilibrium is unstable it is reactive.

Theorem 3.3. *If the $x = 0$ equilibrium for $x'(t) = Ax(t)$ is asymptotically stable and A is a Metzler matrix, then the system attenuates in any norm. Likewise if the $x = 0$ equilibrium is unstable then the system is reactive in any norm.*

Proof. Let $\mu(A)$ be the eigenvalue of A with the largest real part. The matrix A is Metzler and so $\mu(A)$ is a real eigenvalue of A with an associated nonnegative eigenvector v (Thm A.43, Thieme (2003)). The system with initial condition $x(0) = v$ then has solution of the form $x(t) = e^{\mu(A)t}v$. Due to the absolute homogeneity property of all norms, $||x(t)|| = ||e^{\mu(A)t}v|| = |e^{\mu(A)t}|||v|| = e^{\mu(A)t}||v||$. Therefore differentiating and setting $t = 0$ yields

$$\frac{1}{||x(t)||}\frac{d||x(t)||}{dt}\bigg|_{t=0} = \mu(A).$$

Now if the $x = 0$ equilibrium is asymptotically stable then $\mu(A) < 0$ and therefore the minimum in the definition of $\underline{\sigma}_\omega$ in eq. (3.5) is negative so the system attenuates. If the $x = 0$ equilibrium is unstable then $\mu(A) > 0$ and therefore the maximum in the definition of $\bar{\sigma}_\omega$ in eq. (3.2) is positive so the system is reactive. □

In this section we have shown how to calculate reactivity and attenuation using the ℓ_1 norm in metapopulations, proven that if the equilibrium of a system is unstable/stable then the system must be reactive/attenuate in any norm, and demonstrated the difference between reactivity in the ℓ_1 and ℓ_2 norms using two salient examples. We now return to the motivating feature of this chapter — systems that are reactive and stable or attenuate and are unstable — and in the following section we provide examples of long lived transients in these systems.

3.3 Metapopulations with arbitrarily large transient growth or decay

Here we examine two different metapopulations, one of which is reactive and can exhibit arbitrarily large transient growth, and the other that attenuates and can decline to arbitrarily small levels. In each case this transient growth differs from the system's long term growth trajectory: the metapopulation that exhibits large growth eventually declines, and the system that declines eventually grows. Both of these example metapopulations are linear systems, and therefore the addition of non-linearities to construct more realistic models could further exacerbate the length of the transient period. These examples are not meant to imply that there are realistic biological metapopulations that can grow arbitrarily large before decaying, but rather to emphasize that the difference between transient dynamics and asymptotic dynamics can be quite stark even in linear systems.

3.3.1 Arbitrarily large transient growth

First we present a reactive metapopulation that can exhibit arbitrarily large transient growth, but eventually declines. In this metapopulation individuals can either give birth to new individuals on the same patch, or give birth to individuals on the other patch, but there is no migration of individuals between patches. As mentioned in the introduction, this type of model is applicable to many marine metapopulations where adults are sedentary but larvae can disperse, to plant populations where seeds can be carried between habitat patches, or other populations governed by birth-jump processes. Let the metapopulation be described by:

$$\begin{aligned} x' &= rx + b_{12}y \\ y' &= b_{21}x + ry \end{aligned} \tag{3.8}$$

so that r is the on patch birth rate minus the death rate, b_{12} is the birth rate of individuals on patch 2 producing new individuals on patch 1, and b_{21} is the birth rate of individuals on patch 1 producing new individuals on patch 2. The system is linear, so assuming that $r^2 \neq b_{12}b_{21}$ the only steady state is $x = y = 0$.

For the metapopulation to eventually decline, both eigenvalues need to be negative. For system (3.8) the eigenvalues are $r + \sqrt{b_{12}b_{21}}$ and $r - \sqrt{b_{12}b_{21}}$ and thus we require that $r < 0$ and $r^2 > b_{12}b_{21}$. Now in order for the metapopulation to be reactive in the ℓ_1 norm we need either $b_{12} > -r$ or $b_{21} > -r$. Here we choose $b_{21} > -r$, so that if we start with one individual on patch 1, i.e. $x(0) = 1$, $y(0) = 0$, the metapopulation initially grows.

To prove that the metapopulation can grow arbitrarily large, we show that the limit as some parameter approaches 0 of $\max_t(x(t) + y(t))$ is unbounded. Along with the initial condition $x(0) = 1$, $y(0) = 0$, this is equivalent to showing that the limit of the maximum amplification in the ℓ_1 norm, $\rho_{\max}$, becomes unbounded. This equivalence is because the initial growth rate for patch 1, λ_1, is greater than the initial growth rate for patch 2, λ_2, and thus by Lemma 3.1 and the linearity of the system, the maximum amplification will be achieved by the unit perturbation $x(0) = 1$, $y(0) = 0$. To take the limit, we must first reduce the parameters in our system until we are left with a single parameter that we can let approach 0, while still maintaining the inequalities above that govern the stability and reactivity of the system. Let $r = -1$, $b_{12} = \epsilon/2$, and $b_{21} = 1/\epsilon$, where ϵ is a small positive parameter that approaches 0.

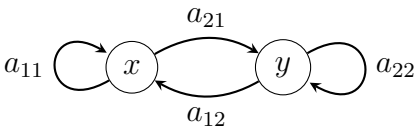

Figure 3.3: General life cycle digraph for a two-patch model, $\mathbf{x} = \mathbf{A}\mathbf{x}$, where $\mathbf{x} = \begin{bmatrix} x & y \end{bmatrix}^T$, and $\mathbf{A} = \begin{bmatrix} a_{11} & a_{12} \\ a_{21} & a_{22} \end{bmatrix}$. The directed edges represent the birth rate of individuals on the outgoing patch producing new individuals on the incoming patch. The self loops are the birth rate minus the death rate on a patch. In system (3.9), $a_{11} = -1$, $a_{12} = \epsilon/2$, $a_{21} = \epsilon^{-1}$, and $a_{22} = -1$. In system (3.12) $a_{11} = -1$, $a_{12} = \epsilon$, $a_{21} = \epsilon$, and $a_{22} = \epsilon$. In system (3.15) if $x_1 = x$ and $x_2 = y$ then $a_{11} = b_{11} - d_1$, $a_{12} = b_{12}$, $a_{21} = b_{21}$, and $a_{22} = b_{22} - d_2$.

Our reduced system can now be written as:

$$\begin{aligned} x' &= -x + \frac{\epsilon}{2} y \\ y' &= \frac{1}{\epsilon} x - y \\ x(0) = 1 \qquad & y(0) = 0. \end{aligned} \tag{3.9}$$

This system is stable and the digraph for this system is shown in fig. 3.3. This system is reactive in ℓ_1 and ℓ_2 for small ϵ and the solution is:

$$x(t) = \frac{1}{2}\left(e^{-(1-\frac{1}{\sqrt{2}})t} + e^{-(1+\frac{1}{\sqrt{2}})t}\right) \tag{3.10}$$

$$y(t) = \frac{1}{\sqrt{2}\epsilon}\left(e^{-(1-\frac{1}{\sqrt{2}})t} - e^{-(1+\frac{1}{\sqrt{2}})t}\right). \tag{3.11}$$

For each fixed t, $\lim_{\epsilon \to 0} y(t) = \infty$, and thus the metapopulation can grow arbitrarily large. For further details, see section 3.8.2.

Therefore even in a two patch metapopulation that is asymptotically stable, there is always a parameter combination for which the total population, and thus also the maximum amplification in the ℓ_1 norm, $\rho_{\max}$, can initially grow arbitrarily large before they decay. This is not meant to imply that there are realistic biological metapopulations that can grow arbitrarily large before decaying, but to emphasize how different the transient and asymptotic dynamics of a system can be.

3.3.2 Transient decay to arbitrarily small levels

We now present an example of a metapopulation that attenuates and can decay to an arbitrarily small population size before eventually growing. We again use a

metapopulation where individuals can either give birth to new individuals on their patch or on the other patch, but cannot migrate between patches. The difference between this metapopulation and the example used in the previous section, is that now the on patch birth and death rates differ between patches, but the between patch birth rates are the same. Let the metapopulation be described by:

$$\begin{aligned} x' &= r_1 x + \epsilon y \\ y' &= \epsilon x + r_2 y \end{aligned}$$

where r_1 is the birth rate minus the death rate on patch 1, r_2 is the birth rate minus the death rate on patch 2, and ϵ is the interpatch birth rate for both patches.

In order for the metapopulation to eventually grow, we assume that the birth rate is greater than the death rate on one of the patches. We choose this to be patch 2, thus we require $r_2 > 0$. We also want our population to initially decline when starting on patch 1, for this to occur we assume $r_1 + \epsilon < 0$. To prove that the metapopulation can decay to an arbitrarily small population size we reduce the system to have a single parameter and then show that the limit as the parameter approaches 0 of $\min_t(x(t) + y(t)) = 0$. Let $r_1 = -1$ and $r_2 = \epsilon$, then our system can be written in terms of a single positive parameter, ϵ, as:

$$\begin{aligned} x' &= -x + \epsilon y \\ y' &= \epsilon x + \epsilon y \\ x(0) = 1 \qquad & y(0) = 0. \end{aligned} \tag{3.12}$$

This system is unstable and the corresponding digraph is shown in fig. 3.3. It attenuates in both the ℓ_1 and ℓ_2 norms for small ϵ.

It is possible to show that the minimum population size can grow arbitrarily small in a manner similar to the previous section, though the calculations are somewhat more complicated. Instead in this section, we perform an asymptotic expansion in terms of ϵ to demonstrate the limiting behaviour of system (3.12). Let $x(t) = x_0(t) + \epsilon x_1(t) + O(\epsilon^2)$ and $y(t) = y_0(t) + \epsilon y_1(t) + O(\epsilon^2)$. Then the zero order system is:

$$\begin{aligned} x_0'(t) &= -x_0(t) \\ y_0'(t) &= 0 \\ x_0(0) = 1 \qquad & y_0(0) = 0, \end{aligned}$$

that has the solution $x_0(t) = e^{-t}$ and $y_0 = 0$. We can proceed in a similar manner to

solve the first order terms, and then our solution up to order ϵ is given by:

$$x(t) = e^{-t} + O(\epsilon^2)$$
$$y(t) = \epsilon(1 - e^{-t}) + O(\epsilon^2).$$

This solution is valid for small t, and is therefore our inner approximation. To find our outer approximation for large t, we rescale $t = \tau/\epsilon$ and arrive at the system:

$$\epsilon X' = -X + \epsilon Y$$
$$\epsilon Y' = \epsilon X + \epsilon Y.$$

We can again solve the zero order and first order equations and arrive at the following solution with two undetermined coefficients:

$$X(\tau) = \epsilon C e^{\tau} + O(\epsilon^2)$$
$$Y(\tau) = Ce^{\tau} + \epsilon(C\tau e^{\tau} + (C + K)e^{\tau}) + O(\epsilon^2).$$

To solve our undetermined coefficients we require that $\lim_{t\to\infty} x(t) = \lim_{\tau\to 0} X(\tau)$, and $\lim_{t\to\infty} y(t) = \lim_{\tau\to 0} Y(\tau)$. From $x(\infty) = X(0^+)$, we find $C = 0$. Substituting $C = 0$ into $y(\infty) = Y(0^+)$ to solve for K we find $K = 1$. Adding our inner and outer solutions together and subtracting the overlap ($x(\infty) = X(0^+) = 0$ and $y(\infty) = Y(0^+) = \epsilon$) we find

$$x(t) = e^{-t} + O(\epsilon^2)$$
$$y(t) = \epsilon(e^{\epsilon t} - e^{-t}) + O(\epsilon^2),$$

thus our total population size behaves as

$$x(t) + y(t) = e^{-t} + \epsilon(e^{\epsilon t} - e^{-t}) + O(\epsilon^2). \tag{3.13}$$

We can see from eq. (3.13) and fig. 3.4 that for very small ϵ, the total population size behaves similarly to e^{-t} before eventually growing. Thus for a minimum population threshold, we can always find an ϵ small enough, such that the solution crosses the threshold before the population grows. Alternatively, this can be proved by solving the full system and taking the minimum.

In this example the zero equilibrium is a saddle and as ϵ becomes arbitrarily small the initial condition becomes arbitrarily close to the stable manifold of the saddle. Therefore the trajectory remains close to the stable manifold for a long time before heading towards the unstable manifold. The construction and dynamics of this example are thus qualitatively different from the previous example where the zero equilibrium is stable and there is no unstable manifold present.

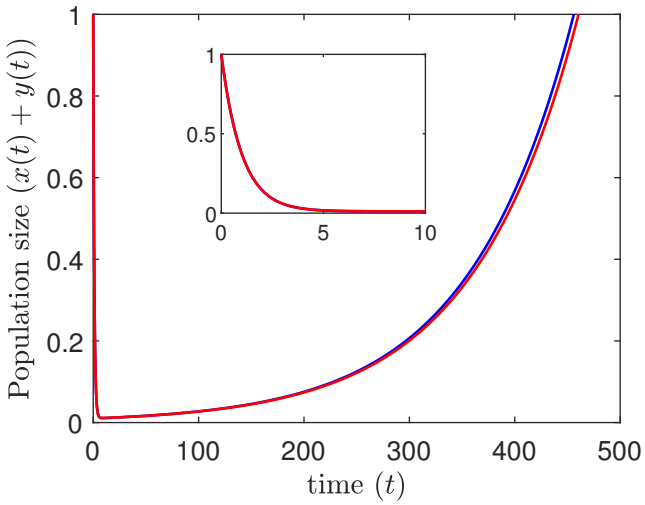

Figure 3.4: Asymptotic approximation of the total population size (red) compared to the true total population size (blue) for system (3.12), with $\epsilon = 0.01$. The asymptotic approximation is given by eq. (3.13).

Here we have shown that there are metapopulations for which the transient population can grow arbitrarily large or small, no matter the asymptotic stability of the system. In the next section we demonstrate how increasing the patch number can increase transient growth in certain metapopulations.

3.4 Increasing patch number increases transient timescale

In this section we show how in certain scenarios increasing the number of habitat patches in birth-jump metapopulations can prolong the transient growth away from a stable equilibrium. In aquatic systems, habitat patches may be quite productive, but strong drift downstream can sweep most larvae to the next patch, leading to large transient growth on downstream patches before the population eventually disappears from the last patch. This phenomenon can occur in metapopulations situated in rivers, ocean channels, or reef systems where reefs are arranged along a coastline with a directional current. Here we explore how advection, or drift, can cause large transient growth in these metapopulations.

Consider a metapopulation on n patches where the dynamics are described by the

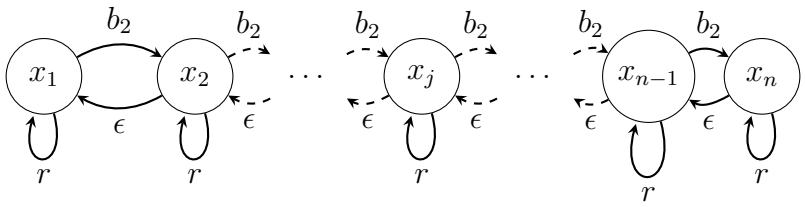

Figure 3.5: Digraph for system (3.14). The directed edges represent the birth rate of individuals on the outgoing patch producing new individuals on the incoming patch. The self loops are the birth rate minus the death rate on a patch.

following system of equations:

$$x' = Ax \qquad x(0) = x_0 \tag{3.14}$$

$$A = \begin{bmatrix} r & \epsilon & 0 & \dots & 0 \\ b_2 & r & \epsilon & \ddots & \vdots \\ 0 & b_2 & r & \ddots & \\ \vdots & \ddots & \ddots & \ddots & \epsilon \\ 0 & \dots & 0 & b_2 & r \end{bmatrix},$$

where r is the birth rate minus the death rate on each patch, b_2 is the birth rate of patch $j-1$ on patch j, ϵ is the birth rate from patch $j+1$ to patch j, and e_1 is a vector with 1 in the first entry and 0s elsewhere. The parameters b_2, and ϵ are positive and r is negative. The digraph for this system is shown in fig. 3.5.

The instantaneous measures of growth, λ_j, and reactivity in the ℓ_1 norm, $\bar{\sigma}_1$, are therefore $\lambda_1 = r+b_2$, $\lambda_j = r+b_2+\epsilon$ for $j = 2, \dots, n-1$, $\lambda_n = r+\epsilon$, and $\bar{\sigma}_1 = r+b_2+\epsilon$. Let $r+\epsilon < 0$ and $r+b_2 > 0$, then the system is reactive ($\bar{\sigma}_1 > 0$), and this maximum initial growth rate is achieved if the initial population is all on any patch except for patch 1 or n, though if the initial population starts on patch 1 the initial growth rate is still positive. In system (3.14) A is a tridiagonal Toeplitz matrix, so it has eigenvalues (Noschese et al., 2013)

$$\lambda_h = r + 2\sqrt{b_2\epsilon}\cos\left(\frac{h\pi}{n+1}\right) \qquad\qquad h = 1, \dots, n,$$

and corresponding right eigenvectors, v_h, where the kth entry is given by

$$v_{h,k} = (b_2/\epsilon)^{k/2}\sin\left(\frac{hk\pi}{n+1}\right) \qquad\qquad k = 1, \dots, n; h = 1, \dots, n.$$

The solution to system (3.14), with initial condition $x_0 = e_1$, can therefore be written as

$$x(t) = We^{Jt}W^{-1}e_1,$$

where W is a matrix containing the eigenvectors, v_h, and J is a diagonal matrix with the eigenvalues, λ_h, on the diagonal. For all but very small t the solution $x(t)$ is approximately equal to the amplification envelope in the ℓ_1 norm, $\rho(t)$, defined by eq. (3.6). Through examination of the eigenvalues, this system is stable if ϵ is small enough such that $r + 2\sqrt{b_2\epsilon} < 0$. Parameters that satisfy the inequalities that determine stability and reactivity in the ℓ_1 norm can be found in the caption of fig. 3.6. In this case the maximum total population size, and also maximum amplification, are given by

$$x_{\max} = \rho_{\max} = \max_{t\geq 0} 1^T W e^{Jt} W^{-1} e_1,$$

with the corresponding time $t_{\max}$, which is the value of t for which the maximum occurs. The last measure of transience that is useful in this system is the total transient time, t_{total}, which we define as the time it takes for the population size to decline below one, after initially starting with one individual, or

$$t_{\text{total}} = \min\{t > 0 : 1^T W e^{Jt} W^{-1} e_1 \leq 1\}.$$

So how does the number of patches affect the magnitude and length of transients? In fig. 3.6, which compares a 5 and 15 patch system, we can see that increasing the patch number increases both the magnitude of growth and the duration.

Here it can be difficult to see the duration of transience exhibited by all patches on a regular scale, but on the log scale we can see that all patches except for patch 1 experience a large period of transient growth, before they decay below 1 individual (fig. 3.6, dashed line). Patch 1 does not experience a large period of growth because the internal growth rate, r, is negative and the birth rate from patch 2 to patch 1, ϵ, is too small to overcome this negative internal growth rate.

What cannot be seen from fig. 3.6 is the dependence of transient growth on system parameters. We find that decreasing b_2 in system (3.14) results in a large decrease in the maximum population size (and maximum amplification), $x_{\max}$ (ρ_{max}), and the total transient time, t_{total}, but only a small decrease in the time at which the maximum population size is achieved, $t_{\max}$. Decreasing r however, results in a large decrease in $x_{\max}$ ($\rho_{\max}$), $t_{\max}$, and t_{total}.

The relationship between increased transient time and number of patches can also be found for a linear metapopulation where all patches have negative initial growth rates, λ_j, except for the last patch which has a positive initial growth rate. In this case the total population size decays for a long time before it eventually grows, and the time that it decays depends on the number of patches.

We can see then that for a linear metapopulation, the length of the linear array

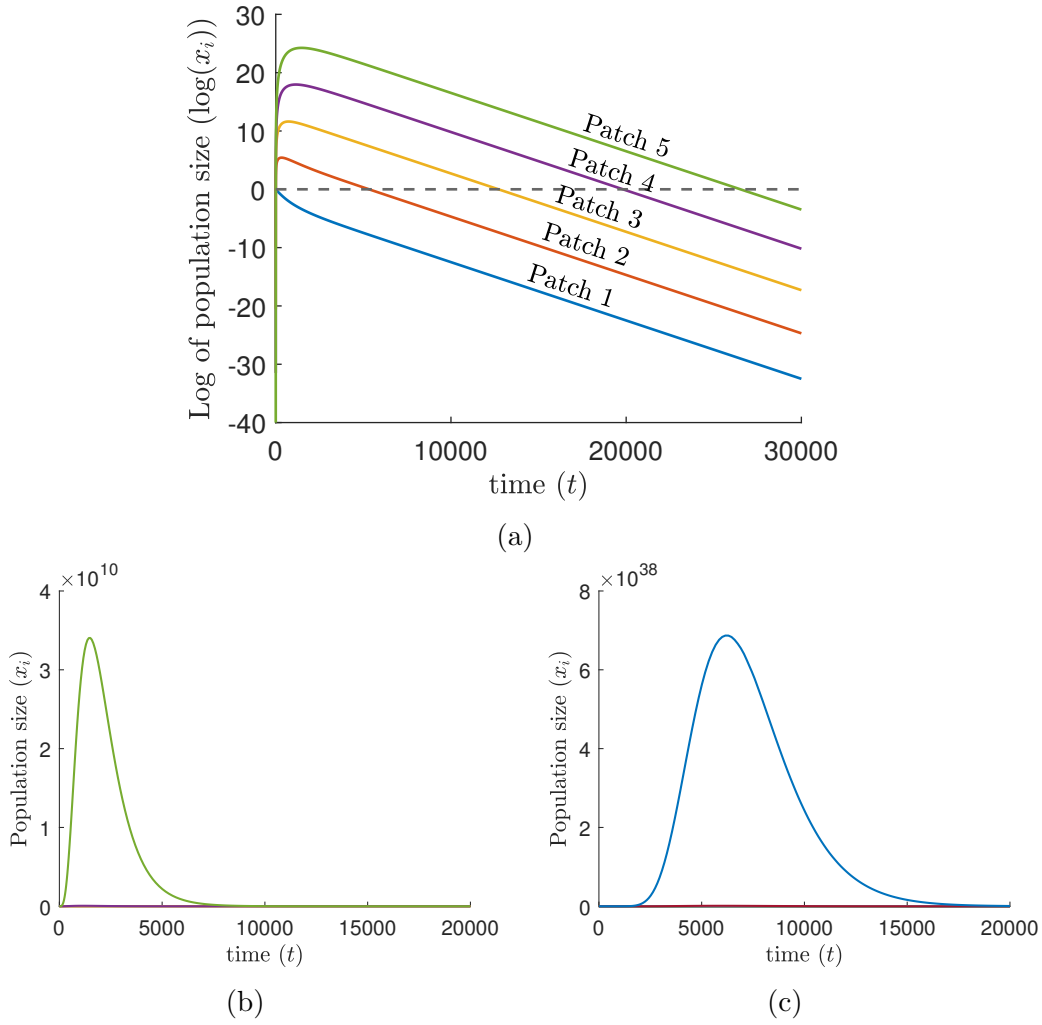

Figure 3.6: The population sizes on each patch for the advective system (3.14) with the initial condition $x_0 = e_1$, so that one individual is initially on patch 1. In a) the population sizes are shown on a log scale for a metapopulation of 5 patches, and in b) and c) the population sizes are shown for a metapopulation of 5 and 15 patches respectively. On the untransformed scale only the population size on the last patch can be seen as it is far larger than on any of the other patches, whereas on the log scale the population sizes of all patches can be seen. Parameters for this simulation are $r = -0.00345$, $\epsilon = 0.000001$, and $b_2 = 2$, chosen so that system (3.14) is reactive but stable.

can accentuate the transient growth that is possible in the system and that this is especially true for advective systems where there is some sort of directed birth in one direction in the array. Systems with this type of advective flow include marine metapopulations located in channels near the mouth of rivers, or long coral reefs that are captured inside of a dominant coastal current flow. To the best of our

knowledge, this form of advection-driven transient has not been previously reported in the literature. However, related literature (eg. Byers and Pringle (2006)) models the effect of advection on population persistence and range shifts.

Having presented some illuminating metapopulation examples that demonstrate the magnitude that transient dynamics can differ from asymptotic dynamics, we now turn back to the general theory of transients in metapopulations and connect it to the source-sink classification of habitat patches.

3.5 Connecting the source-sink dynamics to the transient dynamics

In this section we demonstrate how to connect the transient measures of initial population growth to the source-sink classification of habitat patches in the metapopulation, with a focus on marine metapopulations. There are several marine metapopulations for which habitat patches have been classified as sources or sinks (Bode et al., 2006; Figueira, 2009; Theuerkauf et al., 2021) as defining the contribution of a habitat patch and the classification of habitat patches as sources or sinks is an important aspect in the design of marine reserves (Figueira and Crowder, 2006). Here we connect the source-sink classification of a habitat patch to the transient dynamics that may occur if metapopulations are perturbed at low densities.

For the transient measure of the patch specific contribution to the initial growth of the total population we use λ_j, previously defined in section 3.2. To classify habitat patches as sources or sinks we use the next-generation matrix, K. Next-generation operators have previously been used to classify source and sink regions in heterogenous environments (Harrington and Lewis, 2020; Huang et al., 2016; Krkošek and Lewis, 2010; Mckenzie et al., 2012a). In order to calculate the next-generation matrix for system (3.1) we decompose $A = F - V$, where F is a non-negative matrix with positive entries that describe the birth of new individuals in the metapopulation, and V is a non-singular M matrix (Berman and Plemmons, 1994) with entries that describe the transfer of individuals between compartments or in this case habitat patches, and also includes the death of individuals (van den Driessche and Watmough, 2002). Examples 3, 4, and 5 illustrate the decomposition of A into F and V. Because V is a non-singular M matrix, V^{-1} is non-negative. The next-generation matrix, $K = [k_{ij}]$, can then be calculated as $K = FV^{-1}$ (van den Driessche and Watmough, 2002). This next generation matrix is then commonly used to calculate the basic reproduction number R_0, which is the average number of new individuals produced by one initial individual, and is defined as the spectral radius of K. However we can

also define R_j as the number of new individuals produced on all patches from one initial individual starting on patch j, that can then be calculated as:

$$R_j = \sum_{i=1}^{n} k_{ij}.$$

In Chapter 2 of this thesis we used the notation $R_\delta(j)$ to denote the jth column sum of K, as we were differentiating between $R_\delta(j)$, $R_c(j)$, R_0, R_u, and R_l. In this chapter and the remaining chapters we use R_j instead to simplify the notation as we now only refer to R_j and R_0. We classify patch j as a *source* if $R_j > 1$, as then one individual on patch j would produce more than one individual in the total metapopulation. Likewise we classify patch j as a *sink* if $R_j < 1$, because in this case an individual cannot replace itself in the metapopulation. In the following sections we often refer to R_j as the source-sink classification of a habitat patch because while R_j is a number it can also be used to classify habitat patches as sources ($R_j > 1$) or sinks ($R_j < 1$).

3.5.1 Expressing R_0 as a weighted sum of R_j

Before examining the connection between R_j and the initial growth λ_j, we first highlight a connection between R_j and R_0. It turns out, as shown in the following Lemma, that R_0 can be calculated as a weighted sum of each R_j, and surprisingly this relationship between the spectral radius and the column sums of a matrix does not require any further assumptions on the matrix structure, though if the matrix is not non-negative, the components of the right eigenvector need not be real. Here 1^T is the row vector with each entry equal to 1, and e_j is the vector with the only non-zero entry being 1 in the jth row.

Theorem 3.4. *Let $v = [v_i]$ be the right eigenvector associated with the dominant eigenvalue of the next-generation matrix, $\mathcal{R}_0$, normalized so $\sum_{1\le i\le n} v_i = 1$. Then the basic reproduction number $\mathcal{R}_0 = \sum_{1\le j\le n} R_j v_j$, where $R_j = 1^T K e_j = \sum_{i=1}^{n} k_{ij}$.*

Proof. First, we can rewrite $\mathcal{R}_0$ as

$$\mathcal{R}_0 = \mathcal{R}_0 1^T v = 1^T \mathcal{R}_0 v,$$

because the eigenvector has been normalized to sum to 1. Then, as $\mathcal{R}_0$ is the eigenvalue of K associated with v and the column sums of K are R_j,

$$\mathcal{R}_0 = 1^T \mathcal{R}_0 v = 1^T K v = \begin{bmatrix} R_1 & R_2 & \dots & R_n \end{bmatrix} v = \sum_{j=1}^{n} R_j v_j.$$

□

The entries v_j of the right eigenvector can be interpreted as the probability that a new individual begins on patch j (Cushing and Diekmann, 2016). Therefore $\mathcal{R}_0$ can be interpreted as the sum over all patches, of the probability that an individual is born on patch j, multiplied by the number of new individuals it will produce on all other patches over its lifetime.

Similarly, if we define λ_0 to be the dominant eigenvalue of A, with the associated normalized eigenvector u, then

$$\lambda_0 = 1^T A u = \sum_{j=1}^{n} \sum_{i=1}^{n} a_{ij} u_j = \sum_{j=1}^{n} \lambda_j u_j,$$

where it should be noted that λ_j is the jth column sum of A, rather than an eigenvalue of A.

3.5.2 Connecting the source-sink classification, R_j, to the initial growth rate, λ_j

Now that we have decomposed the dominant eigenvalues, R_0 and λ_0, into weighted sums of the columns of K and A respectively, we proceed to connect the source-sink classification of a particular patch, R_j, to the initial growth from an individual on that patch, λ_j. To do so there are some restrictions that we need to impose on our metapopulation system and this is where we limit our study to marine or birth-jump metapopulation models where juveniles or seeds can disperse between patches while adults remain confined to habitat patches. The mathematical restriction defined by this class of models comes from the decomposition of A into $F - V$. Here V contains all entries that describe the transfer of individuals between compartments or patches. For the results presented in this section, we require that V has the following reducible form:

$$V = \begin{bmatrix} V_{11} & 0 \\ V_{21} & D \end{bmatrix},$$

where V_{11} is $k \times k$, $D = \text{diag}(d_{k+1}, \ldots, d_n)$ with $d_{k+1}, \ldots, d_n$ all positive, $0 \leq k \leq n-1$, and V is a non-singular M matrix.

With this structure, individuals on patches $j = k+1, \ldots, n$ cannot migrate between patches, but can still give birth to new individuals on any patch. Under this structure, we first present proofs connecting our instantaneous and generational growth measures, λ_j and R_j, before presenting a two patch example. If V is completely diagonal, then there is no migration between any patches, only birth on other patches. This is

the case for models of plants with seed dispersal, or simplified marine metapopulation models if the juvenile stage is not explicitly modelled.

Theorem 3.5. *Let $A = F - V$ for system (3.1), where F is non-negative, and V is a non-singular M matrix with the following form:*

$$V = \begin{bmatrix} V_{11} & 0 \\ V_{21} & D \end{bmatrix},$$

where V_{11} is $k \times k$, $D = \mathrm{diag}(d_{k+1}, \ldots, d_n)$ with $d_{k+1}, \ldots, d_n$ all positive, and $0 \leq k \leq n-1$. For $k+1 \leq j \leq n$, λ_j is positive if and only if $R_j > 1$.

Proof. First, we can write λ_j as

$$\lambda_j = \sum_{i=1}^{n} a_{ij} = 1^T A e_j.$$

Then decomposing A into $F - V$, and inserting $V^{-1}V$

$$\lambda_j = 1^T(F-V)e_j = 1^T(F-V)V^{-1}Ve_j = 1^T(FV^{-1} - I)Ve_j.$$

For $k+1 \leq j \leq n$, V is diagonal, so $Ve_j = d_j e_j$. Therefore

$$\lambda_j = 1^T(FV^{-1} - I)d_j e_j = (R_j - 1)d_j.$$

Now $d_j > 0$, and thus $\lambda_j > 0$ if and only if $R_j > 1$. □

Corollary 3.6. *In the notation of Theorem 3.5, if V is diagonal, then $\lambda_j > 0$ if and only if $R_j > 1$ for $j = 1, \ldots, n$.*

Corollary 3.7. *Under the same conditions as Theorem 3.5, $\bar{\sigma}_1 > 0$ if $\max_{k+1 \leq j \leq n} R_j > 1$, and $\underline{\sigma}_1 < 0$ if $\min_{k+1 \leq i \leq n} R_i < 1$.*

Proof. Under the conditions in Theorem 3.5, we know that $R_j - 1$ has the same sign as λ_j for $k+1 \leq j \leq n$. Therefore if $\max_{k+1 \leq j \leq n} R_j > 1$ then $\bar{\sigma}_1 = \max_{1 \leq j \leq n} \lambda_j > 0$, i.e. the system is reactive. Similarly if $\min_{k+1 \leq j \leq n} R_j < 1$ then $\underline{\sigma}_1 = \min_{1 \leq j \leq n} \lambda_j < 0$, i.e. the population attenuates. □

Corollary 3.8. *Under the same conditions of Theorem 3.5, only with V diagonal, then $\bar{\sigma}_1 > 0$ if and only if $\max_{1 \leq j \leq n} R_j > 1$ and $\underline{\sigma}_1 < 0$ if and only if $\min_{1 \leq j \leq n} R_j < 1$.*

Proof. From Corollary 3.6, $\lambda_j > 0$ if and only if $R_j > 1$ for each patch j. Therefore if $\bar{\sigma}_1 = \max_{1 \leq j \leq n} \lambda_j > 0$, then $\max_{1 \leq j \leq n} R_j > 1$, and likewise if $\max_{1 \leq j \leq n} R_j > 1$, then $\bar{\sigma}_1 > 0$. The same argument holds for $\min_{1 \leq j \leq n} \lambda_j$ and $\min_{1 \leq j \leq n} R_j$. □

Now that we have presented theory connecting the initial growth rate, λ_j, to the source-sink classification of patch, R_j, we present an example to illustrate how to calculate these growth rate and source-sink measures and how Theorem 3.5 and Corollaries 3.6 and 3.8 can be used to connect them.

Example 3

Here we present an example of a metapopulation consisting of two habitat patches, patch 1 and patch 2. New individuals can be born on either patch, but no individuals can migrate between patches. This system represents a simplification of the adult dynamics of many marine meroplanktonic metapopulations, where dispersal between patches occurs at the larval stage, rather than the sedentary adult stage. This system could also represent plant metapopulations that spread through seed dispersal, if the habitat landscape is patchy. The metapopulation dynamics can be represented with the following set of ODEs:

$$\begin{aligned} x_1' &= b_{11}x_1 + b_{12}x_2 - d_1x_1 \\ x_2' &= b_{21}x_1 + b_{22}x_2 - d_2x_2, \end{aligned} \tag{3.15}$$

where b_{ij} is the birth rate for births from patch j to patch i, and d_i is the death rate on patch i. The lifecycle graph for this system is shown in fig. 3.3.

We then decompose $A = F - V$ and construct the next generation matrix, $K = FV^{-1}$:

$$A = \begin{bmatrix} b_{11} - d_1 & b_{12} \\ b_{21} & b_{22} - d_2 \end{bmatrix}, \quad F = \begin{bmatrix} b_{11} & b_{12} \\ b_{21} & b_{22} \end{bmatrix}, \quad V = \begin{bmatrix} d_1 & 0 \\ 0 & d_2 \end{bmatrix},$$

$$K = FV^{-1} = \begin{bmatrix} b_{11}/d_1 & b_{12}/d_2 \\ b_{21}/d_1 & b_{22}/d_2 \end{bmatrix}.$$

For an initial individual starting on patch 1, the expected lifetime is $1/d_1$, and the rate that the individual is producing new individuals on both patches is $b_{11} + b_{21}$. Therefore $R_1 = (b_{11} + b_{21})/d_1$ is the total number of individuals born onto both patch 1 and patch 2 over one generation. It is clear that $\lambda_1 = b_{11} + b_{21} - d_1 > 0$ if and only if $R_1 = \frac{b_{11}}{d_1} + \frac{b_{21}}{d_1} > 1$, in accordance with Corollary 3.6. Similarly $\lambda_2 = b_{12} + b_{22} - d_2 > 0$ if and only if $R_2 = \frac{b_{12}}{d_2} + \frac{b_{22}}{d_2} > 1$. The system is therefore reactive if $\max(R_1, R_2) > 1$ (Corollary 3.8).

At first glance it seems obvious that if an individual starts on a source patch the population should have a positive initial growth rate or if the population starts on

a sink patch it should have a negative initial growth rate, and we have shown from Corollary 3.6 and 3.5.2 that this is indeed the case for marine metapopulations. What is perhaps surprising is that this is not the case for general metapopulations when adults can migrate between habitat patches, and thus when the conditions of Theorem 3.5 and Corollary 3.6 are not met. In the general case it is possible to start with an individual on a source patch, but for the population to initially decline and likewise to start on a sink patch but for the population to initially grow. An example of such a metapopulation is shown in section 3.8.1.

Here in this section we have shown that for marine metapopulations and other metapopulations where the population dynamics are defined by birth-jump processes, there is a one-to-one relationship between the source-sink classification of a patch and the initial growth rate when starting with one adult on a patch. That is, the initial population growth rate is positive if we start with one adult on patch j if and only if patch j is a source, and the initial growth rate is negative if and only if patch j is a sink. This is a useful relationship biologically as there are several marine metapopulations where patches have already been classified into sources and sinks, and thus the transient dynamics for these systems can now be better understood.

3.6 Stage structure

In this section we add stage structure to demonstrate some of the nuances in analysing transients in stage structured metapopulation models. The main issue with analysing reactivity and attenuation in models with stage structure is due to the fact that adults often give birth to many more juveniles than will survive to become adults, and that juveniles cannot normally give birth to new juveniles. This presents a few complications.

The first complication is the fact that if we want to analyse the initial growth or decay of a population, starting with an individual in a patch, it now depends if the individual is a juvenile or an adult. If we start with a juvenile, then there is no way that the total population, or even the patch population, can grow, given that the juvenile has to first survive to the adult stage to give birth to new juveniles. Thus we want to start with one adult on a patch.

However, if we start with an adult in a patch, and it gives birth to new juveniles, how do we count these new juveniles? If we are considering a marine metapopulation do we count every larvae as a new individual? If so, every marine metapopulation would exhibit transience, as each adult often produces thousands of larvae. This then begs the question: in a stage structured metapopulation, can we scale the ju-

venile population so that transient measures of population growth, such as reactivity and attenuation, are useful for stage structured models and measure the biologically relevant quantities?

To motivate the necessity of an honest scaling we highlight a discrete time example of transients in Dungeness crabs from Caswell and Neubert (2005). Dungeness crabs give birth to an enormous number of larvae, many of which do not survive to settle and become juveniles after one year. In this case the discrete time model requires a census time to measure new crabs after one year. If the census is taken pre breeding, then the system exhibits little reactivity, as many of the larvae that where initially born have not survived to become one year old juveniles. However, it the census is taken post breeding, then all of the eggs or larvae are counted and the initial amplification is increased by 10^5. The models considered in this chapter are continuous time and do not face this exact problem, but it is easy to see that the addition of a larvae stage in a marine stage structured metapopulation has large effects on the reactivity of the system.

Returning then to our stage structured model with only juvenile and adult stages, how should the juvenile stage be scaled so that an initial growth in juveniles also corresponds in some sense to growth in the total population? Ideally, we would scale the juvenile population so that each juvenile is scaled by the probability that it will become an adult. If we scale our population in this way then the measures of reactivity and attenuation regain their original meaning. If the maximum initial growth rate of our population, now scaled to be in terms of adults, is positive then our system is reactive, and if the minimum is negative then it attenuates.

A biologically relevant measure of reactivity in a stage structured model must then be focused on the initial growth rate of the population, calculated so that the growth rates of juveniles are scaled by their contribution to the adult population. Under this scaling if any adult on any habitat patch produces many juveniles, but less than one become viable adults, then such a metapopulation is not reactive. Whereas if there is a patch such that one adult produces many juveniles and more than one survive to adulthood then the metapopulation is reactive, because the stage structured population, where juveniles are scaled according to their contribution to the adult population, is growing.

In the following sections we formally define such a scaling using a weighted ℓ_1 norm, and contrast it with the unweighted ℓ_1 norm that we have previously been using to calculated reactivity in metapopulations without stage structure.

3.6.1 Unweighted ℓ^1

We want to measure reactivity and attenuation as the total initial growth rate of the population, measured using either the weighted or unweighted norm, when we start with one adult on a patch. We first present the unweighted ℓ^1 measure of the initial growth rate to demonstrate the mathematical framework that we use to examine reactivity in a stage-structured population with juveniles and adults.

Consider a population with juvenile and adult stages on n patches. Let the population dynamics be described by

$$x'(t) = Ax(t), \tag{3.16}$$

where A is a $2n \times 2n$ matrix, arranged A so that all ODEs describing the change in the adult populations are in rows $n+1$ to $2n$. Decompose A into $A = F - V$, where F is non-negative with positive entries that describe the birth of new individuals in the metapopulation, and V is a non-singular M matrix (Berman and Plemmons, 1994) (V^{-1} is non-negative) with entries that describe the transfer of individuals between compartments or in this case habitat patches, and also includes the death of individuals (van den Driessche and Watmough, 2002). We are interested in metapopulations where adults can give birth to juveniles, but juveniles cannot give birth to new juveniles, so F and V can be written in block form as follows:

$$F = \begin{bmatrix} 0 & F_{12} \\ 0 & 0 \end{bmatrix}, \quad V = \begin{bmatrix} V_{11} & 0 \\ V_{21} & V_{22} \end{bmatrix}. \tag{3.17}$$

With this decomposition F_{12} contains all the new juvenile births from each adult patch, V_{11} is a diagonal matrix that contains the rates of juvenile mortality on each patch as well as the maturation from juveniles to adults, V_{22} is a diagonal matrix that contains the rates of adult mortality on each patch, and V_{21} contains the negative of the rates of maturation/migration from juveniles to adults.

We define $\tilde{\lambda}_j$ to be the initial population growth rate, starting with one adult on patch j, measured using the ℓ_1 norm. This can be defined mathematically for $1 \leq j \leq n$ as

$$\tilde{\lambda}_j = \underbrace{\sum_{i=1}^{n} x_i'(0)}_{\text{juvenile}} + \underbrace{\sum_{i=n+1}^{2n} x_i'(0)}_{\text{adult}}, \quad x(0) = e_{j+n}.$$

In terms of F and V

$$\tilde{\lambda}_j = \sum_{i=1}^{n} f_{12ij} - \sum_{i=1}^{n} v_{22ij},$$

where f_{12ij} and v_{22ij} are the (i,j) entries of F_{12} and V_{22} respectively.

We use the tilde to differentiate the initial growth rate in the stage structured population, where we specifically begin with one adult on a patch, from the initial growth rate in a population without stage structure, where there is no difference in the type of individual that we start with. Having presented the mathematical framework that we use to measure reactivity in a stage structured population using the unweighted ℓ_1 norm, we now use a weighted ℓ_1 norm that better captures the biological meaning of reactivity.

3.6.2 Weighted ℓ^1 for each patch

In order to measure reactivity in a biologically meaningful fashion, we introduce a new measure of the initial population growth rate, $\tilde{\lambda}_j^p$. This initial population growth rate is calculated using a weighted ℓ_1 norm so that the adult population is still measured using the regular ℓ_1 norm, but the juvenile population on each patch is scaled by the probability that the juveniles survive to adulthood; the patch specific nature of the weighing is why we denote the initial growth rate $\tilde{\lambda}_j^p$. In this fashion $\tilde{\lambda}_j^p$ measures the initial growth rate of the total population if every member of the metapopulation was weighted according to how much they will contribute to the adult population. Adults are therefore not weighted, and juveniles are weighted by the probability that they survive to adulthood. This weighting recaptures the biological meaning of reactivity, where a system will only be reactive if the adult population will grow, and a system will not be reactive if there is only an initial spike in the juvenile population.

We use the same framework as in the previous section to mathematically calculate $\tilde{\lambda}_j^p$, where we decompose $A = F - V$ and F and V are shown in block form in eq. (3.17). Then we weight the juvenile population growth on each patch i by a factor s_i, where s_i is the probability that a juvenile from patch i eventually becomes an adult. From the block form V, s_i can be calculated as

$$s_i = \sum_{k=1}^{n} (-V_{21}V_{11}^{-1})_{ki}. \tag{3.18}$$

To see how this corresponds to the probability of survival of a juvenile on patch i, consider the different block components of F and V. The matrix V_{11}^{-1} is diagonal, with the (j,j) entry representing the average residence time of a juvenile born onto patch j. The matrix $-V_{21}$ contains the rates of maturation/migration of juveniles becoming adults on different patches, so the (i,j) entry is the rate of maturation/migration of a juvenile on patch j becoming an adult on patch i. This means that when we multiply $-V_{21}$ by V_{11}^{-1} we are multiplying each of these rates by the residence times of the

juveniles in the appropriate patches. In this way, the (i,j) entry of $-V_{21}V_{11}^{-1}$ is then the probability that a juvenile leaving patch j arrives on patch i. Therefore the jth column sum of $-V_{21}V_{11}^{-1}$ is the probability that a juvenile starting on patch j becomes an adult on any other patch.

The initial growth rate using the weighted norm, $\tilde{\lambda}_j^p$, can then be calculated as the sum of the juvenile growth rates, each multiplied by the patch specific survival s_i, and the adult growth rates. Mathematically, this is defined as:

$$\begin{aligned}\tilde{\lambda}_j^p &= \underbrace{\sum_{i=1}^{n} s_i x_i'(0)}_{\text{juvenile}} + \underbrace{\sum_{i=n+1}^{2n} x_i'(0)}_{\text{adult}}, \quad x(0) = e_{j+n} \\ &= \sum_{i=1}^{n} s_i f_{12ij} - \sum_{i=1}^{n} v_{22ij}.\end{aligned}$$

In order to demonstrate that the initial growth rate calculated using the weighted ℓ_1 norm, $\tilde{\lambda}_j^p$, indeed measures the growth rate of the population if all individuals are weighted according to their contribution to the adult population, we show that $\tilde{\lambda}_j^p$ is equivalent to scaling the juvenile population on each patch by the probability of survival to adulthood, and then measuring the initial growth rate using the unweighted ℓ_1 norm, defined previously as $\tilde{\lambda}_j$.

Theorem 3.9. *If each juvenile population in system (3.16) is rescaled by the patch specific survival probability, $s_i = \sum_{k=1}^{n}(-V_{21}V_{11}^{-1})_{ki}$, then the initial growth rate using the unweighted ℓ^1 norm, $\tilde{\lambda}_j$, is equal to the patch specific weighted initial growth rate, $\tilde{\lambda}_j^p$ for the unscaled system.*

Proof. Rescale the juvenile population on patch i by the patch specific survival probability s_i given in eq. (3.18). In terms of system (3.16) this means that $x_i^* = s_i x_i$ for $i = 1, \ldots, n$, $x_i^* = x_i$ for $i = n+1, \ldots, 2n$. Rewriting the system of equations

$$\begin{gathered} x^{*\prime} = A^* x^* \\ A^* = F^* - V^*, \quad F^* = \begin{bmatrix} 0 & SF_{12} \\ 0 & 0 \end{bmatrix}, \quad V^* = \begin{bmatrix} V_{11} & 0 \\ V_{21}S^{-1} & V_{22} \end{bmatrix}, \end{gathered}$$

where $S = \operatorname{diag}(s_1, \ldots, s_n)$. The unweighted initial growth rate for the scaled system is then

$$\tilde{\lambda}_j^* = \sum_{i=1}^{n}(SF_{12})_{ij} - \sum_{i=1}^{n} v_{22ij} = \sum_{i=1}^{n} s_i f_{12ij} - \sum_{i=1}^{n} v_{22ij} = \tilde{\lambda}_j^p.$$

Thus the unweighted initial growth rate for the scaled system is equal to the patch-weighted initial growth rate of the unscaled system, $\tilde{\lambda}_j^p$. □

We believe that it is more intuitive to measure reactivity in a stage-structured system using a weighted norm, rather than scaling the juvenile population and using the unweighted ℓ_1 norm, but for other systems this may not be the case. Recently Mari et al. (2017) have developed a new measure of reactivity called generalized reactivity, or g-reactivity, so that the reactivity of any specific combination of state variables in a system can be measured, and we demonstrate how to place our work in this context. The general framework of g-reactivity allows the reactivity of only the predator to be measured in a predator-prey system, or a single patch in a metapopulation model. Moreover in a stage-structured model, g-reactivity can be used to allow for a differential contribution of the juvenile and adult populations to the reactivity of the system, and so we can compare the calculation of g-reactivity to our calculation using the weighted ℓ_1 norm. To calculate the g-reactivity of a system $x' = Ax$, a linear transformation is introduced, $y = Cx$, where C is a matrix that defines the required contribution of each of the state variables, and then reactivity is calculated for y using eq. (3.2). For system (3.16), if C is a $2n \times 2n$ identity matrix, but with the first n diagonal entries replaced with $s_1, \ldots, s_n$, then g-reactivity is the ℓ_2 norm equivalent of reactivity under our weighted ℓ_1 norm, $\max_j \tilde{\lambda}_j^p$.

Returning to our measure of initial growth rate using a patch weighted norm, we present two examples below to illustrate the calculation of $\tilde{\lambda}_j^p$ in different systems.

Example 4

Consider a two patch system where juveniles are born onto all patches but only mature into adults on the patch where they were born:

$$\begin{aligned} j_1' &= b_{11}a_1 + b_{12}a_2 - m_1 j_1 - d_{j1} j_1 \\ j_2' &= b_{21}a_1 + b_{22}a_2 - m_2 j_2 - d_{j2} j_2 \\ a_1' &= m_1 j_1 - d_a a_1 \\ a_2' &= m_2 j_2 - d_a a_2. \end{aligned} \tag{3.19}$$

Here j_i is the number of juveniles on patch i, a_i is the number of adults on patch i, b_{ij} is the birth rate of juveniles on patch i from adults on patch j, m_i is the maturation rate of juveniles on patch i into adults on patch i, d_{ji} is the death rate of juveniles on patch i, and d_a is the death rate of adults, which is the same on both patches. The lifecycle graph for this system is shown in fig. 3.7.

In this case

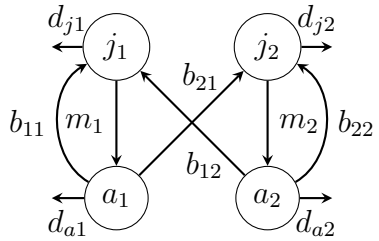

Figure 3.7: Digraph for system (3.19). Here b_{ij} is the birth rate of juveniles on patch i from adults on patch j, m_i is the maturation rate of juveniles on patch i to adults on patch i, d_{ji} is the death rate of juveniles on patch i and d_{ai} is the death rate of adults on patch i.

$$F_{12} = \begin{bmatrix} b_{11} & b_{12} \\ b_{21} & b_{22} \end{bmatrix}, \quad V_{11} = \begin{bmatrix} m_1 + d_{j1} & 0 \\ 0 & m_2 + d_{j2} \end{bmatrix}, \quad V_{21} = \begin{bmatrix} -m_1 & 0 \\ 0 & -m_2 \end{bmatrix},$$

$$V_{22} = \begin{bmatrix} d_a & 0 \\ 0 & d_a \end{bmatrix}, \quad -V_{21}V_{11}^{-1} = \begin{bmatrix} \frac{m_1}{m_1+d_{j1}} & 0 \\ 0 & \frac{m_2}{m_2+d_{j2}} \end{bmatrix},$$

$$\tilde{\lambda}_1^p = s_1 b_{11} + s_2 b_{21} - d_a, \quad \tilde{\lambda}_2^p = s_1 b_{12} + s_2 b_{22} - d_a,$$

$$s_1 = \frac{m_1}{m_1 + d_{j1}}, \quad s_2 = \frac{m_2}{m_2 + d_{j2}}.$$

If we look at $\tilde{\lambda}_1^p$, we see that s_1 is the probability that a juvenile born onto patch 1 survives to become an adult and it is multiplying b_{11}, the birth rate of juveniles onto patch 1 from adults on patch 1. Therefore the first component of $\tilde{\lambda}_1^p$ represents the rate of birth of new juveniles onto patch 1 from one adult on patch 1, but scaled by the probability that these juveniles survive to become adults. Likewise the second component, $s_2 b_{21}$, is the rate of birth of new juveniles onto patch 2 from one adult on patch 1, scaled by the probability that those juveniles also become adults. Thus $\tilde{\lambda}_1^p$ is the initial growth rate of the total population, scaled in terms of the contribution to the adult population, when the population begins with one adult on patch 1.

Example 5

We also consider a system in which juveniles are born onto the same patch as adults, but can then migrate between patches as they mature into adults:

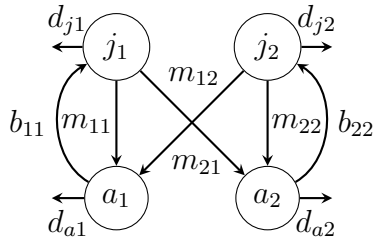

Figure 3.8: Digraph for system (3.20). Here b_{ii} is the birth rate of juveniles on patch i from adults on patch i, m_{ij} is the maturation rate of juveniles on patch j to adults on patch i, d_{ji} is the death rate of juveniles on patch i and d_{ai} is the death rate of adults on patch i.

$$\begin{aligned} j_1' &= b_{11}a_1 - m_{11}j_1 - m_{21}j_1 - d_{j1}j_1 \\ j_2' &= b_{22}a_2 - m_{22}j_2 - m_{12}j_2 - d_{j2}j_2 \\ a_1' &= m_{11}j_1 + m_{12}j_2 - d_a a_1 \\ a_2' &= m_{22}j_2 + m_{21}j_1 - d_a a_2. \end{aligned} \tag{3.20}$$

from which we calculate

$$F_{12} = \begin{bmatrix} b_{11} & 0 \\ 0 & b_{22} \end{bmatrix}, \quad V_{11} = \begin{bmatrix} m_{11}+m_{21}+d_{j1} & 0 \\ 0 & m_{12}+m_{22}+d_{j2} \end{bmatrix},$$

$$V_{21} = \begin{bmatrix} -m_{11} & -m_{12} \\ -m_{21} & -m_{22} \end{bmatrix}, \quad V_{22} = \begin{bmatrix} d_a & 0 \\ 0 & d_a \end{bmatrix}, \quad -V_{21}V_{11}^{-1} = \begin{bmatrix} \frac{m_{11}}{m_{11}+m_{21}+d_{j1}} & \frac{m_{12}}{m_{12}+m_{22}+d_{j2}} \\ \frac{m_{21}}{m_{11}+m_{21}+d_{j1}} & \frac{m_{22}}{m_{12}+m_{22}+d_{j2}} \end{bmatrix}$$

$$\tilde{\lambda}_1^p = s_1 b_{11} - d_a, \quad \tilde{\lambda}_2^p = s_2 b_{22} - d_a$$

$$s_1 = \frac{m_{11}+m_{21}}{m_{11}+m_{21}+d_{j1}} \quad s_2 = \frac{m_{12}+m_{22}}{m_{12}+m_{22}+d_{j2}}.$$

Now if we examine the first component of $\tilde{\lambda}_1^p$, $s_1 = (m_{11}+m_{21})/(m_{11}+m_{21}+d_{j1})$, we can see that because juveniles from patch 1 can now migrate (as they mature) to both patches, s_1 is the probability that juveniles from patch 1 become adults on either patch. Likewise s_2 is the probability that juveniles from patch 2 become adults on either patch. Biologically we are scaling the birth rate on a patch by the probability that a juvenile survives to adulthood on any patch.

Here we have shown that if we use a weighted ℓ_1 norm to scale the initial growth rate so that the juvenile population is scaled by the patch specific probability that juveniles become adults, then our scaled initial growth rate, $\tilde{\lambda}_j^p$ matches the biological intuition that we would like when measuring initial growth of the population. It is positive if

the population, scaled so that every individual is measured by its contribution to the adult population, is growing, and negative if the population is decreasing. Measures of reactivity and attenuation then also represent their intuitive biological properties, and we are no longer in the situation (as if the initial growth rate was unscaled) that most marine metapopulations are reactive.

It is also possible to create a weighted norm where the juvenile populations on each patch are weighted by the same probability of survival, rather than by patch-specific probabilities s_i. In some cases it may be useful to scale all patches by the same survival probability, though under this weighted norm reactivity no longer corresponds exactly to the intuitive biological meaning mentioned previously.

3.7 Discussion

Transient dynamics often differ drastically from the asymptotic dynamics of a system and require different analytical tools. In this chapter we have presented a framework for analysing transient dynamics in birth-jump metapopulations, from the choice of norms to the incorporation of stage structure. We began by using the ℓ_1 norm to define reactivity and attenuation in single species metapopulations and used examples to compare reactivity in the ℓ_1 norm with reactivity in the more commonly used ℓ_2 norm. We presented two models that gave rise to long transients: one stable system that exhibits a long period of growth before eventual decay, and one unstable system that exhibits a long period of decay before growth. In birth-jump metapopulations, where patches are connected via larval dispersal, we showed how strong advective flow, coupled with a large number of patches, can lead to large transient growth. We believe that this could be a key new mechanism giving rise to transient dynamics in marine metapopulations where habitat patches are found in a linear array, such as salmon farms along a fjord (see, for example Harrington and Lewis (2020)). We then connected the initial growth rate of the metapopulation to the source-sink classification of patches and lastly we demonstrated how to measure reactivity meaningfully in stage-structured marine metapopulations.

We are by no means the first to analyze the transient dynamics of systems, and in fact there has been an increase in the study of transient dynamics over the last few decades. In a pair of recent papers, several authors have identified mechanisms as the main causes of long transients in ecological systems (Hastings et al., 2018; Morozov et al., 2020). These identified mechanisms that cause the long transients present in the examples in this chapter are slow-fast systems, crawl-bys, and high dimensionality. Slow-fast systems cause long transients when the system rapidly converges to a slow

manifold, then moves slowly towards or away from an equilibrium, depending on the stability of the system. This occurs in both examples in section 3.3. The second example in section 3.3 is also an instance of a crawl-by where the initial perturbation is near a saddle equilibrium but the movement away from the equilibrium occurs over a long timescale. Lastly in section 3.4 we explicitly demonstrated how increasing the dimension of a system, by increasing the patch number in a linear metapopulation, leads to longer transients.

Our work also reinforces the fact that reactivity is a property specific to the norm under which it is measured. This has been mentioned in the first paper on reactivity by Neubert and Caswell (1997), who also recognize that it is always possible to find a norm such that a stable system is never reactive. It has also been noted by Lutscher and Wang (2020), who mention that reactivity must be analysed in the dimensional version of a system rather than the non-dimensionalized version. The reactivity may be different between the two systems but the dimensional system is where the measure of reactivity is biologically meaningful. When analysing reactivity in metapopulations this fact is significant in two ways: first by using the ℓ_1 norm rather than the ℓ_2 norm to measure reactivity we can explicitly measure the growth rate of a population, and second by using a weighted ℓ_1 norm we prevent the juvenile population from disproportionately affecting the reactivity of the system.

Differentially weighting certain classes of a population to calculate reactivity has been mentioned in passing by Verdy and Caswell (2008), and more extensively by Mari et al. (2017) who developed a new measure of reactivity called general reactivity, or g-reactivity. This is a method of only measuring the reactivity of the components of interest in a population, e.g. predators in a predator-prey model, and can also be used more generally to scale the contribution of different components of the population. Our method of using a weighted ℓ_1 norm for stage-structured models has an equivalent formulation using g-reactivity that is discussed in section 3.6.2, though Mari et al. (2017) use the ℓ_2 norm to measure reactivity, rather than the ℓ_1 norm, and are thus using a different measure of population growth.

While we believe the ℓ_1 norm is the most biologically relevant norm to measure reactivity, we are among the first to use it to analyse reactivity in continuous time models. Townley et al. (2007) show how to calculate reactivity for stage-structured models in continuous time using the ℓ_1 norm, but in following papers proceed to analyse reactivity in the ℓ_1 norm only in discrete time systems (Stott et al., 2010; Stott et al., 2011; Townley and Hodgson, 2008). Most authors measure reactivity with the ℓ_2 norm, presumably due to the nice mathematical property that reactivity in the ℓ_2 norm is given simply as the maximum eigenvalue of $(A + A^T)/2$ (Caswell

and Neubert, 2005; Lutscher and Wang, 2020; Neubert and Caswell, 1997; Neubert et al., 2002; Neubert et al., 2004; Snyder, 2010; Verdy and Caswell, 2008). But while mathematically tractable, the biological meaning of Euclidean distance (ℓ_2) is less clear than population size (ℓ_1) and as shown in section 3.2.2, there are times when reactivity in ℓ_2 does not correspond to an increase in population size.

The reactivity of an equilibrium can also be understood geometrically, as shown in figs. 3.1 and 3.2. Under the ℓ_1 norm the zero equilibrium of a single species metapopulation (2.1) is reactive if the dot product of the derivative vector of any initial perturbation and the outward normal vector of the plane $x_1 + x_2 + \dots x_n = 1$ is positive. This geometric interpretation is applicable when the matrix A describing the dynamics of the linearized system, $x'(t) = Ax(t)$, is Metzler. If instead we want to examine the reactivity of a positive steady state of a metapopulation, x^*, where the dynamics are given by $(x(t) - x^*)' = A(x(t) - x^*)$ and A is no longer Metzler, then we need to extend our geometric interpretation of the ℓ_1 norm. In this case an equilibrium is reactive if the dot product of the derivative vector of any initial perturbation and the outward normal vector to the hypercube $|x_1 - x_1^*| + |x_2 - x_2^*| + \dots |x_n - x_n^*| = 1$ is positive. We could no longer use $\max_j \sum_{i=1}^{n} a_{ij} > 0$ to calculate reactivity, because $x(t) - x^*$ need not remain in the non-negative cone. Thus an interesting area for future work would be to mathematically formulate reactivity in terms of the matrix A for positive equilibria of metapopulations.

No matter the norm in which reactivity and attenuation are measured, they are defined in terms of the linearization of a non-linear system around an equilibrium. As mentioned in the Introduction, reactivity and attenuation are therefore most relevant around hyperbolic equilibria, where the dynamics of the non-linear system are well approximated by the linearized system. In section 3.3 we have shown that even in the linearized system it is possible for the population size to grow arbitrarily large before decaying or decay arbitrarily small before growing. In the latter case the zero equilibrium is unstable mathematically, but biologically the metapopulation could first go extinct if the total population size decays below one individual before it eventually increases.

It is also possible for an equilibrium of a non-linear system to not be reactive, but for a perturbation of the non-linear system to still cause a large excursion away from the stable equilibrium before eventually returning. Excitable systems, such as the FitzHugh-Nagumo system, have stable equilibria with attracting regions, but small perturbations still trigger large excitations (FitzHugh, 1961; Nagumo et al., 1962). These systems may not be reactive from the linearized definition of reactivity, but can still exhibit similar behaviour to reactivity in the non-linear system, given a sufficient

perturbation.

In this chapter we use systems of differential equations to study reactivity, attenuation, and transients in birth-jump metapopulations. It may also be possible to study transients in metapopulations using methods by Wang et al. (2019) for reaction-diffusion equations, where the spread of individuals between patches can be modelled mechanistically.

The final extension that we would like to highlight is the relationship between reactivity of continuous time models and reactivity of their discrete counterparts. Many marine metapopulations are modelled in discrete time due to yearly breeding cycles, however some are modelled in discrete time due to ease of simulation. For these models, where the time step is on the order of hours or days, we can connect the reactivity of the continuous time system with the discrete time system using a Taylor expansion. The continuous time system, $x' = Ax$, has the solution $x(t) = e^{At}x_0$ that could be sampled at discrete time steps τ to create the discrete time system $x(t+\tau) = Bx(t)$, where $B = e^{A\tau}$.

The continuous time system $x' = Ax$ is reactive in ℓ_1 if A has a positive column sum (Theorem 3.1). In discrete time the system $x(t+\tau) = Bx(t)$ is reactive in ℓ_1 if B has a column sum that is greater than 1 (Townley et al., 2007). Assuming τ is a small timestep then we can approximate $B = e^{A\tau} = I + A\tau + O(\tau^2)$. Thus we can see that if the system is reactive in continuous time, i.e. there is a positive column sum of A, then we can find a sufficiently short time step τ such that the discrete time system is also reactive, i.e. there is a column sum of B greater than 1. However for a predetermined time-step τ there are continuous time systems $x' = Ax$ that are reactive but for which their discrete counterparts $x(t+\tau) = e^{A\tau}x(t)$ are not reactive. One such example is system (3.9) with $\epsilon = 0.9$ and $\tau = 1$.

Lastly, we hope our work can be used to better understand the transient dynamics in marine metapopulations for which habitat patches have already been classified as sources and sinks. For these systems the transient dynamics that may occur following a disturbance depend directly on the new distribution of the population. If the remaining population is distributed amongst sink patches then it initially declines, even if it eventually recovers. Likewise if the population is distributed amongst source patches then it initially grows, though this growth may not necessarily occur on the source patch itself. In addition, the relationship between transient dynamics and sources and sinks in marine metapopulations may also be useful when examining the dynamics that can occur following the protection of new marine environments, such as newly implemented Marine Protected Areas.

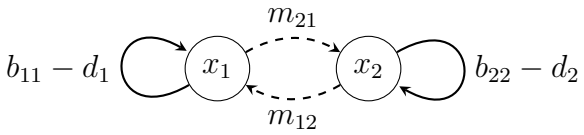

Figure 3.9: Digraph for system (3.21). The directed edges represent the movement of individuals from the outgoing patch to the incoming patch. The self loops are the birth rate minus the death rate on a patch.

3.8 Appendices to Chapter 3

3.8.1 Two patch example with migration

Here we present an example of a two-patch metapopulation where individuals are born only onto their patch, but can now also migrate between patches. This is the case for many terrestrial species that live on patchy landscapes, where individuals can migrate between habitat patches. We present this example to demonstrate how Theorem 3.5 breaks down when V is not of the correct form. The dynamics of this metapopulation are described by the following set of ODEs:

$$\begin{aligned} x_1' &= b_1 x_1 - m_{21} x_1 + m_{12} x_2 - d_1 x_1 \\ x_2' &= b_2 x_2 - m_{12} x_2 + m_{21} x_1 - d_2 x_2, \end{aligned} \tag{3.21}$$

where b_i is the birth rate on patch i, m_{ij} is the migration rate from patch j to patch i, and d_i is the death rate on patch i. The lifecycle graph for this system is shown in fig. 3.9.

We again decompose $A = F - V$ and construct our next generation matrix, $K = FV^{-1}$, though now V is not diagonal nor in the same form as required for Theorem 3.5.

$$A = \begin{bmatrix} b_1 - m_{21} - d_1 & m_{12} \\ m_{21} & b_2 - m_{12} - d_2 \end{bmatrix}$$

$$F = \begin{bmatrix} b_1 & 0 \\ 0 & b_2 \end{bmatrix}$$

$$V = \begin{bmatrix} d_1 + m_{21} & -m_{12} \\ -m_{21} & d_2 + m_{12} \end{bmatrix}$$

$$K = FV^{-1} = \begin{bmatrix} \frac{b_1(d_2+m_{12})}{d_1d_2+d_1m_{12}+d_2m_{21}} & \frac{b_1m_{12}}{d_1d_2+d_1m_{12}+d_2m_{21}} \\ \frac{b_2m_{21}}{d_1d_2+d_1m_{12}+d_2m_{21}} & \frac{b_2(d_1+m_{21})}{d_1d_2+d_1m_{12}+d_2m_{21}} \end{bmatrix}$$

The entries of K may seem counter intuitive, but they represent the infinite sum of a geometric series. Consider the first entry, k_{11}. If we are tracking the total number of new individuals produced by one individual starting on patch 1, then this individual can either produce new offspring in patch 1 immediately, or it can migrate to patch 2, then back to patch 1 and produce offspring, or migrate again and produce more offspring. The entry k_{11} is then the birth rate in patch 1 multiplied by the residence time in patch 1, multiplied by a geometric series where the ratio is the probability of surviving the migration from patch 1 to patch 2 and then back to patch 1. Mathematically

$$k_{11} = \frac{b_1}{m_{21} + d_1} \left[\sum_{i=0}^{\infty} \left(\frac{m_{21}}{m_{21} + d_1} \frac{m_{12}}{m_{12} + d_2} \right)^i \right]$$

Now consider λ_1 and R_1, the measures of transient growth for patch 1:

$$\lambda_1 = b_1 - d_1$$
$$R_1 = \frac{b_1d_2 + b_1m_{12} + b_2m_{21}}{d_1d_2 + d_1m_{12} + d_2m_{21}}.$$

We can see that

$$\lim_{d_2 \to \infty} R_1 = \frac{b_1}{d_1 + m_{21}}.$$

Therefore even if $\lambda_1 > 0$, and so $b_1 > d_1$, as m_{21} becomes large, $R_1 < 1$.

In the other direction, if $d_1 = 2b_1$, then

$$\lim_{b_1 \to 0} R_1 = \frac{b_2}{d_2}.$$

Therefore even if $R_1 > 1$, we can still have $\lambda_1 = b_1 - d_1 < 0$. We present this example to demonstrate that if the assumptions of theorem 3.4 are not met, there is no longer a one-to-one relationship between λ_j and R_j.

Now we might also consider moving the off diagonal entries of V into F so that V becomes diagonal. This is similar to considering migrating individuals as new individuals entering a patch. In this case

$$F = \begin{bmatrix} b_1 & m_{12} \\ m_{21} & b_2 \end{bmatrix}$$
$$V = \begin{bmatrix} d_1 + m_{21} & 0 \\ 0 & d_2 + m_{12} \end{bmatrix}$$
$$K = FV^{-1} = \begin{bmatrix} \frac{b_1}{d_1+m_{21}} & \frac{m_{12}}{d_2+m_{12}} \\ \frac{m_{21}}{d_1+m_{21}} & \frac{b_2}{d_2+m_{12}} \end{bmatrix}$$

Here $\lambda_1 = b_1 - d_1 > 0$ is equivalent to $b_1 > d_1$, which is then equivalent to $R_1 = (b_1 + m_{21})/(d_1 + m_{21}) > 1$. However, in this case R_1 no longer tracks the total number of new individuals produced on all patches over one generation. This new R_1 could perhaps be interpreted as the total number of new individuals produced on patch 1 by a single individual on patch 1 before that individual dies or migrates, plus the probability that the individual migrates to patch 2 before it dies. However, this will no longer be a biologically useful measure of a source or a sink.

3.8.2 Details for proof in section 3.3.1

Here we provide further details for the proof at the end of section section 3.3.1 that follow after system (3.11). We want to show that

$$\lim_{\epsilon \to 0} \max_t (x(t) + y(t)) = \lim_{\epsilon \to 0} \rho_{\max} = \infty.$$

Normally to calculate the maximum we would take the derivative of $(x(t) + y(t))$, set it equal to 0, solve for t, and then evaluate $(x(t) + y(t))$ at this value of t. However it turns out this is rather complicated, so we will simplify this process by first noting that $x(t) > 0$ for all t. Therefore

$$\max_t (x(t) + y(t)) > \max_t y(t).$$

Now we only have to perform the above process on $y(t)$, rather than $(x(t) + y(t))$.

Setting $y'(t) = 0$ and solving for t, we find that the time that the maximum of $y(t)$ is achieved, $t_{\max}$, along with the corresponding maximum in y, $y(t_{\max})$, are:

$$t_{\max} = \frac{1}{\sqrt{2}} \left(\log(1+\sqrt{2}) - \log(-1+\sqrt{2}) \right)$$
$$y(t_{\max}) = \frac{\sqrt{2}}{\epsilon} (1+\sqrt{2})^{(-\frac{1}{2}-\frac{1}{\sqrt{2}})} (-1+\sqrt{2})^{(\frac{1}{\sqrt{2}}-\frac{1}{2})}.$$

We can clearly see that $\lim_{\epsilon \to 0} y(t_{\max}) = \infty$ and thus also $\lim_{\epsilon \to 0} \max_t x(t) + y(t) = \lim_{\epsilon \to 0} \rho_{\max} = \infty$.

Chapter 4

Next-generation matrices for marine metapopulations: the case of sea lice on salmon farms

4.1 Introduction

Metapopulations consist of subpopulations located on isolated habitat patches that are connected via dispersal (Hanski, 1998; Kritzer and Sale, 2004; Levins, 1969). In most benthic marine species, this dispersal comes from the pelagic larval stage (Cowen and Sponaugle, 2009). Larvae disperse between, and then settle on habitat patches, and once settled the remaining stages are sedentary and remain confined to a specific habitat patch. In marine systems the metapopulation concept, where subpopulations are connected but have their own demographic rates, has been used in the planning of Marine Protected Areas and the citing of marine reserves (Bode et al., 2006; Burgess et al., 2014; Costello et al., 2010; Crowder et al., 2000; Figueira, 2009; Watson et al., 2011).

In a metapopulation framework, habitat patches are often classified into sources and sinks based on how the subpopulations on these patches contribute to the overall metapopulation. The source-sink classification of habitat patches was first described concretely by Pulliam (1988), where habitat patches were classified as sources if they could persist in isolation and sinks if they could not. However, this classification ignores the effect of dispersal, which is especially critical in marine metapopulations, and so Runge et al. (2006) and Figueira and Crowder (2006) updated the classification of source and sink patches to include both the local productivity of a patch, as well as dispersal away from the habitat patch. Under this new classification a source patch is a patch on which an adult will more than self replace over the entire metapopulation and a sink is a patch on which an adult will not. Self-replacement need not occur on

the same habitat patch as the adult originated, and thus under this classification a source patch may not be able to persist in isolation.

Due to the large scale larval dispersal that occurs in most marine species, it is common that source patches cannot persist in isolation (White et al., 2019), and thus preserving a persistent metapopulation, especially in the context of MPAs, often requires more than simply preserving source patches. To maintain persistent marine metapopulations it is necessary to preserve sufficient larval exchange between closed loops of habitat patches in the metapopulation so that an average adult can eventually self replace over multiple generations (Burgess et al., 2014; Hastings and Botsford, 2006). This may require preserving both source and sink patches, if the sink patches provide sufficient larval exchange back to the source patches to create a closed loop of habitat patches over which an adult can self replace. Evaluating the persistence of marine metapopulations is difficult as it requires accurate measures of larval connectivity between habitat patches, as well as accurate local demographic rates of adult stages on each habitat patch (Burgess et al., 2014). Despite the difficulties, evaluating metapopulation persistence is critical in designing Marine Protected Areas in which the protected habitat patches can persist even when outside patches are exploited (Carson et al., 2011; Dedrick et al., 2021; Garavelli et al., 2018; Puckett and Eggleston, 2016; Theuerkauf et al., 2021; White et al., 2010).

Next-generation matrices are a useful tool that can both be used to evaluate the persistence of a metapopulation as well as identify the contribution of local habitat patches under a variety of moedling frameworks. Originally popularized in epidemiology as a simple method of calculating the basic reproduction number, R_0, in compartmental models (van den Driessche and Watmough, 2002), they convert population models into generational time, so that the entries are the number of new individuals produced in each compartment, or patch in the case of metapopulations, after one generation. The individual contribution of habitat patches or evaluation of metapopulation persistence can therefore be measured for different model structures (discrete time, continuous time, etc.) under the same framework of the next-generation matrix. The column sums can be used to measure the contribution of each habitat patch over a generation and the spectral radius can be used to evaluate metapopulation persistence. Next-generation operators have previously been used in ecology to calculate source and sink regions in heterogeneous environments (Harrington and Lewis, 2020; Huang et al., 2016; Krkošek and Lewis, 2010; Mckenzie et al., 2012a), and to evaluate the level of control required to suppress invasive species (Lewis et al., 2019).

In this chapter we focus on using the next-generation matrix for evaluate local patch contribution and metapopulation persistence in marine metapopulations, but

the framework used here is also applicable to many other birth-jump metapopulations (Hillen et al., 2015), where there is a single juvenile stage which can disperse between habitat patches and the remaining stages remain on a single habitat patch. Examples of non-marine species that exhibit this structure include plant species where seeds are caried between habitat patches (Husband and Barrett, 1996), or insect species with a single large dispersal event such as the spruce budworm (Williams and Liebhold, 2000) or mountain pine beetle (Safranyik and Carroll, 2007) . In fact, the next-generation matrix approach can even be extended to metapopulations in which adults also disperse, though the calculations become more complicated and so here we focus on species with a single dispersing stage.

Specifically, to demonstrate the utility of the method, we use the next-generation matrix to calculate the contribution of a single salmon farm to the spread of sea lice in a salmon farming region on the west coast of British Columbia. Sea lice are a parasitic marine copepod that feed on the epidermal tissues, muscles, and blood of salmon (Costello, 2006). With a free living larval stage they can disperse tens of kilometres, spreading between salmon farms in a region and between wild and farmed salmon (Krkošek et al., 2006a; Peacock et al., 2020; Stucchi et al., 2011). Lesions and stress from high sea lice infestation make adult salmon more susceptible to secondary infections, leading to large economic consequences for the salmon farming industry (Costello, 2009b). On wild juvenile salmon, infestation with sea lice can lead to mortality and elevated exposure to sea lice from salmon farms can contribute to population level declines in pink salmon (Krkošek et al., 2007). In the context of sea lice on salmon farms we are not concerned with preserving a persistent metapopulation of sea lice parasites, but instead we use the next-generation matrix to evaluate the effect of environmental variables on the overall growth of the sea louse metapopulation.

The specific salmon farming region that we focus on to calculate farm contribution is the Broughton Archipelago. The Broughton Archipelago is located on the west coast of Canada, between Vancouver Island and the mainland of British Columbia and has been central in evaluating the effect of sea lice from salmon farms on wild salmon (Brooks, 2005; Brooks and Stucchi, 2006; Krkošek et al., 2011b; Krkošek et al., 2008; Krkošek et al., 2007; Krkošek et al., 2006a; Krkošek et al., 2005; Krkošek et al., 2006b; Marty et al., 2010; Riddell et al., 2008). The area has historically had around 20 active salmon farms (Foreman et al., 2015), though currently certain farms are being removed from this region in an agreement between the government of British Columbia and the Kwikwasut'inuxw Haxwa'mis, 'Namgis, and Mamalilikulla First Nations (Brownsey and Chamberlain, 2018). After 2023 many of the remaining farms will have be approved by both the local First Nations and the government in

order to continue to operate and thus determining the farms which are acting as the largest sources of sea lice is critical during this transition period.

The chapter is structured as follows. First we demonstrate how to use the next-generation matrix to calculate the contribution of local habitat patches to the metapopulation and evaluate metapopulation persistence. Next, we highlight how to construct the next-generation matrix for different types of models. Then we calculate a next-generation matrix for sea louse populations in the Broughton Archipelago to idenfity which salmon farms are the largest sources of sea lice in this region, evaluate the effect of the current farm removals, and investigate the effect of environmental variables on metapopulation growth. Finally, we discuss how the calculations of patch contribution and metapopulation persistence from other studies compare to the calculations using the next-generation matrix.

4.2 Materials and Methods

In this section we present details on the construction of the next-generation matrix and show how it can be used to determine the contribution of a population on a single habitat patch to the metapopulation as well as determine the persistence of the metapopulation. We then present the explicit construction of the next-generation matrix for models with age dependent demography, and present the construction for ordinary differential equation models and discrete time models in the appendix. Finally, we detail the construction of the next-generation matrix for a system of sea lice populations on salmon farms in the Broughton Archipelago.

4.2.1 Next-generation matrices

Next-generation matrices, as they were first introduced in epidemiology, track the number of new infections produced in each compartment of a multi-compartment model by a single infected individual in a given compartment after one generation (Diekmann et al., 1990; van den Driessche and Watmough, 2002). In ecology, next generation matrices have been used to track the number of new individuals produced in different compartments, rather than new infections. For marine metapopulations, next-generation matrices can be used to couple the local demographic rates on habitat patches with larval connectivity between patches to determine the relative contribution that each patch has to the metapopulation and to classify habitat patches as sources or sinks, as will be shown in section 4.2.2.

We use the next-generation matrix to calculate local patch contribution to the

metapopulation in the context of low population density. To calculate the next-generation matrix it is necessary to linearize a potentially density dependent model around the zero equilibrium so that the effect of density dependence at higher population sizes is ignored when calculating patch contribution. This approach of ignoring density dependence is common when determining persistence or patch contribution of marine metapopulations, as the focus is either on determining if a metapopulation can persist at all, or determining which habitat patches are acting as population sinks and which are acting as population sources (Burgess et al., 2014; Harrington and Lewis, 2020; Hastings and Botsford, 2006; Krkošek and Lewis, 2010). Alternatively it is also useful for determining patch contribution in metapopulations of species that are being actively controlled to remain at low densities, such as sea lice on salmon farms, which is our focus in section 4.2.4. Another common assumption in the theory of persistence also made here is that there is no discernible Allee effect in any of the patches.

We construct the next generation matrix for a single species marine metapopulation with a single larval stage that can disperse between patches and where the remaining stages are confined to the habitat patch on which the larvae settle. Here we assume that the last stage is the only stage that produces new larvae. This assumption can be relaxed, though the entries of the next-generation matrix become slightly more complicated. We construct the next-generation matrix for models where the metapopulation is divided into l patches and the m attached stages are modelled explicitly. The larval stage is modelled implicitly, so that the birth rate into the first attached stage includes both the birth rate of larvae and the probability of larvae successfully dispersing between patches and attaching on a new patch. The lifecycle diagram for such a metapopulation is shown in Figure 5.1. Before specifying a particular model structure we describe the entries of the next generation matrix so that intuition around the next generation matrix can be gained for all model structures.

Under any model structure, the element in row i and column j of the next-generation matrix gives the number of new individuals produced on patch i by one new initial individual on patch j. However, how 'new' individuals are defined is subject to interpretation. Here, we use construct the next-generation matrix under modeling frameworks that only consider the sessile stages explicitly, and so 'new' individuals will be newly attached stage 1 individuals. Then, when the number of new individuals on patch i produced from one new individual on patch j are tracked, the new individual must first survive and reproduce on patch j, before larvae disperse and arrive on patch i. In this way patch contribution, as will be calculated in section

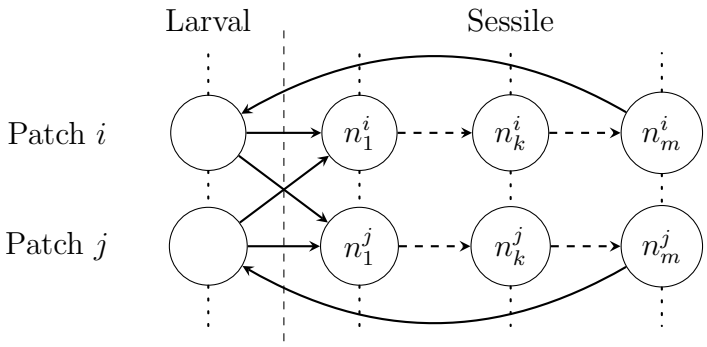

Figure 4.1: The lifecycle graph for two patches in a metapopulation of a species with a single larval stage that disperses between habitat patches and m sessile stages that remain on a habitat patch. The population on patch i in stage k is given by n_k^i.

4.2.2, is primarily a function of the local patch demography which is then coupled with dispersal to other patches. Under this framework, the entries of the next-generation matrix, K, for all model structures can be given by:

$$k_{ij} = \Pr(\text{survival through sessile stages on patch } j) \times \#\text{ larvae produced on patch } j \times \Pr(\text{dispersal from patch } j \text{ to patch } i). \quad (4.1)$$

However if the next-generation matrix is constructed for models that explicitly model the larval stage, then the larval stage is often considered the first stage. The next-generation matrix will be slightly different in this case as well as the calculation of patch contribution, though the calculation of metapopulation persistence will be the same. We illustrate the differences between constructions of the next-generation matrix in the Discussion and show how the calculation of persistence remains the same under all constructions.

4.2.2 Determining patch contribution and metapopulation persistence

Here we show how to use the next-generation matrix, K, to determine the contribution of each patch to the metapopulation and evaluate metapopulation persistence. To determine the contribution of a specific patch to the metapopulation we track the total number of new individuals produced across the metapopulation after one generation from an initial individual starting on that patch. The entries of the next-generation matrix, k_{ij} give the number of new individuals produced on patch i from an initial

individual on patch j. Therefore if we define

$$R_j = \sum_i k_{ij}, \tag{4.2}$$

so that R_j is the jth column sum of K, then R_j is the total number of new individuals produced across all patches from an initial individual starting on patch j and can be used to define the contribution of patch j to the entire metapopulation.

This definition of patch contribution easily lends itself to classifying local habitat patches as population sources or sinks. If $R_j < 1$, then an individual on patch j cannot replace itself over the entire metapopulation, and thus patch j is defined as a sink (Harrington and Lewis, 2020). If $R_j > 1$ then one individual on patch j is producing more than one individual over the entire population and so patch j is defined as a source. To calculate persistence we can use the basic reproduction number, R_0, which can be calculated as

$$R_0 = \rho(K), \tag{4.3}$$

where $\rho()$ is the spectral radius. If $R_0 > 1$ then the metapopulation will persist and if $R_0 < 1$ then the metapopulation will go extinct, a relationship which holds under any of the model formulations considered here (Cushing and Yicang, 1994; Harrington and Lewis, 2020; Li and Schneider, 2002; van den Driessche and Watmough, 2002). The only condition required is that K be irreducible, which is biologically satisfied if there is some small positive probability that larvae leaving one patch can arrive on any other patch.

There are several biological reasonable properties that also exist mathematically under this framework. First, it is easy to show that if the population on any single habitat patch can persist on its own, so that $k_{ii} > 1$, then the entire metapopulation will persist and $R_0 > 1$ (Harrington and Lewis, 2020). Second, a metapopulation consisting only of sink patches cannot persist and a metapopulation consisting only of sources cannot go extinct. The mathematical underpinning of these relationships is that the spectral radius must be between the minimum and maximum column sums of a matrix, so in terms of our metapopulation quantities

$$\min_j R_j \leq R_0 \leq \max_j R_j. \tag{4.4}$$

Having defined patch contribution and persistence in terms of the next-generation matrix, we now demonstrate how to calculate the next-generation matrix for a model with age dependent demography, as this is the modeling structure commonly used for sea lice on salmon farms. We also present the construction of the next-generation matrix for discrete time models and ordinary differential equation models in the

Appendices 4.6.1 and 4.6.2, so that the details are present for the most commonly used population models

4.2.3 Calculating the NGM for models with age dependent demography

Here we calculate the next-generation matrix for models which allow for the maturation, survival, birth, and dispersal rates to depend not only on the stage and patch location of an individual, but also on the time that they have spent in a stage. This time is often referred to as stage-age and so in these models there are two time variables: the global time of the system, t, and the time that an individual has spent in a particular stage, their stage-age, a. These models can be specified either as McKendrick von-Foerster partial differential equations, integrodifferential equations, or renewal equations (Feng and Thieme, 2000). In all cases, the dependence of the maturation rate on time spent in a stage allows for the addition of more realistic maturation functions where most individuals mature at some intermediate stage-age, or after some minimum time spent in the stage. In contrast, if models are formulated using ordinary differential equations the time in a stage is always exponentially distributed.

However, the specification of the model equations for these models can be rather complicated and so here we construct the next-generation matrix directly from the maturation, survival, birth, and dispersal functions, but the full model and the derivation of the next-generation matrix can be found in Appendix 4.6.3 as well as in Harrington and Lewis (2020). Essentially the construction involves tracking the probability that an individual survives through the different stages on a specific patch, the number of larvae that they produce, and the probability that they successfully disperse from one patch from another. If the probability of survival in stage k on patch j at stage-age a is $S_k^j(a)$, the maturation rate from stage k to $k+1$ is $m_k^j(a)$, the birth rate of larvae on patch j is $b^j(a)$, and the probability of a larva leaving patch j and successfully attaching on patch i is p^{ij}, then the entries of the next-generation matrix, K, are given by

$$k_{ij} = \underbrace{\left[\prod_{k=1}^{m-1} \overbrace{\left(\int_0^\infty S_k^j(a) M_k^j(a) m_k^j(a) da\right)}^{\Pr(\text{stage } k \to k+1)}\right]}_{\text{survival through sessile stages}} \underbrace{\left(\int_0^\infty S_m^j(a) b^j(a) da\right)}_{\#\text{ larvae produced}} \times \overbrace{p^{ij}}^{\Pr(\text{patch } j \text{ to patch } i)} \tag{4.5}$$

where $M_k^j(a)$ is the probability that an individual has not yet matured from stage k

to $k+1$ and can be calculated as $M_k^j(a) = \exp(-\int_0^a m_k^j(\tau)d\tau)$.

4.2.4 Application: sea lice on salmon farms in the Broughton Archipelago

In this section we construct a next-generation matrix to determine the contribution of a single salmon farm to the spread of sea lice in a salmon farming region on the west coast of British Columbia, the Broughton Archipelago. The Broughton Archipelago is a group of islands between the northeast coast of Vancouver Island and the mainland of British Columbia. The region has historically had around 20 active salmon farms, though several of these farms are currently being removed in an agreement between local First Nations and the government of British Columbia. To determine the level of sea lice dispersal away from salmon farms, a hydrodynamic model has been run for the region and sea lice particles were released from 20 historical farms in the Broughton Archipelago. We construct one next-generation matrix for the 20 historical farms in the region (Cantrell et al., 2018) for which the hydrodynamic particle tracking model was run, as well as one for the 11 remaining farms in the area after 2023, subject for First Nations and governmental approval (Brownsey and Chamberlain, 2018).

Modeling framework

Sea lice maturation through stages is often modelled with stage-age dependent maturation functions (Aldrin et al., 2017; Revie et al., 2005; Stien et al., 2005) and thus we construct the next-generation matrix for sea lice using age dependent demography, as shown in section 4.2.3.

Dispersal

The probability that a sea louse larvae leaves from one farm and successfully arrives on another depends on several factors including ocean current, temperature, and salinity and to accurately capture this probability it is necessary to use a computational hydrodynamic model that can track the spread of larvae originating from a given farm and the dependence of larval survival on temperature and salinity. To determine the probability of larvae dispersing between farms we use connectivity matrices from Cantrell et al. (2018). These connectivity matrices are calculated by applying Kernel Density Estimation (KDE) to particle tracking simulations to calculate the infectious density of sea lice at each farm, originating from a given farm. The particle tracking simulations are run on output generated by a Finite Volume Community Ocean Model (FVCOM) which uses data on tides, wind surface-heating, and river discharge to

simulate three-dimensional ocean velocity, temperature, and salinity. In the particle tracking simulation the survival of sea louse particles is dependent on temperature and their maturation from non-infectious to infectious larvae is dependent on temperature. Details on the calculation of the KDEs as well as the particle tracking simulations and FVCOM model can be found in Cantrell et al. (2018) and Foreman et al. (2009), as well as Chapter 5 of this thesis.

The infectious densities of sea lice are calculated for each particle release day by applying Kernel Density Estimation to accumulated daily snapshots over 11 days of particle locations for particles which are still alive and are able to attach to salmon over the lifetime of sea louse larvae. A connectivity matrix is then calculated for each particle release day, where the entry in row i and column j of the connectivity matrix is the infectious density of larvae over farm i, produced by larvae initially leaving farm j. In Cantrell et al. (2018) the infectious densities were calculated from 24 hours of particle releases, where 50 particles were released each hour and so to calculate the infectious density of one initial release particle we divide the entries in each connectivity matrix by 1200 (50×24). Then, to create a single connectivity matrix, C, for the 20 farms in the Broughton Archipelago we take the average over all the connectivity matrices created for particles released between March 14th and July 20th, 2009.

The necessary quantity to construct the next-generation matrix is p^{ij}, the probability that larvae leaving farm j will successfully attach on farm i. To estimate p^{ij} from the entries of the connectivity matrix, c_{ij}, there are several assumptions that need to be made. As will be shown in Chapter 5, if we assume that the number of lice that arrive onto farms is small compared to the total number of lice in the water column, so that lice arriving onto farms do not significantly affect the density of lice in the water column, then

$$p^{ij} = \int_0^\infty \beta \int_{\text{farm } i} p_h^j(x,t) d\Omega dt,$$

where $p_h^j(x,t)$ is the two dimensional density of infectious lice produced from farm j that are still alive in the water column at position x and time t, and β is the arrival rate of lice moving over the farm arriving onto the farm. However the entries of the connectivity matrix, c_{ij}, are the infectious density of larvae over farm i, produced by larvae leaving farm j. The infectious densities are calculated by applying Kernel Density Estimation to daily snapshots of infectious particles over 11 days, starting at time $t = 0$, so roughly

$$c_{ij} = p_h^j(x_i, 0) + p_h^j(x_i, 1) + \cdots + p_h^j(x_1, 11).$$

We can therefore roughly calculate p^{ij} from c_{ij} by assuming that the integrals over time and space can be approximated using their Riemann sums, and that the area of a farm is roughly 0.01 km^2, where

$$p^{ij} = \int_0^\infty \beta \int_{\text{farm } i} p_h^j(x,t) d\Omega dt \tag{4.6}$$

$$\approx \beta \times \text{Area of farm } i \times 1 \text{ day} \times \left(p_h^j(x_i,0) + p_h^j(x_i,1) + \cdots + p_h^j(x_i,11)\right) \tag{4.7}$$

$$= \beta \times 0.01 \times c_{ij}. \tag{4.8}$$

Therefore to calculate p^{ij} from c_{ij} we need to estimate the arrival rate β. However, very little is known about the arrival rate of lice dispersing from one farm to another, and so the estimate presented here is very uncertain and could be orders of magnitude off from the true arrival rate. We assume here that $\beta = 100$/day, and thus the average waiting time for infectious sea lice in the water column surrounding the farm to arrive on the farm is roughly 15 minutes ($1/\beta = (1 \text{ day}/100) \times (24 \text{ hrs}/1 \text{ day}) \times (60 \text{ minutes}/1 \text{ hr}) = 14.4$ minutes). However the waiting time could be as little as 1 minute or as long as 1 hour. Moreover, this is ignoring the fact that some infectious lice may never attach, and the estimates of the proportion of lice which successfully attach at all varies from 80% to 0.5% under different lab conditions (Skern-Mauritzen et al., 2020). The purpose of this paper is not to accurately estimate the basic reproduction number, R_0, for the Broughton Archipelago, or to accurately estimate the contribution of an individual farm, R_j, but rather to compare the relative contributions of different salmon farms in the system, and to investigate the effect of environmental variables on the basic reproduction number. Therefore we present our estimate of the arrival rate for these purposes only, and our estimate of R_0 found in the results should not be taken as an accurate estimate.

Demography

Once infectious sea lice larvae attach to their salmonid hosts they must survive and mature through several attached life stages before they can produce offspring. These demographic rates are dependent on salinity and temperature, and thus some salmon farms may be more productive than others due to favourable environmental conditions. To capture the dependence of demography on salinity and temperature we simplify the attched sea lice life cycle down to three main stages: chalimus, pre-adult, and adult. Survival in each stage is salinity dependent, maturation is temperature dependent, and egg viability and production depends on both salinity and temperature. The demographic functions that we use are from models which have previously been fit to sea louse population data and are shown in Table 4.1.

Table 4.1: The maturation, survival, and birth functions used to create the next-generation matrix for sea louse populations on salmon farms in the Broughton Archipelago. The sea louse life cycle is simplified to three attached stages: chalimus, pre-adult and adult. For the maturation rate out of stage i, $i \in (c, p)$, where c refers to the chalimus stage and p refers to the pre-adult stage.

Description	Function	Units	Reference
Survival probability of all stages	$S(a) = \exp(-(24a)^{(1/0.512)} \times \exp(-(1/0.512)(4.12 + 0.124S)))$		Connors et al. (2008)
			Rittenhouse et al. (2016)
Maturation rate out of stage i	$m_i(a) = \log(2)\delta_{si}((\delta_{mi}(10/T)^{\delta_{pi}})^{-\delta_{si}})a^{\delta_{si}-1}$	$\frac{1}{\text{day}}$	Aldrin et al. (2017)
	$\delta_{mc} = 18.869$, $\delta_{sc} = 7.945$, $\delta_{pc} = 1.305$, $\delta_{mp} = 10.742$,		
	$\delta_{sp} = 1.643$, $\delta_{pp} = 0.866$		
Egg batch size	$B = 2\exp(5.6 - 0.43\log(T/10) - 0.78(\log(T/10))^2)$	eggs	Stige et al. (2021)
Egg development time	$D = (41.98/(T - 10 + 41.98 * 0.338))^2$	days	Stige et al. (2021)
Egg viability (salinity)	$V_{sal} = \exp(-11.92 + 0.538S)/(1 + \exp(-11.92 + 0.538S))$		Stige et al. (2021)
Egg viability (temperature)	$V_{temp} = \exp(-1.765 + 0.494T)/(1 + \exp(-1.765 + 0.494T))$		Stige et al. (2021)
Birth rate	$b(a) = B \times V_{sal} \times V_{temp}/D$	$\frac{\text{larvae}}{\text{day}}$	Stige et al. (2021)
Arrival rate	$\beta = 100$	$\frac{1}{\text{day}}$	

We calculate the on-patch component of the elements of next-generation matrix, k_{ij}, by integrating the demographic functions over all time,

$$\underbrace{\left[\prod_{k=1}^{m-1}\overbrace{\left(\int_0^\infty S_k^j(a)M_k^j(a)m_k^j(a)da\right)}^{\Pr(k\to k+1)}\right]}_{\text{sessile stages}}\underbrace{\left(\int_0^\infty S_m^j(a)b^j(a)da\right)}_{\#\text{ larvae}}, \tag{4.9}$$

and refer to this as the productivity of patch j. To determine the specific temperature and salinity dependent demographic rates at each farm we find the temperature and salinity that each sea louse particle experiences in the particle tracking simulation when initially released from a farm. We then use the average temperature and salinity of particles over all releases.

We also investigate the effect of varying temperature and salinity on the relative growth and persistence of the metapopulation. To do so, we must calculate survival and maturation rates for temperatures and salinities that farms may not experience in the period for which the FVCOM was run. To keep the variability of temperatures and salinities that exists between farms, we multiply the new temperature or salinity at which we want to evaluate persistence, by the ratio of the mean farm temperature or salinity divided by the mean total temperature or salinity experienced by all farms.

4.3 Results

In this section we present the next-generation matrix for sea lice populations on salmon farms in the Broughton Archipelago, the construction of which is detailed in section 4.2.4, and determine the relative patch contribution of each farm. We use this system to highlight to potential differences between the connectivity matrix, which only contains information surrounding the probability of dispersal from one farm to another, and the next-generation matrix, which combines dispersal between farms and local productivity of sea lice on a salmon farm. We then demonstrate how the next-generation matrix can be used to investigate the effect of changing demographic rates on growth and persistence in this system. Finally, in the context of salmon farm removal from the Broughton Archipelago, we investigate how the removal of habitat patches affects patch contribution and persistence in this sea louse metapopulation.

The next-generation matrix for sea lice populations on salmon farms in the Broughton Archipelago is shown in Figure 4.3a). The patch contribution of each salmon farm is given by R_j, the jth column sum, which is presented at the bottom of each column. We also present the row sums to the left each row, to identify which farms are receiving the most sea lice from other farms in the region. Farm 2 is the largest contributor

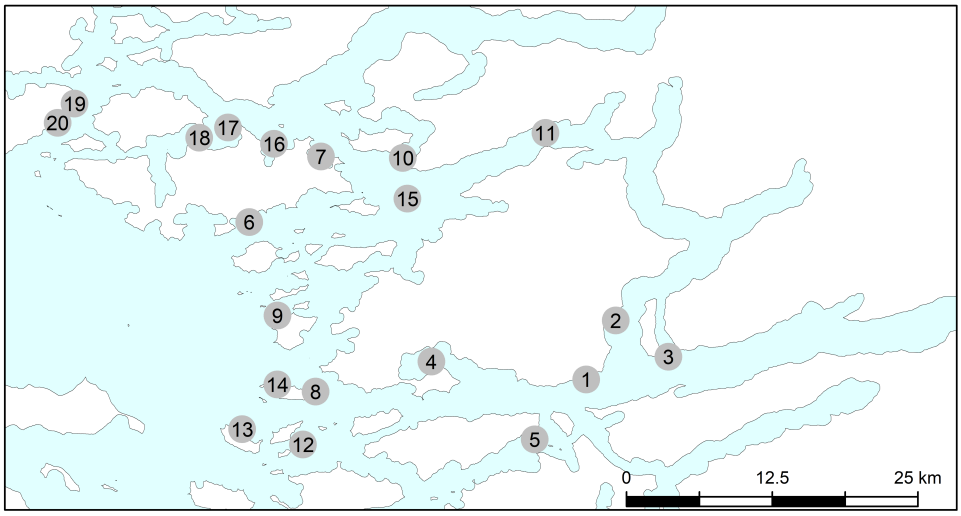

Figure 4.2: Map of the 20 historically active salmon farms in the Broughton Archipelago, for which the next-generation matrix is calculated.

of sea lice to the metapopulation, followed by farms 17 and 18, whereas farm 12 has the lowest contribution. The farms receiving the most sea lice, in declining order, are farms 3, 16, and 7.

To better understand the details and construction of the next-generation matrix, we also present the connectivity matrix for this system in Figure 4.4 and the productivity (total number of new larvae produced from one attached chalimus louse) of each farm in Table 4.1. The (i, j)th entry of the connectivity matrix, c_{ij}, is the infectious density over farm i of lice leaving farm j and the (i, j)th entry of the next-generation matrix is constructed by multiplying the productivity of farm j (equation 4.2.4) $p^{ij} = \beta \times 0.01 \times c_{ij}$, the probability that a larvae leaving farm j attaches on farm i (4.8). The farms with the largest column sums of the connectivity matrix are, in declining order, farms 18, 2, and 17. However, farm 2 has a higher productivity than farms 17 or 18, and when the productivity of farm 2 is multiplied by the connectivity then it becomes the largest source of sea lice in the region, as identified by the next-generation matrix.

A further look into the connectivity matrix and productivity table provides more insight into the underlying drivers of the contribution of each farm to the sea louse population. Many of the farms with low connectivity also have low productivity, which may be due to the fact that temperature and salinity affect on farm demographic rates as well as survival and maturation in the particle tracking simulation which underlies the connectivity matrix. However, there are certain farms, such as 11 and 15, which have a comparably high productivity compared to their connectivity. These farms are located in favourable environments with respect to temperature and salinity, but

low connectivity due to either distance from other farms or unfavourable currents prevents these farms from acting as larger sources of sea lice.

Here we also examine how temperature and salinity affect the overall growth and relative persistence of the sea louse metapopulation, as shown in Figure 4.5. The persistence of the metapopulation is determined by the basic reproduction number, R_0, which is calculated as the spectral radius of the next-generation matrix. As we do not have an accurate estimate for β, we examine the effect of temperature and salinity on the relative change in persistence or growth of the metapopulation, but refrain from commenting on the absolute growth, as measured by R_0. We can see that as both temperature and salinity increases, the overall growth of the metapopulation increases, and that salinity has a larger effect on metapopulation growth than temperature. What is also interesting, but cannot be seen from the figure, is that as salinity increases, the farm that receives the most lice switches from farm 3 to farm 7.

In light of the removal of salmon farms in the Broughton Archipelago we also create a next-generation matrix consisting only of the farms which will remain after 2023 subject to First Nations and government approval, shown in Figure 4.3b), and examine the differences between this matrix and the next-generation matrix with all farms. Most of the farms which are acting as the largest sources of sea lice in this region remain, with the exception of farm 11, the fifth largest source in the original network, which has now been removed. Farm 11, while not the largest source, did have the largest betweenness score based solely on the connectivity matrix (Cantrell et al., 2018), and thus may have been acting as a connecting farm between the two large clusters of source farms. However, since none of the other large source farms have been removed, the overall growth of the metapopulation has only decreased from $R_0 = 2.33$ (original next-generation matrix) to $R_0 = 2.25$. Again these numbers are calculated using a very rough estimate of the arrival rate onto farms, detailed in section, and thus it is their relative similarity that is important, rather than the absolute magnitude.

4.4 Discussion

In this chapter we demonstrated how to use the next-generation matrix to calculate the contribution of each habitat patch to the metapopulation and measure the overall persistence of a metapopulation. We detailed the construction of the next-generation matrix under different model structures to demonstrate the breadth of the approach to several systems. We then constructed the next-generation matrix under

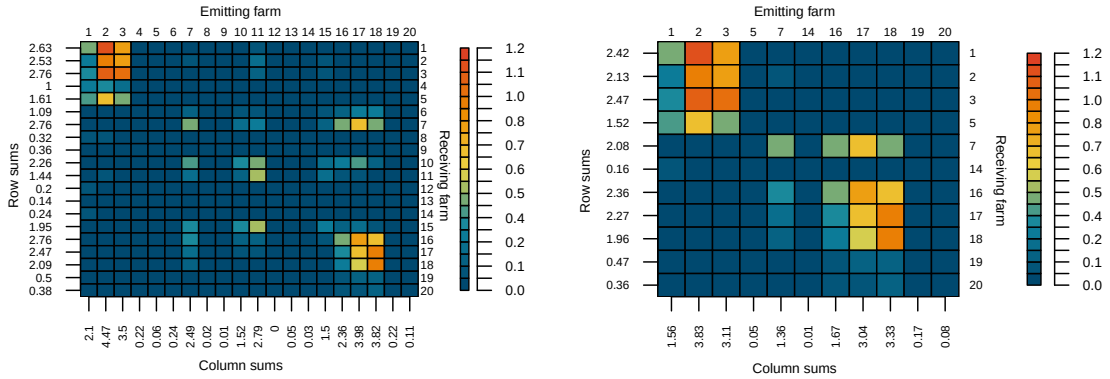

(a) (b)

Figure 4.3: a) The next-generation matrix for the 20 historically active farms in the Broughton Archipelago, and b) the next-generation matrix containing only the farms remaining in the Broughton Archipelago after 2023, subject to First Nations and governmental approval (Brownsey and Chamberlain, 2018). The entries of the next-generations matrices, k_{ij} are the number of new chalimus stage lice produced on farm i from one initial chalimus on farm j. The column sums, R_j, are the total number of chalimus produced on all farms from an initial chalimus on farm j and are shown below each column. Likewise the row sums are the number of new chalimus received by each farm from all other farms and are shown on the left of each row. These numbers should be taken as relative, rather than absolute, as we do not have a very accurate estimate for the arrival rate of sea lice onto farms, β.

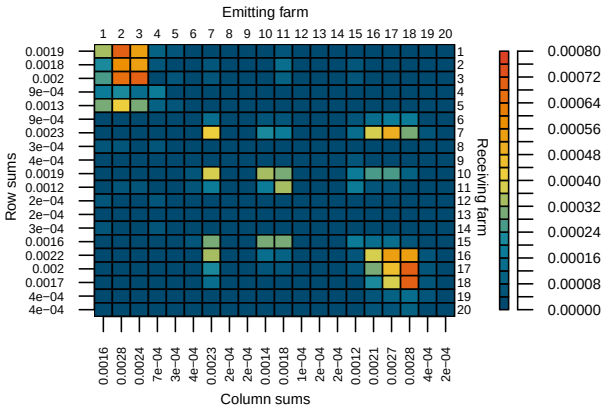

Figure 4.4: The connectivity matrix for sea lice larvae dispersing between salmon farms. The (i, j)th entry is the infectious density of larvae ($1/\text{km}^2$) over farm i that have left from farm j. Column and row sums are shown below and to the left of each column and row, respectively.

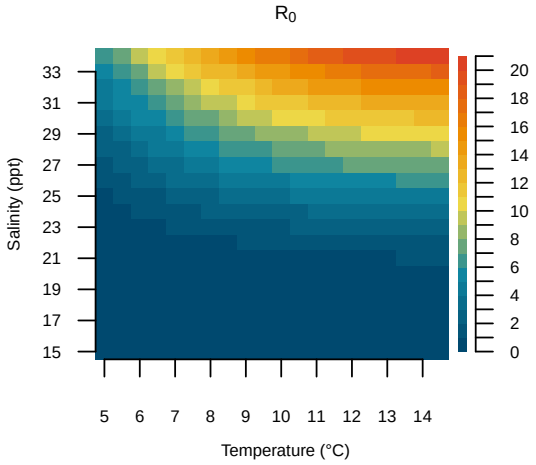

Figure 4.5: The effect of temperature and salinity on the overall growth or persistence of the original sea lice metapopulation of 20 farms, as described by the basic reproduction number, R_0. We do not have a good estimate for the arrival rate of sea lice onto farms, β, and so the R_0 values should only be interpreted relative to each other, rather than as absolute values.

Table 4.2: The number of new larvae produced on each farm by a single louse starting in the chalimus stage. The first row is the farm number and the second row is the number of larvae produced.

1	2	3	4	5	6	7	8	9	10
1355	1582	1462	239	244	612	1064	111	56	1060
11	12	13	14	15	16	17	18	19	20
1529	33	331	175	1255	1143	1483	1348	584	464

an age dependent modeling framework for sea lice populations on salmon farms in the Broughton Archipelago to illustrate how this approach can be applied to a real system. We determined which salmon farms may be acting as the largest sources of sea lice in this region, how the metapopulation will change once certain farms are removed, and examined the effect of temperature and salinity on the relative growth and persistence of this metapopulation.

Next-generation matrices have been used extensively in epidemiology to study the spread of infectious diseases but have recently been introduced in ecology (Huang and Lewis, 2015; Krkošek and Lewis, 2010; Lewis et al., 2019; Mckenzie et al., 2012a) and evolutionary analysis (Hurford et al., 2010). One of the key benefits of using next-generation matrices in epidemiology is that the basic reproduction number, R_0, for a disease can be calculated as the spectral radius of the NGM, which is often much simpler than calculating the eigenvalues of the full system to determine spread. In ecology, one main advantage of this approach is that the mathematical calculation of R_0 can be broken down into biologically relevant quantities, for example the contribution of different dispersal pathways to growth in a population (De-Camino-Beck and Lewis, 2007) or the contribution of populations on different habitat patches (Harrington and Lewis, 2020). While not novel, we hope next-generation matrices can be used more frequently as a simple and easily biologically interpretable method to measure the contribution of local habitat patches to a metapopulation and determine overall persistence.

We are also by no means the first to attempt to calculate the contribution of a local population, classify patches into sources and sinks, or attempt to measure the persistence of metapopulations. In the context of low densities Pulliam (1988) defined a source as a habitat patch that would grow in the absence of immigration and emigration and a sink as a habitat patch that would decline in the absence of immigration and emigration. This is similar to only using the entries along the diagonal of the next-generation matrix to classify sources or sinks, except growth or decline was measured after one time step in a discrete time model, rather than one generation. However, as discussed at the end of section 4.2.2, it is possible to have a metapopulation composed only of sinks based on this definition ($k_{ii} < 1$ for all i), that persists.

Recognizing that dispersal between patches should also considered when classifying habitat patches as sources or sinks, both Runge et al. (2006) and Figueira and Crowder (2006) defined new metrics to classify habitat patches that track the contribution of adults on a patch in one time step to the total population on all patches in the next timestep. These metrics are similar to our patch contribution metric R_j,

except they measure the contribution over one time step rather than one generation, similar to using the dominant eigenvalue of the projection matrix A to determine the stability of the discrete system $n(t+1) = An(t)$, rather than the spectral radius of the next-generation matrix K. However, the calculations can become complicated if the population is stage structured and A is large (Appendix A, Runge et al. (2006)) and the metrics do not easily generalize to systems described by ordinary differential equations.

There are other measures of persistence in metapopulations which do track the number of new individuals contributed to the metapopulation after one generation from an initial individual on one patch, though they use different starting stages for the initial and new individuals. Krkošek and Lewis (2010) define a next-generation operator for general heterogeneous populations which tracks the number of new adults produced in the population from one initial adult after one generation. If b_j is the reproductive output on patch j, p_{ij} is the probability of larvae dispersing between patch j successfully arrives on patch i, and a_i is the survival to adulthood on patch i, then the contribution of patch j to patch i according to Krkošek and Lewis (2010) can be calculated as $b_j p_{ij} a_i$. This patch contribution metric cannot be calculated directly from the next-generation matrices shown in this chapter unless there is only one stage. Burgess et al. (2014), following Hastings and Botsford (2006), track the number of new larvae on all patches produced by an initial larvae. The entries of their 'connectivity matrix' (similar to our next-generation matrix), c_{ij}, are given by $p_{ij} a_i b_i$. The entries of their connectivity matrix would be the entries of the next-generation matrix if it was calculated from a model with an explicit larval stage. However under this construction the contribution of patch j, as calculated by the jth column sum of their connectivity matrix, is primarily a function of the demography of the patches on which larvae dispersing from j settle, rather than the local patch demography of patch j itself, as it is when using the next-generation matrix as we have formulated it in this chapter.

The contribution of each habitat patch to the metapopulation will depend on the stage at which the generational output is measured, but the persistence of the metapopulation is equivalent under all of these frameworks. This is because there is only one component of the life cycle where movement can occur between patches (larval stage) and at all other stages individuals remain on a patch. Let P be a matrix with entries p_{ij}, B be a diagonal matrix with entries b_j and A be a diagonal matrix with entries a_j, where p_{ij}, b_j and a_j are the same as the preceding paragraph. If we measure generational output starting at the first attached stage, as we do in this chapter, the next-generation matrix can be written as PBA, if we measure

generational output starting at the larval stage according to Burgess et al. (2014), the matrix can be written as BAP, and if we measure generational output starting at the adult stage according to Krkošek and Lewis (2010) then the matrix can be written as APB. This is because when P is multiplied by a diagonal matrix on the right, the entries of the diagonal matrix multiply each column of P and when P is multiplied on the left, the entries multiply each row. Now the matrices XY and YX have the same eigenvalues, and because matrix multiplication is associative each of the matrices PBA, BAP, and APB all have the same eigenvalues as well, and therefore also the same spectral radius. Therefore in any of the formulations the metapopulation will only persist if $\rho(PBA) = \rho(BAP) = \rho(APB) > 1$.

While the metapopulation persistence criteria is equivalent to other formulations (Burgess et al., 2014; Hastings and Botsford, 2006; Krkošek and Lewis, 2010) we believe using the next-generation matrix provides several advantages. First, the framework is the same for discrete time, continuous time, and age structured systems of equations. Second, it is easy to convert between the full system of equations and the next-generation matrix, thus if a system of equations has already been parameterized for a given region, it is easy to calculate the contribution of each habitat patch using the next-generation matrix. Third, there is natural extension of the next-generation matrix to systems where multiple stages can reproduce, or when adults can migrate between patches. In discrete time and continuous time the composition of the matrix in terms of the fecundity and transition matrix still holds, only the formulas given in terms of the survival, maturation, and birth rates no longer hold. The next-generation matrix can also be extended as an operator to integro-difference equations (Krkošek and Lewis, 2010; Mckenzie et al., 2012a). Lastly, in continuous time systems it is possible to connect the patch contribution computed from the next-generation matrix, R_j, and the transient dynamics of the metapopulation (Chapter 3 of this thesis).

When calculating the next-generation matrix for a specific system, such as our application of sea lice populations on salmon farms, there are some technical aspects which should be considered. In order to use the next-generation matrix to calculate patch contribution or persistence we are assuming that our system is autonomous, and that the demographic rates do not change with time. In reality for most systems, including sea lice on salmon farms, environmental variables will fluctuate over time, potentially changing the demographic rates of the population. In our case temperature and salinity change over the course of the spring, but we calculate the next-generation matrix using the mean temperature and salinity that sea lice experience during the particle tracking simulation window. Therefore the entries in our next-generation matrix may be slightly different than the true number of newly at-

tached lice produced on other farms from one initially attached louse, depending on the exact time that the louse began its lifecyle during the spring. For temporally oscillating systems it is possible to correct for this difference, though the entries of the next-generation matrix no longer have a simple form and must be computed computationally (Rittenhouse et al., 2016).

Over time periods where temperature and salinity are relatively constant, we can use the next-generation matrix to examine the overall effect of environmental variables on the growth of the metapopulation. The demographic rates at each stage depend explicitly on temperature and salinity but alone, or in a full system of equations, it can be difficult to examine the overall effect of changing environmental variables. However, the basic reproduction number R_0, calculated from the spectral radius of the next-generation matrix, provides a useful metric of the overall effect. We can infer how the growth of the metapopulation may change among seasons, or as the ocean warms. For sea lice on salmon farms in the Broughton Archipelago the effect that of temperature and salinity on R_0 is very similar to previous results found for a single farm (Rittenhouse et al., 2016). With updated temperature and salinity at each farm, we could calculate the change in growth over years in the springtime, which may help explain the recent sea louse outbreaks during warm years in the Broughton Archipelago (Bateman et al., 2016). When examining the effect of temperature and salinity on R_0 we do not rerun the hydrodynamic and particle tracking models to recreate the connectivity matrices under new temperature and salinity scenarios, as this is very computationally intensive, but we expect connectivity to increase as temperature and salinity increases due to higher survival of sea lice and faster maturation. However, we believe it would be valuable to rerun hydrodynamic models under different projected ocean scenarios, to investigate the precise changes in connectivity that may occur.

Specific to management of sea lice populations on salmon farms in the Broughton Archipelago, there are several insights to be gained from our results. The first is that the farms that in the most productive environments are also the most highly connected, and thus become the largest contributors of sea lice to this sea louse metapopulation. They occur in two main clusters (shown in Figure 4.3) and both clusters of farms will remain in the Broughton Archipelago in the current removal plan, subject to First Nations and governmental approval (Brownsey and Chamberlain, 2018). It should be noted that these farms may not necessarily be producing the most number of lice compared to other farms in the region at a given time if their louse population is currently lower than other farms, rather they are the farms that have the largest potential to contribute to spread when sea louse numbers are even

across farms. However, due to the highly connected nature of these clusters, coordinated treatment between farms in the clusters or all farms in the region could reduce the number of treatments required and number of sea lice produced on all farms (Peacock et al., 2016). An interesting avenue of future research would be to connect the productivity of the remaining farms in the Broughton Archipelago with the Kernel Density Estimates of sea louse dispersal from Cantrell et al. (2018) to measure the exposure of migrating wild salmon to sea louse infection from these farms.

4.5 Conclusion

We have illustrated how to use the next-generation matrix to calculate the contribution of each habitat patch in a metapopulation and how to measure metapopulation persistence. The measures of patch contribution, R_j, and metapopulation persistence, R_0, have useful biological interpretations in terms of the number of new individuals produced after one generation and can easily be calculated. We presented the general construction of the next-generation matrix for different formulations of metapopulation models to demonstrate how to apply the approach to many different systems. Then, we constructed the next-generation matrix for sea louse populations on salmon farms in the Broughton Archipelago to show how this approach can be applied to real systems and to provide insight into which farms may be the drivers of spread in this system. Finally, we discussed how previous measures of patch contribution and metapopulation persistence relate to our measures from the next-generation matrix for different systems. Overall, we believe that the next-generation matrix provides a simple and broadly applicable connection between explicit population models and the calculation of patch contribution and persistence in metapopulations.

4.6 Appendices for Chapter 4

4.6.1 Calculating the NGM for differential equation models

Here we briefly formalize the calculation of the next-generation matrix for differential equation models. Again, we are considering a model for a species with m sessile stages on l patches with a larval stage that can disperse between patches and all other stages are sedentary and confined a patch. Let n_k^j be the population in sessile stage k on patch j, then the population dynamics at low population densities can be described by

$$\frac{d\mathbf{n}}{dt} = A\mathbf{n} \tag{4.10}$$

where $\mathbf{n}$ is a population vector of size $m \times l$ describing the population size on all patches at all stages and A is a matrix describing the population dynamics at low population densities. We model the population size at low densities because we are interested in identifying which patches are acting as sources and supporting the population at low densities and which are acting as sinks. Therefore equation 4.10 should be thought of as the linearization about the zero equilibrium of a potentially more complex model that may include density dependence. The elements of A contain the maturation and death rates of sedentary stages confined to patches as well as the rates of larval dispersal and attachment between patches.

The next-generation matrix for this system can be calculated by first decomposing $A = F - V$ where F is a non-negative matrix with entries that describe the rates of larval birth and probability of dispersal between patches and attachment as the first sedentary phase, and V is a non-singular M matrix (Berman and Plemmons, 1994) with entries that describe the maturation rates between stages and death rates in a stage (van den Driessche and Watmough, 2002). Because V is a non-singular M matrix, V^{-1} is non-negative. Following van den Driessche and Watmough (2002) with notation from Diekmann et al. (2010), the next-generation matrix with large domain, K_L, can then by calculated as

$$K_L = FV^{-1}. \tag{4.11}$$

The elements of K_L contain the number of new individuals in each stage and patch produced by one initial new individual in each stages and patch. However, since new individuals are only produced in stage 1, K_L will only have l non-zero rows. If equation 4.10 is arranged so that the populations of stage 1 individuals are in the first l rows, then K_L will have a $l \times l$ submatrix in the upper left-hand corner (Diekmann et al., 2010). This submatrix is the next-generation matrix K, where the elements of K, k_{ij}, give the number of new (stage 1) individuals produced on patch i from one initial stage 1 individual on patch j. In equation 4.10, if the maturation rates from stage k to $k+1$ on patch j are m_k^j, the death rates in stage k are d_k^j, the birth rate in the last stage on patch j is b^j, and the probability of successful attachment on patch i as a larvae leaving patch j is p^{ij}, then the entries of K can be written as:

$$k_{ij} = \underbrace{\left[\prod_{k=1}^{m-1} \overbrace{\left(\frac{m_k^j}{m_k^j + d_k^j}\right)}^{\Pr(\text{stage } k \to k+1)}\right]}_{\text{survival through sessile stages}} \times \underbrace{\left(\frac{b^j}{d_m^j}\right)}_{\#\text{ larvae produced}} \times \overbrace{p^{ij}}^{\Pr(\text{patch } j \text{ to patch } i)} . \tag{4.12}$$

Example of the next-generation matrix for a two patch metapopulation

Here we illustrate the construction of the next-generation matrix using a two patch example for a species which has two sessile stages. The population of sessile stage k on path j is given by n_k^j and the maturation rates, death rates, birth rate, probability of dispersal are defined as in the preceding paragraph. The dynamics of the system can be described by

$$\begin{bmatrix} n_1^1 \\ n_1^2 \\ n_2^1 \\ n_2^2 \end{bmatrix}' = \overbrace{\begin{bmatrix} -d_1^1 - m_1^1 & 0 & b^1 p^{11} & b^2 f^{12} \\ 0 & -d_1^2 - m_1^2 & b^1 p^{21} & b^2 f^{22} \\ m_1^1 & 0 & -d_2^1 & 0 \\ 0 & m_1^2 & 0 & -d_2^2 \end{bmatrix}}^{A} \begin{bmatrix} n_1^1 \\ n_1^2 \\ n_2^1 \\ n_2^2 \end{bmatrix},$$

where we have arranged the system of equations so that individuals in the first stage appear in the top rows. We decompose $A = F - V$ where F contains all the births of new stage 1 individuals and V contains all the remaining transitions, so that F and V are given by

$$F = \begin{bmatrix} 0 & 0 & b^1 p^{11} & b^2 p^{12} \\ 0 & 0 & b^1 p^{21} & b^2 p^{22} \\ 0 & 0 & 0 & 0 \\ 0 & 0 & 0 & 0 \end{bmatrix}, V = \begin{bmatrix} d_1^1 + m_1^1 & 0 & 0 & 0 \\ 0 & d_1^2 + m_1^2 & 0 & 0 \\ -m_1^1 & 0 & d_2^1 & 0 \\ 0 & -m_1^2 & 0 & d_2^2 \end{bmatrix}.$$

The next-generation matrix with large domain, K_L, can then be calculated as $K_L = FV^{-1}$, where

$$K_L = \begin{bmatrix} \frac{m_1^1}{m_1^1+d_1^1}\frac{b^1}{d_2^1}p^{11} & \frac{m_1^2}{m_1^2+d_1^2}\frac{b^2}{d_2^2}p^{12} & \frac{b^1}{d_2^1}p^{11} & \frac{b^2}{d_2^2}p^{12} \\ \frac{m_1^1}{m_1^1+d_1^1}\frac{b^1}{d_2^1}p^{21} & \frac{m_1^2}{m_1^2+d_1^2}\frac{b^2}{d_2^2}p^{22} & \frac{b^1}{d_2^1}p^{21} & \frac{b^2}{d_2^2}p^{22} \\ 0 & 0 & 0 & 0 \\ 0 & 0 & 0 & 0 \end{bmatrix}$$

and then the next-generation matrix, K, will be given by the 2×2 submatrix in the upper left-hand corner of K_L, so

$$K = \begin{bmatrix} \frac{m_1^1}{m_1^1+d_1^1}\frac{b^1}{d_2^1}p^{11} & \frac{m_1^2}{m_1^2+d_1^2}\frac{b^2}{d_2^2}p^{12} \\ \frac{m_1^1}{m_1^1+d_1^1}\frac{b^1}{d_2^1}p^{21} & \frac{m_1^2}{m_1^2+d_1^2}\frac{b^2}{d_2^2}p^{22} \end{bmatrix}.$$

The contribution of patch 1 is therefore

$$R_1 = \underbrace{\frac{m_1^1}{m_1^1 + d_1^1}\frac{b^1}{d_2^1}}_{\text{productivity}} \underbrace{\left(p^{11} + p^{12}\right)}_{\text{connectivity}}$$

and the contribution of patch 2 is

$$R_2 = \frac{m_1^2}{m_1^2 + d_1^2}\frac{b^2}{d_2^2}\left(p^{12} + p^{22}\right).$$

In order for a patch to be a source ($R_j > 1$), both the on-patch productivity and the connectivity to other patches need to multiply to be larger than 1. If either is too low, i.e. if a patch is highly productive but not well connected, or highly connected but not productive, then the patch will be a sink ($R_j < 1$). There are two ways for the entire metapopulation to persist. Either a single patch can persist on its own ($k_{ii} > 1$), or there must be sufficient production and connectivity within patches such that $R_0 = \rho(K) > 1$.

4.6.2 Calculating the NGM for discrete time models

The construction of the next-generation matrix for discrete time models is very similar to that of continuous time, though with some minor differences. The population dynamics can now be described by

$$\mathbf{n}_{t+1} = A\mathbf{n}_t \tag{4.13}$$

where again $\mathbf{n}$ is a population vector of size $m \times l$ (number of stages $\times$ number of patches) describing the population size on all patches at all sessile stages, but now A is a population projection matrix with transition and survival probabilities as well as births.

To calculate the next-generation matrix for the discrete time system, we now decompose $A = F + T$, where again F is a matrix that contains all the birth rates and probabilities of successful of larval dispersal between patches, and now T is a matrix that contains all of the survival probabilities and transition probabilities between stages. Under this decomposition, the next-generation matrix with large domain, K_L, can by calculated by

$$K_L = F(I - T)^{-1}. \tag{4.14}$$

If Equation 4.13 is arranged so that the populations of all stage 1 individuals are in the top l rows, then again the next-generation matrix, K, will be the $l \times l$ submatrix in the upper left hand corner of K_L. In the discrete time framework if the probability

of transitioning from stage k to $k+1$ is m_k^j, the probability of survival in stage k is s_k^j, the fecundity in patch j is b^j, and the probability that a larvae leaving patch j successfully arrives on patch i is p^{ij}, then the entries of K can be written as

$$k_{ij} = \underbrace{\left[\prod_{k=1}^{m-1} \overbrace{\left(\frac{m_k^j}{1-s_k^j}\right)}^{\Pr(\text{stage } k \to k+1)}\right]}_{\text{survival through sessile stages}} \times \underbrace{\left(\frac{b^j}{1-s_m^j}\right)}_{\#\text{ larvae produced}} \times \overbrace{p^{ij}}^{\Pr(\text{patch } j \text{ to patch } i)} . \tag{4.15}$$

4.6.3 Details of the model with age dependent demography in section 4.2.3

The full set of age density equations for the density of individuals in sessile stage k on patch i at time t and age a, $n_k^i(t,a)$, is

$$n_k^i(t,a) = \begin{cases} \underbrace{B_k^i(t-a)S_k^i(a)M_k^i(a)}_{\text{entered at } t-a\text{, survived to } a} & t > a \\ \underbrace{n_{k,0}^i(a-t)\dfrac{S_k^i(a)M_k^i(a)}{S_k^i(a-t)M_k^i(a-t)}}_{\text{present at } a-t\text{, survived to } a} & 0 < t < a \\ \underbrace{n_{k,0}^i(a)}_{\text{initial density}} & t = 0 \end{cases} \quad k = 1, \ldots, m-1, \tag{4.16}$$

$$n_m^i(t,a) = \begin{cases} B_m^i(t-a)S_m^i(a) & t > a \\ n_{m,0}^i(a-t)\frac{S_m^i(a)}{S_m^i(a-t)} & 0 < t < a \\ n_{m,0}^i(a) & t = 0 \end{cases} \quad k = m,$$

$$B_1^i(t) = \sum_{j=1}^{l} \int_0^\infty n_m^i(t,a) b^i(a) p^{ij} da \qquad k = 1$$

$$B_k^i(t) = \textstyle\int_0^\infty n_{k-1}^i(t,a) m_{k-1}^i(a) da \qquad k = 2, \ldots, m,$$

where $S_k^j(a)$ is the probability of survival in stage k on patch j at stage-age a, $m_k^j(a)$ is the maturation rate from stage k to $k+1$, $b^j(a)$ is the birth rate of larvae on patch j, and the probability of a larva leaving patch j and successfully attaching on patch i is p^{ij}. $M_k^j(a)$ is the probability that an individual has not yet matured from stage k to $k+1$ and can be calculated as $M_k^j(a) = \exp(-\int_0^a m_k^j(\tau)d\tau)$. Additional details of the model equations can be found in Harrington and Lewis (2020), though there the first larval stage is modelled explicitly and so the set of equations is slightly different.

To construct the next-generation matrix for this system, we need to track the number of stage 1 individuals produced on each patch from one initial stage 1 individual

on a given patch. We briefly present the idea of the construction here, and more details can be found in Harrington and Lewis (2020).

Let $\gamma_{ij}(t)$ be the rate of production of new stage 1 individuals on patch i from an initial stage 1 individual on patch j. For an initial individual to be producing offspring it must survive through each of the sessile stages and then produce larvae which settle on another patch. Let r_k be the time that an individual spends in stage k. Then in the first $m-1$ sessile stages $k = 1, \ldots, m-1$ the probability that the individual survives up to r_k is $S_k^j(r_k)M_k^j(r_k)$ and the rate that they are maturing to the next stage at r_k is $m_k^j(r_k)$. In the last stage the probability that they survive up to r_m is $S_m^j(r_m)$ and the rate that they are producing larvae from patch j which successfully arrive on patch i is $b^j(r_m)p^{ij}$.

To calculate the rate of production at time t, $\gamma_{ij}(t)$ we multiply all the survival probabilities, maturation rates, and birth rate in each stage and integrate over all possible r_k, where $0 \leq \sum_{k=1}^{m} r_k \leq t$. To ensure this bound we rewrite $r_m = t - \sum_{k=1}^{m-1} r_k$. Thus

$$\gamma_{ij}(t) = \int_0^t \int_0^{t-r_{m-1}} \int_0^{t-r_{m-1}-r_{m-2}} \cdots \int_0^{t-\sum_2^{m-1} r_k} S_1^j(r_1)M_1^j(r_1)m_1^j(r_1)\ldots$$
$$S_{m-1}^j(r_{m-1})M_{m-1}^j(r_{m-1})m_{m-1}^j(r_{m-1})S_m^j(t-\sum_1^{m-1} r_k)b^j(t-\sum_1^{m-1} r_k)p^{ij}dr_1\ldots dr_{m-1}. \tag{4.17}$$

Then we can integrate the rate of production, $\gamma_{ij}(t)$ over all time to find the total number of new individuals produced on i from an initial individual on j, this is the entry in the ith row and jth column of the next-generation matrix, k_{ij}. We can use the convolution theorem,

$$\int_0^\infty f(t) * g(t)dt = \int_0^\infty f(t)dt \int_0^\infty g(t)dt \tag{4.18}$$

to calculate $\int_0^\infty \gamma_{ij}(t)dt = k_{ij}$ as

$$k_{ij} = \left[\prod_{k=1}^{m-1} \left(S_k^j(t)M_k^j(t)m_k^j(t)dt\right)\right] \left(\int_0^\infty S_m^j(t)b^j(t)dt\right) p^{ij}. \tag{4.19}$$

Chapter 5

Calculating the timing and probability of arrival for sea lice dispersing between salmon farms

5.1 Introduction

Marine populations are often connected over large distances due to larval dispersal. Once thought to be open populations with continuous exchanges of larvae, it is now understood that many marine populations depend directly on the degree of larval exchange between population patches, and that these connected patches act as metapopulations (Cowen et al., 2006; Cowen et al., 2000; Cowen and Sponaugle, 2009). The degree of connectivity between habitat patches in a metapopulation is a function of many variables, including the strength of the ocean currents on which the larvae depend to disperse and the environmental conditions of the ocean which impact biological processes such as maturation and survival. Research into larval dispersal in marine metapopulations has led to a greater understanding of the population dynamics of corals (Mayorga-Adame et al., 2017), coral reef fish (Jones et al., 2009) and sea turtles (Robson et al., 2017), as well as the efficacy of Marine Protected Areas (Botsford et al., 2009; Fox et al., 2016). It has also been used to determine the level of sea lice dispersal between salmon farms and the effect of coordinated treatment plans in salmon farming regions (Adams et al., 2015; Cantrell et al., 2018; Kragesteen et al., 2018; Samsing et al., 2017).

Sea lice (*Lepeophtheirus salmonis*) are parasitic marine copepods that feed on the epidermal tissues, muscle, and blood of salmon (Costello, 2006). A free living nauplius stage allows sea lice to disperse tens of kilometers in the ocean while developing into infectious copepodites that can attach to their salmonid hosts, on which sea lice complete the remainder of their life cycle (see Figure 5.1) (Amundrud and Murray,

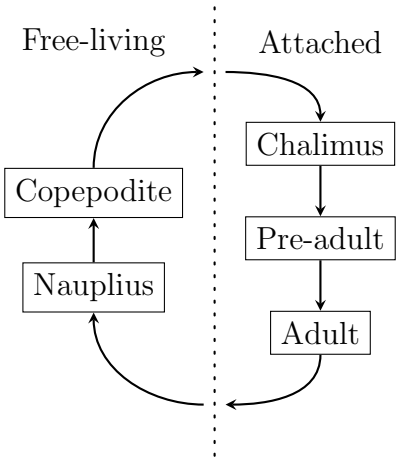

Figure 5.1: A simplified schematic of the life cycle of the sea louse, *Lepeophtheirus salmonis*. The attached stages live on wild or farmed salmon and the free-living stages disperse in the water column. Larvae must mature through the nauplius stage into the copepodite stage before they are able to attach to a salmonid host.

2009; Stucchi et al., 2011). High infestation levels on adult salmon have been shown to lead to mortality and morbidity (Pike and Wadsworth, 1999), and lesions and stress from infestations make adult salmon susceptible to secondary infections, which have led to large economic consequences for the salmon farming industry (Costello, 2009b). On wild juvenile salmon, infestation with sea lice can lead to mortality (Krkošek et al., 2007) or other physiological (Brauner et al., 2012) and behavioural effects (Godwin et al., 2015; Krkošek et al., 2011a). In near coastal areas, elevated levels of sea lice from salmon farms have been detected on juvenile salmon up to tens of kilometers away and these high levels of infection have contributed to population level declines in pink salmon (Krkošek et al., 2007; Krkošek et al., 2006a; Krkošek et al., 2005; Peacock et al., 2020).

In dense salmon farming regions such as Norway, Scotland, and Canada there is evidence that sea lice populations on salmon farms are connected via larval dispersal and thus act as a connected metapopulation (Adams et al., 2015; Aldrin et al., 2017; Aldrin et al., 2013; Cantrell et al., 2021; Cantrell et al., 2018). In Norway, where most salmon farms are located in fjords along the coast, seaway distance has been used as a simple measure of farm connectivity over a large scale (Aldrin et al., 2013). At a smaller scale, hydrodynamic models have been used to measure the level of connectivity between farms (Adams et al., 2015; Cantrell et al., 2018; Foreman et al., 2015; Samsing et al., 2017) in several salmon farming regions. Hydrodynamic models simulate ocean currents and can then be coupled with particle tracking models to

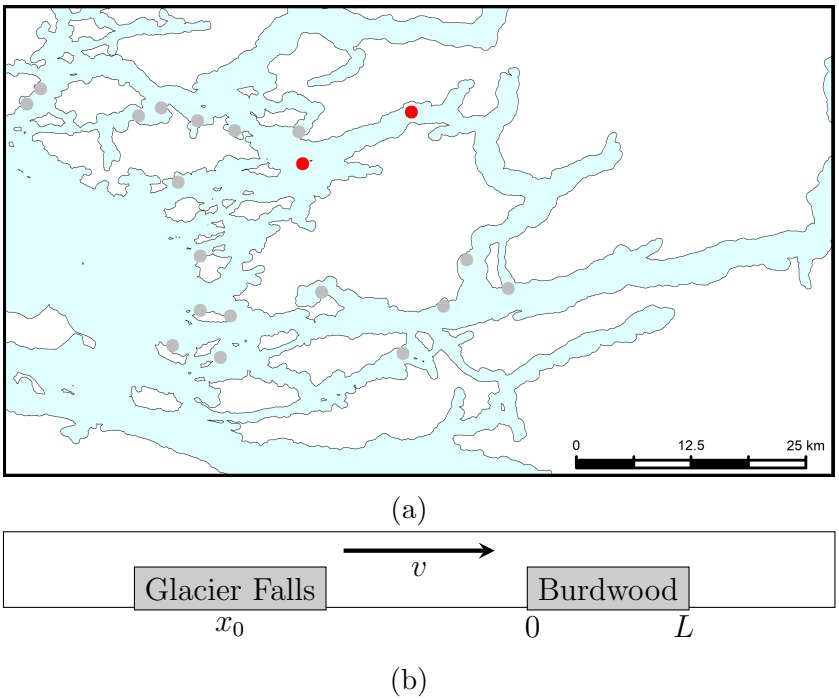

Figure 5.2: The two salmon farms that are used to calculate the time and probability of arrival for sea lice dispersing between farms. a) A map of the Broughton Archipelago with all active farms from 2009 shown in grey, and the two farms used in this study highlighted in red. The release farm is the eastern farm, Glacier Falls, which is located in Tribune Channel and the receiving farm is the western farm, Burdwood. b) The one dimensional representation of Tribune Channel used in the mathematical analysis. Note that the position of the farms has been switched so the advective coefficient, v, is positive.

determine how sea lice disperse when released from a farm (Stucchi et al., 2011).

The degree of interfarm connectivity, even between two farms, can have large consequences in terms of treating for sea louse outbreaks, and can even lead to chaotic dynamics under threshold treatment regimes (Peacock et al., 2016). Calculating the probability of sea lice dispersing to other farms is integral in determining which farms may be the largest sources of sea lice spread in a salmon farming region and thus which may be driving spread (Cantrell et al., 2018; Harrington and Lewis, 2020). Lastly and perhaps most importantly, determining the probability of sea lice arrival onto other farms is critical in understanding where to place farms in a salmon farming region, or which to first remove.

To date, most of the research into the degree of connectivity between salmon farms has either been region specific, using hydrodynamical models (Cantrell et al., 2018; Samsing et al., 2017) or at a large scale, with statistical analyses (Aldrin et al., 2013; Kristoffersen et al., 2013). Hydrodynamic models can be very useful in determining connectivity in the specific regions for which they are run, but results from these specific regions may be difficult to generalise to other regions. Conversely, statistical analyses are useful at determining the broad drivers of spread over large regions but often do not allow for detailed investigations into how certain parameter interactions affect the degree of connectivity between two farms. Thus there are still many general questions surrounding interfarm connectivity that require new approaches to investigate.

In this chapter, we aim to answer the following questions surrounding the probability of sea lice dispersing between salmon farms:

(i) How does the degree of cross-infection, giving by arrival probability, depend on the spacing between farms?

(ii) Are there scenarios where an intermediate spacing between farms leads to the highest level of cross-infection?

(iii) Does the relationship between cross-infection and farm spacing change in advection dominated versus diffusion dominated systems?

(iv) How does the maturation time for nauplii to develop into infectious copepodites affect cross-infection?

In order to answer these questions it is necessary to have a mechanistic model that is both sufficiently simple to investigate analytically and numerically in detail, but sufficiently realistic to capture the essential components of ocean circulation and

sea louse biology. For credible analysis the simple model must be fit to realistic sea lice dispersal data to ensure accurate estimates of oceanic advection and diffusion as well as sea louse maturation times. The approach here is to use numerical flows from a three dimensional computational hydrodynamic model, along with a particle tracking model, to fit a simple one dimensional analytical model that describes the movement of sea lice between two salmon farms in a channel in the Broughton Archipelago, British Columbia(Figure 5.2). The calibrated model is then used to investigate questions (i)-(iv).

The numerical flows are generated from a Finite Volume Community Ocean Model (FVCOM) which has been applied to the Broughton Archipelago, located between the northeast coast of Vancouver Island and the mainland of British Columbia. The Broughton Archipelago has many active salmon farms and has been at the center of the debate of the effect of sea lice on wild salmon (Brooks, 2005; Brooks and Stucchi, 2006; Krkošek et al., 2011b; Krkošek et al., 2008; Krkošek et al., 2007; Krkošek et al., 2006a; Krkošek et al., 2005; Krkošek et al., 2006b; Marty et al., 2010; Riddell et al., 2008). The rivers in the Broughton are major migration routes for both pink and chum salmon, and sea lice from salmon farms in this region have contributed to population level declines in pink salmon (Krkošek et al., 2007). Currently, certain salmon farms are being removed under a new agreement between the governments of British Columbia and the Kwikwasut'inuxw Haxwa'mis, 'Namgis, and Mamalilikulla First Nations (Brownsey and Chamberlain, 2018). The abundance of sea lice data from counts on farmed and wild salmon as well as the complex hydrodynamical particle tracking simulations run for this region make the Broughton Archipelago an ideal area to investigate the cross-infection of sea lice between salmon farms.

In this chapter we develop a simple mechanistic model for the arrival time distribution of sea lice dispersing between two different salmon farms. The arrival time distribution is necessary to calculate the level of cross-infection between farms, which is given by the probability of arrival for sea lice dispersing between salmon farms. We begin by presenting the analytical results for simple particles dispersing, ignoring the maturation required for sea lice to become infectious, before presenting the full arrival time distribution for sea lice that encompasses the non-infectious nauplius stage and infectious copepodite stage. Next, we calculate the arrival time directly using the numerical flows from FVCOM coupled with a particle tracking model to fit our simple mechanistic model and find parameter estimates. Lastly, we use our parameterized mechanistic model to investigate the questions (i)-(iv) surrounding cross-infection and farm placement.

5.2 Methods

5.2.1 Mechanistic model

In order to calculate the arrival time of sea lice travelling between salmon farms and the probability of arrival, we first need a model for how sea lice disperse along a channel and arrive at a salmon farm. We begin by ignoring the maturation time required for newly released nauplii to develop into infectious copepodites to gain a comprehensive understanding of the arrival time distribution and to simplify the details of the initial mathematical analysis. Therefore we are assuming that all sea lice released from a salmon farm are infectious and model their dispersal using the following advection-diffusion equation:

$$\frac{\partial}{\partial t}p(x,t) = -\underbrace{\frac{\partial}{\partial x}\left(vp(x,t)\right)}_{\text{advection}} + \underbrace{\frac{\partial^2}{\partial x^2}\left(Dp(x,t)\right)}_{\text{diffusion}} - \underbrace{\mu p(x,t)}_{\text{mortality}} - \underbrace{h(x)\alpha p(x,t)}_{\text{arrival onto farm}} \tag{5.1}$$

$$p(x,0) = p_0(x) \tag{5.2}$$

$$h(x) = \begin{cases} 1 & x \in [0,L] \\ 0 & \text{otherwise} \end{cases}, \tag{5.3}$$

where $p(x,t)$ is the density of sea lice at position x and time t, $p_0(x)$ is the initial distribution of sea lice, and the farm at which sea lice are arriving is located between $[0,L]$. The rate at which sea lice arrive onto the farm, through successful attachment to salmonid hosts, is given by α; the mortality rate of lice is μ; advection, which represents the general seaward flow due to river output, is given by v; and diffusion, representing mixing due to winds and tidal flow, is given by D. This equation has previously been used to model sea lice movement in the Broughton Archipalego, to demonstrate the distribution of sea lice on wild salmon caused by salmon farms along salmon migration routes (Krkošek et al., 2006a; Krkošek et al., 2005; Peacock et al., 2020). The necessary boundary conditions that accompany equation 5.1 are:

$$\lim_{x\to-\infty} p(x,t) = 0 \tag{5.4}$$

$$\lim_{x\to\infty} p(x,t) = 0 \tag{5.5}$$

$$\lim_{x\to-\infty} \frac{\partial}{\partial x}p(x,t) = 0 \tag{5.6}$$

$$\lim_{x\to\infty} \frac{\partial}{\partial x}p(x,t) = 0 \tag{5.7}$$

To calculate the time of arrival onto the farm, we first rescale the density of lice by their probability of survival up to time t, $p(x,t) = e^{-\mu t}\tilde{p}(x,t)$, so that $\tilde{p}(x,t)$ represents the probability density that lice are in the channel at position x at time t given that they have survived, and $e^{-\mu t}$ is the probability that they have survived up to time t. The reasoning behind this rescaling is that now when we are tracking $\tilde{p}(x,t)$, the probability density function for the movement of lice that have survived, the only way that lice can be removed from the channel is by arriving onto the farm. The equation describing $\tilde{p}(x,t)$ is

$$\frac{\partial}{\partial t}\tilde{p}(x,t) = -\frac{\partial}{\partial x}\left(v\tilde{p}(x,t)\right) + \frac{\partial^2}{\partial x^2}\left(D\tilde{p}(x,t)\right) - h(x)\alpha\tilde{p}(x,t) \tag{5.8}$$

$$\tilde{p}(x,0) = p_0(x) \tag{5.9}$$

$$h(x) = \begin{cases} 1 & x \in [0,L] \\ 0 & \text{otherwise} \end{cases}, \tag{5.10}$$

with the same necessary boundary conditions as before.

Let T be the random variable describing the time of arrival onto the farm. We are interested in calculating $f(t)$, the distribution of arrival times, where $\int_0^t f(\tau)d\tau = \Pr(T < t)$. Now consider $\int_{-\infty}^{\infty}\tilde{p}(x,t)dx$. This is the probability that lice are still in the water column and have not yet arrived onto the farm, thus $\int_{-\infty}^{\infty}\tilde{p}(x,t)dx = \Pr(T > t) = 1 - \Pr(T < t)$. The arrival time distribution $f(t)$ can therefore be given by

$$f(t) = -\frac{d}{dt}\int_{-\infty}^{\infty}\tilde{p}(x,t)dx.$$

If we integrate equation 5.8 in space from $-\infty$ to ∞, then the advection and diffusion terms disappear due to the boundary conditions and we are left with

$$\frac{d}{dt}\int_{-\infty}^{\infty}\tilde{p}(x,t)dx = -\alpha\int_0^L \tilde{p}(x,t)dx.$$

Substituting this equation into the one for $f(t)$ we find that

$$f(t) = \alpha\int_0^L \tilde{p}(x,t)dx. \tag{5.11}$$

Therefore in order to solve $f(t)$ we must in turn solve $\tilde{p}(x,t)$. Before turning our attention to this solution, there are a couple details which are important to note. First, because $f(t)$ is the distribution of arrival times of sea lice that arrive on the farm, $\int_0^{\infty} f(t)dt$ will only equal 1 if all lice are eventually arrive onto the farm. While

this will be the case if $v = 0$, if $v > 0$ or $v < 0$ then this need not be the case. In fact for sea lice passing by salmon farms, the arrival rate α will probably be quite small, as farms are often located on the edge of large channels, and we are approximating the entire channel with a one dimensional domain. Therefore most of the lice released will not arrive onto the farm, an assumption which we will make explicit in the following section. Second, because we have removed mortality from the equation describing $\tilde{p}(x,t)$, $f(t)$ is the probability density of arrival at time t, given that lice survive up to time t. The probability density that lice survive up to time t and then arrive onto the farm is $e^{-\mu t}f(t)$.

Calculating arrival time via asymptotic analysis

The solution, $\tilde{p}(x,t)$, to equation 5.8 is difficult to solve exactly and so to find an analytical solution to $\tilde{p}(x,t)$ and $f(t)$ we perform an asymptotic analysis and solve the first order solution. For simplicity of asymptotic analysis we will assume that $p_0(x) = \delta(x - x_0)$, so that all lice are initially released from another farm at position x_0. To find a small parameter around which to perform the asymptotic analysis we first need to non-dimensionalize our system. There are many different possibilities for non-dimensionalization, but in our case we choose to non-dimensionalize time as $\tilde{t} = \frac{D}{L^2}t$ and space as $\tilde{x} = \frac{x}{L}$. Using these non-dimensional parameters we can re-write equation 5.8 as

$$\frac{\partial}{\partial \tilde{t}}\tilde{p}(\tilde{x},\tilde{t}) = -\frac{\partial}{\partial \tilde{x}}\left(\frac{vL}{D}\tilde{p}(\tilde{x},\tilde{t})\right) + \frac{\partial^2}{\partial \tilde{x}^2}\tilde{p}(\tilde{x},\tilde{t}) - h(\tilde{x})\frac{\alpha L^2}{D}\tilde{p}(\tilde{x},\tilde{t}) \tag{5.12}$$

$$\tilde{p}(\tilde{x},0) = \delta(\tilde{x} - \frac{x_0}{L}) \tag{5.13}$$

$$h(\tilde{x}) = \begin{cases} 1 & \tilde{x} \in [0,1] \\ 0 & \text{otherwise} \end{cases}. \tag{5.14}$$

Along with non-dimensionalizing the equations for $\tilde{p}(\tilde{x},\tilde{t})$, we must also write $f(t)$ in terms of its non-dimensional form so that it is clear how to redimensionalize $f(t)$ to fit to data. Previously, we demonstrated that $f(t)$ could be calculated as

$$f(t) = -\frac{d}{dt}\int_{-\infty}^{\infty}\tilde{p}(x,t)dx.$$

In terms of the new non-dimensional time and space variables, $\tilde{t}$ and $\tilde{x}$, this can be rewritten as

$$f(\tilde{t}) = -\frac{D}{L}\frac{d}{d\tilde{t}}\int_{-\infty}^{\infty}\tilde{p}(\tilde{x},\tilde{t})d\tilde{x}.$$

From the formulation of $\tilde{p}(\tilde{x},\tilde{t})$ in equation (5.12) we can see that the non-dimensional rate of removal of $\tilde{p}$ will be $-d/d\tilde{t}\int_{-\infty}^{\infty}\tilde{p}(\tilde{x},\tilde{t})d\tilde{x}$, in the same manner as the dimensional removal rate, $f(t)$, was calculated in the previous section. Therefore if we let

$$\tilde{f}(\tilde{t}) = -\frac{d}{d\tilde{t}}\int_{-\infty}^{\infty}\tilde{p}(\tilde{x},\tilde{t})d\tilde{x}$$

be the non-dimensional arrival time distribution, then we can write the dimensional arrival time as

$$f(\tilde{t}) = \frac{D}{L}\tilde{f}(\tilde{t}). \tag{5.15}$$

In the non-dimensionalization process of $\tilde{p}(\tilde{x},\tilde{t})$ three dimensionless parameters appear: x_0/L, vL/D, and $\alpha L^2/D$. In the Broughton Archipelago, advection and diffusion have previously been estimated as $v = 0.0645$ km/hr and $D = 0.945$ km^2/hr (Table 5.2), and the length of the average farm is around $L = 0.1$ km. To roughly estimate the magnitude of the arrival rate in 1 dimension, α, we must first make some assumptions about the arrival rate of sea lice over a salmon farm in two dimensions. Let β be the actual rate of arrival of lice onto a farm when they are in the water column directly over a farm. In the previous chapter of this thesis we assumed that $\beta = 100/$ day, and thus the average waiting time for infectious sea lice in the water column surrounding the farm to arrive on the farm is roughly 15 minutes ($1/\beta$ = (1 day/100) $\times$ (24 hrs/1 day) $\times$ (60 minutes/1 hr) = 14.4 minutes). In this chapter the timescale that we use is hours, and so $\beta = 25/6$ hrs $= 4.17/$ hrs. Even if infectious lice pass over a farm, there may be only some proportion which attach successfully at all, and this proportion has been estimated to be as high as 80% and as low as 0.5% under different lab conditions (Skern-Mauritzen et al., 2020). Because of the variability in these estimates we do not scale β by the proportion of lice that eventually attach, but note that our estimate may be large and for the purposes of asymptotic analysis we assume our estimate of β is at the upper end of the true estimate. Then, we assume that the ratio of $\alpha/\beta = 0.012$, which in physical terms means that the two dimensional area taken up by the farm is roughly 0.012 of the area of the channel at the location of the farm. At the particular farm we fit the model to the farm is roughly 50m wide and the channel is 4km wide, and 0.05/4=0.0125). When we fit the model we find that the estimate of α/β in fact ranges from 0.012 to 0.006 (Table 5.1). Thus taking the values of $\alpha/\beta = 0.012$ and $\beta = 4.17$ as rough maximum estimates, we assume $\alpha \leq 0.05$. Based on these parameter estimates and assumptions we choose $\alpha L^2/D$ to be the small parameter around which we perform our asymptotic approximation.

Let $z = x_0/L$, $\epsilon = \alpha L^2/D$ ($< 5.29 \times 10^{-4}$) and $\omega = vL/D$ (6.83×10^{-3}). Then we can rewrite equation 5.12 as

$$\frac{\partial}{\partial \tilde{t}}\tilde{p}(\tilde{x},\tilde{t}) = -\frac{\partial}{\partial \tilde{x}}\left(\omega \tilde{p}(\tilde{x},\tilde{t})\right) + \frac{\partial^2}{\partial \tilde{x}^2}\tilde{p}(\tilde{x},\tilde{t}) - \epsilon h(\tilde{x})\tilde{p}(\tilde{x},\tilde{t}) \tag{5.16}$$

$$\tilde{p}(\tilde{x},0) = \delta(\tilde{x} - z) \tag{5.17}$$

$$h(\tilde{x}) = \begin{cases} 1 & \tilde{x} \in [0,1] \\ 0 & \text{otherwise} \end{cases}. \tag{5.18}$$

In terms of $\tilde{f}(\tilde{t})$, if we integrate both sides of equation 5.16 on space from $-\infty$ to ∞, then we can write

$$\tilde{f}(\tilde{t}) = \epsilon \int_0^1 \tilde{p}(\tilde{x},\tilde{t}) d\tilde{x}.$$

We assume that $\tilde{p}(\tilde{x},\tilde{t})$ can be expressed as a regular asymptotic expansion in epsilon,

$$\tilde{p}(\tilde{x},\tilde{t}) = \tilde{p}_0(\tilde{x},\tilde{t}) + \epsilon \tilde{p}_1(\tilde{x},\tilde{t}) + O(\epsilon^2)$$

and then can express $\tilde{f}(\tilde{t})$ as

$$\tilde{f}(\tilde{t}) = \epsilon \int_0^1 \tilde{p}_0(\tilde{x},\tilde{t}) d\tilde{x} + O(\epsilon^2).$$

Substituting the expansion for $\tilde{p}(\tilde{x},\tilde{t})$ into equation 5.16 and matching terms of order ϵ^0, we have

$$\frac{\partial}{\partial \tilde{t}}\tilde{p}_0(\tilde{x},\tilde{t}) = -\frac{\partial}{\partial \tilde{x}}\left(\omega \tilde{p}_0(\tilde{x},\tilde{t})\right) + \frac{\partial^2}{\partial \tilde{x}^2}\tilde{p}_0(\tilde{x},\tilde{t}) \tag{5.19}$$

$$\tilde{p}_0(\tilde{x},0) = \delta(\tilde{x} - z), \tag{5.20}$$

which has the solution

$$\tilde{p}_0(\tilde{x},\tilde{t}) = \frac{1}{\sqrt{4\pi\tilde{t}}} e^{-(\tilde{x}-z-\omega\tilde{t})^2/4\tilde{t}}. \tag{5.21}$$

Therefore $\tilde{f}(\tilde{t})$, up to order ϵ^2, is given by

$$\tilde{f}(\tilde{t}) = \epsilon \int_0^1 p_0(\tilde{x},\tilde{t}) d\tilde{x} + O(\epsilon^2) \tag{5.22}$$

$$= \epsilon \int_0^1 \frac{1}{\sqrt{4\pi\tilde{t}}} e^{-(\tilde{x}-z-\omega\tilde{t})^2/4\tilde{t}} d\tilde{x} + O(\epsilon^2) \tag{5.23}$$

Returning to our original dimensional parameters, the dimensional form of the arrival time distribution is

$$f(t) = \alpha \int_0^L \frac{1}{\sqrt{4\pi Dt}} e^{-(x-x0-vt)^2/4Dt} dx \tag{5.24}$$

$$= \frac{\alpha}{2}\left(\text{erf}\left(\frac{x_0+vt}{\sqrt{4Dt}}\right) - \text{erf}\left(\frac{x_0+vt-L}{\sqrt{4Dt}}\right)\right). \tag{5.25}$$

5.2.2 Including survival and maturation

In the previous section we ignored the fact that sea lice larvae can be divided into two main stages: a non-infectious nauplius stage, and an infectious copepodite stage. In the nauplius stage, sea lice larvae cannot attach to salmonid hosts even if they come in close contact, it is only in the copepodite stage that sea lice are able to attach to hosts. To capture this infectious stage, we model the densities of the nauplius ($p_n(x,t)$) and copepodite ($p_c(x,t)$) stages with the following differential equations:

$$\frac{\partial}{\partial t}p_n(x,t) = -\underbrace{\frac{\partial}{\partial x}\left(vp_n(x,t)\right)}_{\text{advection}} + \underbrace{\frac{\partial^2}{\partial x^2}\left(Dp_n(x,t)\right)}_{\text{diffusion}} - \underbrace{\mu_n p_n(x,t)}_{\text{nauplius mortality}} - \underbrace{m(t)p_n(x,t)}_{\text{maturation}} \tag{5.26}$$

$$p_n(x,0) = \delta(x-x_0) \tag{5.27}$$

$$\frac{\partial}{\partial t}p_c(x,t) = \underbrace{m(t)p_n(x,t)}_{\text{maturation}} - \underbrace{\frac{\partial}{\partial x}\left(vp_c(x,t)\right)}_{\text{advection}} + \underbrace{\frac{\partial^2}{\partial x^2}\left(Dp_c(x,t)\right)}_{\text{diffusion}} \tag{5.28}$$

$$- \underbrace{\mu_c p_c(x,t)}_{\text{copepodite mortality}} - \underbrace{\alpha h(x) p_c(x,t)}_{\text{arrival onto farm}}$$

$$p_c(x,0) = 0 \tag{5.29}$$

$$h(x) = \begin{cases} 1 & x \in [0,L] \\ 0 & \text{otherwise} \end{cases}, \tag{5.30}$$

where μ_i is the mortality rate in stage i, and $m(t)$ is the maturation rate of nauplii to copepodites.

We are again interested in calculating the time it takes for larvae leaving one farm to arrive on another. Now that we have divided the larvae into a non-infectious stage and an infectious stage, the larvae must mature into the infectious stage in order to arrive onto the second farm. Therefore to calculate the arrival time of larvae onto the second farm, we are really interested in the removal rate of infectious larvae from the water column. However, we do not want to count infectious larvae that die, so first we need to separate out mortality from the two equations. Let $p_c(x,t) = e^{-\mu_c t}\tilde{p}_c(x,t)$ and $p_n(x,t) = e^{-\mu_n t}\tilde{p}_n(x,t)$, where $e^{-\mu_c t}$ and $e^{-\mu_n t}$ are the probabilities that lice survive

up to time t in the copepodite and nauplius stages respectively. In the previous section where there was only one stage the arrival time distribution was given by $f(t) = -d/dt \int_{-\infty}^{\infty} \tilde{p}(x,t)dx$, but now that there are two stages with different death rates the arrival time distribution will be given by

$$e^{-\mu_c t} f(t) = -e^{\mu_c t} \frac{d}{dt} \int_{-\infty}^{\infty} \tilde{p}_c(x,t)dx - e^{-\mu_n t} \frac{d}{dt} \int_{-\infty}^{\infty} \tilde{p}_n(x,t)dx. \tag{5.31}$$

To calculate the arrival time we can rewrite equations (5.26)-(5.30) as

$$e^{-\mu_n t} \frac{\partial}{\partial t} \tilde{p}_n(x,t) = -e^{-\mu_n t} \frac{\partial}{\partial x} \left(v \tilde{p}_n(x,t)\right) + e^{-\mu_n t} \frac{\partial^2}{\partial x^2} \left(D \tilde{p}_n(x,t)\right) - e^{-\mu_n t} m(t) \tilde{p}_n(x,t) \tag{5.32}$$

$$\tilde{p}_n(x,0) = \delta(x - x_0) \tag{5.33}$$

$$\begin{aligned} e^{-\mu_c t} \frac{\partial}{\partial t} \tilde{p}_c(x,t) = {} & e^{-\mu_n t} m(t) \tilde{p}_n(x,t) - e^{-\mu_c t} \frac{\partial}{\partial x} \left(v \tilde{p}_c(x,t)\right) + e^{-\mu_c t} \frac{\partial^2}{\partial x^2} \left(D \tilde{p}_c(x,t)\right) \\ & - e^{-\mu_c t} \alpha h(x) \tilde{p}_c(x,t) \end{aligned} \tag{5.34}$$

$$\tilde{p}_c(x,0) = 0 \tag{5.35}$$

$$h(x) = \begin{cases} 1 & x \in [0, L] \\ 0 & \text{otherwise} \end{cases}. \tag{5.36}$$

Then adding them together, integrating over all space, and substituting the resulting expression into equation 5.31 we have

$$f_c(t) = \alpha \int_0^L \tilde{p}_c(x,t)dx,$$

where we use the subscript c to denote the arrival time of lice which have matured into copepodites.

Once again, to calculate the arrival time density we will need to solve the equations governing the lice distribution in the channel using an asymptotic analysis, this time with the addition of Green's functions.

First, let us formulate the copepodid density, $\tilde{p}_c(x,t)$, in terms of a Green's function. The Green's function describes the movement of copepodites, as described by equation (5.34), but without the source of maturing nauplii. The Green's function is then convolved with the source function: the maturing nauplii which are entering the copepodid stage. The copepodid density can then be written as

$$\tilde{p}_c(x,t) = \int_0^t \int_{-\infty}^{\infty} G(x - \xi, t - \tau) s(\xi, \tau) d\xi d\tau, \tag{5.37}$$

where $s(\xi, \tau) = e^{(\mu_c - \mu_n)\tau} m(\tau) \tilde{p}_n(\xi, \tau)$ and $G(x,t)$ solves

$$\frac{\partial}{\partial t}G(x,t) = -\frac{\partial}{\partial x}\left(vG(x,t)\right) + \frac{\partial^2}{\partial x^2}\left(DG(x,t)\right) - \alpha h(x)G(x,t) \tag{5.38}$$

$$G(x,0) = \delta(x) \tag{5.39}$$

$$h(x) = \begin{cases} 1 & x \in [0,L] \\ 0 & \text{otherwise} \end{cases}. \tag{5.40}$$

Similar to before, the equation governing $G(x,t)$ is difficult to solve directly, and so we non-dimensionalize the equations and then perform an asymptotic analysis in a small parameter. We non-dimensionalize equations (5.38)-(5.40) and non-dimensionalize the formula for $\tilde{p}_c(x,t)$ (equation (5.37)) directly. As before, let $\tilde{t} = \frac{D}{L^2}t$ and $\tilde{x} = \frac{x}{L}$, then the nauplius and copepodid system can be reformulated in a non-dimensional form as:

$$\frac{\partial}{\partial \tilde{t}}\tilde{p}_n(\tilde{x},\tilde{t}) = -\frac{\partial}{\partial \tilde{x}}\left(\frac{vL}{D}\tilde{p}_n(\tilde{x},t)\right) + \frac{\partial^2}{\partial \tilde{x}^2}\tilde{p}_n(\tilde{x},\tilde{t}) - \frac{L^2}{D}m(\tilde{t})p_n(\tilde{x},\tilde{t}) \tag{5.41}$$

$$\tilde{p}_n(\tilde{x},0) = \delta(\tilde{x} - \frac{x_0}{L}) \tag{5.42}$$

$$\frac{\partial}{\partial \tilde{t}}G(\tilde{x},\tilde{t}) = -\frac{\partial}{\partial \tilde{x}}\left(\frac{vL}{D}G(\tilde{x},\tilde{t})\right) + \frac{\partial^2}{\partial \tilde{x}^2}G(\tilde{x},\tilde{t}) - \frac{\alpha L^2}{D}h(x)G(x,t) \tag{5.43}$$

$$G(\tilde{x},0) = \delta(\tilde{x}) \tag{5.44}$$

$$h(x) = \begin{cases} 1 & x \in [0,L] \\ 0 & \text{otherwise} \end{cases} \tag{5.45}$$

$$\tilde{p}_c(\tilde{x},\tilde{t}) = \frac{L^3}{D}\int_0^{\tilde{t}}\int_{-\infty}^{\infty} G(\tilde{x}-\tilde{\xi},\tilde{t}-\tilde{\tau})e^{(\mu_c-\mu_n)(L^2\tilde{\tau}/D)}m(\tilde{t})\tilde{p}_n(\tilde{\xi},\tilde{\tau})d\tilde{\xi}d\tilde{\tau}. \tag{5.46}$$

Similar to the previous section, we also need to write $f(t)$ in terms of the new non-dimensional space and time variables. Rescaling equation (5.31) we have

$$e^{-\mu_c(L^2\tilde{t}/D)}f_c(\tilde{t}) = \frac{D}{L}\left(-e^{\mu_c(L^2\tilde{t}/D)}\frac{d}{d\tilde{t}}\int_{-\infty}^{\infty}\tilde{p}_c(\tilde{x},\tilde{t})d\tilde{x} - e^{-\mu_n(L^2\tilde{t}/D)}\frac{d}{d\tilde{t}}\int_{-\infty}^{\infty}\tilde{p}_n(\tilde{x},\tilde{t})d\tilde{x}\right), \tag{5.47}$$

so if we let the non-dimensional version of our arrival time distribution be given by

$$e^{-\mu_c(L^2\tilde{t}/D)}\tilde{f}_c(\tilde{t}) = \left(-e^{\mu_c(L^2\tilde{t}/D)}\frac{d}{d\tilde{t}}\int_{-\infty}^{\infty}\tilde{p}_c(\tilde{x},\tilde{t})d\tilde{x} - e^{-\mu_n(L^2\tilde{t}/D)}\frac{d}{d\tilde{t}}\int_{-\infty}^{\infty}\tilde{p}_n(\tilde{x},\tilde{t})d\tilde{x}\right) \tag{5.48}$$

then the relationship between the dimension and non-dimensional forms of the arrival time is

$$f_c(\tilde{t}) = \frac{D}{L}\tilde{f}_c(\tilde{t}).$$

For our small parameter we again choose $\epsilon = \alpha L^2/D$, around which we perform our expansion, and $\omega = vL/D$ as the other non-dimensional parameter. We can then expand $G(\tilde{x},\tilde{t}) = G_0(\tilde{x},\tilde{t}) + \epsilon G_1(\tilde{x},\tilde{t}) + O(\epsilon^2)$, along with the corresponding $\tilde{p}_c(\tilde{x},\tilde{t}) = \tilde{p}_{c0}(\tilde{x},\tilde{t}) + \epsilon\tilde{p}_{c1}(\tilde{x},\tilde{t}) + O(\epsilon^2)$.

Then using these new parameters and adding together the terms on the right hand side of equation (5.48), the non-dimensional version of the arrival time distribution, $\tilde{f}(\tilde{t})$, is

$$\tilde{f}_c(\tilde{t}) = \epsilon \int_0^1 \tilde{p}_{c0}(\tilde{x},\tilde{t})d\tilde{x} + O(\epsilon^2). \tag{5.49}$$

Therefore to find $\tilde{f}_c(\tilde{t})$ we need to calculate $G_0(\tilde{x},\tilde{t})$ and $\tilde{p}_0(\tilde{x},\tilde{t})$. Focusing first on $G(\tilde{x},\tilde{t})$ we can match terms of order ϵ^0 in equation (5.43) to arrive at

$$\frac{\partial}{\partial\tilde{t}}G_0(\tilde{x},\tilde{t}) = -\frac{\partial}{\partial\tilde{x}}\left(\omega G_0(\tilde{x},\tilde{t})\right) + \frac{\partial^2}{\partial\tilde{x}^2}G_0(\tilde{x},\tilde{t}) \tag{5.50}$$

$$G_0(\tilde{x},0) = \delta(\tilde{x}) \tag{5.51}$$

which has the solution

$$G_0(\tilde{x},\tilde{t}) = \frac{1}{\sqrt{4\pi\tilde{t}}}e^{-(\tilde{x}-\omega\tilde{t})^2/4\tilde{t}} \tag{5.52}$$

with the corresponding solution in $\tilde{p}_{c0}(\tilde{x},\tilde{t})$,

$$\tilde{p}_{c0}(\tilde{x},\tilde{t}) = \frac{L^3}{D}\int_0^{\tilde{t}}\int_{-\infty}^{\infty} G_0(\tilde{x}-\tilde{\xi},\tilde{t}-\tilde{\tau})e^{(\mu_c-\mu_n)(L^2\tilde{\tau}/D)}m(\tilde{t})\tilde{p}_n(\tilde{\xi},\tilde{\tau})d\tilde{\xi}d\tilde{\tau}. \tag{5.53}$$

Therefore the arrival time distribution, up to order ϵ^2, is given by $\tilde{f}_c(\tilde{t}) = \epsilon\int_0^1 \tilde{p}_{c0}(\tilde{x},\tilde{t})d\tilde{x} + O(\epsilon^2)$ along with equations (5.52) and (5.53). Before writing out $\tilde{f}_c(\tilde{t})$ explicitly, we will first redimensionalize the arrival time distribution, as this is what will be fit to data. In its dimensional form with the original time and space variables we have:

$$f_c(t) \approx \alpha\int_0^L\int_0^t\int_{-\infty}^{\infty} G_0(x-\xi,t-\tau)e^{(\mu_c-\mu_n)\tau}m(t)\tilde{p}_n(\xi,\tau)d\xi d\tau \tag{5.54}$$

$$G_0(x,t) = \frac{1}{\sqrt{4\pi Dt}}e^{-(x-vt)^2/4Dt} \tag{5.55}$$

$$\tilde{p}_n(x,t) = \frac{1}{\sqrt{4\pi Dt}}e^{-(x-vt)^2/4Dt}e^{-\int_0^t m(u)du} \tag{5.56}$$

5.2.3 Coupled biological-physical particle tracking simulation

The region in which we are interested in fitting the arrival time model to data is the Broughton Archipelago, located between the northeast coast of Vancouver Island and the mainland of British Columbia. To measure the arrival time for sea lice dispersing between farms in the Broughton Archipelago we use a bio-physical particle tracking simulation. This particle tracking simulation uses an underlying ocean circulation model, the Finite Volume Community Ocean Model (FVCOM) (Chen et al., 2006). The simulation period of the FVCOM was between March 1st and July 31st 2009, to coincide with the outmigration of juvenile pink and chum salmon in that year. More details on the FVCOM simulation can be found in Foreman et al. (2009) and Cantrell et al. (2018), but briefly the FVCOM uses data on tides, wind, surface heating, and river discharge from the six major rivers in the Broughton as input to simulate three-dimensional ocean velocity, temperature and salinity. The FVCOM uses an unstructured grid to solve the necessary hydrodynamic equations, which allows for a more realistic simulation of ocean circulation near the complex coastlines of the Broughton Archipelago. The FVCOM currents arising from this 2009 simulation were compared with observations from twelve current meter moorings and found to be in relatively close agreement (Foreman et al., 2009).

Hourly output from the FVCOM model was used as input into an offline bio-physical particle tracking simulation, details of which can be found in Cantrell et al. (2018). The physical component of the particle tracking simulation determines how sea lice particles move based on the current that they experience from the output of the FVCOM model, and the biological component determines how they survive and mature based on the local salinity and temperature that they experience. Particles are first released from farms as pre-infectious nauplii and then mature into infectious copepodites. The development time from nauplii to copepodite is based on the temperature (T) that particles experience, and is given by the simplified Bělehrádek function

$$\tau(T) = \left[\frac{\beta_1}{T - 10 + \beta_1\beta_2}\right]^2. \tag{5.57}$$

As a particle will experience different temperatures over its lifetime, to track maturity each particle is given a maturity value (M). The maturity value starts at 0 for a newly released nauplius and then updates via

$$M_t = M_{t-1} + \Delta t/\tau(T). \tag{5.58}$$

Once the maturity value, M, reaches 1, the particle molts into a copepodite.

The survival probability of each particle is given by

$$S(t) = e^{-\mu t},$$

where the survival coefficient, μ, is constant at 0.31 per day when salinity (S) is above 30 ppt for the nauplius stage, and at less than 30 ppt is given by

$$\mu = 5.11 - 0.16S. \tag{5.59}$$

Once the particles mature into copepodites (with a maturity coefficient ≥ 1), then the survival coefficient is constant at 0.22 per day. The constant survival in the mature copepodite stage is due to a lack of consensus among studies on how copepodite survival changes with temperature and salinity.

To determine the trajectories of sea lice originating from farms in the Broughton Archipelago, 50 particles were released per hour from each of the 20 active farms (during 2009) and tracked for 11 days using the offline particle tracking model. The first day of release was March 14, and the last day of release was July 20, 2009. In this chapter, to fit the analytical arrival time distribution, we use the particles released on May 2, 2009 as this is a typical release day from 2009 (CRD 50 in Cantrell et al. (2018)).

The 24 hours of particle releases (24 releases $\times$ 50 particles per release) on May 2, 2009 were combined into one cohort so that the time of release of the entire cohort begins at $t = 0$. The amalgamation of 24 hours of releases on one day is to smooth out the effect that the tidal cycle may have on any given individual release. For this particular cohort, Kernel Density Estimates (KDEs) were created using the particle locations at every hour over the 11 days that they were tracked, for a total of 265 KDEs. The idea behind kernel density estimation is to create a distribution from individual particle locations by applying a smoothed Gaussian kernel around each particle location and then adding each kernel to create a distribution. The specific details behind the Kernel Density Estimation process for the sea lice particles can be found in Cantrell et al. (2018).

5.2.4 Model fitting

In order to fit the analytical model of arrival time to the Kernel Density Estimates calculated from the particle tracking simulation we need to calculate a form of arrival time from the KDEs. The first step in this process is to determining which farm to set as the release farm for sea lice and which to use as the receiving farm. In the Broughton Archipelago the use of a one dimensional advection diffusion model to

determine the distribution of sea lice on wild salmon from source farms has been fit to data mainly in Tribune channel and so to compare parameter estimates we choose farms also in Tribune. Our release farm is Glacier Falls, located in the center of Tribune channel, and our receiving farm is Burdwood, which lies at the opening of Tribune (see Figure 5.2).

The KDE represents the distribution of particles over space and has units of particles per kilometer squared. In order to convert this density distribution into a probability distribution, we first must divide the KDE by the total number of particles released, in this case 1200 (50 particles $\times$ 24 releases (1 per hour)). Then the new KDE represents the two dimensional probability distribution of particles, with the integral over the entire domain equal to one; this is now the two dimensional equivalent of $p(x,t)$.

Recall that in the one dimensional mechanistic model, arrival time was calculated as

$$f(t) = \alpha \int_0^L p(x,t)dx$$

and so to calculate the arrival time for the particle tracking simulations we take the value of the rescaled KDE at the position of the receiving farm and multiply it by the area of the raster cell (approximately the size of the farm), which is 0.01 km^2. The only unknown quantity is the rate of arrival of lice onto the farm over which they are passing, which we call β, this is the two dimensional equivalent of α. In Chapter 4 of this thesis we assumed that the arrival rate was roughly $\beta = 25/6$ hr, but we did not scale the arrival rate by the proportion of lice that may successfully attach upon arrival, and so the actual estimate of β is very uncertain. No matter the rate, the key assumption that we make here is that the number of lice that arrive onto the farm is small compared to the total number of lice in the rest of the domain, and thus we do not discount future KDEs by any proportion of lice that have potentially arrived on a farm.

The hydrodynamic equivalent of the arrival time distribution can then be calculated as

$$f_h(t) = \beta \int_{farm} p_h(x,t)d\Omega,$$

to which we want to fit our original arrival time distribution $f(t) = \alpha \int_0^L p(x,t)dx$. We could use our assumption of the arrival rate for the hydrodynamic model, β, to fit the arrival rate of the one dimensional model α, however due to the uncertainties in β we instead fit

$$\left(\frac{\alpha}{\beta}\right) \int_0^L p(x,t)dx$$

to $\int_{farm} p_h(x,t)d\Omega$, calculated from kernel density estimation. For simplicity we use $\beta = 1$ rather than $\beta = 25/6$ to calculate the arrival time in Figures 5.4 through 5.8.

There are three different mechanistic models that we fit to the arrival time from the Kernel Density Estimates: arrival time of inert particles, arrival time of particles which have survived, and arrival time of sea lice particles that have survived and matured to their infective stage. These three models each use slightly different KDEs. For the inert particles, the KDEs are constructed solely from the positions of the sea lice particles at each time step. For the arrival time of only the particles that have survived up to t, the KDEs are constructed by weighting each particle by its individual survival coefficient, which depends on the local salinity that it has experienced, as described in the previous section. Details on this weighting can be found in Cantrell et al. (2018). Lastly, for the arrival time of sea lice particles that have both survived up to time t and matured into infectious copepodites, the KDEs are constructed using only particles that have a maturity value greater or equal to 0.8, and then these particles are again weighted by their survival coefficient during the construction of the KDEs. The value of 0.8 was chosen as it has been previously been found that using a maturity value of 1 may be overly sensitive to temperature (Cantrell et al., 2018).

To fit our arrival time models to the arrival time from the KDEs we use non-linear least squares, with the size of the farm and distance of release farm fixed at $L = 0.1$ km and $x_0 = -13.5$ km respectively. All of the other parameters were allowed to vary during the fitting process and the best fit parameter estimates can be found in Table 5.1.

In the arrival time model which includes maturation, it is necessary to specify a maturation function in order to fit the model to the KDE data. We choose to use a Weibull maturation function, also used by Aldrin et al. (2017) to model sea lice maturation, as it gave a much better fit to our maturation data (Figure 5.3) than the alternatives often used in the sea lice literature: a constant maturation rate (Krkošek et al., 2006a; Peacock et al., 2020) or strict minimum development time followed by a constant maturation rate (Adams et al., 2015; Revie et al., 2005). The Weibull distribution is a two parameter distribution and can be parameterized in a number of ways. We choose to follow Aldrin et al. (2017) and use the median time to development, δ_m, and a shape parameter, δ_s, to define the distribution. Using these parameters the maturation rate (often called the hazard rate in survival analysis) is

$$m(t) = \log(2)\delta_s(\delta_m)^{-\delta_s}t^{\delta_s - 1}.$$

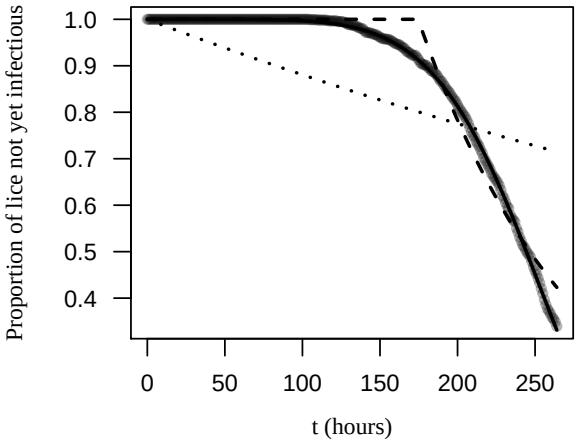

Figure 5.3: The proportion of larvae that have not yet reached a maturation level of 0.8 in the hydrodynamic model, with the best fit lines for three different maturation functions. The dotted line is the maturation function corresponding to a constant maturation rate (e^{-mt}), the dashed line is the maturation function for a minimum development time followed by a constant maturation rate ($1-H(t-t_{\min})(1-e^{-m*(t-t_{\min})}$), and the solid line is the Weibull maturation function ($e^{-\log(2)(t/\delta_m)^{\delta_s}}$).

5.3 Results

5.3.1 Arrival time of inert particles

First we present the arrival time distribution of inert sea lice particles, which do not have any survival or maturation characteristics associated with them, but are still confined to the top five meters of the water column. The formula for the arrival time distribution from the analytical model, given in section 5.2.1, is

$$f(t) = \alpha \int_0^L \frac{1}{\sqrt{4\pi D t}} e^{-(x-x0-vt)^2/4Dt} dx.$$

The fit of this distribution to the output from the hydrodynamic simulation can be seen in Figure 5.4, along with the best fit parameter estimates in Table 5.1.

5.3.2 Arrival time including survival

Next, we present the fit of the arrival time distribution of particles that have survived, to Kernel Density Estimates that are weighted by survival, as described in section 5.2.3. Therefore the distribution we are now fitting is

$$e^{-\mu t} f(t) = \alpha e^{-\mu t} \int_0^L \frac{1}{\sqrt{4\pi D t}} e^{-(x-x0-vt)^2/4Dt} dx.$$

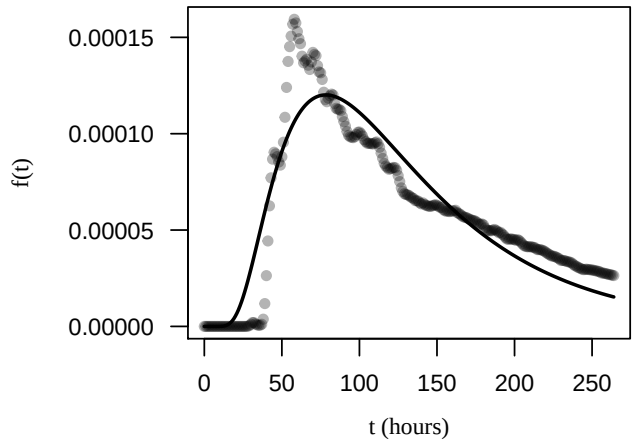

Figure 5.4: Arrival time distribution of inert particles. The points are the arrival time densities calculated from the hydrodynamic model and the curve is the best fit line of the simple analytical model fit to these points via non-linear least squares. Parameter estimates for the model are given in Table 5.1, with $\beta = 1$.

The survival function, $e^{-\mu t}$, is the probability that a sea louse has survived up to time t, and $\int_{t-\epsilon}^{t+\epsilon} f(\tau)d\tau$ is the probability that a sea louse arrives on the second farm between $t-\epsilon$ and $t+\epsilon$, given that it has survived. The fit of $e^{-\mu t}f(t)$ to the hydrodynamic model is shown in Figure 5.5.

5.3.3 Arrival time of sea lice (maturation and survival)

Lastly, we present the fit of the arrival time distribution of infectious sea lice particles. In the hydrodynamic simulation these particles each mature and have a survival probability based on the local salinity and temperature that they experience over their lifetime. For the one dimensional mechanistic model, we are fitting the arrival time distribution of copepodites, $f(t)$, offset by the probability that a copepodite survives up to time t, $e^{-\mu_c t}$. In short, we are fitting

$$e^{-\mu_c t}f_c(t) = \alpha \int_0^L \int_0^t \int_{-\infty}^{\infty} G_0(x-\xi, t-\tau)e^{-\mu_c(t-\tau)}e^{-\mu_n \tau}m(\tau)p_n(\xi,\tau)d\xi d\tau \quad (5.60)$$

$$G_0(x,t) = \frac{1}{\sqrt{4\pi Dt}}e^{-(x-vt)^2/4Dt} \quad (5.61)$$

$$p_n(x,t) = \frac{1}{\sqrt{4\pi Dt}}e^{-(x-vt)^2/4Dt}e^{-\int_0^t m(u)du} \quad (5.62)$$

$$m(t) = \log(2)\delta_s(\delta_m)^{-\delta_s}t^{\delta_s - 1} \quad (5.63)$$

to the Kernel Density Estimates of sea lice particles that have survived and have matured from nauplii to infectious copepodites. The fit of $e^{-\mu_c t}f_c(t)$ is shown in

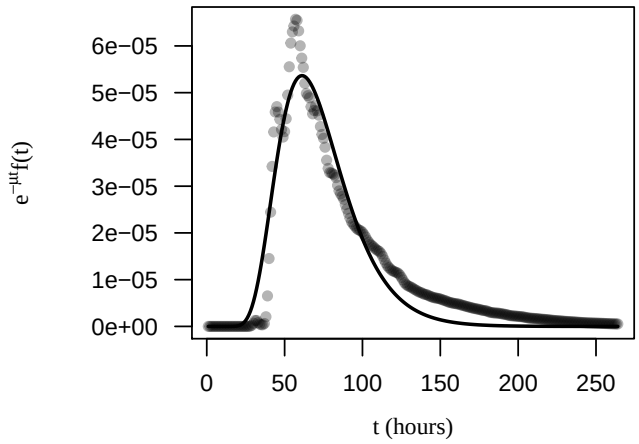

Figure 5.5: Arrival time distribution of particles with survival included. The points are the arrival time densities calculated from the hydrodynamic model with KDE estimates weighted by survival and the curve is the best fit line of the simple analytical model fit to these points via non-linear least squares. Parameter estimates for the model are given in Table 5.1, with $\beta = 1$.

Figure 5.6 and the best fit parameters are in Table 5.1. The probability of arrival of sea lice on the farm is given by

$$\int_0^\infty e^{-\mu_c t} f_c(t) dt,$$

which is how we will measure the level of cross infection between farms.

5.3.4 Applications

Now that we have fit our arrival time model to the hydrodynamic simulation, we aim to answer the questions posed in the Introduction, surrounding the placement of salmon farms in a channel:

(i) How does the degree of cross-infection, giving by arrival probability, depend on the spacing between farms?

(ii) Are there scenarios where an intermediate spacing between farms leads to the highest level of cross-infection?

(iii) Does the relationship between cross-infection and farm spacing change in advection dominated versus diffusion dominated systems?

(iv) How does the maturation time for nauplii to develop into infectious copepodites affect cross-infection?

Table 5.1: Parameter estimates of best fit models under non-linear least squares.

Parameter	Description	Inert	With survival	With survival and maturation
v	Advection	0.143 km/h	0.175 km/h	0.149 km/h
D	Diffusion	0.371 km^2/h	0.165 km^2/h	0.617 km^2/h
α/β	Ratio of 1D to 2D arrival rate	0.012	0.012	0.006
μ	Combined mortality rate	-	0.020/h	-
μ_n	Nauplius mortality rate	-	-	0.009/h
μ_c	Copepodite mortality rate	-	-	0.012/h
δ_m	Median nauplius maturation time	-	-	251h
δ_s	Maturation shape parameter	-	-	8.94

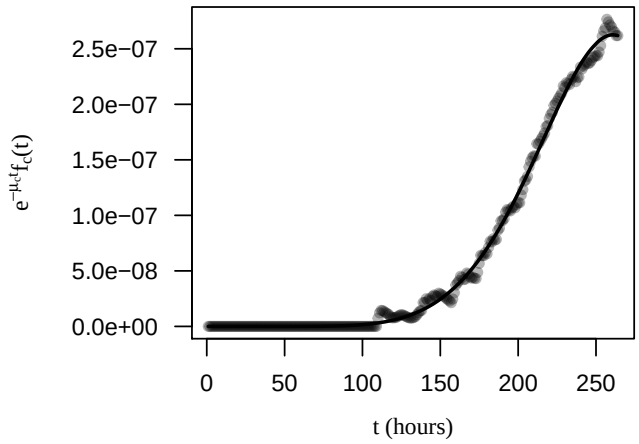

Figure 5.6: Arrival time distribution of infectious copepodites. The points are the arrival time densities calculated from the hydrodynamic model and the curve is the best fit line of the simple analytical model fit to these points via non-linear least squares. Parameter estimates for the model are given in Table 5.1, with $\beta = 1$.

We have a model for the distribution of arrival times of sea lice coming from a second farm, and so there are a variety of analyses that can be done with such a distribution. In this section we will focus on how various factors affect cross infection between farms, as measured by the probability of arrival, $\int_0^\infty e^{-\mu_c t} f_c(t) dt$. but one could also investigate how the mean arrival time or variance of the distribution also changes. For our analyses we will use our full arrival time model that includes both maturation and survival of sea lice, as we focus on how different parameters affect the total probability that lice arrive on the farm, but for other questions relating to how the advection and diffusivity affect the arrival of particles, the simpler models may be more suitable.

To answer the above questions we explore how three different interactions of parameters affect the probability of arrival: advection (v) and diffusion (D), advection and initial farm placement (x_0), and median maturation time (δ_m) and initial farm placement. Each of these interactions reveals a glimpse into a different component of the model, as it is difficult to gain insight if all of these parameters are changed at once. Apart from the parameters that are varying, all others will be held constant at their best fit estimates from the non-linear least squares fit, shown in Table 5.1. We begin by answering the last three questions before turning our attention to the first.

Are there scenarios where an intermediate spacing between farms leads to the highest level of cross-infection?

By examining the effect of varying the advection coefficient and the placement of the first farm, we can see from Figure 5.7b) there are indeed scenarios where an intermediate spacing leads to the highest level of cross infection. At even small advection coefficients, for example $v = 0.05$, the arrival probability is maximized when the second farm is placed around 14km away from the first. However, even if transmission to a farm 1km away may be lower than transmission to a farm 14km away, when considering self infection of a farm, local currents may allow sea lice to directly mature around the farm so that within farm infection remains high, as sea lice outbreaks on farms in the Broughton have been shown to be primarily driven by self-infection (Krkošek et al., 2012a).

In fact, the probability of arrival is maximized along the line $v = mx_0 + b$, for some slope m and intercept b, and the probability decrease symmetrically as the intercept b moves away from the intercept at which the probability is maximized. Intuitively this seems to be due to the relationship between the spatial mean of the solution to equation 5.1, when the initial condition is a delta function. The solution is

$$p(x,t) = \frac{1}{\sqrt{4\pi Dt}} e^{-\mu t - (x - x_0 - vt)^2/4Dt},$$

which has the spatial mean $x_0 + vt$. So for a fixed maturation time, the probability of arrival should be maximized if most lice have matured before the mean density of lice moving through the channel passes by the second farm.

Does the relationship between cross-infection and farm spacing change in advection dominated versus diffusion dominated systems?

The relationship between the advection and diffusion of the system and the arrival probability is shown in Figure 5.7a). We can see that for any diffusion coefficient, there is a single advection coefficient that maximizes the probability of arrival. At this maximized advection coefficient, increasing the diffusion coefficient simply reduces the probability of arrival. Now this is in the context of a fixed release location and median maturation time, but for these fixed parameters the advection coefficient plays a large role in determining whether lice will arrive at all, and the value of the diffusion coefficient determines how large the probability of arrival will be.

How does the maturation time for nauplii to develop into infectious copepodites affect cross-infection?

The relationship between the median maturation time, δ_m, the placement of the release farm, x_0, and the arrival probability is shown in Figure 5.7c). Here we chose the minimum median development time of 70 hours as this was approximately the lower end of the 95% confidence interval for the median maturation time at 10 degrees found in a large analysis of salmon farms in Norway (Aldrin et al., 2017), and thus is most likely the fastest that nauplii would develop into copepodites in the Broughton Archipelago. Again we can see that for many median maturation times, the arrival probability is maximized at intermediate values of release farm position, x_0, and therefore placing farms closer to each other may not always lead to higher transmission. However for a given release farm position, the arrival probability is always maximized at the lowest possible development time. Therefore for two farms at fixed locations, warmer temperatures that cause faster louse development times will lead to higher spread between farms.

How does the degree of cross-infection, giving by arrival probability, depend on the spacing between farms?

We can see that the degree of cross-infection between farms depends on a variety of factors, and there is no specific farm spacing that minimizes or maximizes cross-infection across all variables. If there is very little advection in the system then cross-infection will be highest when farms are closest together. In channels with an underlying advective current, cross-infection will be maximized at some intermediate spacing, though the spacing leading to maximum cross-infection depends on the current. This is due in part to the maturation time required for sea lice to become infectious, if lice are swept by the farm before they have a chance to mature then cross-infection will be low. Complicating this relationship further is that for a given farm spacing, cross-infection may change throughout the year or among years as advection changes with river discharges and winds, as diffusion changes over spring-neap and longer tidal cycles, and as maturation time changes due to changing temperatures.

5.4 Discussion

The degree of sea louse connectivity between salmon farms has been well studied in specific salmon farming regions but there are few general models that can answer broad questions surrounding the effect of farm spacing and environmental variables on interfarm connectivity. In this chapter we used a simple mechanistic model to

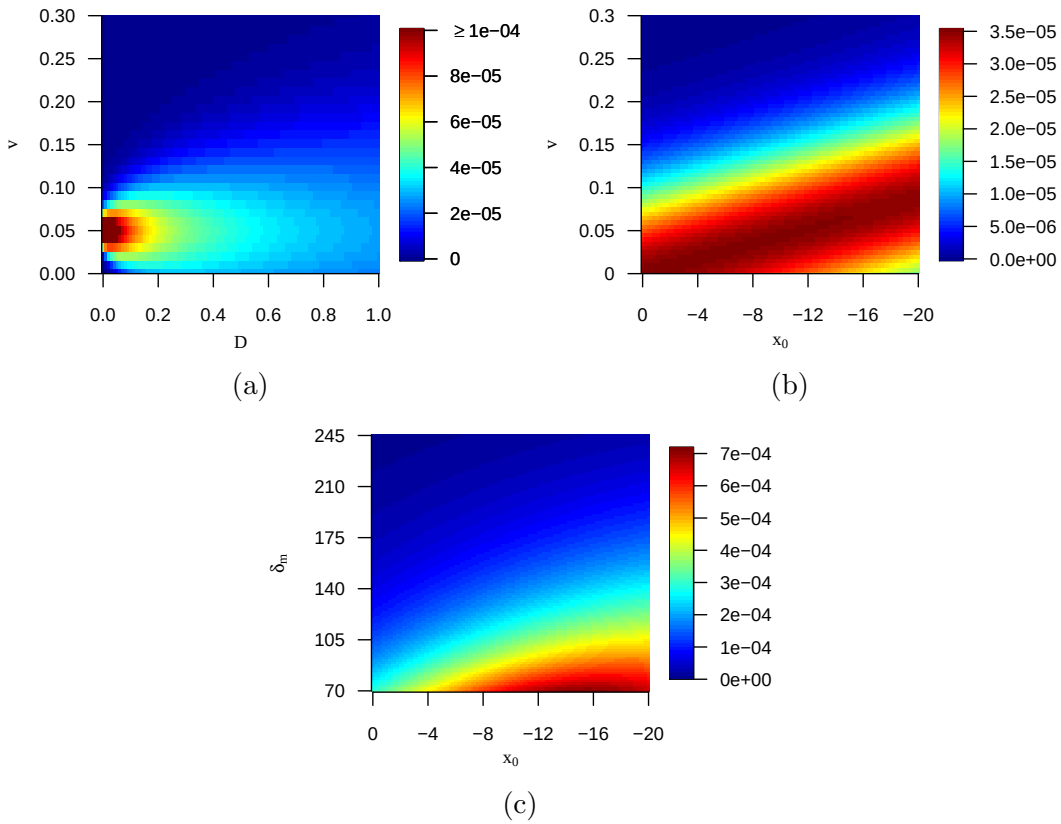

Figure 5.7: Total probability of sea lice arriving from one farm to another, $\int_0^\infty e^{-\mu_c t} f(t) dt$, as different parameters vary: a) advection and diffusion, b) advection and initial farm placement, c) initial farm placement and median development time. Apart from the parameters that are varying, all other parameters are held constant at their best fit estimates shown in Table 5.1, with $\beta = 1$.

calculate the timing and probabilty of arrival for sea lice dispersing between salmon farms. We then calculated the same quantities directly from complex hydrodynamical and particle tracking simulations in the Broughton Archipelago and demonstrated that our simple model captures the necessary effects of environmental and physical variables on timing and probability of arrival for sea lice in this region. Using our simple model calibrated to the Broughton Archipelago, we then investigated the effect of farm spacing, maturation time, and ocean advection and diffusion on the degree of cross-infection between farms and found that there are several scenarios in which intermediate farm spacing leads to the highest levels of cross infection.

Previous studies from the Broughton Archipelago have used hydrodynamic simulations and mechanistic models to model the dispersal of sea lice from salmon farms onto wild salmon and these studies provide useful comparisons of parameter estimates in this region (Table 5.2). The main parameters to compare are the advection coefficient v, the diffusion coefficient D, the mortality rates μ_c and μ_n. There were no parameter estimates for the nauplius mortality rate from Krkošek et al. (2005) or Krkošek et al. (2006a), as in these studies nauplius mortality rate was estimated in conjunction with nauplius maturation rate, but most of our other parameters estimates are similar to those found previously, lending support to the accurate calibration of our simple model. The only parameter estimate which seems high compared to other studies is the advection coefficient v. This could be because in the other studies the advection coefficient is estimated over a larger region of Tribune channel than our study, and so varying coefficients in other parts of the channel could lead to a lower overall advection coefficient. In particular, Cantrell et al. (2018) found that sea lice from farms in the lower part of the channel move in the opposite direction as the advection is estimated from Krkošek et al. (2006a), which would therefore lead to a lower overall advection coefficient when estimated over the entire channel. Alternatively, our advection estimate is taken from the particle tracking simulation for a single day and may change if our model is fit against a simulation from a different time period.

In addition to confirming our parameter estimates, previous studies in the Broughton Archipelago also support our result that the highest density of farm origin sea lice in a channel may be at an intermediate distance away from the farm, leading the highest degree of cross-infection of sea lice. In particular, Cantrell et al. (2018) found that the simulated density of infectious copepodites from the five south-easterly farms (Figure 5.2) was highest further than fifteen kilometers away from the nearest farm using a hydrodynamic model. Less drastically, Peacock et al. (2020) also found that the highest density of copepodites was a few kilometers away from each farm along the measured migration corridor using a mechanistic model fit to empirical data. These

differing results may be a result of the different scales or methods used and are perhaps accentuated by the different maturation functions. Cantrell et al. (2018) used the same maturation process as described in this chapter (equation (5.58)), which can be well approximated by a Weibull function (5.3) and allows for a delay before sea lice larvae can become infections, whereas the exponential maturation function used by Peacock et al. (2020) does not allow for such a delay and thus some larvae will instantly become infectious.

When farms are not located in a channel but on nearby islands or along a common coastline the ocean dynamics will likely be diffusion dominated and thus cross infection will decrease as farms become further apart, rather than cross-infection being maximized at intermediate distances in the presence of advective currents. We found that our simple model also fits well to these scenarios (fits not shown), though in this case the absorption rate will be lower as the one dimensional approximation now effectively represents a radial slice of a two dimensional diffusion process. In these cases the probability of arrival is likely to be well-approximated by the seaway distance kernels used in other studies (Aldrin et al., 2017; Aldrin et al., 2013).

The simplicity of our mechanistic model coupled with the knowledge of how median development time changes with respect to temperature also allows us to investigate how connectivity may change as ocean temperatures warm. We found that for any fixed farm separation distance, shorter development times, which are caused by warmer temperatures, increased the probability of sea lice dispersing between farms. This result confirms previous work demonstrating that warmer temperatures increase the connectivity of farms, using a bio-physical model (Cantrell et al., 2020), and the failure to control sea louse outbreaks on wild salmon in 2015 when the water temperature was anomalously warm (Bateman et al., 2016). Moreover, the simple analytical nature of our arrival time model and the dependence of maturation time on temperature allows us to explicitly demonstrate the dependence of connectivity on temperature, so that for the temperature of a given year, we can calculate the level of interfarm connectivity.

While our simple model can be used to understand how connectivity changes as temperatures warm, it may be beneficial to updated connectivity estimates in future years. In this case GPS drifters released from farms could be used to calculate the advection and diffusion of the ocean and determine spatial spread while average temperature and salinity data could be used to determine the appropriate maturation and survival times (equations 5.57-5.59). GPS drifters have previously been used to determine ocean diffusivity (Corrado et al., 2017; De Dominicis et al., 2012), and could be used to update connectivity as re-running the hydrodynamic model is com-

Table 5.2: Comparison of parameter estimates in this study to others in the Broughton Archipelago.

Parameter	Description	Analytical Model	Krkošek et al. (2006a)	Brooks (2005)	Krkošek et al. (2005)
v	Advection	0.149 km/h	-	0.0648 km/h	0.0379 km/h
D	Diffusion	0.617 km^2/h	0.945 km^2/h	-	0.321 km^2/h
μ_n	Nauplius mortality rate	0.009/h	-	-	-
μ_c	Copepodite mortality rate	0.012/h	0.0083/h	-	-

putationally expensive. In British Columbia, particle tracking models with sea lice releases from farms have only been run in the Broughton Archipelago and so drifters, combined with temperature and salinity data, could be used to estimate connectivity between salmon farms in other regions across BC.

In this chapter we have estimated the timing and probability of arrival using advection and diffusion estimates from particle releases that have been averaged over 24 hours to smooth the effect of the tidal cycle. However, there may be certain situations where the timing of arrival needs to be estimated at a specific point in the tidal cycle. It is also possible to calculate the arrival time distribution for this case and we present the results in the Appendix. We calculate the arrival time using two different methods and compare to the arrival time calculated from the complex hydrodynamical simulations with a single particle release. One method simply allows the advection coefficient to oscillate in magnitude with the tidal cycle, and the second builds on the first and also allows sea lice move between the main channel and small bays or connecting channels where they are free of the oscillating tidal flow.

Lastly, this chapter has been written in the context of the current agreement between the governments of British Columbia and the Kwikwasut'inuxw Haxwa'mis, 'Namgis, and Mamalilikulla First Nations to remove salmon farms from their traditional territories (Brownsey and Chamberlain, 2018). Currently 9 farms are being removed before 2023 and after 2023 7 of the remaining 11 farms will require agreements with the Kwikwasut'inuxw Haxwa'mis, 'Namgis, and Mamalilikulla First Nations and valid DFO licenses to continue to operate. Our work reinforces the notion that it is not always obvious how farm placement affects sea louse spread between farms, as there are certain instances where placing two farms further away from each other can lead to more spread than if they were closer. We hope that our work builds on past research to help understand the level of sea louse spread between salmon farms Broughton Archipelago and that our research may help understand which farms could be the primary drivers of sea louse spread in other regions as well.

5.5 Appendix for Chapter 5

5.5.1 Model extension — including tidal flow

In this chapter we have modelled larval dispersal from a farm using an advection-diffusion equation, as others have done in this region (Krkošek et al., 2006a; Krkošek et al., 2005; Peacock et al., 2020). When modelling dispersal using this framework, the constant advection coefficient captures directional water movement due to river

runoff and the diffusion coefficient captures the average mixing due to tidal flow and wind currents. In order to capture the average mixing due to tidal flow we have fit our arrival time model to hydrodynamic data where the spatial distribution of sea lice is drawn from 24 hours of release times. The strongest constituent tide in the Broughton is M2, which has a period of 12.4 hours, and so by sampling 24 hours of releases we capture releases from approximately two tidal periods.

However, it is also possible to augment the advection-diffusion equation with constant coefficients that governs larval dispersal so that tidal flow is explicitly captured, which can then be compared to the hydrodynamic model consisting of only one release time. We briefly present two different models of larval dispersal with time varying advection coefficients to capture tidal flow and discuss their implications. Both models describe the dispersal of larvae that have survived, $\tilde{p}(x,t)$, and so their constant advection counterpart is given by equation 5.8. For simplicity we will also ignore the maturation period required for nauplii to develop into infectious copepodites before arriving onto a farm, similar to the first model presented in this chapter.

The first method of modeling larval dispersal subject to tidal flow is to replace the constant advection coefficient, v, by an oscillating advection coefficient, $v_0 + v_1 \cos(\frac{2\pi}{12}(t-t_0)$, where v_0 is the constant advection of the system, v_1 is the magnitude of the tidal flow oscillation and t_0 is the time in the tidal cycle at which sea lice are initially released. We assume a period of 12 hours here to demonstrate the method, though in reality the tidal period is slightly longer and would be better approximated by a summation of sinusoids each with different amplitudes, phase lags, and periods to capture the different tidal constituents. The first model for larval dispersal is then given by:

$$\frac{\partial}{\partial t}\tilde{p}(x,t) = -\frac{\partial}{\partial x}\left((v_0 + v_1\cos(\frac{2\pi}{12}(t-t_0))\tilde{p}(x,t)\right) + \frac{\partial^2}{\partial x^2}\left(D\tilde{p}(x,t)\right) - h(x)\alpha\tilde{p}(x,t) \tag{5.64}$$

$$\tilde{p}(x,0) = \delta(x-x_0) \tag{5.65}$$

$$h(x) = \begin{cases} 1 & x \in [0,L] \\ 0 & \text{otherwise} \end{cases}. \tag{5.66}$$

The benefit of this framework is that it is again possible to non-dimensionalize, perform an asymptotic expansion in the small parameter, $\epsilon = \alpha L^2/D$, solve for the arrival time distribution, $f(t)$, up to order ϵ^2, and then re-dimensionalize $f(t)$ which

is then given by:

$$f(t) = \frac{\alpha}{2}\left(\operatorname{erf}\left(\frac{x_0 + v_0 t + v_1 \frac{12}{2\pi}\left(\sin\left(\frac{2\pi}{12}(t-t_0)\right) + \sin\left(\frac{2\pi}{12}(t_0)\right)\right)}{\sqrt{4Dt}}\right)\right. \tag{5.67}$$

$$\left. - \operatorname{erf}\left(\frac{x_0 + v_0 t + v_1 \frac{12}{2\pi}\left(\sin\left(\frac{2\pi}{12}(t-t_0)\right) + \sin\left(\frac{2\pi}{12}(t_0)\right)\right) - L}{\sqrt{4Dt}}\right)\right), \tag{5.68}$$

shown in Figure 5.8a). The downside to this approach is that the average over all tidal release times, t_0, is simply the constant advection diffusion equation with the same diffusion coefficient as the oscillating advection case. This seems somewhat biologically unrealistic, as the addition of modeling tidal flow was meant to allow for a smaller diffusion coefficient, as the mixing due to tidal flow should now be accounted for in the oscillating advection term.

In order to construct more realistic equations where the oscillating tidal flow mimics the diffusion in the constant advection diffusion equation, for the second model we split the ocean environment into two compartments, a lateral compartment that represents movement along the channel, and a cross channel compartment where larvae remain stationary in the lateral direction. This cross channel compartment represents larvae that may be swept into eddies, small bays along the shore, or into any connecting channels that are perpendicular to the lateral channel. We let $\tilde{p}(x,t)$ denote the larvae that are in the lateral compartment, $q(x,t)$ to be the larvae that are in the cross channel compartment, λ_1 to be the rate of transfer from the lateral to cross channel compartment, and λ_2 to be the rate of transfer between the cross channel and lateral compartment. The model is

$$\frac{\partial}{\partial t}\tilde{p}(x,t) = -\frac{\partial}{\partial x}\left((v_0 + v_1\cos(\frac{2\pi}{12}(t-t_0))\tilde{p}(x,t)\right) + \frac{\partial^2}{\partial x^2}\left(D\tilde{p}(x,t)\right) - h(x)\alpha\tilde{p}(x,t)$$
$$- \lambda_1\tilde{p}(t,x) + \lambda_2 q(t,x) \tag{5.69}$$

$$\frac{d}{dt}q(x,t) = \lambda_1\tilde{p}(x,t) - \lambda_2 q(x,t) \tag{5.70}$$

$$\tilde{p}(x,0) = \delta(x - x_0) \tag{5.71}$$

$$q(x,0) = 0 \tag{5.72}$$

$$h(x) = \begin{cases} 1 & x \in [0,L] \\ 0 & \text{otherwise} \end{cases}. \tag{5.73}$$

With the addition of this cross channel compartment, where larvae can remain stationary along the channel, this model can replicate similar arrival times as the previous model but with much smaller diffusion coefficients. The cross channel compartment

allows some larvae to be swept forward in the lateral compartment, transfer to the cross channel compartment and remain there while other larvae may be swept back, before re-entering the lateral compartment and moving forward. The only downside to this model is it is no longer simple to perform an asymptotic analysis and arrive at an analytical expression for the arrival time.

To demonstrate that this model can replicate a similar arrival time distribution as the previous model, we compare the arrival time distributions for the two models and the arrival time calculated from a single louse release in the hydrodynamic mode in Figure 5.8. For this figure we set $\lambda_1 = \lambda_2 = 1/12$, so that the average time spent in either compartment was 12 hours, the same as the tidal period. Here we can see that the two arrival time distributions are similar, but the arrival time from the two compartment model has a much lower diffusion coefficient.

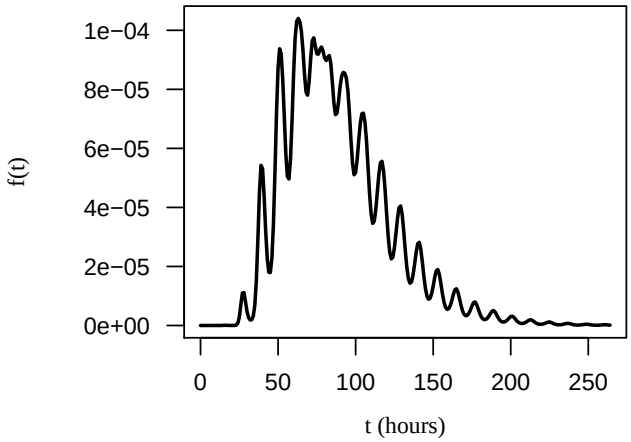

(a)

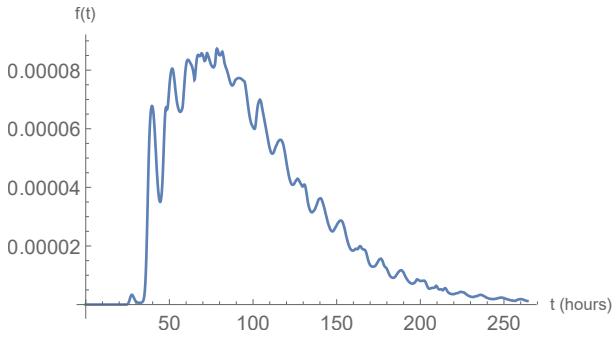

(b)

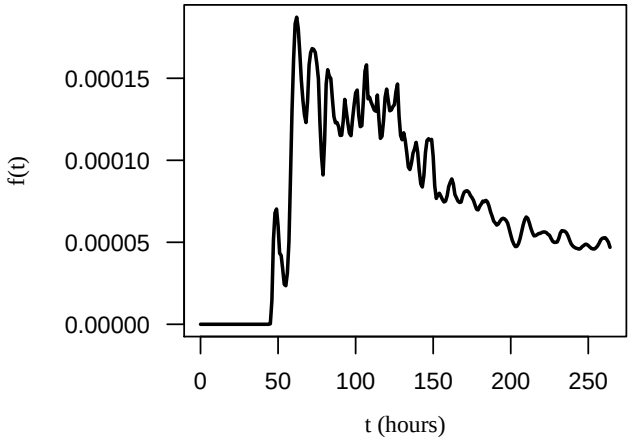

(c)

Figure 5.8: Arrival time distribution incorporating tidal flow. In a) the arrival time is calculated from equations 5.64 and 5.68, where the parameters are the same as the best fit parameter estimates in Table 5.1 for the model which includes survival, with the addition of $v_1 = 1$, and $\beta = 1$. In b) the arrival time is calculated from equation 5.69, with $\alpha/\beta = 0.012$, $\beta = 1$, $v_0 = 0.3$, $v_1 = 1$, $D = 0.01$, and $\lambda_{12} = \lambda_{21} = 1/12$. In c) the arrival time is calculated directly from the KDEs and the hydrodynamic model, for a single hourly release.

Chapter 6

Conclusion

In this thesis I used mathematics to understand sea louse transmission between salmon farms in the Broughton Archipelago, and contributed more broadly to the understanding of transient and asymptotic dynamics of birth-jump metapopulations. As posed at the start of the introduction this thesis was focused on answering the following questions:

- Chapter 2:
  - How do we classify habitat patches as sources or sinks in a continuous time, continuous age metapopulation?
  - How does this relate to the contribution of sea lice populations on individual salmon farms located in a channel?
- Chapter 3:
  - How are the transient dynamics different from the long-term dynamics of birth jump metapopulations?
  - How can we connect the transient dynamics to the source-sink classification of habitat patches?
- Chapter 4:
  - Which farms are acting as the largest sources of sea lice in the Broughton Archipelago?
  - What is the effect of farm removal the sea louse metapopulation?
- Chapter 5:

- Can simple advection-diffusion equations adequately describe the arrival of sea lice dispersing between two farms?
- How does the interaction between farm spacing and sea louse maturation affect the level of cross-infection between farms?

In this concluding chapter I summarize the main results of this thesis, discuss their significance, limitations, connections to future work, and their applications to sea lice on salmon farms and other marine and birth-jump metapopulations.

6.1 Summary

In Chapter 2 I used next-generation matrices to classify habitat patches into sources and sinks in stage-structured marine metapopulations where dispersal occurs in a larval stage and where survival and maturation in each stage depend on age. To capture the age dependent survival and maturation, and so that dispersal between patches could be accurately described by advection diffusion equations, I formulated the model using continuous age-density equations. These allow for the probability of transitioning between stages to depend on the amount of time already spent in the stage. While most species must spend some minimum time in each stage before transitioning to the next stage, a general modelling framework that can accommodate this minimum time is especially necessary for sea lice, where many models explicitly require a minimum development time in each stage or use a non-exponential distribution of maturation times (Adams et al., 2015; Aldrin et al., 2017; Revie et al., 2005; Stien et al., 2005). The general age-density modeling framework is complex, and thus to classify specific patches as sources or sinks I used the next-generation matrix to distill the essential elements of the model required to calculate the contribution of a local habitat patch to the metapopulation. I proved that the basic reproduction number of the next-generation matrix determines the stability of the zero steady state of the system of age-density equations, and that the column sums of the next-generation matrix determine whether a specific habitat patch is a source or sink.

In the context of sea lice on salmon farms in a channel I demonstrated how the spacing between farms affects both the source-sink distribution of farms, as well as the overall growth of the sea louse metapopulation. I showed how increased advection in this system can increase the difference in metapopulation contribution between farms and affect the overall growth of the sea louse metapopulation. I also demonstrated how the additional of environmental gradients can complicate the source-sink distribution of habitat patches and showed that on a generational time scale that the transient

dynamics can be very different than the asymptotic dynamics in these advective systems.

In Chapter 3 I further investigated how transient dynamics can be different than the asymptotic dynamics of marine and related birth-jump metapopulations. To simplify the analysis the metapopulations were formulated using ordinary differential equations, rather than age-density equations. I presented examples of simple two patch metapopulation models where the populations could grow arbitrarily large before eventually decreasing or grow arbitrarily small before eventually growing. While it has previously been recognized that transient dynamics can be very different than the asymptotic dynamics of systems (Hastings et al., 2018; Morozov et al., 2020), here I have shown that they can in fact be arbitrarily different even in very simple linear models. For marine metapopulations in advective environments, increasing the number of habitat patches can increases the length of the transient dynamics that can occur. Focusing on the early transient behaviour of birth-jump metapopulations, I demonstrated that reactivity and attenuation, measures of the maximum possible initial growth rate that occur after a perturbation and the minimum possible growth rate that can occur, are different depending on whether they are measured in the ℓ_1 or ℓ_2 norms. The ℓ_1 norm measures actual population size, whereas the ℓ_2 norm measures the Euclidean distance of the population away from the equilibrium, and thus there are systems that are reactive in the commonly used ℓ_2 norm, but where the actual population size does not increase. Using the ℓ_1 norm I connected the initial growth rate following a perturbation to the source-sink classification of habitat patches in birth jump metapopulations, and demonstrated that if an individual starts on a source patch the population will initially grow and if it starts on a sink the population will initially decline. This at first seems intuitive, but is not the case when adults can migrate between habitat patches. Lastly, I demonstrated how to meaningfully measure reactivity when marine metapopulations are stage structured, where adults typically produce a large number of offspring and thus most systems would be considered reactive under the classical definition.

In Chapter 4 I extended and applied the results from Chapter 2 to demonstrate that the next-generation matrix can be used to determine the contribution of local habitat patches to the metapopulation and determine metapopulation persistence. These results were derived for cases where metapopulation models are formulated in continuous time and discrete time, as well as with the age-density formulation of Chapter 2.

I then specifically constructed next-generation matrix for sea louse populations on salmon farms in the Broughton Archipelago to determine which farms are the largest

sources of sea lice in this region. Temperature and salinity dependent maturation and survival functions were used to accurately capture sea louse sea louse demography and local farm productivity. The connectivity of larval dispersal between farms was calculated by applying Kernel Density Estimation to particle tracking simulations computed from a computational hydrodynamic model previously run in the Broughton Archipelago. In the Broughton, the most highly connected farms were found to often also the most productive, and thus contributed the most to the overall production of sea lice in this region. In the context of removal of salmon farms in the Broughton (Brownsey and Chamberlain, 2018), the farms that are the largest sources of sea lice in the farm network are currently slated to remain in the Broughton if they can be approved by both the local First Nations and BC government. I used the basic reproduction number of the next-generation matrix, R_0, to investigate how temperature and salinity affect the overall growth of the sea louse metapopulation, distilling the complex dependence of temperature and salinity dependent maturation and survival at each stage into a single operator. Finally I compared how the source-sink classification of habitat patches and calculations of metapopulation persistence under the next-generation matrix compare to other metrics of patch contribution and persistence under other currently used metrics.

In Chapter 5 I calculated the arrival time distribution of sea lice dispersing between two salmon farms. First, I calculated the arrival time for lice dispersing according to a simple-advection diffusion equation and use an asymptotic approximation to calculate the arrival time distribution. Then, I calculated the arrival time directly from the output of a particle tracking simulation run on numerical flows from a realistic hydrodynamic model of the currents in the Broughton Archipelago. I fit the simple mechanistic arrival time model based on the advection diffusion equation to the arrival time calculated from the hydrodynamic model to find realistic parameter estimates and to demonstrate that the simple model could accurately capture the complexities of larval dispersal between two farms in the Broughton Archipelago. Using the parameterized model, I investigated how farm spacing affected the cross-infection between farms, as measured by the probability that sea lice leaving one farm eventually arrive on the other farm. I found that often there is an intermediate farm spacing that maximizes the cross infection between farms, and that the farm spacing that maximizes cross infection depends on the degree of advection between the farms as well as the median maturation time required for non-infectious larvae to develop into infectious larvae. If farms are too close together, then high advection or low maturation time can sweep most larvae past the second farm before they are infectious and able to attach.

Having summarized the main chapters of this thesis, I now contextualize the results of this thesis within the two main themes: transient and asymptotic dynamics of marine and other birth-jump metapopulations, and sea louse transmission between salmon farms in the Broughton Archipelago.

6.2 Dynamics of marine and other birth-jump metapopulations

This thesis has two main contributions to the theory of birth-jump metapopulations: the use of the next-generation matrix to calculate the contribution of a habitat patch and determine the persistence of the metapopulation, and the analysis of reactivity and attenuation in these metapopulations. In Chapters 2 and 4 I demonstrate how the column sums of the next-generation matrix determine the number of new individuals produced over the entire metapopulation from an initial individual on a patch, and how the spectral radius of the next-generation matrix determines the overall persistence of the metapopulation. In Chapter 2 I construct the next-generation matrix for a stage-structured metapopulation model that allows for age-dependent maturation and survival, and to my knowledge I am the first to do so. Then in Chapter 4 I also show how the framework of next-generation matrices can also be used more broadly to determine patch contribution in metapopulation models formulated as ordinary differential equations or in discrete time.

I am not the first to calculate the contribution of individual habitat patches to the overall metapopulation or to calculate metapopulation persistence. Pulliam (1988) originally calculated the contribution of habitat patches based on local birth and death rates in the absence of immigration and emigration and classified source patches as those with positive growth rates and sink patches as those with negative growth rates, however it is possible under this classification for a metapopulation consisting only of sink patches to persist (Armsworth, 2002). In order to rectify this, both Figueira and Crowder (2006) and Runge et al. (2006) created classifications that account for productivity on a patch and dispersal away from patches, and in this framework a metapopulation consisting of sink patches cannot persist. Their classification is very similar to classifying sources and sinks with the next-generation matrix. However their classification is only applicable to discrete time (models), whereas the next-generation matrix is also applicable to ordinary differential equation models and as well as models formulated as age density equations, and can easily be extended into continuous space systems as well (Krkošek and Lewis, 2010).

In terms of metapopulation persistence, Hastings and Botsford (2006) demon-

strated that, in order for marine metapopulations to persist, either a single patch must be able to persist in isolation, or there must be closed loops with sufficient larval production between them that an adult can more than self-replace over many generations. This result was originally formulated in discrete time, and the result relies on the non-negativity of the population projection matrix to identify closed loops of patches. In this thesis I simply use the spectral radius of the next-generation matrix to determine metapopulation persistence, but their results could be extended from discrete to continuous time systems using the next-generation matrix, as the next-generation matrix also has the necessary qualities on which the discrete time proof relies. Both their results and ours demonstrate that it is important to consider both productivity of local habitat patches as well as connectivity between patches in order to determine metapopulation persistence.

In terms of transient dynamics in metapopulations, to our knowledge I am the first to consider reactivity and attenuation in the ℓ_1 norm for continuous time systems, even though the ℓ_1 norm provides the true biological measure of population growth. Most other studies use the ℓ_2 norm to measure reactivity, perhaps because it can be easily calculated around both zero and non-zero steady states, but as I have shown in this thesis reactivity is not always the same under both norms. A more in-depth comparison of reactivity under the two norms for metapopulation models parameterized to real systems would be an exciting area of future work to understand how often reactivity differs between the norms. I am also the first to connect reactivity and attenuation to the source-sink classification of habitat patches, which can only be done in the ℓ_1 norm.

The two main limitations of the work in this thesis in the area of marine metapopulations are that non-linear interactions and stochasticity are not included when modeling the transient dynamics of metapopulations, or calculating the source-sink classification of habitat patches and persistence of the metapopulation. Non-linear interactions could either be in the form of Allee effects or negative density dependence, and thus by not including them in the models here I am assuming they are not essential at the level of the questions being asked in this thesis. This could either be because they are not present, or because populations are small and so can be approximated by a linearization of the true non-linear dynamics. This is a common assumption when determining the persistence of marine metapopulations and calculating the contributions of local habitat patches so that linear models can be used (Burgess et al., 2014; Hastings and Botsford, 2006; Krkošek and Lewis, 2010). It would be an interesting area of future research to explicitly include non-linear interactions when calculating metapopulation persistence and patch contribution so that the they can be applied

more widely to systems where Allee effects or density dependence are significant.

When calculating the reactivity or attenuation around an equilibrium I also ignore non-linear interactions, and am assuming that the system is either linear or that the true non-linear system is well approximated by its linearization. The linear system is used to calculate the amplification envelope, which measures the maximum transient growth that can occur around an equilibrium, and in this thesis I show that the amplification envelope can grow arbitrarily large in a two patch metapopulation and that the amplification envelope increases with patch size in a metapopulation where dispersal is dominated by advection. However, as the population grows away from the equilibrium the linearization may no longer well approximate the non-linear system, and the non-linearities could either amplify or diminish the level of transient growth that could occur. Transient dynamics may be extremely common in natural systems, and the existence of many long transients in ecology may come from non-linearities in the system, such as those driven by ghost attractors, chaotic saddles, and stable limit cycles (Hastings et al., 2018; Morozov et al., 2020).

While not considered in this thesis, stochasticity can also affect the transient dynamics of systems, and can either shorten or lengthen transient timescales (Hastings et al., 2021). In some species such as the Dungeness crab, stochasticity due to environmental fluctuations may be the primary driver of transient dynamics (Higgins et al., 1997). In advective systems, stochasticity has been shown to allow metapopulations to persist in environmental conditions in which they would not be able to without stochasticity, as the stochastic perturbations cause recurring transient dynamics (Aiken and Navarrete, 2011). In the system of habitat patches where dispersal was dominated by advection considered in Chapters 2 and 3, environmental stochasticity may in fact allow these metapopulations to persist, even in regions where $R_0 < 1$.

6.3 Sea lice on salmon farms in the Broughton Archipelago

The main contributions of this thesis to the study of sea lice on salmon farms involve the use of the next-generation matrix to calculate the contribution of specific salmon farm to the overall sea louse population on all farms, identifying which salmon farms are acting as the largest sources in the Broughton Archipelago, and determining the arrival time of sea lice dispersing between two farms.

In Chapter 2 I constructed a next-generation matrix for a general stage-structured sea louse metapopulation with age dependent survival and maturation. The next-generation matrix is a method of distilling the complexities of the age structure model

down to a simple matrix, from which the contribution of each farm can be calculated. Various different survival and maturation functions can be used to calculated farm contribution. In Chapter 4 I follow Aldrin et al. (2017) and use a Weibull distribution to parameterize the median maturation time as a function of temperature, but instead I could have used a strict maturation time, as used by Revie et al. (2005), or a minimum maturation time followed by a constant maturation rate, as used by Stien et al. (2005). The ability for many different modeling structures to be compared in the same framework is one of the advantages of using the next-generation matrix to calculate the contribution of different salmon farms, and it would be a useful future investigation to examine the sensitivity of the relative farm contributions to different maturation and survival functions.

Due to the complexities of the sea louse life cycle, some studies simply use larval connectivity to identify the contributions of individual farms, and have used graph theoretic clustering algorithms to determine connected clusters of farms (Adams et al., 2012; Cantrell et al., 2018; Samsing et al., 2017; Samsing et al., 2019). Running these same graph theoretic clustering algorithms on the next-generation matrix instead of a connectivity matrix of larval connectivities would be a useful way to incorporate the demographic information stored in the next-generation matrix. In this way stronger connections would represent a higher production of lice occurring between certain farms, rather than simply higher connectivity. This could be especially fruitful in identifying clusters of farms for coordinated management, as the effectiveness of coordinated treatment between farms at reducing overall sea louse levels depends both on farm connectivity as well as differences in local farm productivity (Peacock et al., 2016).

In Chapter 4 I identified which farms were the largest sources of sea lice in this network of salmon farms. I found that there were two main clusters of farms that produced relatively higher levels of sea lice than other farms. The cluster with the highest source farm is also located directly on the migration route of wild juvenile salmon, and this cluster of farms produces the highest density of larvae that wild salmon must migrate through in the Broughton Archipelago (Cantrell et al., 2018; Peacock et al., 2020). Moreover, this cluster of farms is not being currently removed under the agreement between the BC government and the Kwikwasut'inuxw Haxwa'mis, 'Namgis, and Mamalilikulla First Nations (Brownsey and Chamberlain, 2018). If it is approved to remain by both the First Nations and the BC government after 2023 sea lice levels on the farm should be carefully monitored so as to not present a risk to migrating wild salmon. A useful avenue of future research should the farms remain would be to couple the local productivity of farms with the dispersal kernels from

Cantrell et al. (2018) to determine if there are other migratory routes that pose a risk to wild salmon if sea lice levels on farms are elevated.

With respect to identifying the largest source farms in the Broughton Archipelago with the next-generation matrix, there are several limitations to note. First, our estimation of the arrival rate onto farms (β) is very uncertain, and thus the next-generation matrix should be primarily be used to look the relative contribution of farms in this system, rather than the absolute generational output given by the column sums. Second, while I believe that the hydrodynamic model captures the spread of sea lice between farms with relative accuracy, the resolution of the hydrodynamic model may not be fine enough to capture the local hydrodynamics of a salmon farm that may keep some lice in the vicinity of the farm, so that even if the model shows that most lice disperse away from a farm there may be some proportion that remain. Again this would not change the relative farm contributions, but would change their absolute contributions, as well as the estimated value of R_0. Lastly, I assume for these analyses that all farms have similar numbers of salmon, but if the next-generation matrix is to be used to determine the contribution of specific farms at a given time, the entries should be scaled by the salmon on each farm.

In Chapter 5, to calculate arrival time and investigate the effect of farm spacing on cross infection, I model larval dispersal with a simple advection diffusion equation and fit the resulting arrival time distribution to the arrival time calculated directly from a complex hydrodynamic model that accurately captures the intricacies of the currents in the Broughton Archipelago. Some of the earliest work connecting elevated sea lice levels on wild salmon with sea lice numbers on salmon farms used the same advection diffusion equations I use in this thesis to model dispersal away from salmon farms (Krkošek et al., 2006a; Krkošek et al., 2005). There the dispersal model was fit using empirical data of sea lice on wild salmon to detect elevated lice levels on salmon that were migrating past the farms. However, hydrodynamic models of sea lice dispersal were used to question these results, as the particle tracking simulations estimated that lice would be swept further away from the farm than the stationary distribution estimated (Brooks, 2005; Brooks and Stucchi, 2006). This is the first study which compares the arrival time calculated from a simple advection diffusion equation and a hydrodynamic model to determine dispersal of sea lice in the Broughton Archipelago and it shows that the simpler model yields a good approximation to the more complex.

Fitting dispersal models using advection diffusion equations to those with hydrodynamic models could also be useful in other marine metapopulations, especially those located along the coast with a directional coastal current, so that questions can be investigated using the simple advection diffusion equation, with the knowledge that

it is well parameterized to capture dispersal in the metapopulation. In California, the dispersal of several species along the coastline have been modelled using advection diffusion equations, and at certain scales, alongshore larval dispersal kernels generated by hydrodynamic models can be adequately captured by those generated by advection-diffusion equations (Botsford et al., 1994; Largier, 2003; Lubina and Levin, 1988; Mitarai et al., 2008; Roughgarden et al., 1988; Siegel et al., 2003).

6.4 Concluding remarks

Overall, the work in this thesis contributes to a new understanding of marine metapopulations and specifically to sea louse populations on salmon farms in the Broughton Archipelago. I have demonstrated how to use the next-generation matrix to calculate the contribution of local habitat patches and overall growth of the metapopulation for sea louse and other marine metapopulations and investigated the transient dynamics that can occur in these and other birth-jump metapopulations. In the Broughton Archipelago I determined how various factors affect the dispersal of sea lice between salmon farms and found which salmon farms may be the largest sources of sea lice in this region. The results in these thesis have both broad implications for theoretical ecologists interested in marine metapopulations and specific management implications for salmon farms in the Broughton Archipelago. In the Broughton Archipelago, connectivity between salmon farms is complex, and even in channels seaway distance may not be a useful measure of connectivity in this region. Therefore accurate estimates of sea louse dispersal should be used when evaluating the removal of farms or placement of new farms, to reduce the level of cross infection between farms. Location is also important, as some areas have higher sea louse productivity due to higher temperatures and salinities, and in the Broughton the farms in the most productive areas are also the most highly connected. These farms are also slated to remain in the current removal plan of farms from the Broughton, subject to local First Nations and provincial governmental approval, and thus careful management of these farms is necessary to reduce the spread of sea lice between the network of salmon farms in the Broughton, and to reduce the spread of sea lice from farms onto wild salmon.

Bibliography

Aaen, S. M., K. O. Helgesen, M. J. Bakke, K. Kaur, and T. E. Horsberg (2015). "Drug resistance in sea lice: A threat to salmonid aquaculture". *Trends Parasitol.* 31.2, pp. 72–81.

Abolofia, J., F. Asche, and J. E. Wilen (2017). "The Cost of Lice: Quantifying the Impacts of Parasitic Sea Lice on Farmed Salmon". *Mar Resour Econ* 32.3, pp. 329–349.

Adams, T. P., K. D. Black, C. MacIntyre, I. MacIntyre, and R. Dean (2012). "Connectivity modelling and network analysis of sea lice infection in Loch Fyne, west coast of Scotland". *Aquac. Environ. Interact.* 3.1, pp. 51–63.

Adams, T. P., R. Proud, and K. D. Black (2015). "Connected networks of sea lice populations: dynamics and implications for control". *Aquac. Environ. Interact.* 6.3, pp. 273–284.

Aiken, C. M. and S. A. Navarrete (2011). "Environmental fluctuations and asymmetrical dispersal: Generalized stability theory for studying metapopulation persistence and marine protected areas". *Mar. Ecol. Prog. Ser.* 428, pp. 77–88.

Aldrin, M., R. B. Huseby, A. Stien, R. N. Grøntvedt, H. Viljugrein, and P. A. Jansen (2017). "A stage-structured Bayesian hierarchical model for salmon lice populations at individual salmon farms - Estimated from multiple farm data sets". *Ecol. Modell.* 359, pp. 333–348.

Aldrin, M., B. Storvik, A. B. Kristoffersen, and P. A. Jansen (2013). "Space-Time Modelling of the Spread of Salmon Lice between and within Norwegian Marine Salmon Farms". *PLoS One* 8.5, pp. 1–10.

Alexander, S. E. and J. Roughgarden (1996). "Larval transport and population dynamics of intertidal barnacles: a coupled benthic/oceanic model". *Ecol. Monogr.* 66.3, pp. 259–275.

Amarasekare, P. and R. M. Nisbet (2001). "Spatial Heterogeneity, Source-Sink Dynamics, and the Local Coexistence of Competing Species". *Am. Nat.* 158.6, pp. 572–584.

Amundrud, T. and A. Murray (2009). "Modelling sea lice dispersion under varying environmental forcing in a Scottish sea loch". *Journal of fish diseases* 32.1, pp. 27–44.

Arino, J. and P. van den Driessche (2003). "A multi-city epidemic model". *Math. Popul. Stud.* 10.3, pp. 175–193.

Armsworth, P. R. (2002). "Recruitment limitation, population regulation, and larval connectivity in reef fish metapopulations". *Ecology* 83.4, pp. 1092–1104.

Bani, R., M.-J. Fortin, R. M. Daigle, and F. Guichard (2019). "Dispersal traits interact with dynamic connectivity to affect metapopulation growth and stability". *Theor Ecol* 12.1, pp. 111–127.

Bateman, A. W., S. J. Peacock, B. Connors, Z. Polk, D. Berg, M. Krkošek, and A. Morton (2016). "Recent failure to control sea louse outbreaks on salmon in the Broughton Archipelago, British Columbia". *Can. J. Fish. Aquat. Sci.* 73.8, pp. 1164–1172.

Berg, H. (1983). *Random Walks in Biology*. Princeton, NJ: Princeton University Press.

Berman, A. and R. J. Plemmons (1994). *Nonnegative matrices in the mathematical sciences*. Society for Industrial and Applied Mathematics.

Bode, M, L Bode, and P. R. Armsworth (2006). "Larval dispersal reveals regional sources and sinks in the Great Barrier Reef". *Mar. Ecol. Prog. Ser. Ser.* 308, pp. 1–9.

Botsford, L. W., C. L. Moloney, A. Hastings, J. L. Largier, T. M. Powell, K. Higgins, and J. F. Quinn (1994). "The influence of spatially and temporally varying oceanographic conditions on meroplanktonic metapopulations". *Deep. Res. Part II* 41.1, pp. 107–145.

Botsford, L. W., J. W. White, M. A. Coffroth, C. B. Paris, S. Planes, T. L. Shearer, S. R. Thorrold, and G. P. Jones (2009). "Connectivity and resilience of coral reef metapopulations in marine protected areas: Matching empirical efforts to predictive needs". *Coral Reefs* 28.2, pp. 327–337.

Brauner, C. J., M. Sackville, Z. Gallagher, S. Tang, L. Nendick, and A. P. Farrell (2012). "Physiological consequences of the salmon louse (Lepeophtheirus salmonis) on juvenile pink salmon (Oncorhynchus gorbuscha): Implications for wild salmon

ecology and management, and for salmon aquaculture". *Philos. Trans. R. Soc. B Biol. Sci.* 367.1596, pp. 1770–1779.

Brooks, K. M. (2005). "The effects of water temperature, salinity, and currents on the survival and distribution of the infective copepodid stage of sea lice (Lepeophtheirus salmonis) originating on atlantic salmon farms in the Broughton Archipelago of British Columbia, Canada". *Rev. Fish. Sci.* 13.3, pp. 177–204.

Brooks, K. M. and D. J. Stucchi (2006). "The effects of water temperature, salinity and currents on the survival and distribution of the infective copepodid stage of the salmon louse (Lepeophtheirus salmonis) originating on Atlantic salmon farms in the Broughton Archipelago of British Columbia, " *Rev. Fish. Sci.* 14.1-2, pp. 13–23.

Brownsey, L. and R. Chamberlain (2018). *Collaborative solutions for finfish aquaculture farms in the Broughton Area, steering committee recommendations*. Government of British Columbia.

Burgess, S. C., K. J. Nickols, C. D. Griesemer, L. A. Barnett, A. G. Dedrick, E. V. Satterthwaite, L. Yamane, S. G. Morgan, J. W. White, and L. W. Botsford (2014). "Beyond connectivity: How empirical methods can quantify population persistence to improve marine protected-area design". *Ecol. Appl.* 24.2, pp. 257–270.

Byers, J. E. and J. M. Pringle (2006). "Going against the flow: Retention, range limits and invasions in advective environments". *Mar. Ecol. Prog. Ser.* 313, pp. 27–41.

Cantrell, D., R. Filgueira, C. W. Revie, E. E. Rees, R. Vanderstichel, M. Guo, M. G. Foreman, D. Wan, and J. Grant (2020). "The relevance of larval biology on spatiotemporal patterns of pathogen connectivity among open-marine salmon farms". *Can. J. Fish. Aquat. Sci.* 77.3, pp. 505–519.

Cantrell, D., R. Vanderstichel, R. Filgueira, J. Grant, and C. W. Revie (2021). "Validation of a sea lice dispersal model: principles from ecological agent-based models applied to aquatic epidemiology". *Aquac. Environ. Interact.* 13, pp. 65–79.

Cantrell, D. L., E. E. Rees, R. Vanderstichel, J. Grant, R. Filgueira, and C. W. Revie (2018). "The Use of Kernel Density Estimation With a Bio-Physical Model Provides a Method to Quantify Connectivity Among Salmon Farms: Spatial Planning and Management With Epidemiological Relevance". *Front. Vet. Sci.* 5.269, pp. 1–14.

Carson, H. S., G. S. Cook, P. C. López-duarte, L. A. Levin, H. S. Carson, G. S. Cook, P. C. Lopez-duarte, and L. A. Levin (2011). "Evaluating the importance of demographic connectivity in a marine metapopulation". *Ecology* 92.10, pp. 1972–1984.

Caswell, H. (2000). *Matrix population models*. Sunderland, MA, USA: Sinauert.

Caswell, H. and M. G. Neubert (2005). "Reactivity and transient dynamics of discrete-time ecological systems". *J. Differ. Equations Appl.* 11.4-5, pp. 295–310.

Chen, C., R. Beardsley, and G. Cowles (2006). "An Unstructured Grid, Finite-Volume Coastal Ocean Model (FVCOM) System". *Oceanography* 19.1, pp. 78–89.

Connors, B. M., E. Juarez-Colunga, and L. M. Dill (2008). "Effects of varying salinities on Lepeophtheirus salmonis survival on juvenile pink and chum salmon". *J. Fish Biol.* 72.7, pp. 1825–1830.

Corrado, R., G. Lacorata, L. Palatella, R. Santoleri, and E. Zambianchi (2017). "General characteristics of relative dispersion in the ocean". *Sci. Rep.* 7, pp. 1–11.

Costello, C., A. Rassweiler, D. Siegel, G. De Leo, F. Micheli, A. Rosenberg, and S. D. Gaines (2010). "The value of spatial information in MPA network design". *PNAS* 107.43, pp. 18294–18299.

Costello, M. J. (2009a). "How sea lice from salmon farms may cause wild salmonid declines in Europe and North America and be a threat to fishes elsewhere". *Proc. R. Soc. B Biol. Sci.* 276.1672, pp. 3385–3394.

Costello, M. J. (2006). "Ecology of sea lice parasitic on farmed and wild fish". *Trends Parasitol.* 22.10, pp. 475–483.

Costello, M. J. (2009b). "The global economic cost of sea lice to the salmonid farming industry". *J. Fish Dis.* 32.1, pp. 115–118.

Cowen, R. K., C. B. Paris, and A. Srinivasan (2006). "Scaling of connectivity in marine populations". *Science* 311.5760, pp. 522–527.

Cowen, R. K., K. M. Lwiza, S. Sponaugle, C. B. Paris, and D. B. Olson (2000). "Connectivity of marine populations: Open or closed?" *Science.* 287.5454, pp. 857–859.

Cowen, R. K. and S. Sponaugle (2009). "Larval dispersal and marine population connectivity". *Ann. Rev. Mar. Sci.* 1, pp. 443–466.

Crowder, L. B., S. J. Lyman, W. F. Figueira, and J. Priddy (2000). "Source-sink population dynamics and the problem of siting marine reserves". *Bull. Mar. Sci.* 66.3, pp. 799–820.

Cushing, J. M. and O. Diekmann (2016). "The many guises of R_0 (a didactic note)". *J. Theor. Biol.* 404, pp. 295–302.

Cushing, J. M. and Z. Yicang (1994). "The net reproductive value and stability in matrix population models". *Nat. Resour. Model.* 8.4, pp. 297–333.

De-Camino-Beck, T. and M. A. Lewis (2007). "A new method for calculating net reproductive rate from graph reduction with applications to the control of invasive species". *Bull. Math. Biol.* 69.4, pp. 1341–1354.

De Dominicis, M., G. Leuzzi, P. Monti, N. Pinardi, and P. M. Poulain (2012). "Eddy diffusivity derived from drifter data for dispersion model applications". *Ocean Dyn.* 62.9, pp. 1381–1398.

Dedrick, A. G., K. A. Catalano, M. R. Stuart, J. W. White, H. R. Montes, and M. L. Pinsky (2021). "Persistence of a reef fish metapopulation via network connectivity: theory and data". *Ecol. Lett.* 24.6, pp. 1121–1132.

Diekmann, O., J. A. P. Heesterbeek, and J. A. J. Metz (1990). "On the definition and the computation of the basic reproduction ratio R_0 in models for infectious diseases in heterogeneous populations". *J. Math. Biol.* 28.4, pp. 365–382.

Diekmann, O., J. A. P. Heesterbeek, and M. G. Roberts (2010). "The construction of next-generation matrices for compartmental epidemic models". *J. R. Soc. Interface* 7.47, pp. 873–885.

Fauchald, P. and T. Tveraa (2003). "Using first-passage time in the analysis of area-restricted search and habitat selection". *Ecology* 84.2, pp. 282–288.

Feng, Z. and H. R. Thieme (2000). "Endemic Models with Arbitrarily Distributed Periods of Infection I: Fundamental Properties of the Model". *SIAM J. Appl. Math.* 61.3, pp. 803–833.

Feng, Z., D. Xu, and H. Zhao (2007). "Epidemiological models with non-exponentially distributed disease stages and applications to disease control". *Bull. Math. Biol.* 69.5, pp. 1511–1536.

Figueira, W. F. (2009). "Connectivity or demography: Defining sources and sinks in coral reef fish metapopulations". *Ecol. Modell.* 220.8, pp. 1126–1137.

Figueira, W. F. and L. B. Crowder (2006). "Defining patch contribution in source-sink metapopulations: the importance of including dispersal and its relevance to marine systems". *Popul. Ecol.* 48.3, pp. 215–224.

FitzHugh, R. (1961). "Impulses and physiological states in theoretical models of nerve membrane". *Biophys. J.* 1.6, pp. 445–466.

Foreman, M. G. G., P. C. Chandler, D. J. Stucchi, K. A. Garver, M Guo, J Morrison, and D Tuele (2015). *The ability of hydrodynamic models to inform decisions on the siting and management of aquaculture facilities in British Columbia*. Tech. rep. Fisheries and Oceans Canada.

Foreman, M. G. G., P. Czajko, D. J. Stucchi, and M. Guo (2009). "A finite volume model simulation for the Broughton Archipelago, Canada". *Ocean Model.* 30.1, pp. 29–47.

Fox, A. D., L. A. Henry, D. W. Corne, and J. M. Roberts (2016). "Sensitivity of marine protected area network connectivity to atmospheric variability". *R. Soc. Open Sci.* 3.11.

Frazer, L. N., A. Morton, and M. Krkosek (2012). "Critical thresholds in sea lice epidemics: evidence, sensitivity and subcritical estimation." *Proc. Biol. Sci.* 279.1735, pp. 1950–8.

Garavelli, L., J. W. White, I. Chollett, and L. M. Chérubin (2018). "Population models reveal unexpected patterns of local persistence despite widespread larval dispersal in a highly exploited species". *Conserv. Lett.* 11.5.

Godwin, S. C., L. M. Dill, J. D. Reynolds, and M. Krkošek (2015). "Sea lice, sockeye salmon, and foraging competition: Lousy fish are lousy competitors". *Can. J. Fish. Aquat. Sci.* 72.7, pp. 1113–1120.

Godwin, S. C., M. Krkošek, J. D. Reynolds, L. A. Rogers, and L. M. Dill (2017). "Heavy sea louse infection is associated with decreased stomach fullness in wild juvenile sockeye salmon". *Can. J. Fish. Aquat. Sci.* 75.10, pp. 1587–1595.

Groner, M. L., G. Gettinby, M. Stormoen, C. W. Revie, and R. Cox (2014). "Modelling the impact of temperature-induced life history plasticity and mate limitation on the epidemic potential of a marine ectoparasite". *PLoS One* 9.2, pp. 1–12.

Gurtin, M. E. and R. C. MacCamy (1974). "Non-linear age-dependent population dynamics". *Arch. Ration. Mech. Anal.* 54.3, pp. 66–76.

Gyllenberg, M. and I. Hanski (1997). "Habitat deterioration, habitat destruction, and metapopulation persistence in a heterogenous landscape". *Theor. Popul. Biol.* 52.3, pp. 198–215.

Gyllenberg, M., A. Hastings, and I. Hanski (1997). "5 - Structured metapopulation models". *Metapopulation Biology*. Ed. by I. Hanski and M. E. Gilpin. San Diego: Academic Press, pp. 93–122.

Hanski, I. (1998). "Metapolulation dynamics". *Nature* 396, pp. 41–49.

Hanski, I. (1999). *Metapopulation ecology*. Oxford University Press.

Hanski, I. and C. D. Thomas (1994). "Metapopulation dynamics and conservation: a spatially explicit model applied to butterflies". *Biol. Conserv.* 68.2, pp. 167–180.

Harrington, P. D. and M. A. Lewis (2020). "A next-generation approach to calculate source–sink dynamics in marine metapopulations". *Bull. Math. Biol.* 82.1, pp. 1–44.

Hastings, A. (2001). "Transient dynamics and persistence of ecological systems". *Ecol. Lett.* 4.3, pp. 215–220.

Hastings, A. (1982). "Dynamics of a single species in a spatially varying environment: The stabilizing role of high dispersal rates". *J. Math. Biol.* 16.1, pp. 49–55.

Hastings, A. (2004). "Transients: the key to long-term ecological understanding?" *Trends Ecol. Evol.* 19.1, pp. 39–45.

Hastings, A., K. C. Abbott, K. Cuddington, T. Francis, G. Gellner, Y. C. Lai, A. Morozov, S. Petrovskii, K. Scranton, and M. L. Zeeman (2018). "Transient phenomena in ecology". *Science* 361.6406.

Hastings, A., K. C. Abbott, K. Cuddington, T. B. Francis, Y.-C. Lai, A. Morozov, S. Petrovskii, and M. L. Zeeman (2021). "Effects of stochasticity on the length and behaviour of ecological transients". *J R Soc Interface* 18.180, p. 20210257.

Hastings, A. and L. W. Botsford (2006). "Persistence of spatial populations depends on returning home". *Proc. Natl. Acad. Sci. U. S. A.* 103.15, pp. 6067–6072.

Hastings, A. and K. Higgins (1994). "Persistence of transients in spatially structured ecological models". *Science* 263.5150, pp. 1133–1136.

Heesterbeek, J. A. and M. G. Roberts (2007). "The type-reproduction number T in models for infectious disease control". *Math. Biosci.* 206.1, pp. 3–10.

Higgins, K., A. Hastings, J. N. Sarvela, and L. W. Botsford (1997). "Stochastic dynamics and deterministic skeletons: population behavior of Dungeness crab". *Science* 276.5317, pp. 1431–1434.

Hillen, T., B. Greese, J. Martin, and G. de Vries (2015). "Birth-jump processes and application to forest fire spotting". *J. Biol. Dyn.* 9, pp. 104–127.

Horn, R. A. and C. R. Johnson (2012). *Matrix Analysis*. 2nd. New York, NY, USA: Cambridge University Press.

Huang, Q., Y. Jin, and M. A. Lewis (2016). "R_0 analysis of a benthic-drift model for a stream population". *SIAM J. Appl. Dyn. Syst.* 15.1, pp. 287–321.

Huang, Q. and M. A. Lewis (2015). "Homing fidelity and reproductive rate for migratory populations". *Theor. Ecol.* 8.2, pp. 187–205.

Hurford, A., D. Cownden, and T. Day (2010). "Next-generation tools for evolutionary invasion analyses." *J. R. Soc. Interface* 7.45, pp. 561–571.

Husband, B. C. and S. C. H. Barrett (1996). "A metapopulation perspective in plant population biology". *J. Ecol.* 84.3, pp. 461–469.

Johnson, S. C. and L. J. Albright (1991). "Development, growth, and survival of lepeophtheirus salmonis (Copepoda: Caligidae) under laboratory conditions". *J. Mar. Biol. Assoc. United Kingdom* 71.2, pp. 425–436.

Jones, G., G. Almany, G. Russ, P. Sale, R. Steneck, M. van Oppen, and B. Willis (2009). "Larval retention and connectivity among populations of corals and reef fishes: history, advances and challenges". *Coral Reefs* 28, pp. 307–325.

Keyfitz, B. L. and N. Keyfitz (1997). "The McKendrick partial differential equation and its uses in epidemiology and population study". *Math. Comput. Model.* 26.6, pp. 1–9.

Kragesteen, T., K Simonsen, A. Visser, and K. Andersen (2018). "Identifying salmon lice transmission characteristics between Faroese salmon farms". *Aquac. Environ. Interact.* 10.Kabata 1979, pp. 49–60.

Kristoffersen, A. B., E. E. Rees, H Stryhn, R Ibarra, J Campisto, C. W. Revie, and S St-hilaire (2013). "Understanding sources of sea lice for salmon farms in Chile". *Prev. Vet. Med.* 111.1-2, pp. 165–175.

Kritzer, J. P. and P. F. Sale (2004). "Metapopulation ecology in the sea: From Levins' model to marine ecology and fisheries science". *Fish Fish.* 5.2, pp. 131–140.

Kritzer, J. P. and P. F. Sale (2006). *Marine metapopulations*. Elsevier Academic Press.

Krkošek, M., A. W. Bateman, S. Proboszcz, and C. Orr (2012a). "Dynamics of outbreak and control of salmon lice on two salmon farms in the Broughton Archipelago, British Columbia". *Aquac. Environ. Interact.* 1.2, pp. 137–146.

Krkošek, M., B. M. Connors, H. Ford, S. Peacock, P. Mages, J. S. Ford, M. Alexandra, J. P. Volpe, R. Hilborn, L. M. Dill, and M. A. Lewis (2011a). "Fish farms, parasites, and predators: Implications for salmon population dynamics". *Ecol. Appl.* 21.3, pp. 897–914.

Krkošek, M., B. M. Connors, M. A. Lewis, and R. Poulin (2012b). "Allee Effects May Slow the Spread of Parasites in a Coastal Marine Ecosystem". *Am. Nat.* 179.3, pp. 401–412.

Krkošek, M., B. M. Connors, A. Morton, M. A. Lewis, L. M. Dill, and R. Hilborn (2011b). "Effects of parasites from salmon farms on productivity of wild salmon." *Proc. Natl. Acad. Sci. U. S. A.* 108.35, pp. 14700–14704.

Krkošek, M., J. S. Ford, A. Morton, S. Lele, and M. A. Lewis (2008). "Response to comment on "Declining wild salmon populations in relation to parasites from farm salmon"". *Science* 322.5909, pp. 1–4.

Krkošek, M., J. S. Ford, A. Morton, S. Lele, R. A. Myers, and M. A. Lewis (2007). "Declining Wild Salmon Populations in Relation to Parasites from Farm Salmon". *Science.* 318.2, pp. 1772–1775.

Krkošek, M. and M. A. Lewis (2010). "An R_0 theory for source-sink dynamics with application to Dreissena competition". *Theor. Ecol.* 3.1, pp. 25–43.

Krkošek, M., M. A. Lewis, A. Morton, L. N. Frazer, and J. P. Volpe (2006a). "Epizootics of wild fish induced by farm fish". *Proc. Natl. Acad. Sci. U. S. A.* 103.42, pp. 15506–15510.

Krkošek, M., M. A. Lewis, and J. P. Volpe (2005). "Transmission dynamics of parasitic sea lice from farm to wild salmon." *Proc. Biol. Sci.* 272.1564, pp. 689–696.

Krkošek, M., M. A. Lewis, J. P. Volpe, and A. Morton (2006b). "Fish farms and sea lice infestations of wild juvenile salmon in the Broughton Archipelago - A Rebuttal to Brooks (2005)". *Rev. Fish. Sci.* 14.1-2, pp. 1–11.

Kurella, V., J. C. Tzou, D. Coombs, and M. J. Ward (2015). "Asymptotic Analysis of First Passage Time Problems Inspired by Ecology". *Bull. Math. Biol.* 77.1, pp. 83–125.

Largier, J. L. (2003). "Considerations in estimating larval dispersal distances from oceanographic data". *Ecol Appl* 13.sp1, pp. 71–89.

Le Corre, M., C. Dussault, and S. D. Côté (2014). "Detecting changes in the annual movements of terrestrial migratory species: using the first-passage time to document the spring migration of caribou". *Movement ecology* 2.1, pp. 1–11.

Levins, R. (1969). "Some demographic and genetic consequences of environmental heterogeneity for biological control". *Bull. Entomol. Soc. Am.* 15.3, pp. 237–250.

Lewis, M. A., Z. Shuai, and P. van den Driessche (2019). "A general theory for target reproduction numbers with applications to ecology and epidemiology". *J. Math. Biol.* 78.7, pp. 2317–2339.

Li, C. K. and H. Schneider (2002). "Applications of Perron-Frobenius theory to population dynamics". *J. Math. Biol.* 44.5, pp. 450–462.

Lloyd, A. L. and R. M. May (1996). "Spatial heterogeneity in epidemic models". *J. Theor. Biol.* 179.1, pp. 1–11.

Lubina, J. A. and S. A. Levin (1988). "The Spread of a Reinvading Species: Range Expansion in the California Sea Otter". *Am. Nat.* 131.4, pp. 526–543.

Ludwig, D., D. D. Jones, and C. S. Holling (1978). "Qualitative analysis of insect outbreak systems: the spruce budworm and forest". *J. Anim. Ecol.* 47.1, pp. 315–332.

Lutscher, F. and X. Wang (2020). "Reactivity of communities at equilibrium and periodic orbits". *J. Theor. Biol.* 493, p. 110240.

Marculis, N. G. and A. Hastings (2021). "Simple discrete-time metapopulation models of patch occupancy". *Oikos* 130.2, pp. 310–320.

Mari, L., R. Casagrandi, E. Bertuzzo, A. Rinaldo, and M. Gatto (2019). "Conditions for transient epidemics of waterborne disease in spatially explicit systems". *R. Soc. Open Sci.* 6.5.

Mari, L., R. Casagrandi, A. Rinaldo, and M. Gatto (2017). "A generalized definition of reactivity for ecological systems and the problem of transient species dynamics". *Methods Ecol. Evol.* 8.11, pp. 1574–1584.

Marty, G. D., S. M. Saksida, and T. J. Quinn (2010). "Relationship of farm salmon, sea lice, and wild salmon populations." *Proc. Natl. Acad. Sci. U. S. A.* 107.52, pp. 22599–22604.

Mayorga-Adame, C. G., H. P. Batchelder, and Y. H. Spitz (2017). "Modeling larval connectivity of coral reef organisms in the Kenya-Tanzania region". *Front. Mar. Sci.* 4, p. 92.

McKendrick, A. G. (1925). "Applications of Mathematics to Medical Problems". *Proc. Edinburgh Math. Soc.* 44, pp. 98–130.

Mckenzie, H. W., Y. Jin, J. Jacobsen, and M. A. Lewis (2012a). "R_0 analysis of a spatiotemporal model for a stream population". *SIAM J. Appl. Dyn. Syst.* 11.2, pp. 567–596.

McKenzie, H. W., M. A. Lewis, and E. H. Merrill (2009). "First passage time analysis of animal movement and insights into the functional response". *Bull. Math. Biol.* 71.1, pp. 107–129.

Mckenzie, H. W., E. H. Merrill, R. J. Spiteri, and M. A. Lewis (2012b). "How linear features alter predator movement and the functional response". *Interface Focus* 2.2, pp. 205–216.

Mileikovsky, S. A. (1971). "Types of larval development in marine bottom invertebrates, their distribution and ecological significance: a re-evaluation". *Mar. Biol.* 10, pp. 193–213.

Mitarai, S., D. Siegel, and K. Winters (2008). "A numerical study of stochastic larval settlement in the California Current system". *J. Mar. Sys.* 69.3. Physical-Biological Interactions in the Upper Ocean, pp. 295–309.

Morozov, A., K. Abbott, K. Cuddington, T. Francis, G. Gellner, A. Hastings, Y. C. Lai, S. Petrovskii, K. Scranton, and M. L. Zeeman (2020). "Long transients in ecology: theory and applications". *Phys. Life Rev.* 32, pp. 1–40.

Morris, R. F. (1963). "The dynamics of epidemic spruce budworm populations". *Mem. Entomol. Soc. Canada* 95.S31, pp. 1–12.

Nagumo, J., S. Arimoto, and S. Yoshizawa (1962). "An active pulse transmission line simulating nerve axon". *Proc. IRE* 50.10, pp. 2061–2070.

Neubert, M. G. and H. Caswell (1997). "Alternatives to resilience for measuring the responses of ecological systems to perturbations". *Ecology* 78.3, pp. 653–665.

Neubert, M. G., H. Caswell, and J. D. Murray (2002). "Transient dynamics and pattern formation: reactivity is necessary for Turing instabilities". *Math. Biosci.* 175.1, pp. 1–11.

Neubert, M. G., T. Klanjscek, and H. Caswell (2004). "Reactivity and transient dynamics of predator-prey and food web models". *Ecol. Modell.* 179.1-2, pp. 29–38.

Noschese, S., L. Pasquini, and L. Reichel (2013). "Tridiagonal Toeplitz matrices: properties and novel applications". *Numer. Linear Algebra Appl.* 20.2, pp. 302–326.

Ovaskainen, O. and I. Hanski (2002). "Transient dynamics in metapopulation response to perturbation". *Theoretical population biology* 61.3, pp. 285–295.

Ovaskainen, O. and M. Saastamoinen (2018). "Frontiers in metapopulation biology: The legacy of Ilkka Hanski". *Annu. Rev. Ecol. Evol. Syst.* 49, pp. 231–252.

Peacock, S. J., A. W. Bateman, M. Krkošek, and M. A. Lewis (2016). "The dynamics of coupled populations subject to control". *Theor. Ecol.*, pp. 1–16.

Peacock, S. J., M. Krkošek, A. W. Bateman, and M. A. Lewis (2020). "Estimation of spatiotemporal transmission dynamics and analysis of management scenarios for sea lice of farmed and wild salmon". *Can. J. Fish. Aquat. Sci.* 77.1, pp. 55–68.

Pike, A. and S. Wadsworth (1999). "Sealice on Salmonids: Their Biology and Control". *Adv. Parasitol.* Vol. 44, pp. 233–337.

Planes, S., G. P. Jones, and S. R. Thorrold (2009). "Larval dispersal connects fish populations in a network of marine protected areas". *Proc. Natl. Acad. Sci.* 106.14, pp. 5693–5697.

Puckett, B. J. and D. B. Eggleston (2016). "Metapopulation dynamics guide marine reserve design: Importance of connectivity, demographics, and stock enhancement". *Ecosphere* 7.6.

Pulliam, H. R. (1988). "Sources, sinks and population regulation". *Am. Nat.* 132.5, pp. 652–661.

Redner, S. (2001). *A Guide to First-Passage Processes*. Cambridge University Press.

Revie, C. W., C. Robbins, G. Gettinby, L. Kelly, and J. W. Treasurer (2005). "A mathematical model of the growth of sea lice, Lepeophtheirus salmonis, populations on farmed Atlantic salmon, Salmo salar L., in Scotland and its use in the assessment of treatment strategies". *J. Fish Dis.* 28.10, pp. 603–614.

Riddell, B. E., R. J. Beamish, L. J. Richards, and J. R. Candy (2008). "Comment on "Declining Wild Salmon Populations in Relation to Parasites from Farm Salmon"". *Science* 322.5909, 1790 LP –1790.

Rittenhouse, M. A., C. W. Revie, and A. Hurford (2016). "A model for sea lice (Lepeophtheirus salmonis) dynamics in a seasonally changing environment". *Epidemics* 16, pp. 8–16.

Roberts, M. G. and J. A. Heesterbeek (2003). "A new method for estimating the effort required to control an infectious disease". *Proc. R. Soc. B Biol. Sci.* 270.1522, pp. 1359–1364.

Robson, N. A., Y. Hetzel, S. Whiting, S. Wijeratne, C. B. Pattiaratchi, P. Withers, and M. Thums (2017). "Use of particle tracking to determine optimal release dates and locations for rehabilitated neonate sea turtles". *Front. Mar. Sci.* 4.JUN.

Rogers, L. A., S. J. Peacock, P. McKenzie, S. DeDominicis, S. R. Jones, P. Chandler, M. G. Foreman, C. W. Revie, and M. Krkošek (2013). "Modeling Parasite Dynamics on Farmed Salmon for Precautionary Conservation Management of Wild Salmon". *PLoS One* 8.4.

Roughgarden, J., S. Gaines, and H. Possingham (1988). "Recruitment dynamics in complex life cycles". *Science* 241.4872, pp. 1460–1466.

Runge, J. P., M. C. Runge, and J. D. Nichols (2006). "The role of local populations within a landscape context: Defining and classifying sources and sinks". *Am. Nat.* 167.6, pp. 925–938.

Safranyik, L and A. L. Carroll (2007). "The biology and epidemiology of the mountain pine beetle in lodgepole pine forests." *The mountain pine beetle: a synthesis of biology, management and impacts on lodgepole pine*. Ed. by L Safranyik and B Wilson. Victoria, Canada: Canadian Forest Service, pp. 3–66.

Samsing, F., I. Johnsen, T. Dempster, F. Oppedal, and E. A. Treml (2017). "Network analysis reveals strong seasonality in the dispersal of a marine parasite and identifies areas for coordinated management". *Landsc. Ecol.* 32.10, pp. 1953–1967.

Samsing, F., I. Johnsen, E. A. Treml, and T. Dempster (2019). "Identifying 'firebreaks' to fragment dispersal networks of a marine parasite". *Int. J. Parasitol.* 49.3, pp. 277–286.

Samsing, F., F. Oppedal, S. Dalvin, I. Johnsen, T. Vågseth, and T. Dempster (2016). "Salmon lice (Lepeophtheirus salmonis) development times, body size, and reproductive outputs follow universal models of temperature dependence". *Can. J. Fish. Aquat. Sci.* 73.12, pp. 1841–1851.

Sandvik, A. D., S. Dalvin, R. Skern-Mauritzen, and M. D. Skogen (2021). "The effect of a warmer climate on the salmon lice infection pressure from Norwegian aquaculture". *ICES J. Mar. Sci.* 78.5, pp. 1849–1859.

Sandvik, A. D., I. A. Johnsen, M. S. Myksvoll, P. N. Sævik, and M. D. Skogen (2020). "Prediction of the salmon lice infestation pressure in a Norwegian fjord". *ICES J. Mar. Sci.* 77.2, pp. 746–756.

Siegel, D., B. Kinlan, B Gaylord, and S. Gaines (2003). "Lagrangian descriptions of marine larval dispersion". *Mar. Ecol. Prog. Ser.* 260, pp. 83–96.

Skern-Mauritzen, R., N. H. Sissener, A. D. Sandvik, S. Meier, P. N. Sævik, M. D. Skogen, T. Vågseth, S. Dalvin, M. Skern-Mauritzen, and S. Bui (2020). "Parasite development affect dispersal dynamics; infectivity, activity and energetic status in cohorts of salmon louse copepodids". *J. Exp. Mar. Bio. Ecol.* 530-531, p. 151429.

Snyder, R. E. (2010). "What makes ecological systems reactive?" *Theor. Popul. Biol.* 77.4, pp. 243–249.

Stien, A., P. A. Bjørn, P. A. Heuch, and D. A. Elston (2005). "Population dynamics of salmon lice Lepeophtheirus salmonis on Atlantic salmon and sea trout". *Mar. Ecol. Prog. Ser.* 290, pp. 263–275.

Stige, L., K. Helgesen, H Viljugrein, and L Qviller (2021). "A statistical mechanistic approach including temperature and salinity effects to improve salmon lice modelling of infestation pressure". *Aquac. Environ. Interact.* 13, pp. 339–361.

Stott, I., M. Franco, D. Carslake, S. Townley, and D. Hodgson (2010). "Boom or bust? A comparative analysis of transient population dynamics in plants". *J. Ecol.* 98.2, pp. 302–311.

Stott, I., S. Townley, and D. J. Hodgson (2011). "A framework for studying transient dynamics of population projection matrix models". *Ecol. Lett.* 14.9, pp. 959–970.

Stucchi, D., M. Guo, M. Foreman, P. Czajko, M. Galbraith, D. Mackas, and P. A. Gillibrand (2011). "Modeling sea lice production and concentrations in the Broughton Archipelago, British Columbia". *Salmon lice: an integrated approach to understanding parasite abundance and distribution.* Ed. by R Jones, S., Beamish. 1st ed. Chichester: Wiley, pp. 117–150.

Theuerkauf, S. J., B. J. Puckett, and D. B. Eggleston (2021). "Metapopulation dynamics of oysters: sources, sinks, and implications for conservation and restoration". *Ecosphere* 12.7.

Thieme, H. R. (2003). *Mathematics in Population Biology.* Princeton University Press.

Thieme, H. R. (2009). "Spectral bound and reproduction number for infinite-dimensional population structure and time heterogeneity". *SIAM J. Appl. Math.* 70.1, pp. 188–211.

Townley, S., D. Carslake, O. Kellie-Smith, D. Mccarthy, and D. Hodgson (2007). "Predicting transient amplification in perturbed ecological systems". *J. Appl. Ecol.* 44.6, pp. 1243–1251.

Townley, S. and D. J. Hodgson (2008). "Erratum et addendum: Transient amplification and attenuation in stage-structured population dynamics". *J. Appl. Ecol.* 45.6, pp. 1836–1839.

van den Driessche, P. and J. Watmough (2002). "Reproduction numbers and subthreshold endemic equilibria for compartmental models of disease transmission". *Math. Biosci.* 180.1-2, pp. 29–48.

Verdy, A. and H. Caswell (2008). "Sensitivity analysis of reactive ecological dynamics". *Bull. Math. Biol.* 70.6, pp. 1634–1659.

Wang, X., M. Efendiev, and F. Lutscher (2019). "How Spatial Heterogeneity Affects Transient Behavior in Reaction–Diffusion Systems for Ecological Interactions?" *Bull. Math. Biol.* 81.10, pp. 3889–3917.

Watson, J. R., B. E. Kendall, D. A. Siegel, and S. Mitarai (2012). "Changing Seascapes, Stochastic Connectivity, and Marine Metapopulation Dynamics". *Am. Nat.* 180.1, pp. 99–112.

Watson, J. R., D. A. Siegel, B. E. Kendall, S. Mitarai, A. Rassweiller, and S. D. Gaines (2011). "Identifying critical regions in small-world marine metapopulations". *Proc. Natl. Acad. Sci. U. S. A.* 108.43, pp. 907–913.

Webber, Q. M., M. P. Laforge, M. Bonar, A. L. Robitaille, C. Hart, S. Zabihi-Seissan, and E. Vander Wal (2020). "The ecology of individual differences empirically applied to space-use and movement tactics". *Am. Nat.* 196.1, E1–E15.

White, J. W., L. W. Botsford, A. Hastings, and J. L. Largier (2010). "Population persistence in marine reserve networks: Incorporating spatial heterogeneities in larval dispersal". *Mar. Ecol. Prog. Ser.* 398, pp. 49–67.

White, J. W., M. H. Carr, J. E. Caselle, L. Washburn, C. B. Woodson, S. R. Palumbi, P. M. Carlson, R. R. Warner, B. A. Menge, J. A. Barth, C. A. Blanchette, P. T. Raimondi, and K. Milligan (2019). "Connectivity, Dispersal, and Recruitment". *Oceanography* 32.3, pp. 50–59.

Williams, D. W. and A. M. Liebhold (2000). "Spatial synchrony of spruce budworm outbreaks in eastern North America". *Ecology* 81.10, pp. 2753–2766.